**US Army Corps
of Engineers**
Waterways Experiment
Station

# Noyo Harbor, California, Breakwater Stability and Transmission Tests

*by Ernest R. Smith, Leland L. Hennington*

DTIC
SELECTED
JAN 0 5 1996
F

19960103 237

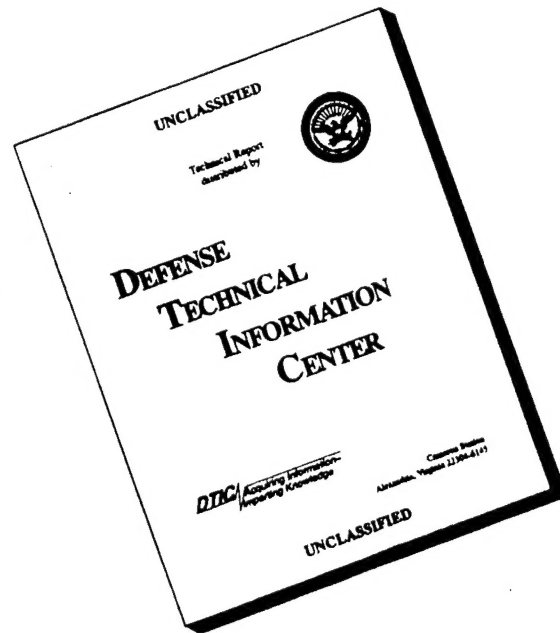Prepared for   U.S. Army Engineer District, San Francisco

The contents of this report are not to be used for advertising,
publication, or promotional purposes. Citation of trade names
does not constitute an official endorsement or approval of the use
of such commercial products.

# DISCLAIMER NOTICE

UNCLASSIFIED

Technical Report
distributed by

**DEFENSE
TECHNICAL
INFORMATION
CENTER**

DTIC Acquiring Information-
Imparting Knowledge

Cameron Station
Alexandria, Virginia 22304-6145

UNCLASSIFIED

# THIS DOCUMENT IS BEST QUALITY AVAILABLE. THE COPY FURNISHED TO DTIC CONTAINED A SIGNIFICANT NUMBER OF PAGES WHICH DO NOT REPRODUCE LEGIBLY.

# Noyo Harbor, California, Breakwater Stability and Transmission Tests

by  Ernest R. Smith, Leland L. Hennington

U.S. Army Corps of Engineers
Waterways Experiment Station
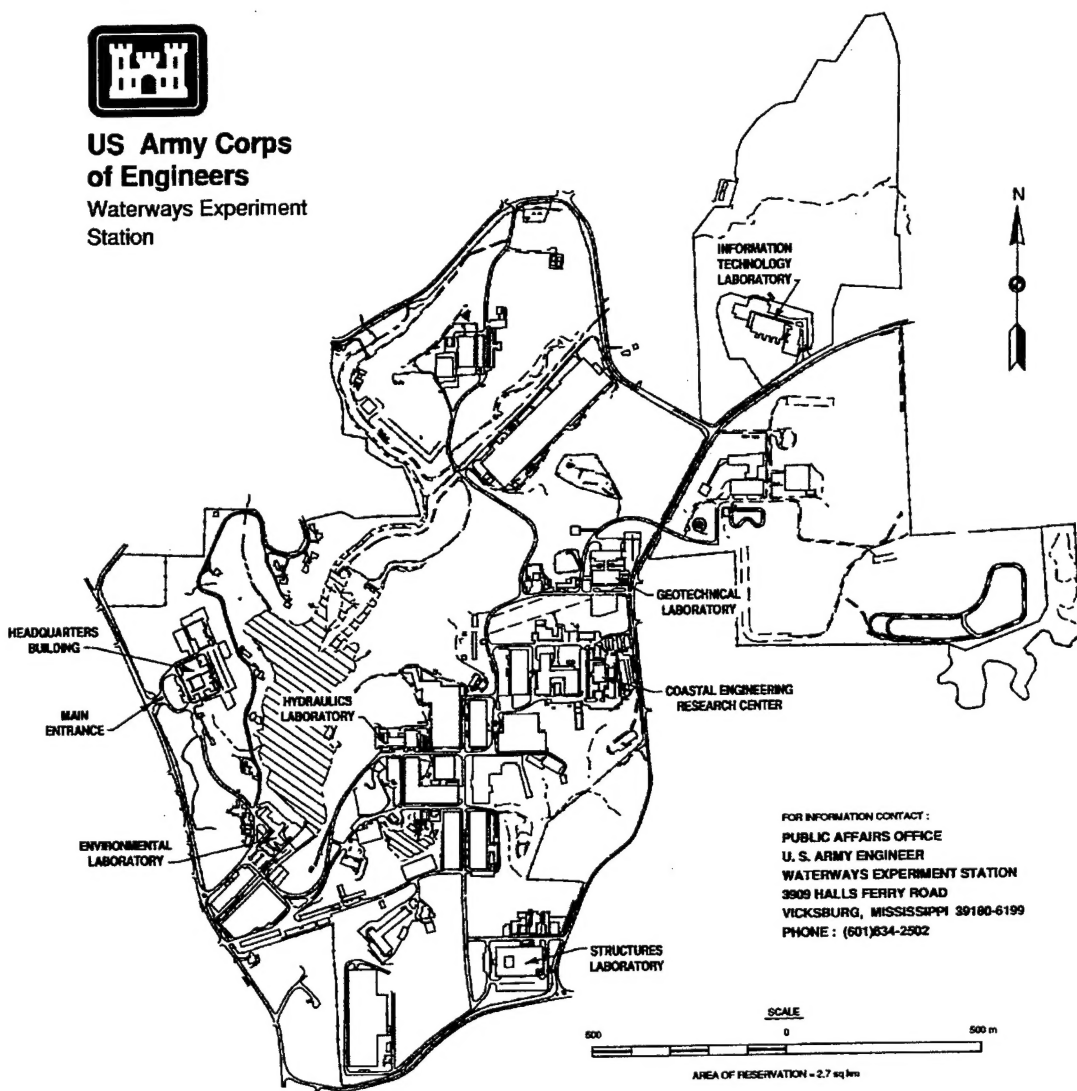3909 Halls Ferry Road
Vicksburg, MS   39180-6199

| Accesion For | | |
|---|---|---|
| NTIS   CRA&I | | ☑ |
| DTIC   TAB | | ☐ |
| Unannounced | | ☐ |
| Justification | | |
| By | | |
| Distribution / | | |
| Availability Codes | | |
| Dist | Avail and / or Special | |
| A-1 | | |

Final report

Approved for public release; distribution is unlimited

Prepared for   U.S. Army Engineer District, San Francisco
211 Main Street, San Francisco, CA   94105-1905

**US Army Corps
of Engineers**
Waterways Experiment
Station



INFORMATION
TECHNOLOGY
LABORATORY

GEOTECHNICAL
LABORATORY

HEADQUARTERS
BUILDING

COASTAL ENGINEERING
RESEARCH CENTER

MAIN
ENTRANCE

HYDRAULICS
LABORATORY

ENVIRONMENTAL
LABORATORY

STRUCTURES
LABORATORY

SCALE

500            0            500 m

AREA OF RESERVATION = 2.7 sq km

# Contents

# List of Figures

## List of Tables

# Preface

The model investigation of Noyo Cove, California, reported herein was requested by the U.S. Army Engineer District, San Francisco (SPN) and conducted at the Coastal Engineering Research Center (CERC) of the U.S. Army Engineer Waterways Experiment Station (WES). Authorization for WES to perform the study was granted in SPN Intra-Army Orders E86933014 dated 8 June 1992 and E86923021 dated 22 January 1993.

Two-dimensional model tests were conducted at WES during the period August 1992 through March 1993 and three-dimensional (3-D) model tests were conducted intermittently from May 1993 through August 1994 by personnel of the Wave Research Branch (WRB) of the Wave Dynamics Division (WDD), CERC, under the direction of Dr. James R. Houston and Mr. Charles C. Calhoun, Jr., Director and Assistant Director of CERC, respectively; and the direct guidance of Messrs. C. E. Chatham, Jr., Chief of WDD; and Mr. D. D. Davidson, Chief of WRB. Tests were conducted by Messrs. Leland L. Hennington, Civil Engineer; Raymond Reed, Civil Engineering Technician; C. Ray Herrington, Civil Engineering Technician; Johnny Heggins, Civil Engineering Technician; David Daily, Instrumentation Services Technician; and Ernest R. Smith, Research Hydraulic Engineer. A supplemental study on structural analysis of concrete armor units is described in Appendix A (Concrete Armor Unit Structural Investigation for the Offshore Noyo, CA, Breakwater) and written by Messrs. Jeff A. Melby and George F. Turk. This report was prepared by Messrs. Smith and Hennington.

Liaison was maintained with SPN through monthly progress reports and telephone conversations during the course of the investigation. Mr. Jeff Cole was SPN's primary point of contact (POC) during two-dimensional (2-D) testing of the breakwater. Prior to construction of the 2-D breakwater cross section, Messrs. Cole and Joe Hooks, SPN; and Michael Deneche and Louis Sanchez, Sogreah Engineering, France, visited WES and demonstrated proper Accropode placement techniques and observed 2-D stability model tests. Mr. Sanchez visited WES prior to construction of the 3-D breakwater to demonstrate proper placement of Accropodes on breakwater heads.

Mr. Tom Bonigut was SPN's POC during the 3-D testing of the breakwater. During 3-D testing of the Noyo breakwater, a meeting was held at SPN to discuss future plans for model testing. Attending the meeting were

Messrs. Bonigut, Hooks, Tom Kendall, Herb Cheong, Ken Harrington, Bill Angeloni, Rod Chisolm, and Gary Ohea, SPN, and Mr. Smith, WES.

At the time of publication of this report, Director of WES was Dr. Robert W. Whalin. Commander of WES was COL Bruce K. Howard, EN.

# Conversion Factors, SI to Non-SI Units of Measurement

SI units of measurement used in this report can be converted to Non-SI units as follows:

| Multiply | By | To Obtain |
|---|---|---|
| centimeters | 0.3937 | inches |
| cubic meters | 35.3198 | cubic feet |
| cubic meters | 2.6489 | tons (U.S.)[1] |
| grams | 0.00220 | pounds |
| kilograms | 2.20462 | pounds |
| kilograms | 0.00110 | tons |
| kilometers | 0.62137 | miles (U.S. statute) |
| megapascal | 20,885.4 | pounds per square foot |
| meters | 3.281 | feet |
| tonnes | 2204.6 | pounds |

[1] For specific weight of concrete of 150 pounds per cubic foot.

# 1 Introduction

## The Prototype

Noyo River and Harbor are located on the California coast at Fort Bragg, approximately 217 km[1] north of San Francisco and 140 km south of Eureka (Figure 1). The shoreline of the area consists of broken irregular cliffs about 12 to 24 m high with numerous rocks extending several hundred meters off-shore. Small pocket beaches front heads of coves in the immediate vicinity. The Noyo River empties into Noyo Cove, which is approximately 550 m wide, north to south, and 610 m long, east to west.

The existing Noyo River and Harbor project was authorized by the River and Harbor Act of 1930 (U.S. Army Engineer District, San Francisco 1979), and construction was completed in 1961. It consists of a jettied entrance at the river mouth; a 3-m-deep, 30.5-m-wide entrance channel; and a 3-m-deep, 45.7-m-wide river channel extending upstream about 1 km. Noyo Mooring Basin is located on the south bank of the river at the upstream limit of the dredged river channel. Dolphin Isle Marina, a privately owned harbor, is located approximately 1.8 km from the river mouth on the south bank. An aerial photograph of the area is shown in Figure 2.

## The Problem

Noyo Cove is open to the Pacific Ocean and is exposed to high waves generated by seas and swell. Waves in excess of 6 m approach the cove covering directions from the southwest to the northwest. The entrance is impassable if heavy seas sweep across the cove and through the jettied river entrance. The harbor has also experienced strong surging problems due to long-period wave energy, which has damaged small moored craft. Shoaling has occurred in the river channel by deposition of material from the river during the winter rainy season, which causes navigational difficulties in the

---

[1] A table of factors for converting SI units of measurement to non-SI units is presented on page x.
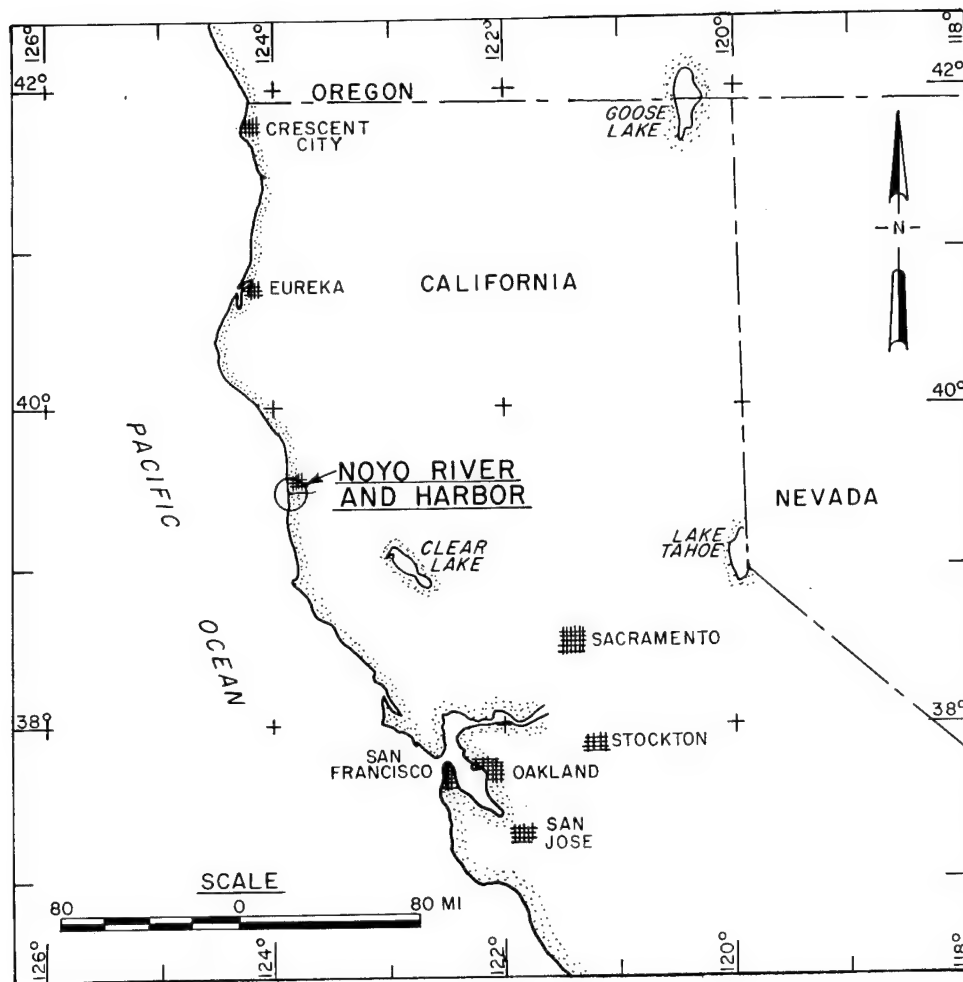
Figure 1.  Location of Noyo Harbor

Figure 2.  Aerial view of Noyo Harbor

shallow river channel. Vessels have been grounded and navigation delayed until favorable tide conditions were present to provide passable depths.

Improvements at Noyo River and Harbor would result in the reduction of boat and harbor damages, increased commercial fish catch, reduction in navigation delays and gear losses, and a reduction in operation and maintenance costs for the existing channel entrance jetties. The proposed breakwater would facilitate safe navigation in the entrance channel, and provide improved protection and shelter without becoming a navigation hazard itself. Project construction would employ local (currently unemployed) labor and enhance area redevelopment. The improvements should also enhance the overall commercial fishing operation, thereby contributing to the local economic base.

## Previous Reported Model Tests

A three-dimensional model of Noyo Harbor was constructed to investigate short- and long-period waves and river flows for a proposed breakwater. A two-dimensional study was also conducted at a 1:31 model scale to determine wave transmission for the proposed breakwater and the results were used to design the 1:75 scale cross section for the three-dimensional tests (Bottin, Acuff, and Markle 1988). Waves generated in the model were as high as 9.8 m, prototype. The optimum protective breakwater developed and reported by Bottin, Acuff, and Markle was a 194-m-long curved dolos breakwater located near the river entrance. However, it was determined that river entrance protection benefits would decrease for storm conditions above a certain threshold because those conditions are too extreme for fishing vessels.

It was later determined that most benefits would be derived for 4.3-m wave heights or less. Additional tests were conducted on the model by Bottin and Mize (1989) for waves 4.3 m and lower. Bottin and Mize found several combinations of breakwaters that would meet the established wave height criteria of 1.8 m or less in the river entrance channel.

## Purpose of Study

Local interests expressed interest in construction of an outer breakwater that would provide navigational protection from the extreme wave conditions at Noyo Cove. At the request of the U.S. Army Engineer District, San Francisco (SPN), two- and three-dimensional wave tests were conducted at the U.S. Army Engineer Waterways Experiment Station (WES) Coastal Engineering Research Center to determine the optimum breakwater cross section and head in terms of stability. Additionally, tests were conducted to determine the proper cross section to be used in the 1:75 Noyo Harbor model, reported separately by Bottin (1994), in terms of wave transmission. The proposed breakwater consisted of Accropode armor units, which are patented by Sogreah, France, and described by Chida, Kaihatsu, and Kobayashi (1992).

Two-dimensional stability tests were also conducted with dolos armor units. Core-Locs, a new armor unit design discussed by Melby and Turk (1994), were used in addition to Accropodes in the three-dimensional stability tests. An important consideration of concrete armor units is the structural integrity of the individual units. Therefore, a structural analysis was performed to compare the structural response of the Accropode, Core-Loc, and dolos armor units.

This report describes the design, facilities used, and results of the two-dimensional stability tests (Chapter 2), three-dimensional stability tests (Chapter 3), and two-dimensional transmission tests (Chapter 4). Conclusions are listed in Chapter 5. Appendix A contains results of the structural stability analysis; Appendices B and C contain photographs of the two- and three-dimensional stability tests, respectively; and Appendix D includes symbol notation used in the report.

# 2 Two-Dimensional Stability Tests

## The Model

### Design of model

Two-dimensional stability tests were conducted at a geometrically undistorted linear scale of 1:43.3, model to prototype. Scale was based on size availability of model Accropodes and dolosse and the capabilities of the available wave generator to produce required wave heights at modeled water depths. Time relations were scaled according to Froude Model Law (Stevens et al. 1942). Model-to-prototype relations were derived in terms of length $l$ and time $t$ shown in Table 1. The model units used in two-dimensional stability tests are shown in Figure 3.

| Table 1<br>Model-Prototype Scale Relations (1:43.3 scale) | | |
|---|---|---|
| Characteristic | Dimension | Scale Relations<br>Model:Prototype |
| Length | $l$ | $l_r =$ 1:43.3 |
| Area | $l^2$ | $a_r =$ 1:1875 |
| Volume | $l^3$ | $v_r =$ 1:81,183 |
| Time | $l^{1/2}$ | $t_r =$ 1:6.6 |

The specific weight of water used in the model was 62.4 pcf with that of the prototype being 64.0 pcf. The specific weights of the model material used for construction differed for the prototype; therefore, the Hudson (1975) transference equation was used to determine model material weights:

$$\frac{(W_a)_m}{(W_a)_p} = \frac{(\gamma_a)_m}{(\gamma_a)_p} \left(\frac{l_m}{l_p}\right)^3 \left[\frac{(S_a)_p - 1}{(S_a)_m - 1}\right]^3 \tag{1}$$
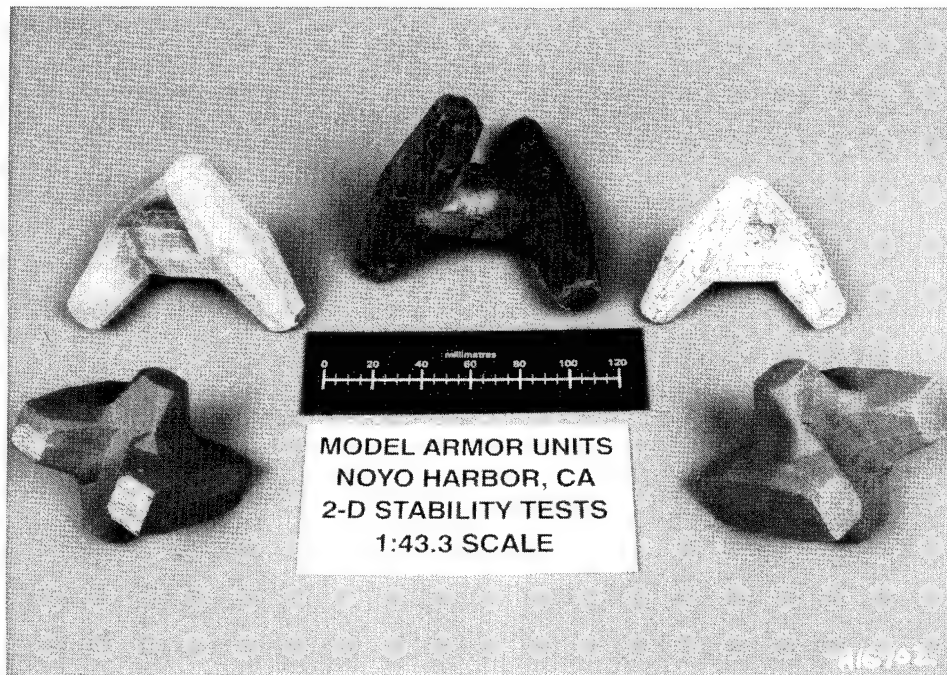
Figure 3. Model armor units used in two-dimensional stability tests, prototype weights from left; 7.6-m³ Accropode, 5.9-m³ dolos, 7.9-m³ dolos, 3.8-m³ dolos, and 9.1-m³ Accropode

where

$m$ = model quantities

$p$ = prototype quantities

$W_a$ = weight of individual armor or stone

$\gamma_a$ = specific weight of an individual armor unit or stone

$l_m/l_p$ = linear scale of the model

$S_a$ = specific gravity of an individual armor unit or stone relative to the water in which it is placed

$S_a$ = $\gamma_a/\gamma_w$, and $\gamma_w$ is the specific weight of water

A consideration of all rubble-mound physical models is the scale effect of viscous forces associated with flow through the underlayers and core of the structure. To reproduce prototype conditions, the model must consist of materials of a sufficient size to ensure turbulent flow through the structure. The method of Keulegan (1973) was used to check, and modify if necessary, the core $W_3$ and underlayer $W_2$ model material sizes for viscous effects. The geometrically scaled underlayer size was found to be satisfactory, but the core size was increased for all plans to account for scale effects. Prototype and model armor layer $W_1$, underlayer $W_2$, core $W_3$, and toe berm $W_4$ material sizes are listed in Table 2.

**Table 2**
**Prototype and Model Material Sizes**

| | Plan 1 | Plan 2 | Plan 3 | Plan 4 | Plan 5 |
|---|---|---|---|---|---|
| **Prototype** | | | | | |
| Armor Type | Accropode | Accropode | Dolos | Dolos | Dolos |
| $W_1$ m³ | 9.1 | 7.6 | 3.8 | 7.9 | 5.9 |
| $W_2$ kg | 1,500 to 3,000 | 1,500 to 3,000 | 453 to 1,814 | 957 to 3,828 | 957 to 3,828 |
| $W_3$ kg | 1 to 500 | 1 to 500 | 1 to 45 | 3 to 96 | 3 to 96 |
| $W_4$ kg | 50 to 500 | 50 to 500 | 227 | 227 | 227 |
| **Model** | | | | | |
| Armor Type | Accropode | Accropode | Dolos | Dolos | Dolos |
| $W_1$ kg | 0.260 | 0.213 | 0.125 | 0.267 | 0.200 |
| $W_2$ kg | 0.018 to 0.029 | 0.018 to 0.029 | 0.011 to 0.018 | 0.018 to 0.029 | 0.018 to 0.029 |
| $W_3$ kg | 0.018 to 0.029 | 0.018 to 0.029 | 0.011 to 0.018 | 0.018 to 0.029 | 0.018 to 0.029 |
| $W_4$ kg | 0.002 to 0.005 | 0.002 to 0.005 | 0.011 to 0.018 | 0.011 to 0.018 | 0.011 to 0.018 |

## Test facilities and equipment

Tests were conducted in a 47.2-m-long, 0.6-m-wide, 1.8-m-deep wave tank. Figure 4 shows tank dimensions, bottom slopes, gage placement, and structure location for stability tests. A concrete-capped, compound slope was installed to represent local bathymetry seaward of the breakwater location. A 1V:20H slope originated at a prototype depth of 20.4 m mean lower low water (mllw), terminated, and was horizontal at the 9.1-m mllw depth. The breakwater cross section was placed on the horizontal section 61 m (prototype distance) from the slope transition.

Waves were generated by a hinge-actuated electronically controlled hydraulic system. Displacement of the wave board was controlled by a command signal transmitted to the wave board by a Digital Equipment Corporation (DEC) MicroVax II computer. Waves were produced by the
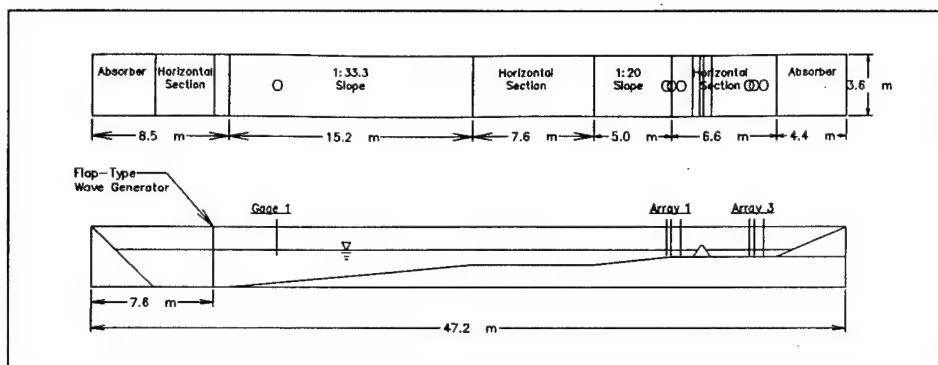
Figure 4. Wave tank used in two-dimensional tests

periodic displacement of the wave board. Random wave command signals to drive the wave board were generated to simulate a Texel Marsen Arsloe (TMA) shallow-water spectrum (Hughes 1984) for the design wave periods. Regular waves were generated by command signals produced by a synthesized function generator.

Water surface elevations were recorded by single wire capacitance-type gages, sampled at 20 Hz. Ten gages were used during calibration of the facility, but only seven were used during stability tests. Gage 1 was placed near the wave board to obtain offshore wave heights, and the remaining gages were placed in arrays of three gages each, which permitted calculation of incident and reflected wave heights by the method of Goda and Suzuki (1976). Array 1 was positioned approximately 105.5 m prototype seaward of the breakwater toe location, Array 2 was placed at the location of the breakwater toe, and Array 3 was placed approximately 105.5 m prototype shoreward of the structure. Array 2 was used only during calibration of the facility, and was removed prior to construction of the initial breakwater cross section. Wave data obtained from Arrays 1 and 3 during tests provided incident and transmitted wave data, respectively, and were stored on a MicroVax II mini-computer and analyzed using the Time Series Analysis computer program (Long and Ward 1987), which can execute several analysis operations. The operations used for two-dimensional stability tests were mean downcrossing analysis to obtain significant, maximum, and average wave heights, significant and average wave periods, and mean water levels at each gage; single channel frequency domain analysis to acquire peak period $T_p$, zero-moment wave height $H_{mo}$, and spectral density plots for each gage; and unidirectional spectral density incident/reflection analysis to determine the incident and reflected parameters at each array.

Prior to conducting tests, the facility was calibrated without the breakwater in place for design wave periods at +2.13 m mllw. Figures 5, 6, and 7 show prototype wave height versus percent of maximum generator stroke for random waves having peak periods of 13, 17, and 20 sec, respectively. The maximum

Figure 5. Wave height versus generator stroke, 13-sec random waves



Figure 6. Wave height versus generator stroke, 17-sec random waves
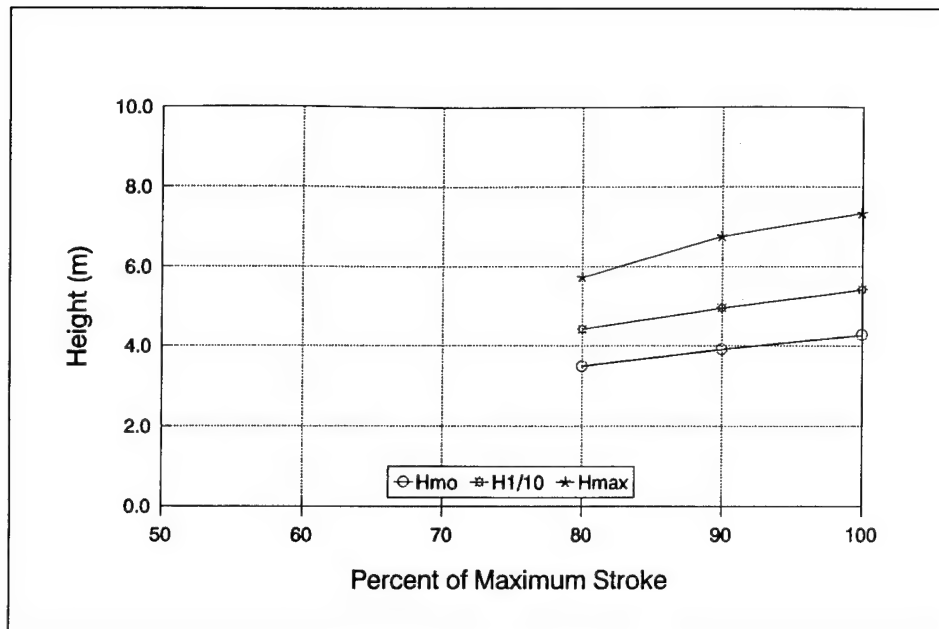
Figure 7. Wave height versus generator stroke, 20-sec random waves

$H_{mo}$ produced at +2.13-m mllw for the slope installed was 5.8 m prototype with a 13-sec period. As generator stroke increased, the higher waves in the spectrum became depth limited and broke. It was desired to subject the breakwater to higher $H_{mo}$ values than could be obtained using random waves. The maximum wave heights $H_{max}$ produced were 8.5 m for the 13- and 17-sec periods, and 7.3 m for the 20-sec period. Therefore, it was expected that $H_{mo}$ values of the magnitude of the $H_{max}$ values could be expected if regular waves were generated at periods $T$ of 13, 17, and 20 sec. Zero-moment wave height is plotted for regular waves versus generator stroke for waves at Array 1 $(H_{mo})_o$ and Array 2 $(H_{mo})_d$ in Figures 8 through 10. The figures show that the off-shore wave height and the wave height at the structure are nearly identical for lower waves, but deviate as offshore height increases and waves approach depth-limited conditions and begin to decay in height. Although Figures 8 and 9 show maximum $(H_{mo})_d$ as 7.6 and 7 m, respectively, it was later found that a height of 8.2 m could be produced at 70 percent of stroke for 13-sec periods, and a 7.6-m wave could be generated with an 83 percent stroke with a 17-sec period. Figure 10 shows no decrease in wave height over the range of stroke, and the maximum wave height was approximately 7.6 m at maximum stroke. The figure indicates that the 20-sec waves were limited by generator stroke and not a depth-limited condition. Breakwater stability tests were con-ducted for the design still-water level (swl) and wave heights listed in Table 3.
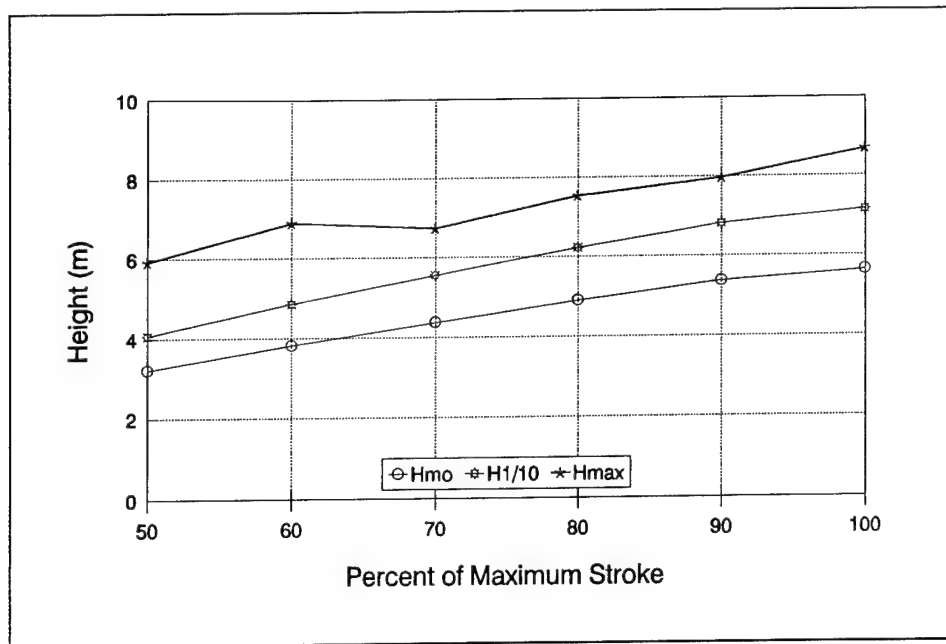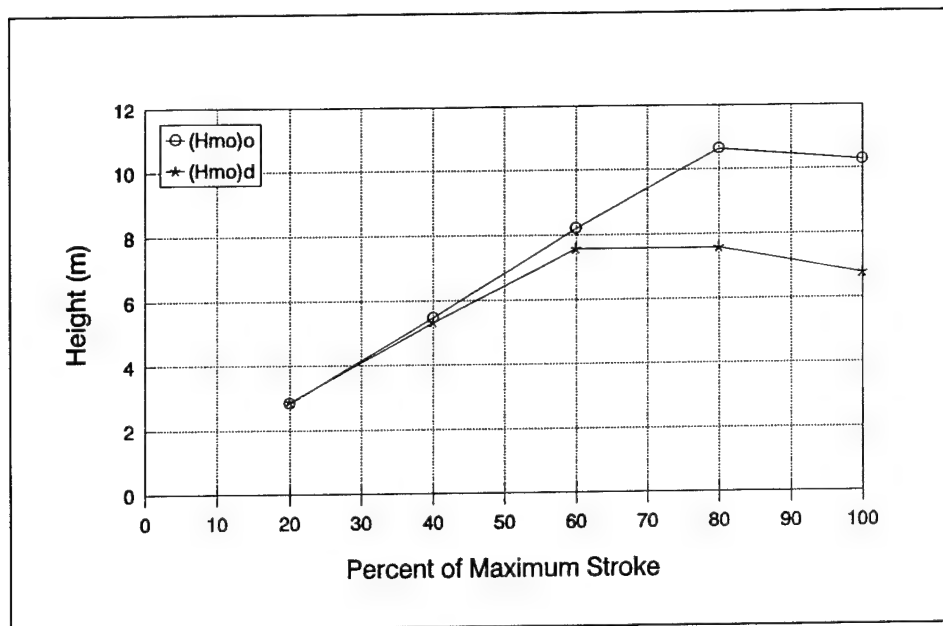
Figure 8.  Wave height versus generator stroke, 13-sec regular waves



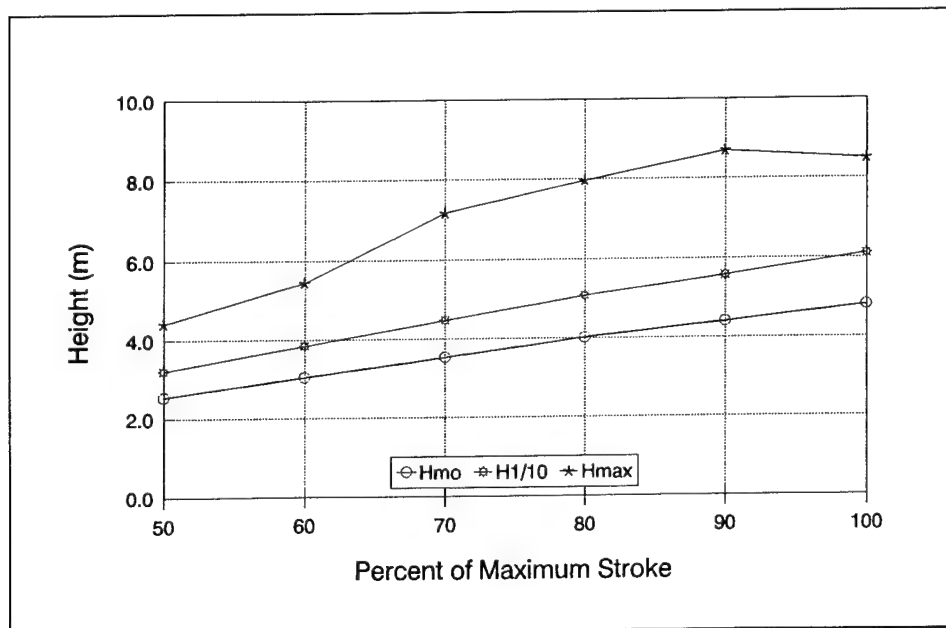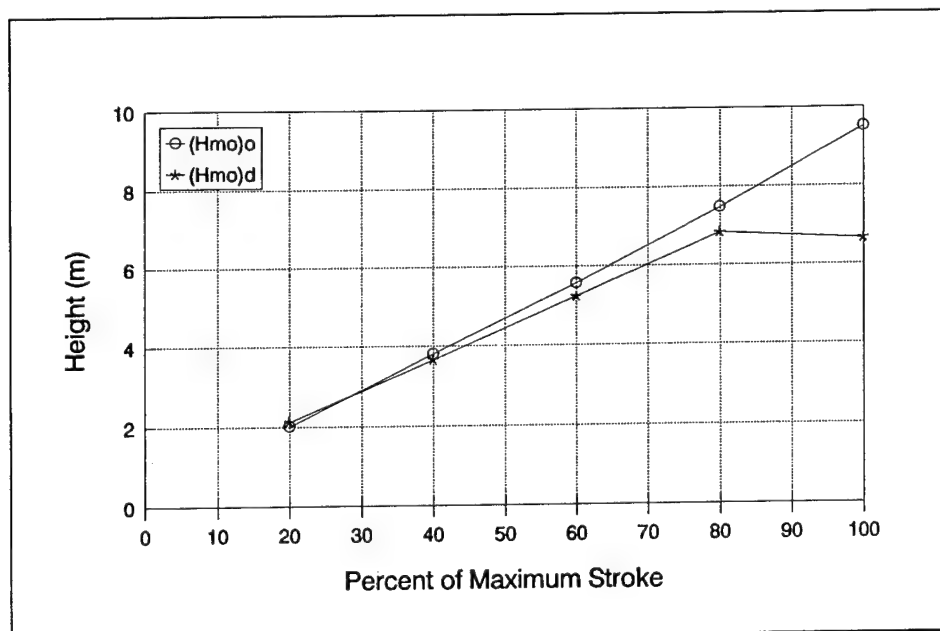Figure 9.  Wave height versus generator stroke, 17-sec regular waves
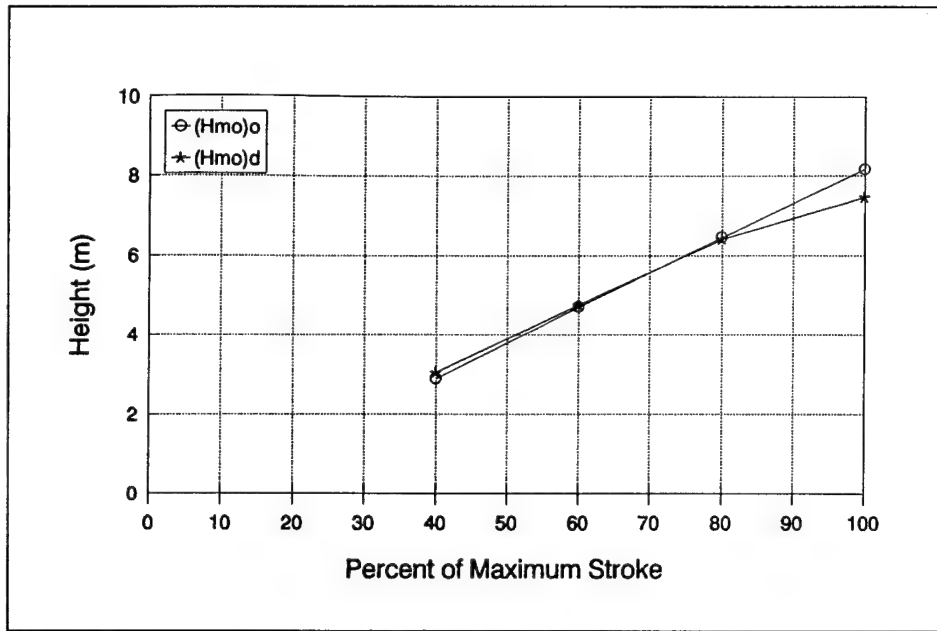
Figure 10. Wave height versus generator stroke, 20-sec regular waves

**Table 3**
**Stability Test Wave Conditions**

| Wave Type | SWL m, mllw | T sec | $H_{mo}$ m | $H_{max}$ m | Cycles | Test Duration model min |
|---|---|---|---|---|---|---|
| Random | +2.13 | 13 | 4.6 | 7.3 | 1 | 15 |
| Random | +2.13 | 17 | 4.6 | 8.5 | 1 | 15 |
| Random | +2.13 | 20 | 4.3 | 7.3 | 1 | 15 |
| Random | +2.13 | 13 | 5.5 | 8.5 | 1 | 15 |
| Random | +2.13 | 17 | 4.9 | 8.2 | 1 | 15 |
| Random | +2.13 | 20 | 4.3 | 7.3 | 1 | 15 |
| Regular | +2.13 | 13 | 6.4 | 6.4 | 5 | 15 |
| Regular | +2.13 | 17 | 6.4 | 6.4 | 5 | 15 |
| Regular | +2.13 | 20 | 6.4 | 6.4 | 5 | 15 |
| Regular | +2.13 | 13 | 7.0 | 7.0 | 5 | 15 |
| Regular | +2.13 | 17 | 7.0 | 7.0 | 5 | 15 |
| Regular | +2.13 | 20 | 7.0 | 7.0 | 5 | 15 |
| Regular | +2.13 | 13 | 7.6 | 7.6 | 5 | 15 |
| Regular | +2.13 | 17 | 7.6 | 7.6 | 5 | 15 |
| Regular | +2.13 | 20 | 7.6 | 7.6 | 5 | 15 |
| Regular | +2.13 | 13 | 8.2 | 8.2 | 5 | 15 |

## Test procedures

Photographs were taken prior to stability tests. The tank was flooded to the appropriate depth and the structure was exposed to one cycle of low-level waves listed in Table 3. These initial waves allowed settling and nesting of the newly constructed section which would occur under typical daily wave conditions prior to being exposed to a design-level storm. The low-level waves also provided transmission data for non-overtopping conditions. After the structure was exposed to low-level waves, the wave conditions listed in Table 3 were generated. Prototype duration for each wave height was 99 min (900 sec model). Test durations were completed with one cycle of random waves for 900 sec, and five cycles of regular waves in bursts of 180 sec each. The procedure of testing in bursts for regular waves prevented contamination of incident waves by waves re-reflected from the wave generator. Wave heights and period varied for the random wave tests; therefore, a longer record was required for the series to obtain a statistically strong confidence interval for calculating the wave spectrum. Reflection and re-reflection between the structure and the wave board could not be avoided in the random wave tests. Upon completion of a cycle, sufficient time was provided for the water surface to settle before the next cycle began.

The response of the structure to each cycle of test waves was recorded. Detailed model observation included movement of units on the structure and a general statement of the structural condition. At the conclusion of the design conditions, the tank was drained and the condition of the structure was summarized in notes and documented with photographs. Before and after test photographs are shown in Appendix B. After documentation of the initial tests was completed, the armor units were removed, and the underlayer stone was straightened as needed. The armor units were replaced and the test was repeated. The purpose of the repeat test was to determine the presence of any uncontrolled variations in model construction technique that might affect stability of the structure.

## Model construction

Construction of the modeled section simulated prototype construction as closely as possible. The core, bedding, and underlayer of material were dumped by bucket or shovel, smoothed to grade, and compacted with hand trowels to simulate consolidation that would have occurred due to wave action. The armor layer was then placed on the structure.

**Accropode placement.** The design of Plan 1, 9-m$^3$ (24-ton) Accropodes, was furnished by Sogreah, France. Accropode breakwaters consist of one layer of armor placed on a 3V:4H slope. Representatives of Sogreah visited WES prior to initiation of the Accropode stability tests. The representatives demonstrated the proper placement of the Accropode cross sections, and assisted with construction of the initial plan. Accropodes are placed according

to a "mesh," which is a function of armor unit size, specifically, the length of the Accropode anvil. The special Accropode placement was used for initial and repeat tests of both 9-m³ and 7.6-m³ (20-ton) Accropode cross sections.

**Dolos placement.** Breakwaters constructed of dolosse are placed in two layers at a 1V:2H slope. The units were placed by hand in a random manner below mllw. Random placement consists of placing the unit in contact with adjacent units on the structure, with no attempt to orient the axes of the dolos or key the unit to the structure. Dolos placed above mllw were placed in contact with adjacent units and keyed in fashion that would be similar to prototype construction.

### Reporting model observations

Visual inspections of the structure were made during and after testing and recorded on log sheets. Two objectives for all tests were to note overtopping and instability in tested armor units. The stability of the test sections could be calculated from the test results by:

$$K_d = \frac{\gamma_a H_d^3}{W_a (S_a - 1)^3 \cot\theta} \qquad (2)$$

in which $K_d$ is the stability coefficient, $H_d$ is the highest wave height at the structure that causes no damage, i.e., wave height at which damage is less than or equal to 2 percent, and $\theta$ is the angle of the structure slope measured from horizontal in degrees. In the present study, the zero moment wave height $H_{mo}$ was used to calculate stability coefficients for both random and regular waves.

## Results

Stability tests were conducted for five breakwater cross sections at a model scale of 1:43.3. Accropodes were used as the primary armor unit for Plans 1 and 2, and dolosse were used in Plans 3, 4, and 5. Each plan was subjected to the series of wave conditions listed in Table 3. The structure was rebuilt following each initial series of wave conditions and stability tests were repeated, with the exception of Plans 4 and 5. The purpose of repeating the tests was to ensure consistency in building the breakwater and to verify results. Repeat tests of Plans 1 through 3 indicated construction of the cross section was consistent with the original building. Repeat tests of Plans 4 and 5 were omitted because repeat tests showed duplicate stability results and it was desired to determine the optimal dolos cross section under time restrictions.

Wave data were collected seaward and shoreward of the structure during stability tests for each plan. Transmission data obtained from the 1:43.3 scale were used to develop a cross section having the same transmission characteristics at a 1:75 scale, which is discussed in Chapter 4. The 1:75 scale

cross section was used in the three-dimensional harbor study of Noyo Cove (Bottin 1994).

Qualitative results were taken for overtopping. The wave period and height and category of overtopping were noted for each run. If overtopping occurred, it was characterized as minor, moderate, or major.

## Plan 1

Plan 1 (Figure 11, Photos B1 through B3), proposed by SPN and Sogreah, consisted of one layer of 9-m$^3$ Accropode armor units placed on a 3V:4H slope. The underlayer consisted of stone ranging from 1,500 to 3,000 kg, core material ranged from 1 to 5,000 kg, and the toe berm was constructed of 50- to 500-kg stone.
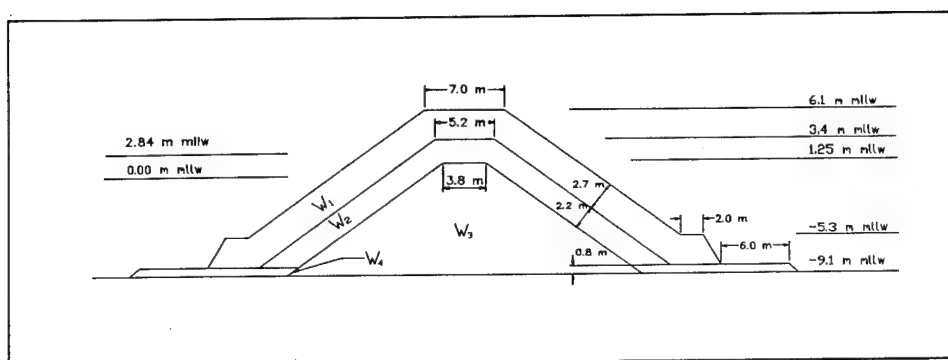


Figure 11. Plan 1, two-dimensional stability tests

The structure was stable for original and repeat tests for the design wave conditions at +2.13 m mllw. Plan 1 suffered no damage for the test conditions with no units displaced or rocking (Photos B4 through B6). A stability coefficient of 19.0 was calculated for Plan 1, using Equation 2 with the maximum $H_{mo}$ of 8.2 m. The structure did not reach a damaged condition and based on observations of the tests, a higher $K_d$ would have been attained if waves were not limited by depth. Although the armor layer was not damaged, the toe berm material fronting the cross section was displaced.

## Plan 2

Results from Plan 1 showed the 9-m$^3$ Accropode units were stable and a less conservative (lighter) armor unit would also be stable. Although the 9-m$^3$ unit was recommended by Sogreah as the appropriate armor size for the design wave conditions, a lighter Accropode was placed on the structure for testing. Plan 2 consisted of the same geometry and underlayer, core, and toe berm material sizes used in Plan 1, but 7.6-m$^3$ Accropodes were used as armor layer (Figure 12, Photos B7 through B9).
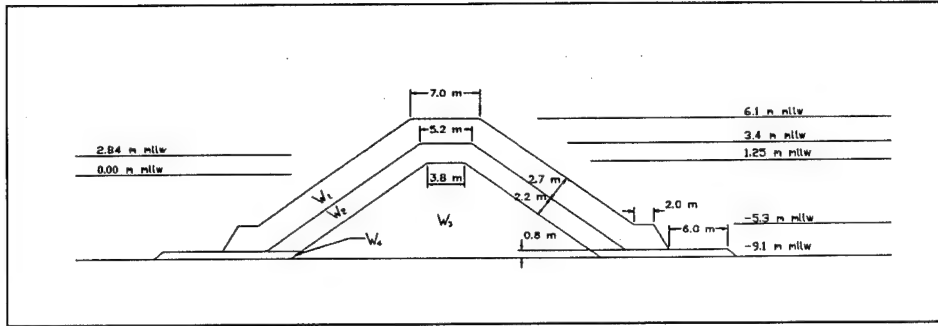
Figure 12. Plan 2, two-dimensional stability tests

The structure was tested for the design wave conditions at +2.13-m mllw
and repeated once. Plan 2 was not damaged for the test conditions with no
displaced armor units (Photos B10 through B12); however, four units were
observed to rock in place during original and repeat tests. The stability
coefficient calculated for Plan 2 was 23.1. The toe berm size was identical to
the size used in Plan 1 and was also damaged.

## Plan 3

Stability tests were conducted for a dolos armor section as an alternative
armor type to Accropodes. An economic analysis conducted by SPN indicated
that a breakwater constructed of 9-m$^3$ Accropodes was feasible to
construct. It was felt that the prototype dolos cross section to be modeled
would need to be equal in cost to the Accropode cross section to be considered
as an option for construction. Dolos size selection was based on the amount
of concrete required to place 9-m$^3$ Accropodes on the proposed breakwater.
Unlike Accropodes, which are placed in one layer on a 3V:4H slope, dolos are
placed in two layers on a 1V:2H slope. A 3.8-m$^3$ (10-ton) dolos cross section
was calculated to have approximately the same volume of concrete as the 9-m$^3$
Accropode section. Many factors are included in an economic analysis;
therefore, the basis of equated concrete volume was not complete but gave a
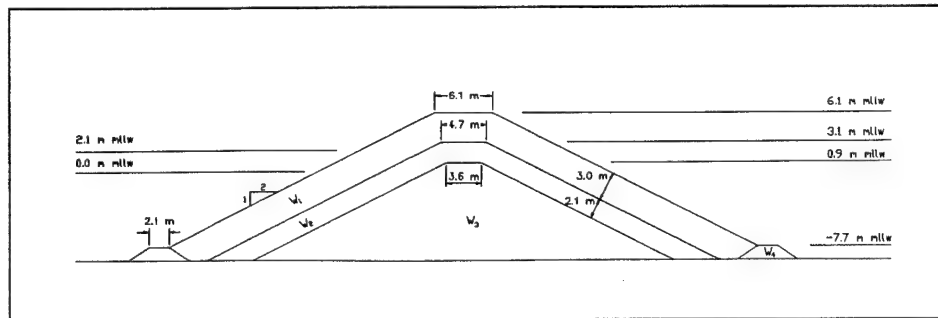relative estimate for comparison. Plan 3, shown in Figure 13 and Photos B13



Figure 13. Plan 3, two-dimensional stability tests

through B15, was designed using the method recommended by the *Shore Protection Manual* (1984), and consisted of 453.6- to 1,814.4-kg underlayer stone and 1.4- to 45.4-kg core stone. The toe berm stone was constructed of 907.2-kg stone.

After the structure was subjected to the conditions in Table 3, 1.6 percent of the units were displaced on the sea side (Photos B16 and B17). The structure did not reach a damaged condition and a $K_d$ of 29.8 was calculated. However, eight units were observed to rock in place during original tests and ten units rocked in place during repeat tests. This movement of units indicates that units would break on the prototype structure, which could result in failure of the structure. Quantitative and qualitative results indicated that Plan 3 was moderately stable for the design wave conditions conducted at +2.13 m mllw. No stone was displaced from the toe berm.

## Plan 4

Results from Plan 3 indicated that a heavier dolos unit was required for a stable cross section. Plan 4 (Figure 14) was constructed of 7.9- and 5.9-m$^3$ (21- and 15.6-ton) dolos placed on the structure to increase stability. The armor layer was constructed of two sizes because the quantity of model 7.9-m$^3$ dolosse available was limited. The 7.9-m$^3$ dolosse were placed on the breakwater sea side, crown, and lee side from the crown to +2.13 m mllw. The 5.9-m$^3$ dolos were placed on the lee side from the toe to +2.13 m mllw. The underlayer was constructed of 957- to 3828-kg stone; core stone ranged from 3.2 to 95.7 kg, and the toe berm consisted of 907-kg stone.

Plan 4 was not damaged by the design wave conditions conducted at +2.13 m mllw (Photos B18 through B20), and a $K_d$ of 14.4 was calculated for the sea-side cross section. Slight rocking of units was observed for wave heights equal to and greater than 6.4 m. Observations during tests indicated that higher waves would not damage the structure and that Plan 4 appeared to be a conservative design. The toe berm was stable with no stone displaced.
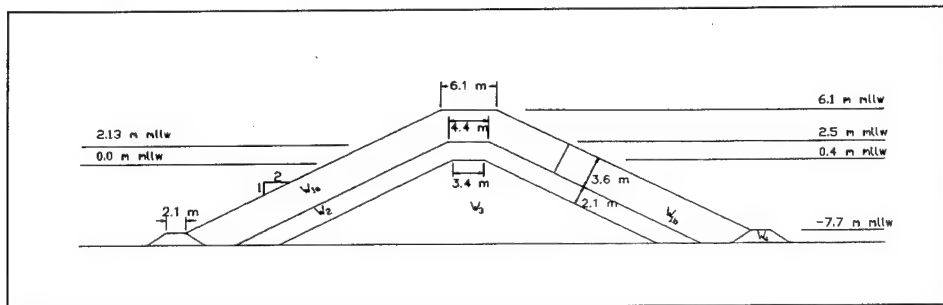


Figure 14. Plan 4, two-dimensional stability tests

## Plan 5

Results from Plans 3 and 4 indicated the optimal dolos size for stability was heavier than 3.8 m³ and lighter than 7.9 m³. Plan 5 (Figure 15, Photos B21 through B23) consisted of 5.9-m³ dolos on the armor layer. The underlayer, core, and toe berm stone sizes remained the same as Plan 4.
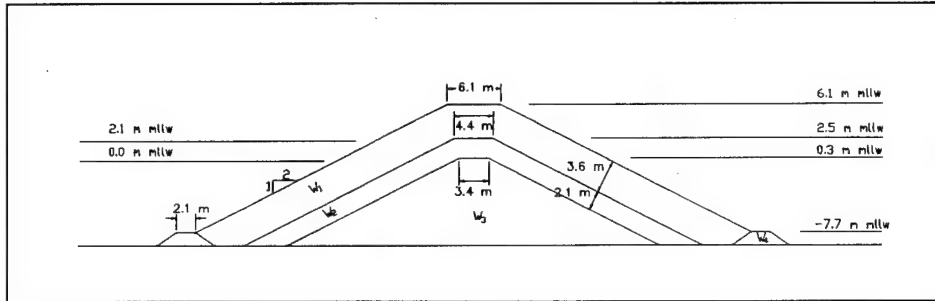


Figure 15. Plan 5, two-dimensional stability tests

No units were displaced from the 5.9-m³ cross section and a $K_d$ of 19.5 was calculated, but five units were observed to rock in place during wave action. Plan 5 was stable and less units were observed to rock in place than with Plan 3. However, the increase in stability between the 3.8-m³ and 5.9-m³ dolos was not significant. The 907.2-kg toe berm was stable.

## Overtopping

The plans tested had two geometric shapes. The Accropode sections, Plans 1 and 2, were constructed on a 3V:4H slope at a crown elevation of +6.1 m mllw and a crown width of 6.4 m. Minor overtopping occurred for these sections with random wave heights $H_{mo} \leq 4.6$ m. Overtopping increased for higher waves, and was moderate for 7-m regular waves. The waves approached depth-limited breaking at this height and overtopping did not increase significantly for 7.6- and 8.2-m wave heights.

Plans 3, 4, and 5 were constructed of two layers of dolosse on a 1V:2H slope at a +6.1-m mllw crown elevation and a 6.1-m width. No overtopping was observed for waves up to 6.4 m. Overtopping was minor to moderate for 17-sec, 7-m waves and higher. Although the Accropode and dolos sections were of the same elevation and approximate width, the flatter slope and two layers of dolosse allowed more energy to dissipate, and less overtopping was observed for Plans 3 through 5.

# Summary of Two-Dimensional Stability Tests

Two-dimensional stability tests are summarized is shown in Table 4. None of the cross sections tested failed under the design wave conditions. Wave heights for the water levels tested were limited by depth for 13- and 17-sec periods. The maximum $H_{mo}$ achieved using regular waves was 8.2 m, and the maximum $H_{mo}$ generated at the structure for random waves was 5.8 m. Stability tests showed no units were displaced for the 9-m$^3$ Accropode and 7.9-m$^3$ dolos sections, Plans 1 and 4, respectively. The cross sections were considered conservatively designed. No units were displaced for the 7.6-m$^3$ Accropode section (Plan 2); however, four units rocked in place at the crown when subjected to 20-sec, 7.6-m waves. The 3.8-m$^3$ and 5.9-m$^3$ dolos sections, Plans 3 and 5, respectively, were found to be marginally stable. No significant increase in stability was gained by the increase in armor unit weight from 3.8 m$^3$ to 5.9 m$^3$.

The toe stone used in Plans 1 and 2, 50 to 500 kg, was not stable and was displaced for the conditions tested. A 907.2-kg stone was used in Plans 3 through 5 and was stable.

| | **Table 4** | | | |
|---|---|---|---|---|
| | **Summary Of 2-D Stability Tests (Seaward Section)** | | | |
| **Plan** | **Armor Type** | **Size (m³)** | **$K_d$** | **Observation** |
| 1 | Accropode | 9.0 | 19.0 | Conservative |
| 2 | Accropode | 7.6 | 23.1 | Stable |
| 3 | Dolos | 3.8 | 29.8 | Moderately stable |
| 4 | Dolos | 7.9 | 14.4 | Conservative |
| 5 | Dolos | 5.9 | 19.5 | Stable |

# 3 Three-Dimensional Stability Tests

Armor units placed on the ends of breakwaters are often vulnerable to waves which overtop and diffract around the structure because the units are subjected to wave forces from the opposing direction of a two-dimensional situation. A heavier unit is often required for breakwater stability on the roundhead of the structure. To determine the stability of the entire structure, in particular the roundheads, three-dimensional tests were conducted for the proposed Noyo breakwater.

## The Model

### Design of model

Three-dimensional stability tests were conducted at a geometrically undistorted linear scale of 1:50, model to prototype. Scale was based on size availability of model armor units and the capabilities of the available wave generator to produce required wave heights at the modeled water depth. Time relations were scaled according to Froude Model Law (Stevens et al. 1942), and model-to-prototype relations were derived in terms of $l$ and $t$ shown in Table 5.

**Table 5**
**Model-Prototype Scale Relations (1:50 scale)**

| Characteristic | Dimension | Scale Relations Model:Prototype |
|---|---|---|
| Length | $l$ | $l_r = 1:50$ |
| Area | $l^2$ | $a_r = 1:2500$ |
| Volume | $l^3$ | $v_r = 1:125000$ |
| Time | $l^{1/2}$ | $t_r = 1:7.07$ |

The armor layer of the original plan for three-dimensional tests consisted of 14- and 9-m$^3$ (37- and 24-ton) Accropodes, but the specific weights of water and construction materials differed between the model and prototype. The transference equation of Hudson (1975), Equation 1, was used to determine the model scale that most closely represented prototype weights for the model Accropodes available at WES and Sogreah. A 1:50 scale and model weights of 0.26 kg and 0.16 kg used in Equation 1 yielded prototype weights of 14 m$^3$ and 8.3 m$^3$ (22 tons), respectively. The two-dimensional stability tests showed a 7.6-m$^3$ Accropode was stable for the conditions tested, and on this basis, it was felt the 8.3-m$^3$ unit would be analogous to a 9-m$^3$ unit for three-dimensional testing. Core-Loc armor units representing prototype sizes of 11.9 m$^3$ and 7 m$^3$ were also used during three-dimensional testing. The model armor units used for three-dimensional stability tests are shown in Figure 16.
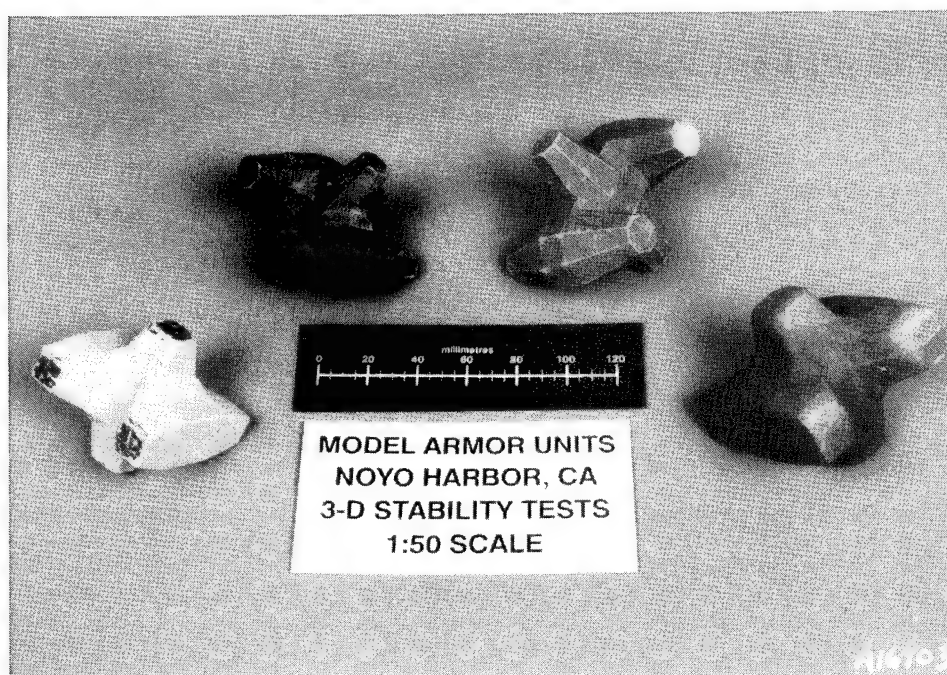


Figure 16. Model armor units used in three-dimensional stability tests, prototype weights from left; 8.3-m$^3$ Accropode, 7.0-m$^3$ Core-Loc, 11.9-m$^3$ Core-Loc, and 14.0-m$^3$ Accropode

Scale effects of viscous forces associated with flow through underlayers and core of the original structure design, shown in plan view in Figure 17, were addressed using the method of Keulegan (1973) to assure that flow through the structure was turbulent. Prototype and model armor layer $W_1$, first and second underlayers $W_2$ and $W_2'$, core $W_3$, and toe berm $W_4$, materials used for the three-dimensional stability tests of the proposed breakwater are listed in Table 6. Cross sections of the Profiles 1-1, 1'-1', 2'-2', and 2-2 denoted in Figure 17 are shown in Figures 18, 19, 20, and 21, respectively.

**Table 6**
**Prototype and Model Material Sizes (Original Design)**

| | Prototype | | | |
|---|---|---|---|---|
| | **Profile 1-1** | **Profile 1'-1'** | **Profile 2'-2'** | **Profile 2-2** |
| $W_1$ $m^3$ | 14.0 | 14.0 | 8.3 | 8.3 |
| $W_2$ kg | 2200 to 4400 | 2200 to 4400 | 1500 to 3000 | 1500 to 3000 |
| $W_2'$ kg | 1500 to 3000 | 1500 to 3000 | - | - |
| $W_3$ kg | 1 to 500 | 1 to 500 | 1 to 500 | 1 to 500 |
| $W_4$ kg | 10 to 500 | 10 to 500 | 10 to 500 | 10 to 500 |
| | Model | | | |
| | **Profile 1-1** | **Profile 1'-1'** | **Profile 2'-2'** | **Profile 2-2** |
| $W_1$ kg | 0.26 | 0.26 | 0.16 | 0.16 |
| $W_2$ kg | 0.018 to 0.029 | 0.018 to 0.029 | 0.011 to 0.018 | 0.011 to 0.018 |
| $W_2'$ kg | 0.011 to 0.018 | 0.011 to 0.018 | - | - |
| $W_3$ kg | 0.005 to 0.011 | 0.005 to 0.011 | 0.005 to 0.011 | 0.005 to 0.011 |
| $W_4$ kg | 0.005 to 0.011 | 0.005 to 0.011 | 0.005 to 0.011 | 0.005 to 0.011 |

## Test facilities and equipment

Tests were conducted in a 36.6-m-long, 24.4-m-wide, 1.2-m-deep wave basin. A photograph of the three-dimensional model, gravel absorber, wave gages, and wave generator is shown in Figure 22. The model was constructed and molded of concrete to represent approximately 425 by 425 m of bathymetry in the vicinity of the proposed breakwater location. Contours were molded to -15 m mllw, and a 1 on 5 transition slope was molded from the -15-m contour to the model floor elevation of -24.4 m mllw. Gravel absorber was placed on the eastern and southern sides of the molded model bathymetry to provide depth and prevent unnatural wave refraction effects around the model.

Waves were generated by a piston-type electronically controlled hydraulic system. Displacement of the wave board was controlled by a command signal transmitted to the board by a DEC MicroVAX II computer, and waves were produced by the periodic displacement of the board. Random wave command
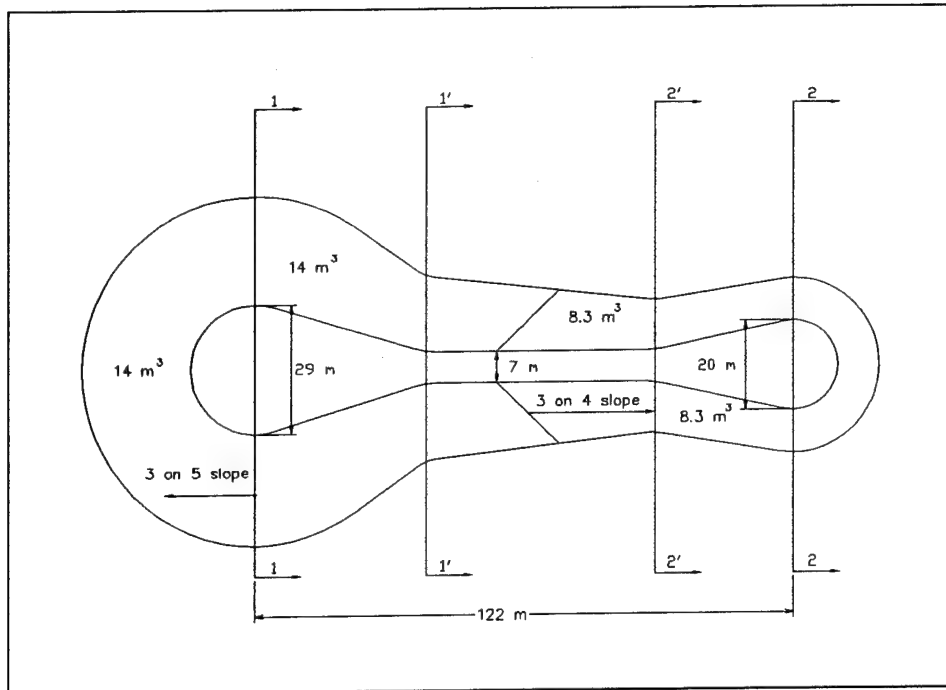
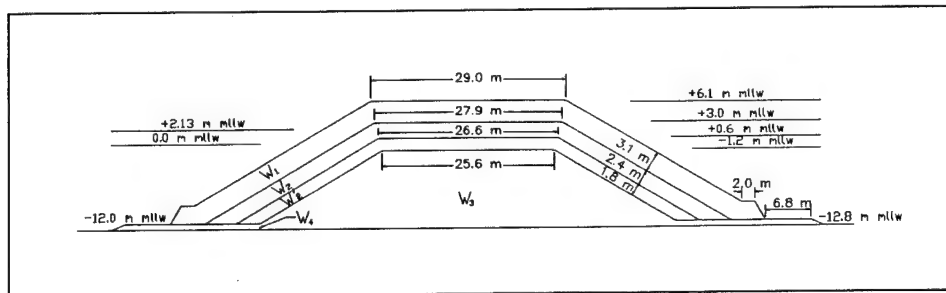Figure 17.  Original Noyo breakwater plan



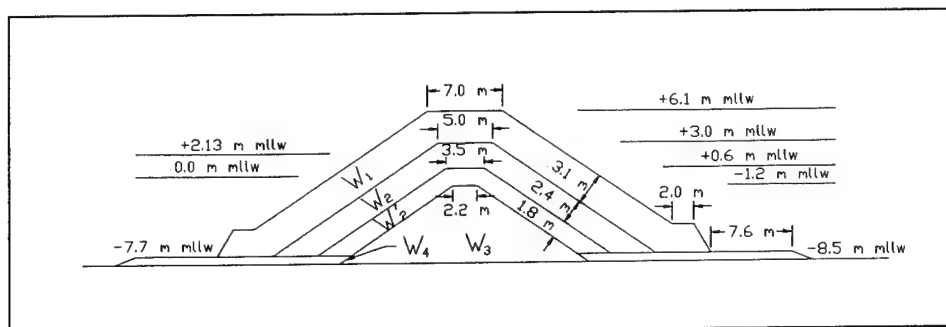Figure 18.  Profile 1-1 of original breakwater plan



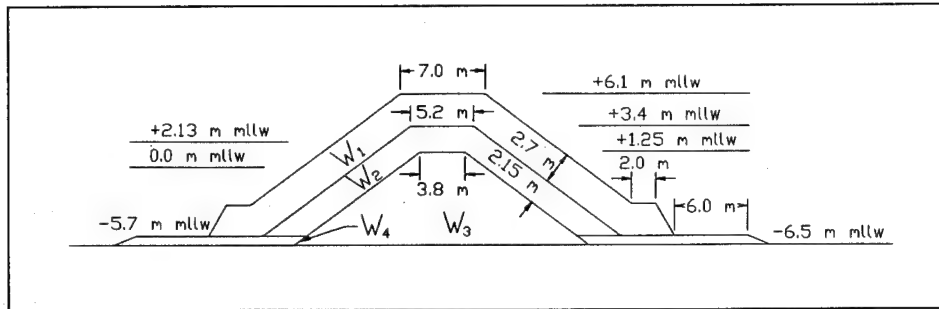Figure 19.  Profile 1'-1' of original breakwater plan

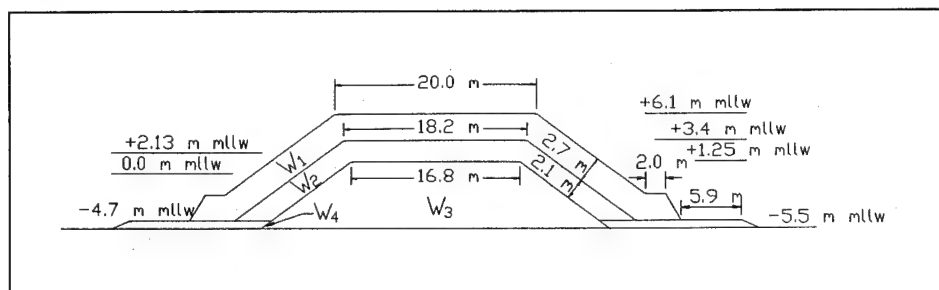Figure 20. Profile 2'-2' of original breakwater plan


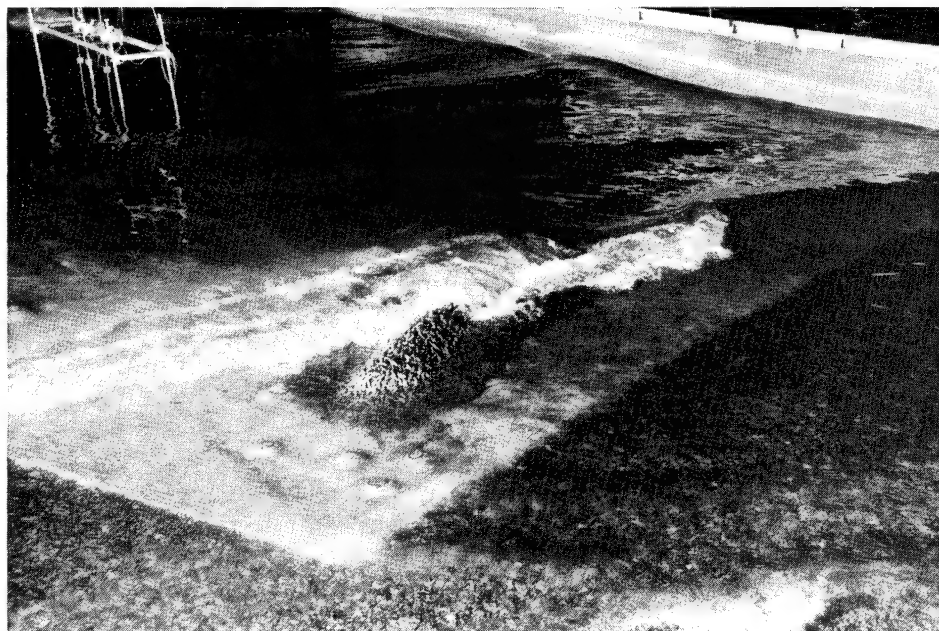
Figure 21. Profile 2-2 of original breakwater plan



Figure 22. Photograph of three-dimensional stability model

signals to drive the board were generated to simulate a TMA shallow-water spectrum (Hughes 1984) for the design wave periods.

Results from wave hindcast studies (Corson et al. 1986) indicated the most severe wave conditions approached the harbor from the west-northwest; therefore, the west-northwest direction was selected as the test direction. Prior to construction of the breakwater, the basin was calibrated for the design periods from the west-northwest. The selected water depth for all tests was +2.13 m mllw for design wave periods of 13, 17, and 20 sec. Design wave heights were based on the maximum incident waves which reached the structure.

Water surface elevations were recorded by single wire capacitance-type gages, sampled at 20 Hz. Six gages were used for calibration in two arrays of three gages each to allow calculation of incident and reflected wave heights by Goda and Suzuki (1976). Array 1 was positioned above the model floor (-24.4 m mllw, prototype) 4.5 m from the generator, which was midway between the generator and model contours. Array 2 was positioned so that the middle gage of the array was directly above the center of the north roundhead of the breakwater. Array 2 was removed after calibration was completed and, during stability tests, wave data were collected at Array 1 only to verify that proper wave conditions were generated. Data obtained from the arrays were analyzed using the TSA computer program of Long and Ward (1987). Operations performed for the three-dimensional stability tests were mean down-crossing analysis to obtain significant, maximum, and average wave heights, significant and average wave periods, and mean water levels at each gage; and unidirectional spectral density incident/reflection analysis to determine the incident and reflected parameters at each array.

Design wave heights at the proposed structure were selected from Figures 23 through 25, which show results of three-dimensional calibration of the facility for peak periods of 13, 17, and 20 sec, respectively. Offshore wave height at the wave generator depth of 24 m $(H_{mo})_{24}$ is plotted versus $(H_{max})_d$, $(H_s)_d$, and $(H_{mo})_d$ at the north roundhead, where $(H_{max})_d$ = maximum wave height at north roundhead, three-dimensional tests, $(H_s)_d$ = significant wave height at north roundhead, three-dimensional tests, and $(H_{mo})_d$ = zero-moment wave height at north roundhead, three-dimensional tests. A depth-limited breaking condition was reached at the structure location for non-breaking conditions at the generator for all periods. Storm I design conditions for stability tests are shown in Table 7. The total duration of Storm I was approximately 30 hr prototype. Some breakwater plans were subjected to additional waves without rebuilding the structure. Storm IA conditions consisted of the ten Storm I waves beginning with the $T_p = 13$ sec, $(H_{mo})_d = 5.8$ m condition and continuing to $T_p = 20$ sec and $(H_{mo})_d = 8.1$ m in Table 7. Storm IB consisted of three Storm I waves which began with $T_p = 17$ sec, $(H_{mo})_d = 7.2$ m and concluded with $T_p = 20$ sec, $(H_{mo})_d = 8.1$ m.
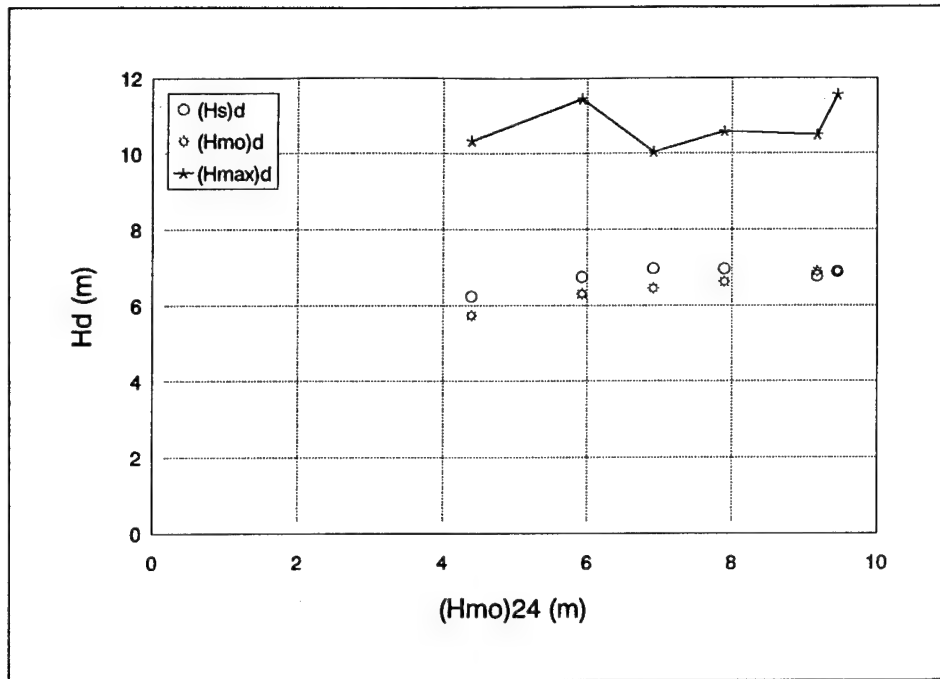
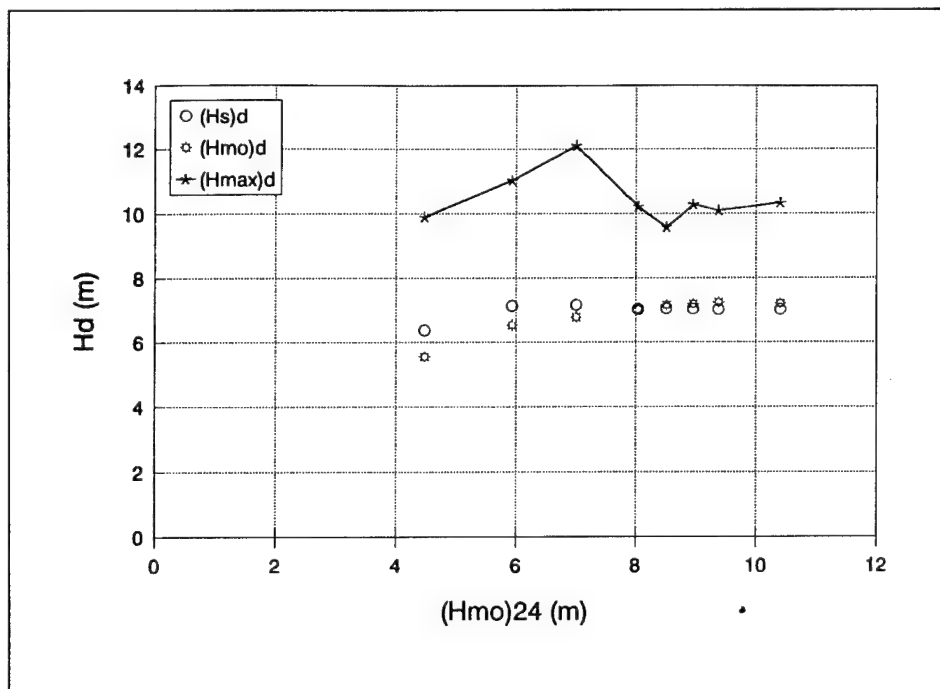Figure 23.  Wave height at north roundhead, 13-sec waves



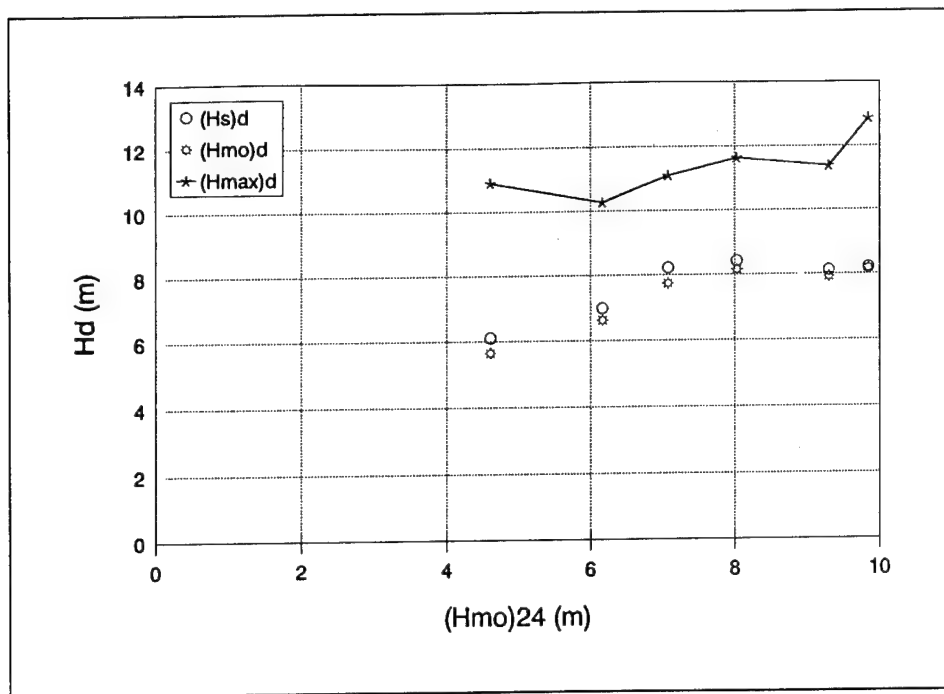Figure 24.  Wave height at north roundhead, 17-sec waves

Figure 25. Wave height at north roundhead, 20-sec waves

## Test procedures

Photographs were taken before testing was initiated without water in the basin. Following before-test photographs, the basin was flooded to +2.13 m mllw and the structure was exposed to low-level waves, $T_p = 13$ s, $(H_{mo})_d = 3.0$ m, wave condition 1 in Table 7. The low-level series allowed settling and nesting of the newly constructed section which would occur under typical daily wave conditions prior to being exposed to a design-level storm. The remainder of the Storm I wave conditions of Table 7 were generated upon completion of the low-level waves. Response of the structure was recorded during and after each wave condition. Photographs were also taken of the north and south roundheads, and the lee side and sea side of the structure while the basin was flooded after each series of waves of constant height was completed. A detailed inspection of the structure was also performed during this time, and effects of the waves on individual units, toe buttress stone, and the general condition of the structure were recorded. The basin was drained, and after-test photographs were taken after all waves of a storm series were generated. The same procedure was followed if the plan was subjected to additional storm conditions. Before and after photographs are located in Appendix C.

**Table 7**
**Storm I Wave Conditions**

| Wave Type | SWL m, mllw | T sec | $(H_{mo})_d$ m | $(H_s)_d$ m | $(H_{max})_d$ m | $(H_{mo})_{24}$ m | Test Duration model min |
|---|---|---|---|---|---|---|---|
| Random | +2.13 | 13 | 3.0 | 3.4 | 5.5 | 2.3 | 15 |
| Random | +2.13 | 13 | 4.6 | 5.0 | 8.3 | 3.5 | 15 |
| Random | +2.13 | 17 | 4.6 | 5.6 | 8.2 | 3.7 | 15 |
| Random | +2.13 | 20 | 4.6 | 5.0 | 9.0 | 3.8 | 15 |
| Random | +2.13 | 13 | 5.2 | 5.6 | 9.4 | 4.0 | 15 |
| Random | +2.13 | 17 | 5.2 | 5.9 | 9.3 | 5.7 | 15 |
| Random | +2.13 | 20 | 5.2 | 5.6 | 10.2 | 4.3 | 15 |
| Random | +2.13 | 13 | 5.8[1] | 6.1 | 10.5 | 4.6 | 15 |
| Random | +2.13 | 17 | 5.8[1] | 6.6 | 10.2 | 4.9 | 15 |
| Random | +2.13 | 20 | 5.8[1] | 6.2 | 10.7 | 4.8 | 15 |
| Random | +2.13 | 13 | 6.4[1] | 6.9 | 10.5 | 6.6 | 15 |
| Random | +2.13 | 17 | 6.4[1] | 7.0 | 10.9 | 5.7 | 15 |
| Random | +2.13 | 20 | 6.4[1] | 6.8 | 10.4 | 5.8 | 15 |
| Random | +2.13 | 13 | 6.9[1] | 6.8 | 10.5 | 9.2 | 15 |
| Random | +2.13 | 17 | 7.2[1,2] | 7.0 | 10.1 | 9.4 | 15 |
| Random | +2.13 | 20 | 7.0[1,2] | 7.4 | 10.4 | 6.2 | 15 |
| Random | +2.13 | 20 | 8.1[1,2] | 8.4 | 11.6 | 8.0 | 15 |

[1] Included in Storm IA conditions.
[2] Included in Storm IB conditions.

## Model construction

Construction of the modeled section simulated prototype construction as closely as possible. The core, bedding, and underlayer of material were dumped by shovel, smoothed to grade, and compacted with hand trowels to simulate consolidation that would have occurred due to wave action.

Plan 1 was based on results of the two-dimensional stability tests and expected wave heights at the breakwater. The initial plan was provided by Sogreah, France, and proper placement of Accropodes on the three-dimensional structure was demonstrated by Mr. Louis Sanchez of Sogreah. The units were placed according to a three-dimensional mesh, which is a function of Accropode size. This special placement of units was performed on all subsequent Accropode plans.

### Reporting model observations

Visual inspections were made during and after wave action on the structure. Because Accropodes are placed in one layer, no displacement of any unit was desired. In essence, the structure either failed or was stable.

Qualitative results were taken for overtopping, and the wave period and height and category of overtopping (minor, moderate, or major) were noted for each wave condition.

# Results

Three-dimensional stability tests were conducted for 17 plans at a model scale of 1:50. The plans consisted of two breakwater configurations, original and modified. Eight toe protection plans were used with the original breakwater and nine toe plans were used with the modified structure. Accropodes were used for all original breakwater plans and both Accropodes and Core-Locs were used during tests with the modified breakwater plans. All wave heights referred to in this section are $(H_{mo})_d$. A 3V:4H slope was used on all original breakwater plans, and a 2V:3H slope was used on modified breakwater plans.

Plans 1 through 9 were subjected to Storm I conditions from the west-northwest direction listed in Table 7, with the exception of Plan 8, which was subjected to only Storm IA conditions described above from the west-north-west. In addition to Storm I waves, Plans 4 through 7 were also subjected to Storm IA waves without rebuilding the structure. It was determined that wave heights lower than $(H_{mo})_d = 5.8$ m had little effect on the stability of the structure. These lesser wave conditions were omitted during tests of Plans 10 through 17, which were subjected to multiple series of Storm IA and/or Storm IB waves. Wave data were collected at the basin floor in -24.4 m mllw water immediately in front of the wave generator to assure the appropriate waves were generated. Three-dimensional harbor tests at a 1:75 scale were simultaneously being conducted by Bottin (1994) to determine the effectiveness of the structure on wave height reduction. Design wave conditions for the 1:75 scale harbor study were lower than the stability test design conditions because it was agreed by SPN and local representatives of Noyo Harbor that fishing vessels would not navigate for offshore wave heights in excess of 4.3 m. However, in the present study it was necessary to determine the stability of the structure for the highest wave conditions that occur at the site because the structure would always be exposed to these conditions. Wave data were not collected shoreward of the structure during the stability tests because it would not be applicable to the harbor model tests.

## Plan 1

Plan 1, the proposed plan, consisted of 14-m$^3$ Accropodes on the north roundhead and 8.3-m$^3$ units on the south roundhead (Figure 17) and was exposed to Storm I conditions. The armor layer became loose and Accropodes were displaced at the toe during tests with 20-s, 6.4-m waves. This period and height were repeated to determine if further damage would occur and if the limiting wave condition had been reached. Damage did not increase when the condition was repeated, but the plan failed after the structure was subjected to the higher waves in the test series. Armor units were observed to slip on the structure slope, which indicated the mechanism of failure to be an unstable toe (Photos C1 through C4).

## Plan 2

Results from Plan 1 indicated failure was due to toe instability. Toe stability in part is a function of the breakwater slope. Because Accropodes are placed on a 3V:4H slope, which is relatively steep, the patent holder Sogreah was consulted for their recommendation for a solution. Sogreah gave two options for Accropode toe stability: (a) place the first row of units in a trench, and (b) add a toe buttress in front of the units. Sogreah stated using a trench was the best method for assuring toe stability, but placement of a toe buttress was the more desirable and less expensive option for SPN. Plan 2 was constructed and tested using 3,350 kg (3.7 tons) buttressing stone around the entire structure (Photos C5 through C8) to reinforce the first row of Accropodes and provide stability to the toe. Stone was placed using the standard toe buttress configuration (two layers thick and minimum three stones wide) on the upper layer (Markle 1989). The toe buttress width was approximately 6.1 m prototype at the base.

The toe was observed to be more stable for Plan 2 after Storm I waves with inclusion of the buttress stone. However, the first layer of 14-m$^3$ Accropodes was displaced on the leeward and seaward sides of the breakwater and the structure failed in these areas (Photos C9 through C11). The buttressing stone appeared to provide sufficient stability at the toe of the 8.3-m$^3$ units (Photo C12).

## Plan 3

To improve stability at the toe, 5,080-kg (5.6-ton) stone was placed two layers high and three stones wide for reinforcement at the toe of the 14-m$^3$ units for Plan 3 (Photos C13 through C16). Results of Plan 2 indicated 3,350-kg buttress stone provided adequate toe protection in front of the 8.3-m$^3$ units. The toe of the 8.3-m$^3$ units remained stable after Storm I waves were generated, but the 5,080-kg stone was displaced, and Accropodes were displaced near the toe on the seaward and leeward sides near the north roundhead (Photos C17 through C20). The 5,080-kg stone buttress extended higher in the

water column than the lighter stone, and was subjected to more of the wave energy, which may have caused the stone to be displaced.

## Plan 4

Results of Plan 3 indicated that use of stone larger than 3,350 kg placed two layers high and 6.1 m wide would not secure the toe. Therefore, a wider toe buttress was placed for Plan 4. The plan consisted of 3,350-kg buttressing stone placed around the entire structure, but unlike Plan 2, the buttress width was extended from 6.1 m to 24.4 m on the lee side in the area of toe instability and to 18.3 m on the sea side in front of the 14-m$^3$ units (Photos C21 through C23). The buttress width fronting the 8.3-m$^3$ Accropodes was again placed 6.1 m wide (Photo C24).

The structure was stable for waves as high as 7 m, but toe instability occurred on the lee side of the north roundhead for the 20-sec, 8.1-m wave condition. Toe instability was located in deeper water on the leeward side than observed in previous plans and at the point where the buttress width began to narrow from 24.4 m to 6.1 m. The unstable toe caused units to slide on the breakwater, and a hole developed in the armor layer, shown in Photos C25 through C28.

The damaged structure was subjected to Storm IA waves. Accropodes were observed to move in the vicinity of the hole and a few were displaced off the structure, but further damage was not significant for the 5.8- to 7-m heights. However, the 20-sec, 8.1-m wave condition removed all Accropodes on the north roundhead above -3 m mllw (Photos C29 through C32). Damage to the breakwater would probably have been more severe, but a cross-sectional template in the model breakwater prevented additional displacement along the trunk. Results of the tests indicated Plan 4 may survive one major storm, but a second storm would destroy the structure if no repairs were performed between the first and second storms.

## Plan 5

The wider toe berm used in Plan 4 provided additional protection to the toe in the problem areas observed in Plans 1 through 3. To determine if less toe buttress material could be placed in these areas to provide stability for one storm, the breakwater was reconstructed and 3,350-kg buttress stone was placed around the structure in the same manner as Plan 4, but reduced to 18.3 m wide on the lee side and 12.2 m wide on the sea side for Plan 5 (Photos C33 through C36). After tests with Storm I and IA waves, the narrower buttress width was displaced on both the sea side and lee side of the structure and was not sufficient to stabilize the toe. (Photos C37 through C40).

## Plan 6

Plan 6 consisted of the proposed breakwater section with a metal strip placed around the entire structure in front of the first row of Accropodes to stabilize the toe (Photos C41 through C44). One 14-m$^3$ Accropode was displaced after Storm I waves, but the structure was in good condition and was not damaged (Photos C45 through C48). The structure was subjected to the additional waves of Storm IA, and no further damage was observed to the breakwater (Photos C49 through C52). Results of Plan 6 showed that the 14- and 8.3-m$^3$ Accropodes placed on the structure would be stable for Storm I and IA wave conditions if the toe was stabilized. Similar results would be expected in the prototype if the first row of Accropodes were placed in a trench or were protected by driven piles.

## Plan 7

Plan 7 was constructed to determine if a stable toe could be achieved without construction of a trench or use of piles. Buttress stone was placed around the entire structure using 3,350-kg stone placed two layers high and 24.4 m wide on the lee side of the north roundhead, which was identical to Plan 4, but the buttress tapered to 18.3 m, rather than 6.1 m, at the end of the north roundhead (Photos C53 and C54). The toe buttress was also placed 18.3 m wide on the sea side fronting the 14-m$^3$ Accropodes (Photo C55). The toe buttress was placed 6.1 m wide in front of the 8.3-m$^3$ Accropodes (Photo C56). The structure was moderately stable for waves up to 7.0 m; however, a hole began to scour within the buttress on the lee side of the breakwater. The scour hole increased in size during 20-sec, 8.1-m waves (Photos C57 and C58), and movement of 14-m$^3$ units was observed. Damage to the breakwater was limited to the lee side of the north roundhead in the vicinity of scour (Photos C59 and C60). The damaged structure was subjected to Storm IA waves which caused the structure to fail on the lee side of the north roundhead (Photos C61 through C64).

## Plan 8

Results of Plan 7 showed the toe buttress remained in place during Storm I and IA conditions, but the 3,350-kg stone scoured within the buttress. Plan 8 was constructed using 3,350-kg buttress stone at the same dimensions of Plan 7, except 5,080-kg stone was placed two layers high in the zone in which scour occurred during Plan 7 tests. To expedite the tests, the plan was subjected to Storm IA tests only. Only one unit was displaced on the leeside of the north roundhead. However, Photos C65 through C68 show that the 5,080-kg stone was not of sufficient weight to prevent scour in the buttress and did not provide necessary toe protection for the structure.

## Breakwater modification tests

With the exception of the lee side of the north roundhead, the toe buttress plans stabilized the toe for the conditions tested. It was observed during tests of Plans 1 through 8 that waves appeared to shoal as they diffracted around the north roundhead. It was felt that the roundhead shape and surrounding bathymetry concentrated breaking wave energy in the area of toe instability. To determine if a different breakwater shape would reduce energy at the toe, wave height measurements were made near the location of toe instability for the original plan for heights of 6.4 m and higher for the design wave periods. Wave heights of the original plan (crest width of 29 m) were compared to two breakwater plans with reduced crown widths of 15.2 m and 9.1 m, shown in Figures 26 through 28. Little difference is observed between the original plan and the 15.2-m crown width plan. However, wave heights in the vicinity of toe instability are 10 to 15 percent lower if a 9.1-m crown width is used. Stability tests were continued with a 9.1-m-wide crown at the north roundhead, shown in Figure 29. The crown width on the remainder of the structure was 6.1 m, including the south roundhead. Cross sections of Profiles 1-1, 1'-1', 2'-2', and 2-2 of the modified breakwater are shown in Figures 30 through 33. Prototype and model core and first underlayer material sizes of the original plan were used for the modified breakwater plans. The second underlayer size used in Profiles 1-1 and 1'-1' of the original plan was eliminated and not used in the modified plans.
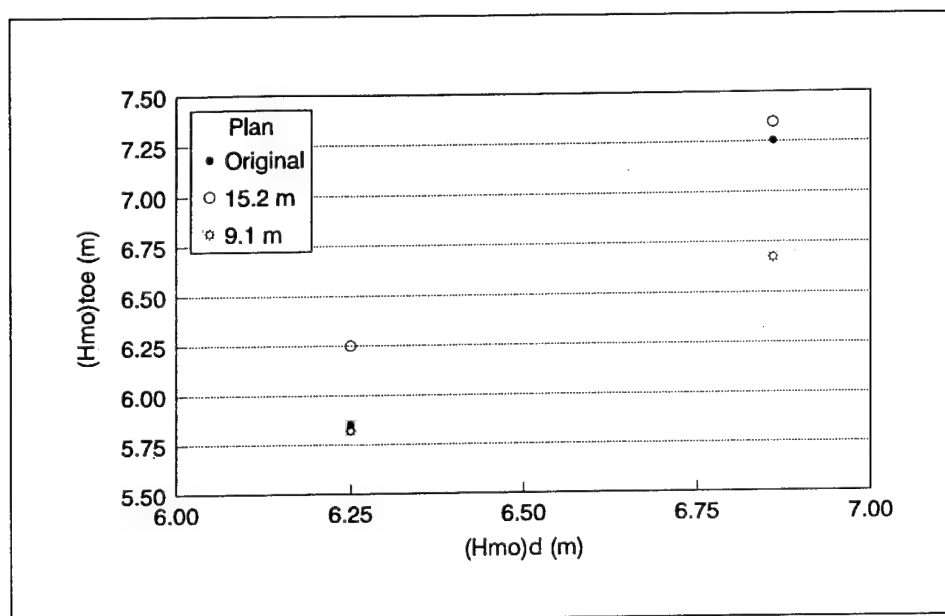


Figure 26. Comparison of 13-sec wave heights at leeside toe to crown width

## Plan 9

Plan 9 was constructed with 14-m³ Accropodes placed on the north roundhead and 8.3-m³ Accropodes on the south roundhead. The effect of the reduced roundhead on required buttress width for toe stability was not known. Therefore, a 6.1-m-wide buttress of 3,350-kg stone was placed around the entire structure (Photos C69 through C72). Despite reduction in energy at the leeside toe of the north roundhead, 20 units were displaced after being subjected to Storm I wave conditions (Photos C73 through C76). Accropodes were displaced at the toe, which caused most of the damage; however, it was observed that some units were displaced from the crown, which was not a result of toe instability.
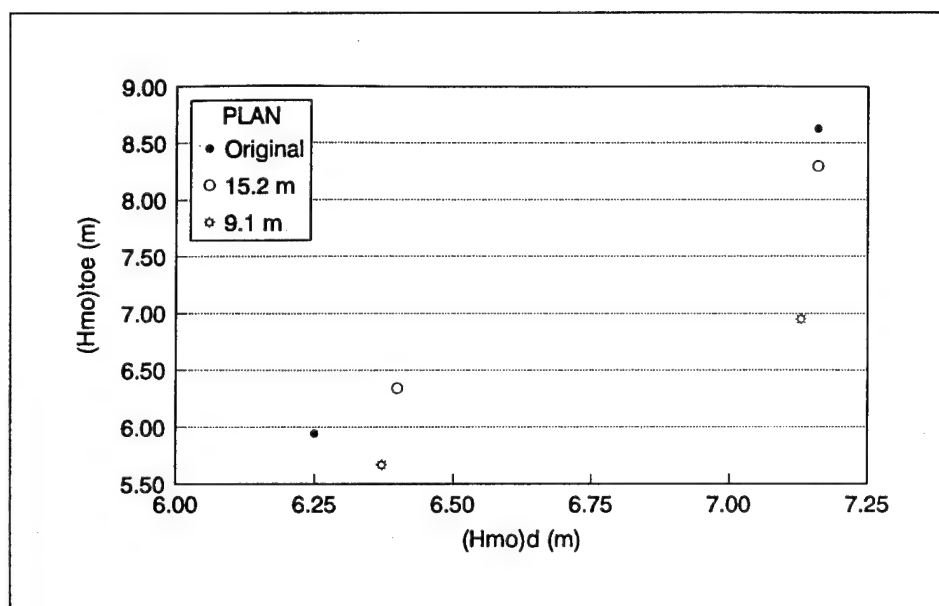


Figure 27. Comparison of 17-sec wave heights at leeside toe to crown width

## Plan 10

Based on results of Plan 9, a wider buttress of 3,350-kg stone was necessary to ensure toe stability on the lee and sea sides of the breakwater. The buttress was extended to 30.5 m on the lee side and to 18.3 m on the sea side in front of the 14-m³ Accropodes (Photos C77 through C80). The structure lost five Accropodes after being subjected to Storm IA waves (Photos C81 through C84), and three additional units were lost after Storm IA waves were repeated without rebuilding (Photos C85 through C88). The toe on the lee side of the north roundhead was not displaced after the tests, and the structure was considered stable (Photo C86).
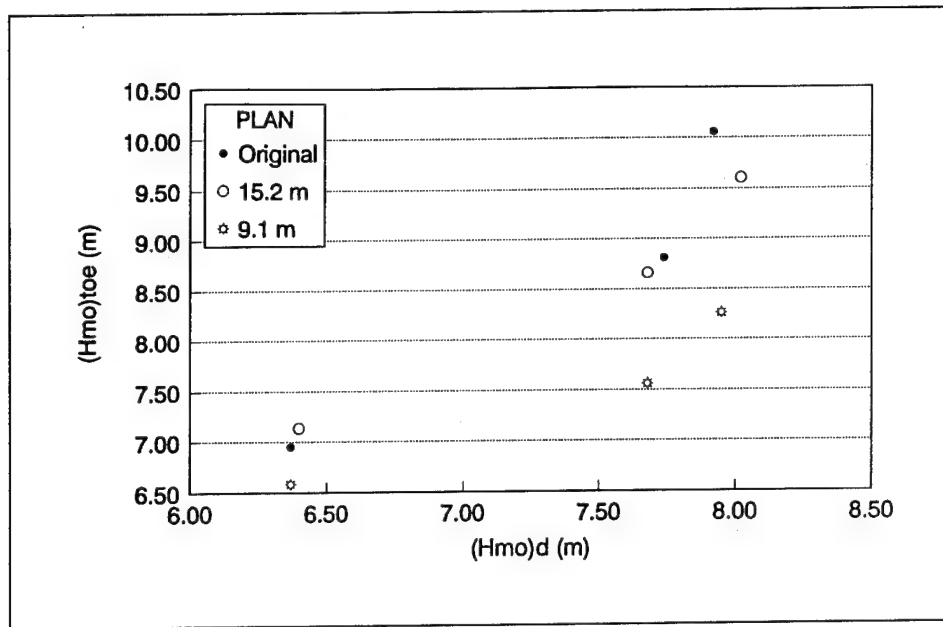
Figure 28. Comparison of 20-sec waves at leeside toe to crown width
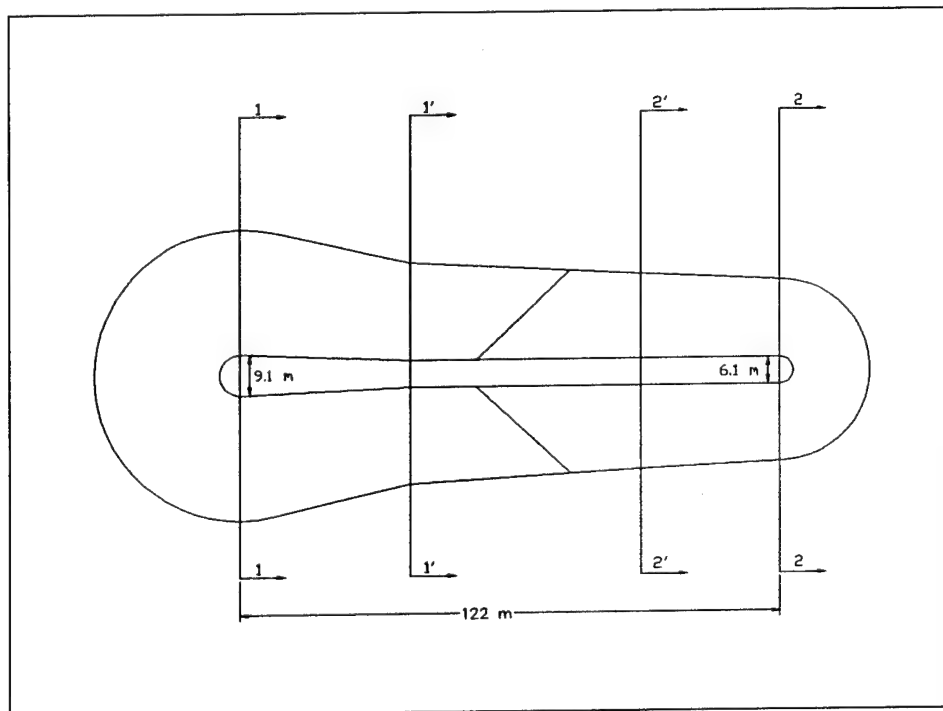


Figure 29. Modified Noyo breakwater plan
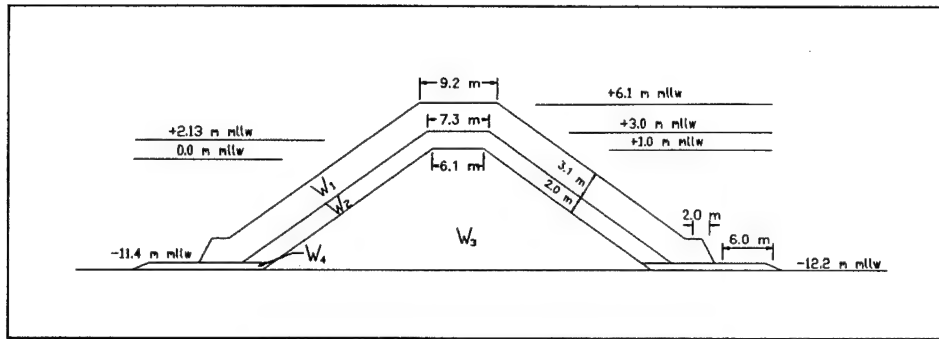
Figure 30. Profile 1-1 of modified breakwater plan
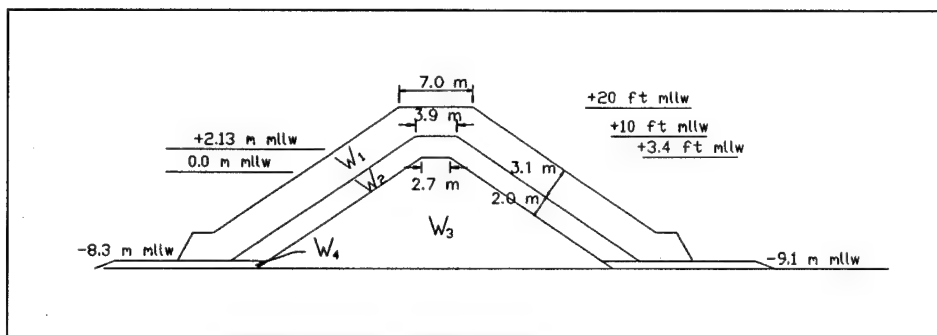


Figure 31. Profile 1'-1' of modified breakwater plan
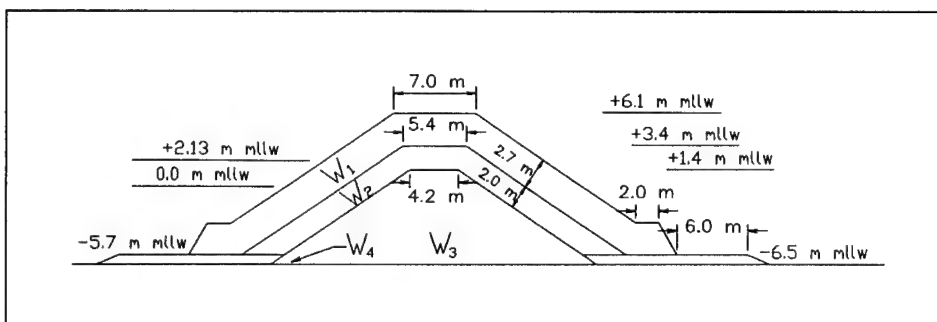


Figure 32. Profile 2'-2' of modified breakwater plan
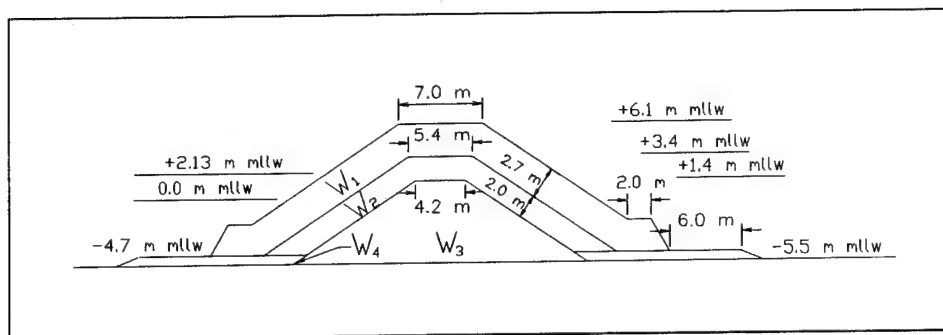
Figure 33. Profile 2-2 of modified breakwater plan

## Plan 11

Plan 11 incorporated 11.9-m$^3$ Core-Loc armor units on the north roundhead, and 7.0-m$^3$ Core-Locs on the south roundhead (Photos C89 through C92). The toe buttress was built of 3,350-kg stone and was 6.1-m wide in front of the south roundhead units and 18.3-m wide in front of the north roundhead units on the sea side. Results of Plan 10 indicated the 30.5-m-wide buttress was stable on the lee side of the north roundhead; therefore, the buttress was narrowed to a width of 24.4 m. Storm IA waves were generated and repeated without rebuilding the structure (Photos C93 through C96 and C97 through C100, respectively). Two Core-Locs were displaced after the tests and the north roundhead displayed general looseness, but the structure was determined to be stable for the test conditions.

## Plan 12

The breakwater was rebuilt with the Core-Locs used in Plan 11. The toe buttress was placed at the same width using the same stone as in Plan 11; however, a 12.2-m-wide buttress was constructed on the lee side of the north roundhead (Photos C101 through C104). The narrower leeside buttress was displaced during Storm IA tests and two 11.9-m$^3$ Core-Locs were displaced (Photos C105 through C108). Six additional 11.9-m$^3$ units were displaced after Storm IA waves were repeated and Plan 12 was considered moderately stable (Photos C109 through C112).

## Plan 13

Plan 13 was constructed of Core-Locs with a toe buttress composed of 3,350-kg stone, 6.1 m wide in front of the 7.0-m$^3$ units and 18.3 m wide at the base of the 11.9-m$^3$ units (Photos C113 through C116). The structure was subjected to Storm IA waves and one unit was displaced off the north round-head on the lee side (Photos C117 through C120). Storm IA waves were generated without rebuilding the structure, and two additional units were

38

displaced on the sea side of the north roundhead (Photos C121 through C124). The toe buttress was in good condition and the structure was stable for the conditions tested.

To determine if damage to the structure would progress with additional wave energy, Plan 13 was subjected to three series of Storm IB waves without rebuilding the breakwater. After a total of five successive storms (two series of Storm IA waves and three of Storm IB waves), 35 units were displaced off the structure (Photos C125 through C128). The buttress was displaced on the sea side in front of the 11.9-m$^3$ Core-Locs near the transition to the 7.0-m$^3$ units. The buttress was also displaced on the south roundhead and on the lee side of the north roundhead. Holes developed in the armor layer on the sea side of the structure and on the north and south roundheads. Most of the Core-Loc displacement was directly caused by toe failure. The results showed the structure would be stable after two storms, but would require rehabilitation after five successive storms if no intermediate repairs were made.

## Plan 14

Plan 14 was constructed using 14- and 8.3-m$^3$ Accropodes with the same buttress configuration used in Plan 13 (Photos C129 through C132). The Accropode structure was subjected to five series of Storm IB waves. Results of Plan 14 tests were similar to Plan 13. The toe buttress was displaced on the sea side near the transition of armor units, the south roundhead, and on the lee side of the north roundhead (Photos C133 through C136). Thirty-one 14-m$^3$ units and ten 8.3-m$^3$ units were displaced. Holes in the armor layer developed along the sea side of the structure and on the north and south roundheads.

## Plan 15

Plan 15 was constructed with 19.9-m$^3$ Accropodes on the north roundhead and 8.3-m$^3$ Accropodes on the south roundhead. The buttress contained 3,350-kg stone and the width was increased to 15.2 m around the south roundhead. The buttress was placed 30.5 m wide at the base of the seaside 8.3-m$^3$ units near the transition to the heavier Accropodes. The buttress tapered to 18.3 m in front of the 19.9-m$^3$ units. The buttress width was maintained at 6.1 m in front of the leeside, 8.3-m$^3$ Accropodes, but the buttress was widened to 30.5 m at the base of the larger, leeside units. Figure 34 shows a plan view of the structure and buttress used for Plan 15. The breakwater lost one 8.3-m$^3$ and seven 19.9-m$^3$ Accropodes after five successive series of Storm IB waves, but was stable (Photos C137 through C140). It was determined that the wider buttress and larger units used on the north roundhead used for Plan 15 were necessary to provide a stable breakwater design for the wave conditions tested.
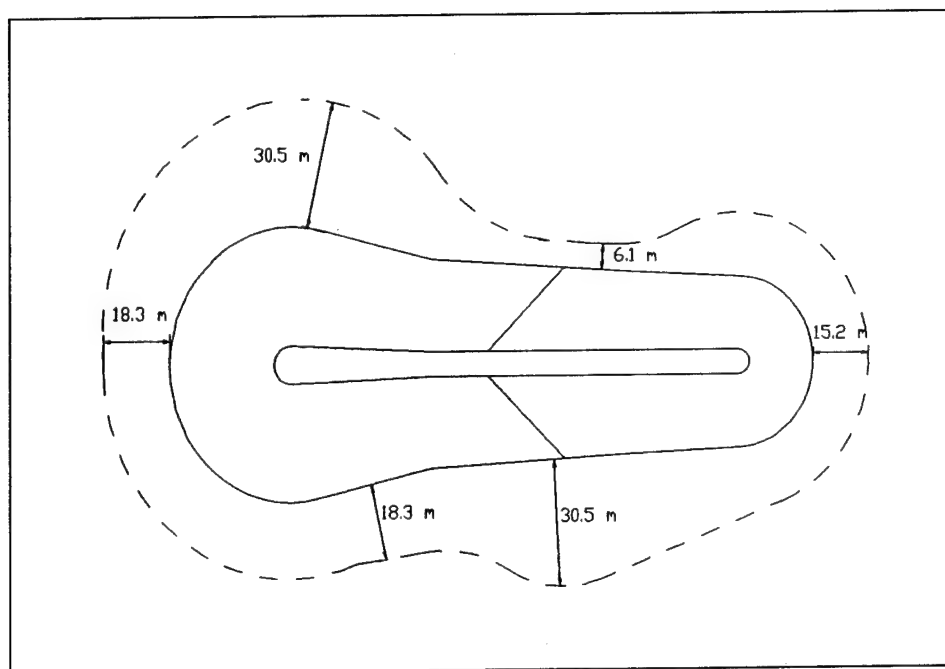
Figure 34. Toe buttress used in Plans 15, 16, and 17

## Plan 16

The breakwater configuration of Plan 15 was determined to be stable for the design wave conditions. However, wave hindcast information showed that deepwater waves higher than 6.7 m for periods greater than 18.7 sec did not occur over a 20-year period of measurement (Corson et. al 1986). It was felt the design conditions were conservative; therefore, the wave conditions were modified to reflect this information. Storm IB waves were generated for five consecutive series, but the 20-sec, 8.1-m wave was omitted from the second, third, and fourth series. Although the high wave condition was rare, it has been observed offshore subsequent to Corson's period of record, and was included in the first and fifth series. Plan 16 was constructed using the same buttress configuration as Plan 15 and with 8.3-$m^3$ Accropodes placed on the south roundhead, but 14.0-$m^3$ Accropodes were placed on the north roundhead (Photos C141 through C144). The plan was stable after five successive storms; three 14.0-$m^3$ units and one 8.3-$m^3$ unit were displaced (Photos C145 through C148). The toe buttress was also found to be stable.

## Plan 17

The breakwater was rebuilt using 11.9- and 7.0-$m^3$ Core-Locs on the north and south roundheads, respectively, and the same buttress configuration used in Plans 15 and 16  (Photos C149 through C152). Plan 17 was subjected to the

modified Storm IB wave conditions of Plan 16 and was stable for the design waves; two 11.9-m$^3$ and two 7.0-m$^3$ were displaced (Photos C153 through C156).

The structure was rebuilt and Plan 17 was tested to determine if the toe was stable for wave conditions at a lower water level. The breakwater was subjected to five successive modified Storm IB waves generated at a +0-m mllw level. The structure and toe buttress were stable; one 11.9-m$^3$ unit was displaced during the test (Photos C157 through C160).

## Summary of Three-Dimensional Stability Tests

Three-dimensional stability tests are summarized in Table 8. The proposed Noyo breakwater was subjected to depth-limited wave conditions generated for three design periods from the west-northwest offshore wave direction. Observations from the tests indicated that the major concern for a stable structure was a stable toe. Two breakwater shapes were tested for the proposed breakwater. Eight toe configurations were tested with the original plan, and nine toe configurations were tested with a modified breakwater plan. All tests with the original plan were conducted with Accropode armor units. The tests with the modified breakwater consisted of both Accropodes and Core-Loc units.

Plan 6, consisting of 14.0- and 8.3-m$^3$ Accropodes and a metal strip placed around the entire structure to simulate a trench or driven piles was the only plan with the original breakwater design to survive Storm I and IA wave conditions. Several Accropode and Core-Loc plans were found to be stable for two storm series which included the 20-sec, 8.1-m wave at the breakwater using a toe buttress of 3,350-kg stone with the modified breakwater plan. However, only Plan 15, consisting of 19.9-m$^3$ Accropodes placed on the north roundhead, was stable for five series of Storm IB waves. A heavier Core-Loc model unit was not available at the time of testing, but based on test observations, a larger Core-Loc used with the toe buttress configuration should also provide adequate stability for all wave conditions. Similar results were obtained between the 14-m$^3$ Accropode and 11.9-m$^3$ Core-Loc; therefore, it was expected that a 16.9-m$^3$ Core-Loc placed on the north roundhead would be required to provide a stable breakwater for five series of Storm IB waves. Plans 16 and 17, which were constructed with 14- and 8.3-m$^3$ Accropodes and 11.9- and 7.0-m$^3$ Core-Locs, respectively, were stable for five series of Storm IB waves, with the 20-sec, 8.1-m wave excluded in three of the series. Wave hindcast data showed this extreme wave condition did not occur during the 20-year prototype wave measurement period. This wave condition has been observed in subsequent field data, and was included in two of the five Storm IB wave series to analyze the breakwater stability.

**Table 8**
**Summary of 3-D Stability Tests**

| Plan | Storm | Cycles | Armor Type | North Roundhead | | South Roundhead | | Units Displaced[1] |
|---|---|---|---|---|---|---|---|---|
| | | | | Armor (m³) | Buttress (kg) | Armor (m³) | Buttress (kg) | |
| 1 | I | 1 | Accropode | 14.0 | - | 8.3 | - | 23 |
| 2 | I | 1 | Accropode | 14.0 | 3350 | 8.3 | 3350 | 7 |
| 3 | I | 1 | Accropode | 14.0 | 5080 | 8.3 | 3350 | 51 |
| 4 | I<br>IA | 1<br>1 | Accropode | 14.0 | 3350 | 8.3 | 3350 | >100 |
| 5 | I<br>IA | 1<br>1 | Accropode | 14.0 | 3350 | 8.3 | 3350 | 8 |
| 6 | I<br>IA | 1<br>1 | Accropode | 14.0 | -[2] | 8.3 | -[2] | 1 |
| 7 | I<br>IA | 1<br>1 | Accropode | 14.0 | 3350 | 8.3 | 3350 | 42 |
| 8 | IA | 1 | Accropode | 14.0 | 3350[3] | 8.3 | 3350 | 1 |
| 9 | I | 1 | Accropode | 14.0 | 3350 | 8.3 | 3350 | 20 |
| 10 | IA | 2 | Accropode | 14.0 | 3350 | 8.3 | 3350 | 8 |
| 11 | IA | 2 | Core-Loc | 11.9 | 3350 | 7.0 | 3350 | 2 |
| 12 | IA | 2 | Core-Loc | 11.9 | 3350 | 7.0 | 3350 | 8 |
| 13 | IA<br>IB | 2<br>3 | Core-Loc | 11.9 | 3350 | 7.0 | 3350 | 35 |
| 14 | IB | 5 | Accropode | 14.0 | 3350 | 8.3 | 3350 | 41 |
| 15 | IB | 5 | Accropode | 19.9 | 3350 | 8.3 | 3350 | 8 |
| 16 | IB[4] | 5 | Accropode | 14.0 | 3350 | 8.3 | 3350 | 4 |
| 17 | IB[4] | 5 | Core-Loc | 11.9 | 3350 | 7.0 | 3350 | 4 |

[1]  Does not include units displaced on structure.
[2]  Toe trench installed.
[3]  Included 5,080-kg stone within buttress.
[4]  20-sec, 8.1-m wave condition omitted from three of five series.

# 4 Two-Dimensional Transmission Tests

## The Model

The purpose of the transmission tests was to develop a breakwater cross section at a small scale that reproduced transmission of the proposed prototype breakwater. The small-scale cross section developed would be used during tests of the proposed Noyo breakwater three-dimensional harbor model tests conducted by Bottin (1994). Ideally, model transmission tests would be compared to field data, but because the breakwater is proposed and does not exist in the prototype, wave data obtained at the small scale were compared to data collected during two-dimensional stability tests at a 1:43 scale.

### Design of model

Transmission tests were conducted at a 1:75 undistorted scale, which was the same scale used in the Noyo three-dimensional harbor model. Table 9 shows model-to-prototype relations defined in terms of $l$ and $t$ at a 1:75 scale. Froude model law (Stevens et al. 1942) was used to scale time relations.

| Table 9 Model-Prototype Scale Relations (1:75 scale) | | |
|---|---|---|
| Characteristic | Dimension | Scale Relations Model:Prototype |
| Length | $l$ | $l_r = $ 1:75 |
| Area | $l^2$ | $a_r = $ 1:5625 |
| Volume | $l^3$ | $v_r = $ 1:421,875 |
| Time | $l^{1/2}$ | $t_r = $ 1:8.7 |

No Accropode armor unit was available to model transmission at a 1:75 scale. Because the tests involved transmission only and not stability, stone was used in the armor layer for the tests.

## Test facilities and equipment

Tests were conducted in the same tank used in the two-dimensional stability tests (Figure 4) and the facilities were operated for the transmission study in the same manner used in the stability tests. The transmission tests, in essence, modeled the two-dimensional stability tests; therefore, it was necessary to place the gages in the same scaled prototype locations used in the two-dimensional stability tests. Data were analyzed using the TSA computer program (Long and Ward 1987) to determine $H$, $H_s$, $H_{max}$, $H_{mo}$, $T$, and $T_p$ mean water levels at each gage, where $H$ = wave height and $H_s$ = significant wave height. Incident/reflected spectra were analyzed using the method of Goda and Suzuki (1976). The cross section was placed on the horizontal section of the slope, 61 m prototype from the 1V:20H slope transition. Transmission was calculated using data obtained from two three-gage arrays placed 105.5 m prototype seaward and shoreward of the structure, respectively.

## Test procedures

Design conditions were based on analyzed data from the two-dimensional stability tests. Measured transmitted wave height $H_t$ from the two-dimensional stability plans is shown as a function of incident wave height $H_i$ in Figures 35 through 37 for regular waves. Prior to testing of small-scale cross sections, comparison criteria were established. The following results and observations were considered to develop transmission test criteria:
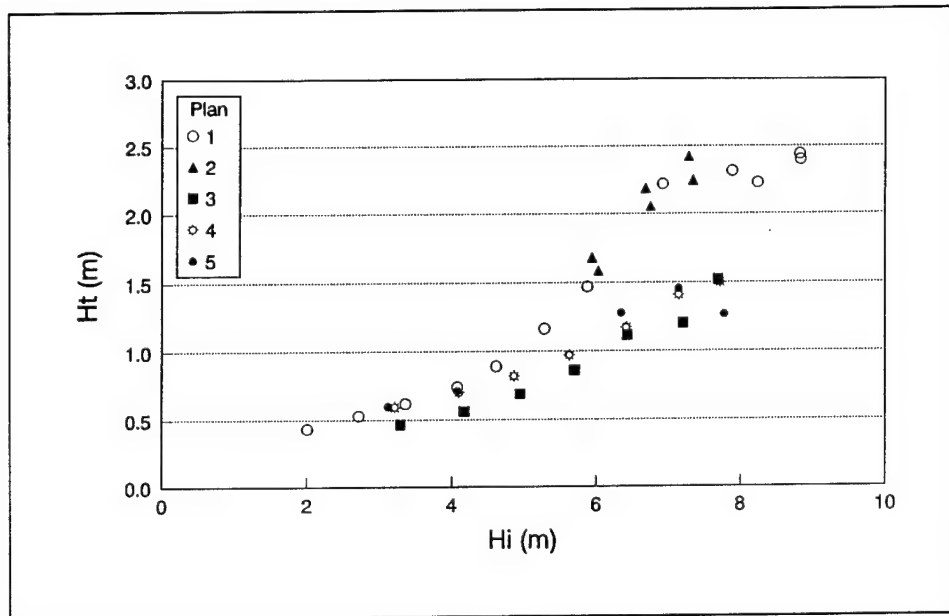


Figure 35. Two-dimensional stability wave transmission, 13-sec waves
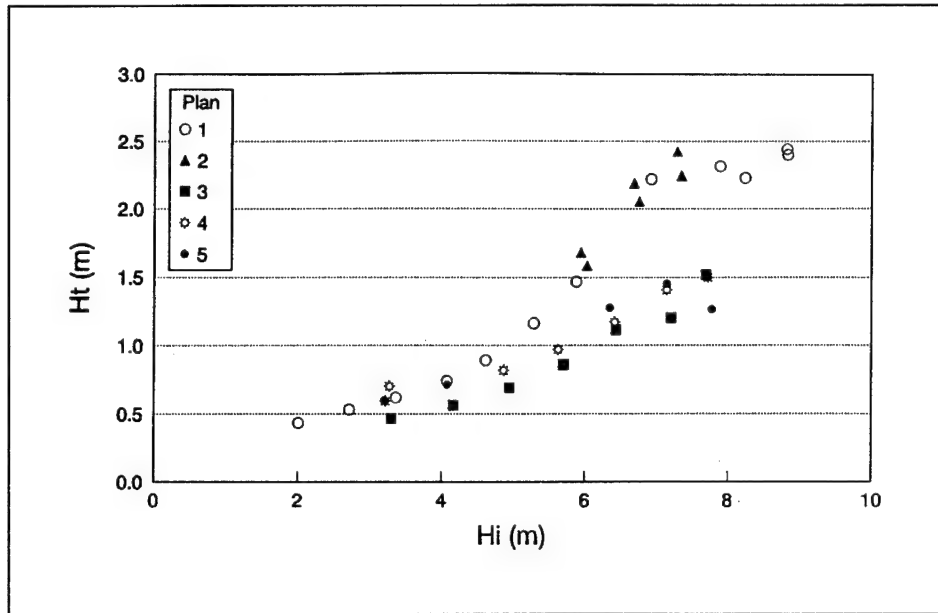
Figure 36. Two-dimensional stability wave transmission, 17-sec waves
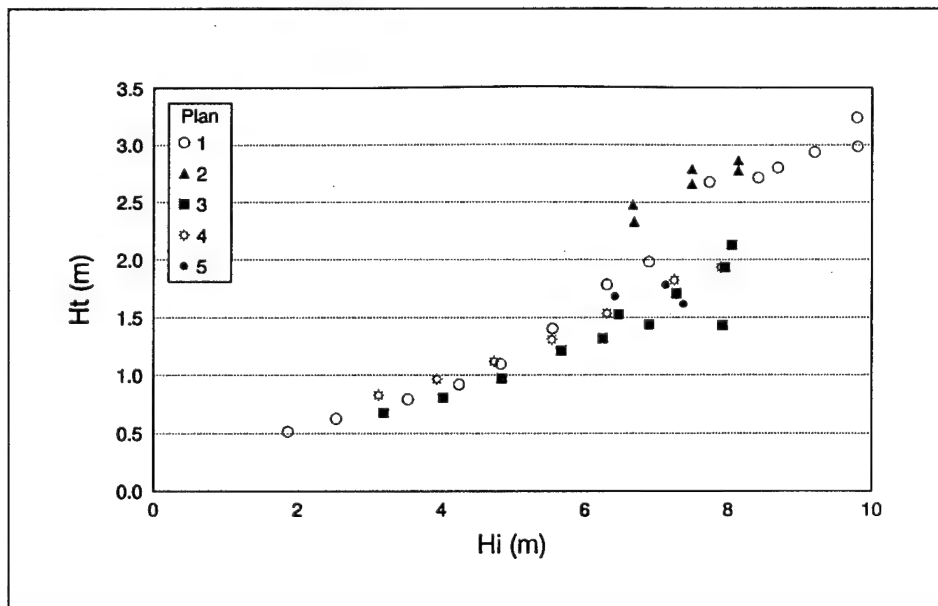


Figure 37. Two-dimensional stability wave transmission, 20-sec waves

*a.* Calibration of the facility showed little difference between wave heights offshore and at the toe of the structure for wave heights less than 6 m (Figures 5 to 10).

*b.* Observations of the stability tests showed wave overtopping did not occur or was minor for heights less than 6 m.

*c.* Tests will be conducted in the three-dimensional harbor model with regular waves only.

*d.* SPN selected Plan 1 as the design cross section from the stability test results.

For the above reasons, comparison of small-scale and large-scale wave transmission was limited to regular waves with heights less than 6 m from Plan 1 tests. Water surface elevations from Array 1, positioned 61 m shoreward of the structure, were used as the incident wave height for the purpose of comparing transmission and computing transmission coefficients.

Regular and random wave heights were generated for periods of 13, 17, and 20 sec; however, only regular waves were used for comparison to Plan 1 transmission values. Incident wave heights were estimated from the calibration curves obtained in the two-dimensional stability study for regular waves (Figures 8 to 10). Some plans were subjected to only a limited number of conditions if it was evident the structure would not duplicate transmission from the 1:43.3-scale cross section.

Photographs were taken prior to conducting transmission tests. Because stability was not a direct concern for transmission, use of low-level waves to settle and nest the units was not necessary. Prototype test duration was 130 min for random waves, and 26 min for regular waves. All wave conditions were conducted for one cycle. Overtopping and general structural stability were noted during and between test cycles, and at the completion of the test series. Photographs were taken of the structure with the tank drained after testing was completed.

## Model construction

The cross section which was determined to have the same transmission characteristics of the large-scale cross section would be used as the design section in the three-dimensional harbor model of Noyo. It was important to construct each cross section in the manner that would be used to construct the breakwater for the three-dimensional harbor study. The core and underlayer of the transmission test sections were placed by bucket or shovel, smoothed to grade, and compacted with hand trowels. The armor layer was placed on the structure by bucket or shovel and smoothed to grade without compaction. The two-dimensional stability plans consisted of an underlayer and core materials of equal size. Therefore, all transmission plans were constructed of an armor layer, geometrically scaled to the proper thickness of the prototype, placed over a core.

## Method of calculating transmission

Transmission is dependent, in part, on incident wave period. Small- and large-scale comparisons of transmission were therefore examined for each period tested in the two-dimensional stability tests. Both transmitted wave heights and the transmission coefficient $K_t$ of the small- and large-scale plans were compared. The transmission coefficient is defined as

$$K_t = \frac{H_t}{H_i} \qquad (3)$$

# Results

Transmission was measured for nine cross sections, which were all built to the same physical dimensions as Plan 1. Each cross section consisted of an armor layer $W_1$, core and underlayer $W_3$, and toe berm $W_4$. Stone was used as the primary armor unit in all plans because no Accropode unit was available to model the 9-m$^3$ (24-ton) unit at a 1:75 scale. Stone and Accropodes have different transmission characteristics; therefore, a thin metal barrier was placed vertically in the cross section for some plans to compensate for these differences. A plan was considered acceptable for a particular period if small-scale values of $K_t$ were within 10 percent of the large-scale $K_t$ values. Results of each plan are described below.

## Plan A

Plan A (Figure 38) consisted of 29- to 44-g armor stone and 0.7- to 2.0-g underlayer and core stone. The armor stone size was selected by directly scaling a 9-m$^3$ stone to a 1:75 scale. The underlayer and core sizes were determined by reducing the prototype stone to a 1:75 scale and increasing the size 50 percent to roughly account for scale effects. Transmitted versus incident wave height is shown in Figures 39, 40, and 41 for 13-, 17-, and 20-sec waves, respectively. Small-scale and Plan 1 transmission coefficients are compared in Figure 42. Differences between Plan A $K_t$ values and Plan 1 values were -17 percent for 13-sec waves, +25 percent for 17-sec waves, and +33 percent for 20-sec waves. The armor stone used was unstable for the tests and it was noted that stones were displaced on the crown. Although stability was not a factor for the tests, the displaced stones at the crown of the cross section lowered the crest elevation and permitted wave energy to overtop the breakwater.

## Plan B

The armor stone of Plan A was replaced with heavier stone, 44 to 86 g, and the core size remained the same for Plan B (Figure 38). It was desired to increase transmission for the 13-sec waves and decrease transmission for 17- and 20-sec waves. The larger armor stone was more porous and would allow more energy to transmit through the breakwater, but it was also more stable and would maintain the design crest elevation and reduce overtopping. Figures 39, 41, and 42 show that the more stable armor stone reduced transmission for the 20-sec waves by 8 percent to +25 percent, but transmission also decreased for 13-sec waves to -28 percent of Plan 1 values of $K_t$. Use of the heavier stone increased transmission for the 17-sec waves to +30 percent of Plan 1 values (Figures 40 and 42).
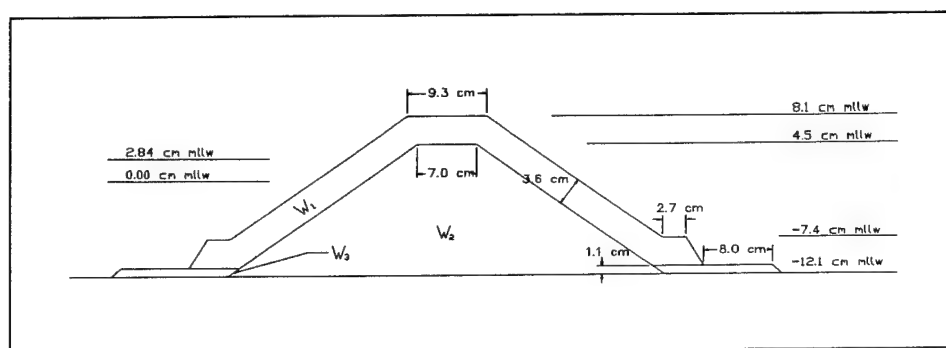


Figure 38.  Cross section of Plans A, B, and C

## Plan C

Smaller core material, 0.09 to 0.7 g, and the armor stone of  Plan B were used for Plan C (Figure 38) to reduce transmission for the 17- and 20-sec waves.  Transmission increased slightly for 13-sec waves to -22 percent of Plan 1 values (Figures 39 and 42), but decreased for 17- and 20-sec waves to +20 percent and +8 percent of Plan 1 values, respectively (Figures 40, 41, and 42).  Use of different armor stone size between Plans A and B and core stone size between Plans B and C had little effect on transmission for the 13-sec period.

## Plan D

A cross section was developed to transmit more energy for the 13-sec waves, yet reduce transmission for the 17- and 20-sec periods.  The shorter
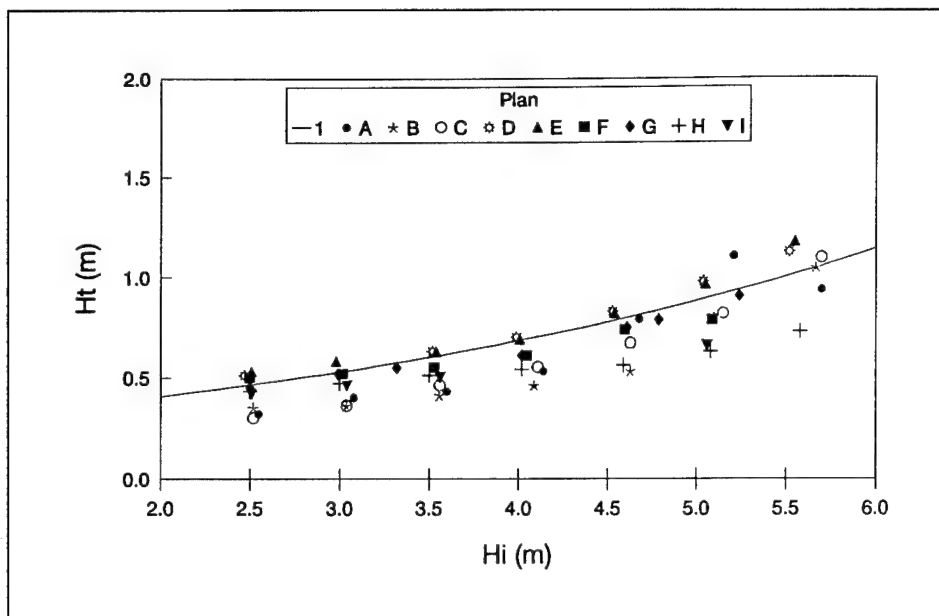
Figure 39. Wave transmission for Plans 1 and A through I, 13-sec waves
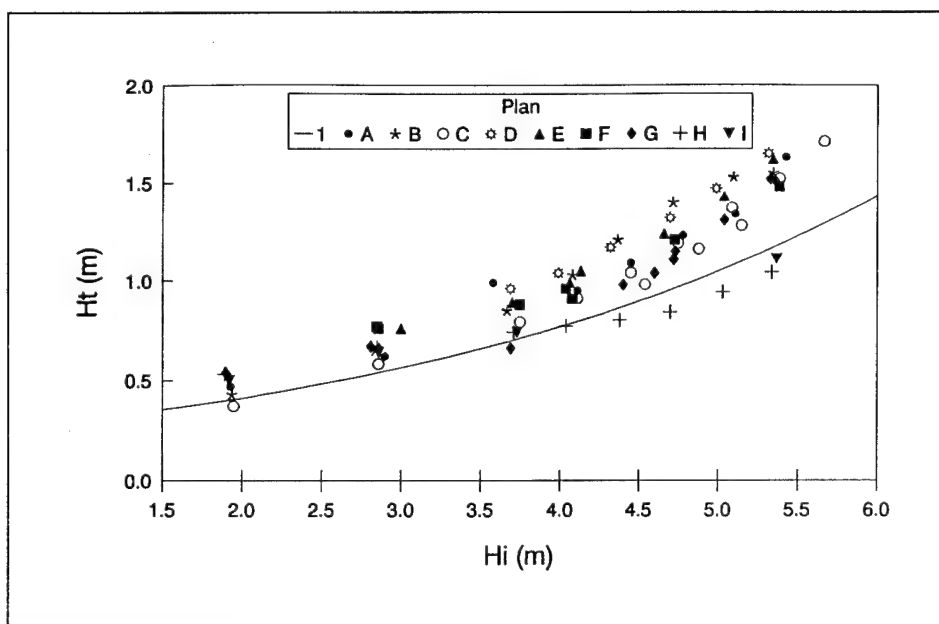


Figure 40. Wave transmission for Plans 1 and A through I, 17-sec waves
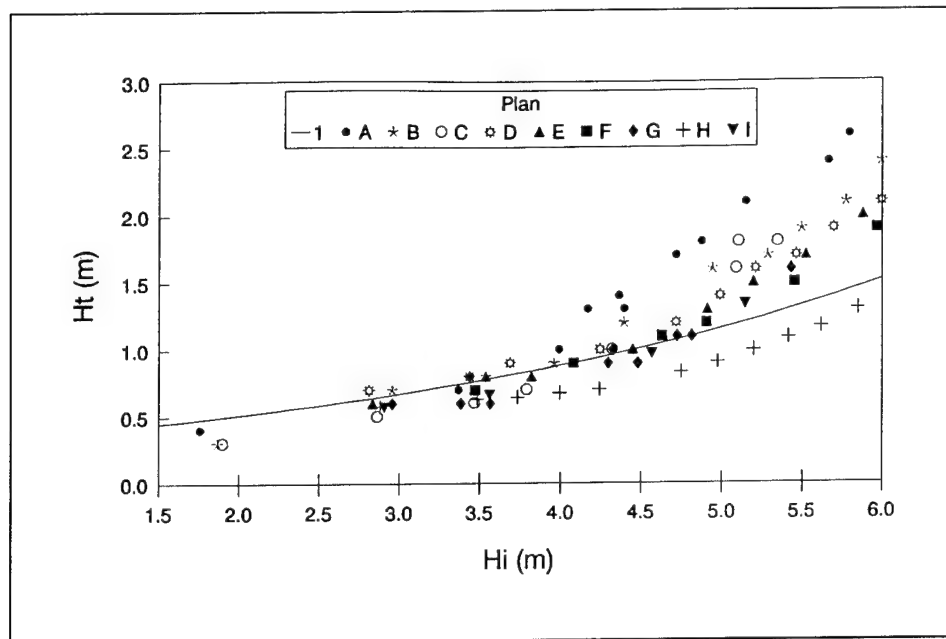
Figure 41. Wave transmission for Plans 1 and A through I, 20-sec waves
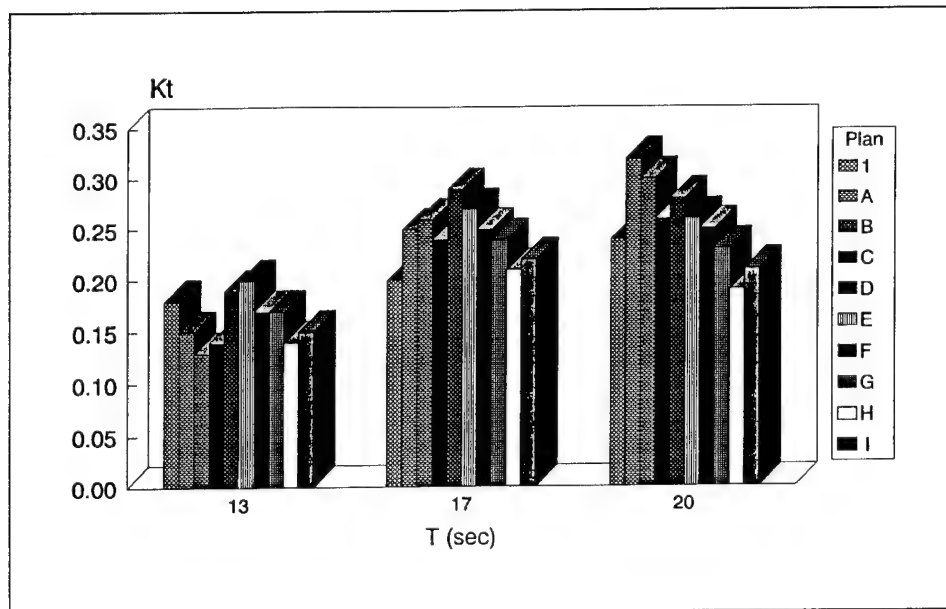


Figure 42. Comparison of $K_t$ between Plan 1 and Plans A through I

period waves approached depth-limited breaking conditions near the cross section, and it was felt that transmission of the 13-sec waves occurred mainly through the core material. Therefore, core and armor stone sizes were increased for Plan D to 86-148 g and 5-11 g, respectively. Reduction of transmission for the 17- and 20-sec periods was attempted by placing a thin metal strip level into the upper portion of the structure. The barrier was placed level with the crown elevation and into the structure a distance $Y_1 = 5.1$ cm (Figure 43). Figures 39 and 42 show that transmitted 13-sec waves for Plan D increased to +6 percent of Plan 1 values. However, transmission for the 17-sec and 20-sec waves also increased to 45 and 17 percent, respectively, higher than desired transmission (Figures 40 through 42).
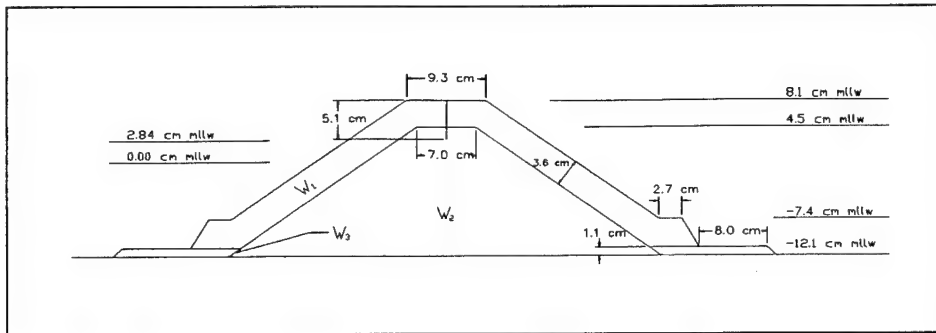


Figure 43. Cross section of Plan D

## Plan E

The stone sizes of Plan D were used for Plan E, but the vertical barrier distance $Y_1$ was increased to 7.3 cm (Figure 44). The longer barrier reduced transmission to +35 percent for the 17-sec waves and +8 percent for 20-sec waves (Figures 40, 41, and 42). The transmitted 13-sec waves increased slightly to +11 percent (Figures 39 and 42). Transmitted heights for the 13- and 20-sec periods were acceptable; however, further reduction in transmission was needed for the 17-sec waves.
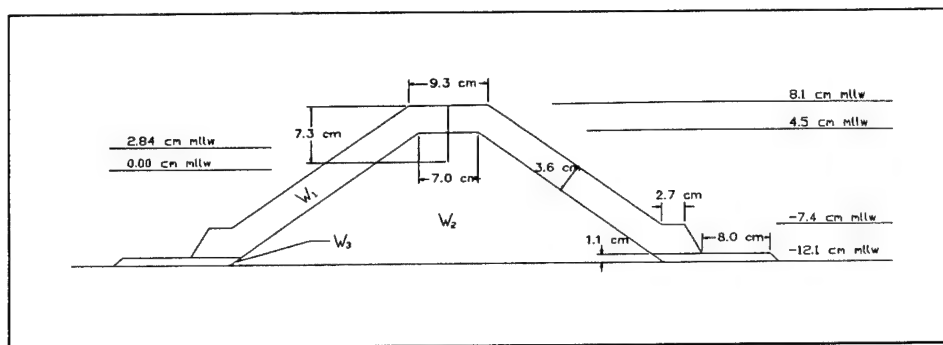
Figure 44.  Cross section of Plan E

## Plan F

To reduce 17-sec transmitted waves, $Y_1$ was increased to 8.9 cm (Figure 45).  Figures 40 and 42 show 17-sec transmitted waves were less than Plan E waves, but were 25 percent higher than Plan 1 $K_t$ values.  Transmitted waves were also reduced for 13-sec and 20-sec periods to -6 and +4 percent, respectively, and were within the acceptable range (Figures 39, 41, and 42).
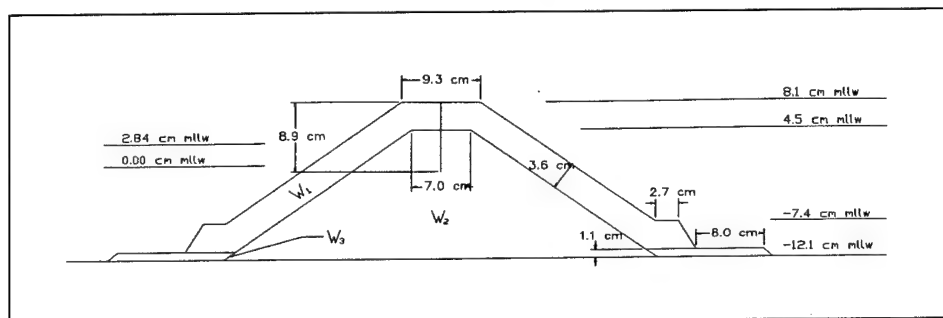


Figure 45.  Cross section of Plan F

## Plan G

The vertical barrier was increased to 11.4 cm for Plan G (Figure 46).  The longer barrier had no effect on transmission coefficients from Plan F for the 13-sec period, -6 percent of Plan 1 values, but reduced 17-sec transmission to +20 percent of Plan 1 transmission, and reduced $K_t$ to -4 percent of Plan 1 values for 20-sec waves. (Figures 37 through 42).  The increase of $Y_1$ in Plans D through G reduced transmission coefficients for all periods tested.

Transmitted wave heights were within ±10 percent for the 13-sec period for Plans D, F, and G, and was +11 percent for Plan E.  Plans E through G gave acceptable $K_t$ values for the 20-sec period, but all vertical-barrier plans gave higher transmitted wave heights than Plan 1 values for the 17-sec period.
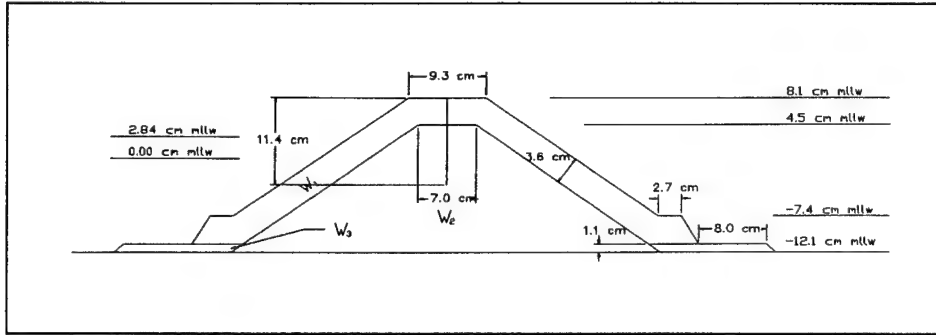
Figure 46. Cross section of Plan G

## Plan H

Plan H was constructed to lower transmission for the 17-sec period and hopefully maintain the transmission characteristics for the 13- and 20-sec periods. Armor and core stone sizes and total barrier length remained the same as in Plan G, but the barrier was raised so that it projected a distance $Y_2 = 2.5$ cm above the crown with $Y_1 = 8.9$ cm (Figure 47). Plan H reduced 17-sec transmission to +5 percent of Plan 1 values, but also lowered the 13-sec and 20-sec transmitted heights to -22 and -21 percent, respectively (Figures 39 through 42).
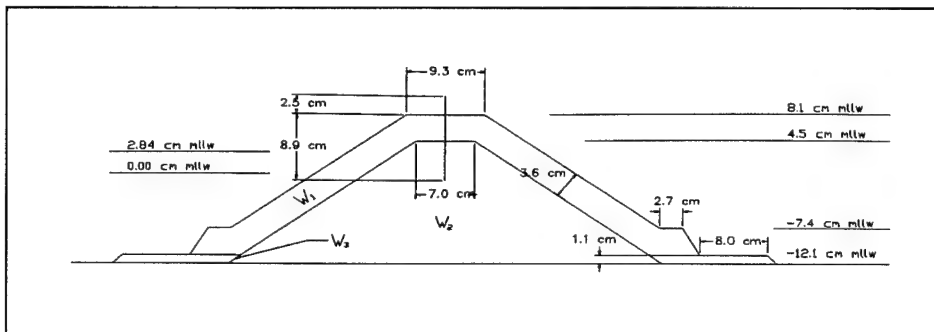


Figure 47. Cross section of Plan H

## Plan I

To increase transmitted energy for 13- and 20-sec waves, the vertical distance above the crest elevation of the transmission barrier $Y_2$ was decreased to 1.3 cm and $Y_1$ was kept at 8.9 cm for Plan I (Figure 48). The 17-sec transmitted waves were 10 percent higher than Plan 1 values, but transmitted waves for the 13- and 20-sec periods were -17 and -12 percent of Plan 1 values, respectively. (Figures 39 through 42).
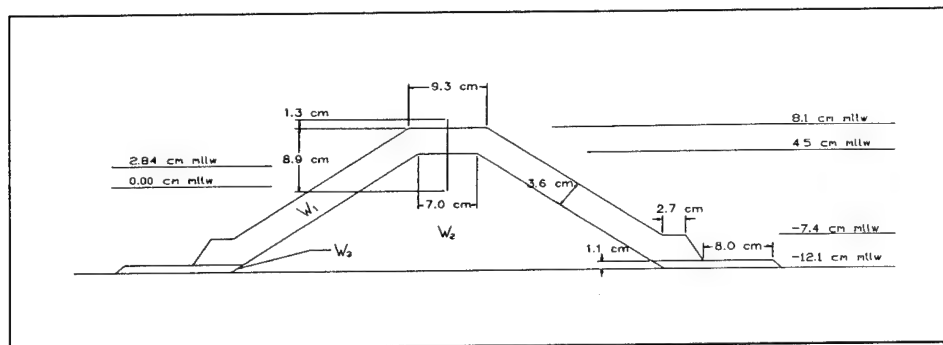
Figure 48.  Cross section of Plan I

## Summary of Transmission Tests

Material sizes and barrier lengths used for transmission tests are summarized in Table 10.  Small-scale transmission tests were used to determine the breakwater cross section at a 1:75 scale that would reproduce transmitted wave heights obtained during the stability tests with a 1:43 scale. The 1:75 cross section developed would be used in the Noyo three-dimensional harbor model.  It was desired to use one cross section for the entire test series to maintain efficient testing of the harbor model.  However, none of the nine plans tested at the small scale reproduced the Plan 1 transmitted heights for all the test periods, but several plans reproduced the desired $H_t$ for one or more periods.  Based on the small-scale test results, the combination of Plans F and H provided the best agreement with transmitted wave heights of Plan 1, and are also the most convenient and practical combination of plans to readily alter.  Plans F and H consist of the same armor and core stone sizes and $Y_1$ is equal.  The difference between the plans is $Y_2 = 0$ in Plan F, whereas $Y_2 = 2.5$ cm in Plan H.  For use in the three-dimensional tests, the breakwater would be constructed to allow placement and removal of the metal strips.  The 8.9-cm barrier (Plan F) would be inserted for 13- and 20-sec waves and the 11.4-cm barrier would be placed for 17-sec waves.

An important detail to note is that the test periods differ between the two-dimensional and three-dimensional studies.  The three-dimensional tests include periods of 7, 9, 11, 13, 15, 17, and 19 sec.  It was felt that Plan F should be used for periods of 13 sec and shorter and for the 19-sec period, but it was uncertain which plan should be used for the 15-sec period.  Because of this uncertainty, four 15-sec waves of varying height were generated with Plan F installed, and incident and transmitted wave heights were obtained. Although no large-scale data were collected for this period, the transmitted wave heights should be within the range of the 13- and 17-sec $H_t$ values if the appropriate plan was used.  Transmitted and incident wave heights were plotted in Figure 49 with 13-sec transmission data using Plan F and 17-sec data using Plan H.  The figure shows 15-sec transmission data with Plan F are higher than 13-sec values and lower than 17-sec values.  Figure 49 indicates

Plan F should be used with the 15-sec period in the three-dimensional harbor model.

| Plan | $W_1$ g | $W_3$ g | $W_4$ g | $Y_1$ cm | $Y_2$ cm |
|------|---------|---------|---------|----------|----------|
| **Table 10**<br>**Transmission Model Material Sizes** | | | | | |
| A | 29 to 44 | 0.7 to 2.0 | 0.09 to 0.7 | - | - |
| B | 44 to 86 | 0.7 to 2.0 | 0.09 to 0.7 | - | - |
| C | 44 to 86 | 0.09 to 0.7 | 0.09 to 0.7 | - | - |
| D | 86 to 148 | 5 to 11 | 0.09 to 0.7 | 5.1 | - |
| E | 86 to 148 | 5 to 11 | 0.09 to 0.7 | 7.3 | - |
| F | 86 to 148 | 5 to 11 | 0.09 to 0.7 | 8.9 | - |
| G | 86 to 148 | 5 to 11 | 0.09 to 0.7 | 11.4 | - |
| H | 86 to 148 | 5 to 11 | 0.09 to 0.7 | 8.9 | 2.5 |
| I | 86 to 148 | 5 to 11 | 0.09 to 0.7 | 10.2 | 1.3 |
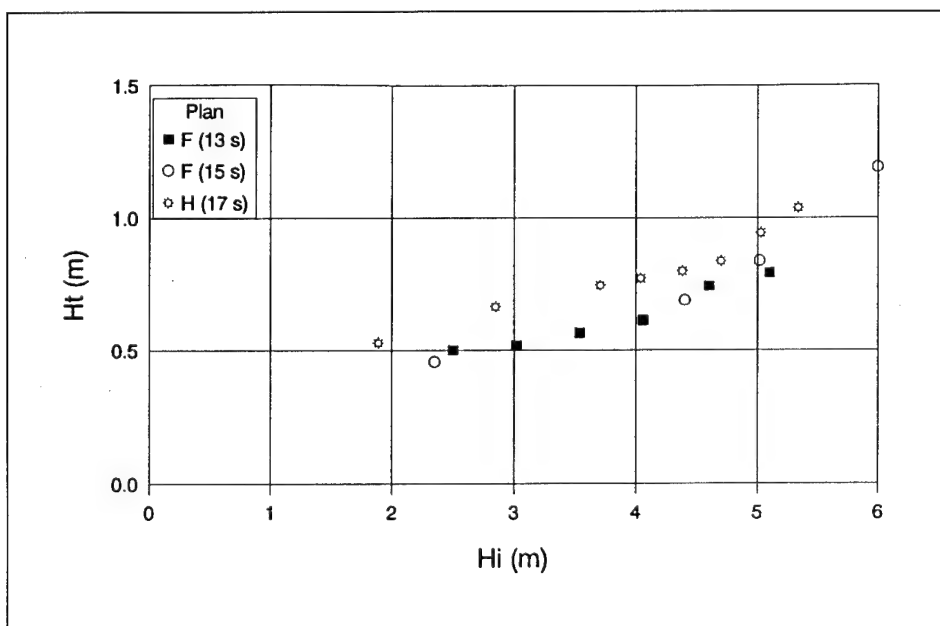


Figure 49. Transmitted versus incident wave height for Plan F, 15-sec waves

# 5 Conclusions

Stability tests were conducted in two and three dimensions to identify a stable breakwater cross section for the proposed Noyo Harbor breakwater. Additionally, two-dimensional transmission tests were performed to determine a small-scale cross section that reproduced transmission of the proposed breakwater cross section. The small-scale cross section was used in three-dimensional harbor tests of Noyo Harbor (Bottin 1994). Results of the stability and transmission tests are summarized in this chapter.

## Two-Dimensional Stability Tests

Based on the results of the two-dimensional stability test conditions reported herein, it was concluded that:

a. The maximum $H_{mo}$ measured at the location of the breakwater for random waves was 5.8 m. The higher waves in the spectra became depth limited and broke if the wave generator stroke was increased. Tests were conducted with regular waves up to 8.2 m to subject the breakwater to higher wave energy.

b. Five two-dimensional stability plans were tested at a 1:43.3 scale, two consisted of an Accropode armor layer, and three consisted of dolosse. Damage did not exceed 2 percent for any of the plans and all were considered not damaged. However, continuous rocking of units was observed during Plan 3 tests (3.8-m$^3$ dolos), and the plan was termed moderately stable. Plan 5 (5.9-m$^3$ dolos) was stable, but numerous units rocked in place, and it was recommended that a dolos breakwater be constructed of units 6 m$^3$ or greater. Plans 1 and 4 (9-m$^3$ Accropodes and 7.9-m$^3$ dolosse, respectively) were considered conservative designs because it was felt the structures could withstand much higher waves than the test conditions generated. Plan 2 was constructed of 7.6-m$^3$ Accropodes and was stable.

# Three-Dimensional Stability Tests

Three-dimensional stability tests were performed with random waves only for offshore conditions from the west-northwest wave direction. Results of Corson et al. (1986) indicated the most severe waves approached the harbor from the west-northwest. Approximately 425 by 425 m of the prototype bathymetry in the vicinity of the proposed structure was modeled by a molded concrete bottom. The contours of the model extended to the 15-m mllw depth and the basin floor represented -24.4 m mllw.

Two breakwater shapes were tested for the proposed breakwater. Eight plans were tested with the original plan, and nine plans were tested with a modified breakwater plan. All tests with the original plan consisted of 14- and 8.3-m$^3$ Accropodes and only the toe configuration differed between plans. Armor units used on the modified plan included 14- and 8.3-m$^3$ Accropodes, 11.9- and 7.0-m$^3$ Core-Locs, and 19- and 8.3-m$^3$ Accropodes. In addition to different armor units, the toe buttress configurations also varied between modified breakwater plans. Based on results of the three-dimensional stability tests for the given test conditions, it was concluded that:

*a.* The armor units selected for the original design were stable if the toe was stable. Plan 6 included a metal strip at the base of the structure to stabilize the toe. Analogous results would be expected if a toe trench or driven piles were used to fix the toe. After tests with Storm I wave conditions (Table 7), one Accropode was displaced, but no further damage occurred after the structure was subjected to Storm IA conditions. Although the structure was stable, it was felt that lighter units would not survive the storm conditions tested.

*b.* Neither of the plans constructed of a standard toe buttress, two stones high and three stones wide, with the original design provided sufficient stability to the toe to support the armor units. Plan 2 contained 3,350-kg stone in the buttress, and 5,080-kg stone was placed at the toe of the 14-m$^3$ Accropodes in Plan 3.

*c.* A wider buttress was found to increase toe stability in most areas of the structure during tests with the original plan. An 18.3-m-wide buttress of 3,350-kg stone fronting the 14-m$^3$ units on the sea side gave sufficient stability to the overlying units (Plans 4, 7, and 8). An 18.3-m-wide buttress on the lee side was displaced and caused Accropodes to slip on the structure slope (Plan 5). A 24.4-m-wide buttress of 3,350-kg stone remained in place during tests; however, a scour hole developed in the wider buttress, which caused the breakwater to fail (Plan 7). Heavier stone (5,080 kg) was placed in the vicinity of the scour hole, but was also dislodged, resulting in breakwater failure (Plan 8).

d. It was determined that the wave height in the vicinity of the lee side of the north roundhead could be reduced by 10 to 15 percent if the crest width at the head was reduced from 29 m to 9.1 m. Although the energy was reduced on the north roundhead lee side, a toe buttress of 3,350-kg stone, three stones wide, used in Plan 9 was not sufficient in stabilizing the toe.

e. The modified structure was found to be stable for two successive series of Storm IA waves with a wider toe buttress of 3,350-kg stone installed with either Accropodes (Plan 10) or Core-Locs (Plans 11 through 13) used in the armor layer. However, the buttress deteriorated if the structure was subjected to five successive storms without rebuilding the structure. Neither the 14-m$^3$ Accropodes (Plan 14) nor the 11.9-m$^3$ Core-Locs (Plan 13) placed on the north roundhead were of sufficient size to stabilize the breakwater. A 19.9-m$^3$ Accropode was required to provide sufficient breakwater stability with a stone toe buttress for five consecutive storms without repair (Plan 15). A heavier Core-Loc model unit was not available at the time of testing, but based on previous test observations, it was assumed that a prototype Core-Loc weight of at least 16.9 m$^3$ would be required for stability for the wave conditions tested.

f. Although it was desired to achieve breakwater stability for all depth-limited wave conditions, wave hindcast data indicated that deepwater waves higher than 6.7 m did not occur over a 20-year period of measurement for wave periods greater than 18.7 sec (Corson et al. 1986). The breakwater was found to be stable using both 14-m$^3$ Accropodes (Plan 16) and 11.9-m$^3$ Core-Locs (Plan 17) placed on the north roundhead for five successive storms if the 20-sec, 8.1-m wave condition at the breakwater was omitted for three of the storms.

## Two-Dimensional Transmission Tests

Transmission tests were conducted at a 1:75 scale and the results were compared to two-dimensional wave heights of Plan 1. The cross section developed was to be used for three-dimensional harbor tests of Noyo with regular waves only. Therefore, regular waves were used for comparison between the small-scale and 1:43-scale tests.

Nine plans were used in transmission tests, but no one plan tested duplicated Plan 1 transmission for all of the test periods (13, 17, and 20 sec). However, 13- and 20-sec transmitted waves with Plan F were comparable to Plan 1 transmission, and 17-sec waves with Plan H gave acceptable transmission values. Both Plans F and H consisted of a vertical barrier inserted at the same depth into the cross section, but the barrier of Plan H extended 2.5 cm above the crown. It was determined that both plans could be used in the harbor model and interchanged readily for the necessary wave period.

# References

Bottin, R. R. (1994). "Noyo River and Harbor, California, design for harbor entrance protection; Coastal model investigation," Technical Report CERC-94-5, U.S. Army Engineer Waterways Experiment Station, Vicksburg, MS.

Bottin R. R., Acuff, H. F., and Markle, D. G. (1988). "Noyo River and Harbor, California, design for wave and surge protection; Coastal model investigation," Technical Report CERC-88-15, U.S. Army Engineer Waterways Experiment Station, Vicksburg, MS.

Bottin, R. R., and Mize, M. G. (1989). "Noyo River and Harbor, California, design for wave protection, supplemental tests; Coastal model investigation," Technical Report CERC-89-18, U.S. Army Engineer Waterways Experiment Station, Vicksburg, MS.

Chida, T., Kaihatsu, S., and Kobayashi, M. (1992). "Introduction of the new type of artificial blocks (Accropode)," *Journal of Electric Power Civil Engineering* 236, 90-99 (in Japanese).

Corson, W. D., Abel, C. E., Brooks, R. M., and Farrar, P. D. (1986). "Pacific Coast hindcast deepwater wave information,"WIS Report 14, U.S. Army Engineer Waterways Experiment Station, Vicksburg, MS.

Goda, T., and Suzuki, Y. (1976). "Estimation of incident and reflected waves in random wave experiments." *Proceedings of the 15th Coastal Engineering Conference*. American Society of Civil Engineers, Honolulu, HI, 828-845.

Hudson, R. Y. (1975). "Reliability of rubble-mound breakwater stability models," Miscellaneous Paper H-75-5, U.S. Army Engineer Waterways Experiment Station, Vicksburg, MS.

Hughes, S. A. (1984). "The TMA shallow-water spectrum description and applications," Technical Report CERC-84-7, U.S. Army Engineer Waterways Experiment Station, Vicksburg, MS.

Keulegan, G. H. (1973). "Wave transmission through rock structures; Hydraulic model investigation," Research Report H-73-1, U.S. Army Engineer Waterways Experiment Station, Vicksburg, MS.

Long, C. E., and Ward, D. L. (1987). "Time series analysis," unpublished computer program, U.S. Army Engineer Waterways Experiment Station, Vicksburg, MS.

Markle, D. G. (1989). "Stability of toe berm armor stone and toe buttressing stone on rubble-mound breakwaters and jetties," Technical Report REMR-CO-12, U.S. Army Engineer Waterways Experiment Station, Vicksburg, MS.

Melby, J. A., and Turk, G. F. (1994). "Core-Loc concrete armor unit design," CETN-III-53, U.S. Army Engineer Waterways Experiment Station, Vicksburg, MS.

*Shore protection manual.* (1984). 4th ed., 2 Vol, U.S. Army Engineer Waterways Experiment Station, U.S. Government Printing Office, Washington, DC.

Stevens, J. C., Bardsley, C. E., Lane, E. W., and Straub, L. G. (1942). "Hydraulic models," *Manuals on Engineering Practice No. 25*, American Society of Civil Engineers, New York, NY.

U.S. Army Engineer District, San Francisco. (1979). "Plan of study for advance engineering and design, Noyo River and Harbor, Mendocino County, California," San Francisco, CA.

# Appendix A
# Concrete Armor Unit Structural Investigation for the Offshore Noyo, California, Breakwater

**by Jeffrey A. Melby and George F. Turk**

## Introduction

This report contains structural analyses of dolos, Core-Loc, and Accropode concrete armor shapes for the offshore breakwater at Noyo Harbor, CA. The PC computer-based program *PC-ARMOR* is used to investigate the structural response of the hydraulically stable dolos options. Structural information on the selected Core-Loc and Accropode units is based on a high-resolution finite element method (FEM) comparison (Melby and Turk 1995). Additional information is provided regarding concrete mix design that may be useful in evaluating the concrete armoring options.

Because the majority of worldwide research conducted to date on concrete armor response has concentrated on hydraulic stability, knowledge of the structural response of many concrete armor unit (CAU) types is limited. Static, in-place wave loading and impact loading are the significant components contributing to mechanical stress levels. For dolosse, the Corps has made significant strides in measuring these structural stresses and in understanding armor unit structural response. But little work has been done to quantify structural response in other armor shapes.

As a result of the dolos measurement program, a stress prediction methodology and an associated reliability-based structural design technique have been developed (Melby 1990, 1993; Melby and Turk 1992). Structural analyses obtained for the hydraulically stable dolos investigated within this report were made in accordance with these methods.

Core-Loc and Accropode armor units react differently than dolosse because they are more stout and are placed in a thinner layer on a steeper slope. On a dolos slope, typically 1 to 2 percent of the units are rocking for even small

wave conditions; and these units can be assumed to break (Melby and Turk 1993). But the Core-Loc and Accropode layers typically have no units rocking for the design wave condition, and, because of their blocky shapes, can be assumed to have no initial breakage, provided a stringent concrete quality control program is followed.

The dolos characteristic shape (slender appendages extending from a slender central section) results in very high stresses in the central section. But because of this slender central section, structural measurements that utilize slender beam theory are relatively easily made. Due to the blocky shape, Core-Loc and Accropode will typically have much smaller stress levels. This is fortuitous as the blocky shape does not lend itself to slender beam theory assumptions and accurate strain measurements require much more complicated and expensive surface strain gage structural instrumentation. Some structural measurements have been made using load-cell-instrumented Accropodes. But because the load cell requires slender beam theory assumptions to interpret the data, these measurements are only qualitatively useful. No surface-mounted strain gage measurements of Core-Loc or Accropode response have been made to date. The structural analyses made herein are therefore restricted to review of some finite element studies of the units under various loading configurations. Because of the blocky shapes it is assumed that the stresses are low under normal loading conditions and that representative FEM analyses are adequate. But, like other concrete armor units, impact stresses in the blocky units will likely be very large if the unit undergoes a rollover either during construction or due to instability on the breakwater. Therefore armor unit-to-unit impacts from large movements should be minimized.

Accropode construction specifications often call for the units to be dynamically placed. In this placement strategy, the units are dropped from a small height, less than a meter, to enhance the wedging and interlocking between units. It is expected that Core-Loc stability will also be enhanced by this placement strategy. Numerical impact loading comparisons of Accropodes and Core-Locs are currently underway to determine if this is a reasonable assumption.

# Structural Design for Dolosse

## Introduction

The dolos design stresses obtained from *PC-ARMOR* were computed based on three primary structural studies:

   a.  Crescent City Prototype Dolosse Study (CCPDS) (Howell, Rhee, and Rosati 1990).

*b.* Large-Scale Dolos Flume Study (LSDFS) (Melby and Turk 1993).

*c.* Small-Scale Dolos Flume Study (SSDFS) (Melby 1992).

The methods used to empirically determine the design stress are from Melby (1993). Within *PC-ARMOR*, static and wave-loading-induced stress probability distri-bution moments are computed based on static data from the LSDFS and pulsating or wave loading data from the CCPDS. Distributions are then calcu-lated and combined to get a total stable stress design distribution. The program assumes that the static and wave-loading stresses are statistically independent.

Relative magnitudes of the maximum tensile stresses in a dolos due to various loads are shown in Figure A1. It can be seen that the stresses induced in dolosse when they are sitting in the casting yard or being picked by a crane are of the same order of magnitude as the largest pulsating stresses. Static mean stresses on the breakwater are double the casting yard stresses. The static stress mean plus one standard deviation is three times the casting yard stress. The impact stress for a moderate drop of one tenth the fluke length is shown for 9- and 18-tonne dolosse. It can be seen that these stresses are nearly ten times the casting yard stress. Measurements of impact stresses for dolosse constituted a major part of the LSDFS. The tests indicated that the impact stress was typically very high and that rocking dolosse would probably break. Therefore, it is imperative that slender CAUs remain hydraulically stable, with a minimal number of units rocking, to avoid impact stresses.

The input parameters for the dolos structural analysis were chosen based on the hydraulic stability study as follows: wave height, $H = 8.5\ m$; waist ratio, $r_w = 0.32$; specific gravity, $S_a=2.34$; slope, $cot\theta = 2$. The design stress exceedance probability was chosen to be $P = 2\ percent$. The results of the dolos structural analysis, as output from PC-ARMOR, are listed in Table A1. These values indicate that the design stress level for the return period of the design event will be exceeded in 2 percent of the on-slope units. This design stress can be interpreted such that, for every 100 stable dolosse on-slope, two will experience a tensile stress level of at least the design stress level during a design event. This stress computation method does not imply that if the unit experiences this stress level it will fail. Also, the prediction methodology used to determine the design stress is approximately 10 to 20 percent conservative. Therefore, it is likely that the stable design stress will be exceeded in very few dolosse.

## Dolos reliability analysis

Although the above stress prediction methods allow incorporation of some of the uncertainties associated with the design stress level measurement, they do not include all of the significant uncertainties nor any of the strength uncer-tainties. For that reason, the dolos structural analysis has been recently
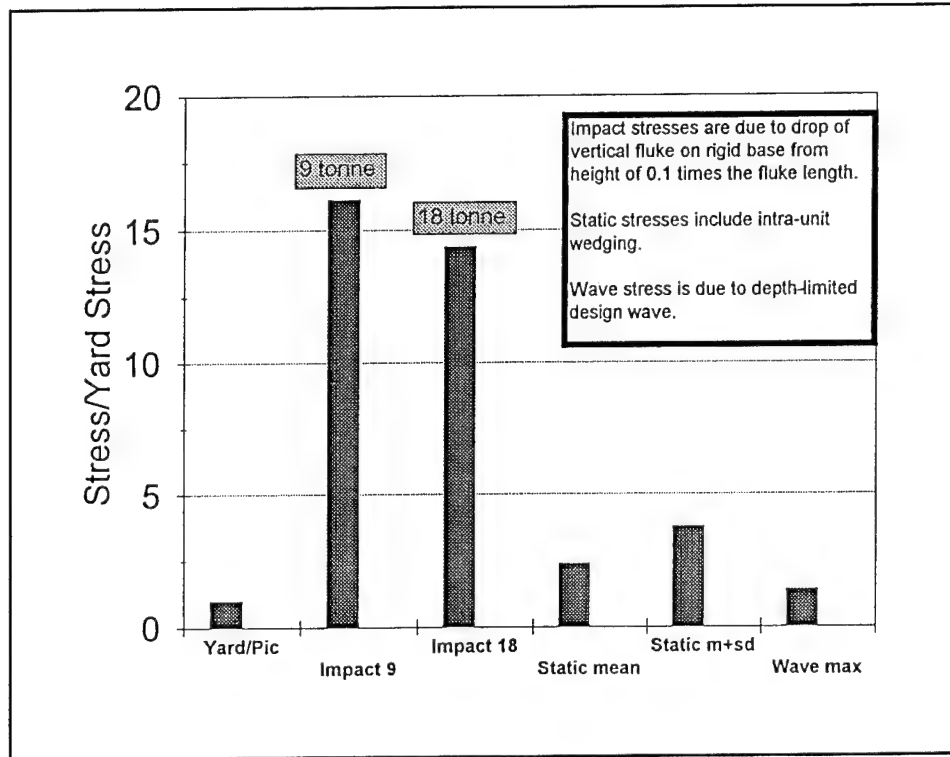
Figure A1. Relative magnitude of dolos stresses for various loads

| Table A1 Dolos Design Stresses from PC-ARMOR | | |
|---|---|---|
| Unit | $W$, tonnes | Stress MPa |
| Dolos | 9 | 3.2 |
| Dolos | 19 | 4.0 |
| Dolos | 14 | 3.7 |

extended using a Level 2 first-order-second-moment reliability analysis. The methods utilize the standard form of the load and resistance factor design (LRFD) equation of the form

$$\gamma Q_n = \phi R_n \qquad \text{(A1)}$$

where the load and resistance factors, $\gamma$ and $\phi$, respectively, provide a measure of the statistical uncertainty associated with the applied loading $Q$ and the structural resistance $R$. Typically, $\gamma$ is greater than one to increase the loads and $\phi$ is less than one to decrease the strength.

For the Noyo breakwater, the values of the load and resistance factors were chosen from Melby and Turk (1993) as $\gamma = 1.0$ and $\phi = 0.9$ for unreinforced flexure. This load factor was chosen so as to preserve the exceedance probability $P = 2$ percent. For flexure, the balanced LRFD equation can be expressed as

$$
\begin{aligned}
\gamma Q_n &= \phi R_n \\
\gamma M_n &= \phi\, 0.89 M_{cr} \\
\gamma S_M k_M \sigma_1 &= \phi\, 0.89 M_{cr} \\
\gamma (0.82\sigma_1) &= \phi\, 0.89 M_{cr}/S_M \\
\gamma (0.82\sigma_1) &= \phi\, (0.89 f_t') \\
0.82\sigma_1 &= 0.80 f_t'
\end{aligned} \tag{A2}
$$

in which $M_n$ is the nominal moment, $M_{cr}$ is the critical moment, $S_m$ is the section modulus, $k_M$ is a stress contribution factor, $\sigma_1$ is the tensile stress, and $f_t'$ is the splitting tensile strength.

Equation A2 is applicable for both unreinforced and reinforced sections. The equation states that the strength must be approximately equal to the design stress, which corresponds to the design exceedance probability.

A factor of safety against armor breakage $FS$ can be defined, using Equation A2, as $FS = f_t'/\sigma_1$. The factor of safety should be 1 for properly specified concrete strength. Table A2 lists the factors of safety for 35-MPa and 45-MPa compressive strength concretes. As can be seen from the structural analysis, in order to maintain at least the design level of stress exceedance, a 28-day concrete compressive strength of 45 MPa must be maintained. Note that although the design exceedance of 2 percent does not include the 1 to 2 percent of units that will break due to impact loads, the stress prediction methodology is 10 to 20 percent conservative. It is therefore expected that, given a minimum compressive strength of 45 MPa, dolos breakage will be limited to those units that undergo impacts and that less than 1 percent of the units will break due to static and pulsating loads.

| Table A2 Dolos Reliability Analysis | | | | |
|---|---|---|---|---|
| Unit | Weight tonnes | Stress MPa | 35-MPa Factor of safety | 45-MPa Factor of safety |
| Dolos | 9 | 3.2 | 1.1 | 1.4 |
| Dolos | 19 | 4.0 | 0.86 | 1.1 |
| Dolos | 14 | 3.7 | 0.94 | 1.1 |

# Finite Element Structural Analysis

The finite element method (FEM) has been used to compare the structural response of dolos, Core-Loc, and Accropode shapes for several static loading modes. Properties of the finite element models are shown in Table A3. The FEM grids for the three units modeled are shown in Figure A2 along with loading and boundary conditions for a torsional load case. Each unit was 9 tonnes and similar loads and boundary condition constraints were applied to each. The units were loaded in flexure, torsion, and a combination of these. Figure A3(A.) shows a Core-Loc loaded in flexure with a 9-tonne point load applied to one fluke end and the other fluke fixed. Figure A3(B.) shows another flexural load condition with a 9-tonne load applied to the center of the fluke. Figure A3(C.) shows a loading condition where 9-tonne flexural and torsional loads were applied to one fluke tip with the opposing fluke fixed rigidly along the outside surface.

| Table A3 Finite Element Model Properties | |
|---|---|
| Model properties | Fully three-dimensional linear elastic model with about 2,000 nodes and 1,500 elements, depending on the unit shape. |
| Armor and material properties | Armor weight $W$ = 9 tonnes<br>Modulus of elasticity $E = 3.5*10^4$ MPa<br>Poisson's ratio $v = 0.21$<br>Specific gravity $S = 2.27$ relative to seawater |

FEM results are summarized in Table A4 in terms of maximum tensile stresses. All load cases were analyzed for the dolos and Core-Loc but only the pure torsion and pure flexure with tip load were analyzed for the Accropode. As illustrated, for equivalent weight units, the Core-Loc maximum tensile stress for static loads ranged from 34 to 62 percent that of dolos, and was 74 percent that of Accropode for both torsion and flexure. These results are graphically depicted in Figure A4.

In conclusion, specifying a 28-day compressive strength of 35 to 45 MPa, as was done for the dolosse, with corresponding tensile strengths of 3.5 to 4.5 MPa, will provide adequate strength to resist even the most severe loads.
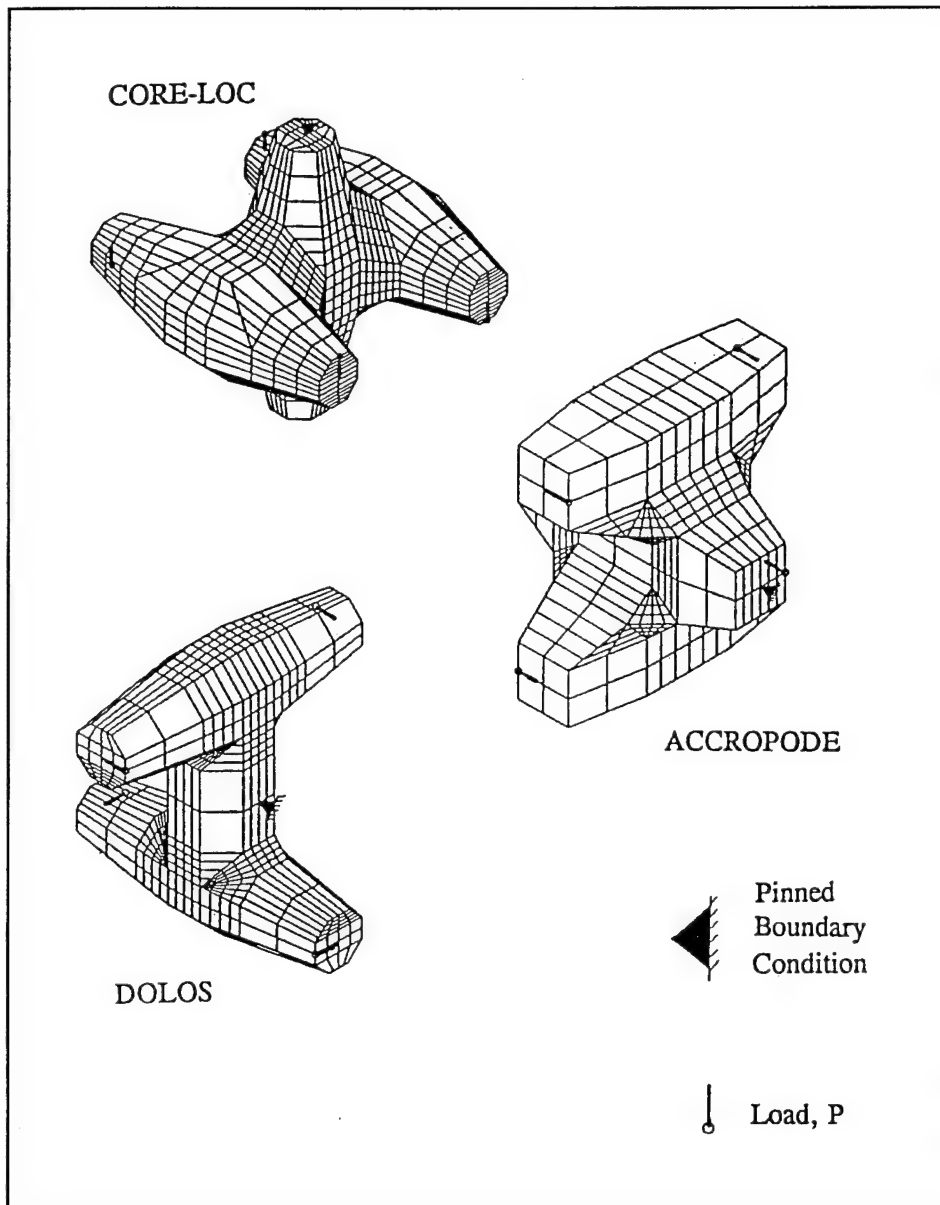
Figure A2. Loading and boundary conditions for torsional loading comparison

**Table A4
FEM Static Stress Comparison**

| Load Case | Stress, $\sigma_s$, MPa | | |
|---|---|---|---|
| | Core-loc | Dolos | Accropode |
| Torsion | 1.12 | 2.08 | 1.52 |
| Flexure - fluke tip load | 1.12 | 2.41 | 1.52 |
| Flexure - fluke center load | 2.10 | 3.42 | – |
| Combined flexure and torsion | 1.91 | 3.83 | – |

# Concrete Mix Design and Strength Enhancements

Quality control testing during the 1986 Crescent City rehabilitation revealed a mean flexural tensile strength of $f_t = 6.3$ MPa (Kendall and Melby 1990) for the steel-fiber reinforced concrete used. The concrete tensile strength at Crescent City was therefore well above the generally specified normal strength of 3.5 MPa. This high strength has contributed to the superior performance of the Crescent City dolosse. The Humboldt dolosse also had high strength concrete, and they too are performing exceptionally.

The necessity for selecting a mixture design capable of producing concrete to withstand design wave loading and harsh marine environments cannot be overstated. Ideally, the concrete produced will have a low porosity, be impervious to seawater attack, be abrasion-resistant, and possess high strength. The concrete would contain a consistent homogeneity throughout all placed units. Quality control and assurance must be implemented during all phases of construction. The quality of concrete produced is a function of the proportions and type of cement, aggregate, water, and admixtures as well as the mixing, placement, and curing.

The following information on a recommended concrete mixture serves only as a starting point for trial mixture design. Many factors affect the integrity of the final product. Variability in the chemical and physical interaction of the individual constituents mandates rigorous testing of the final mixture design. Therefore, it is imperative that the final design be "fine-tuned" and tested in a Division laboratory or certified concrete testing laboratory. It is recommended that three types of tests be performed: (a) axial compression test, (b) splitting-tensile test, and (c) flexure or modulus of rupture test.

**A.** Flexure - fluke tip load

**B.** Flexure - fluke center load

**C.** Combined torsion and flexure
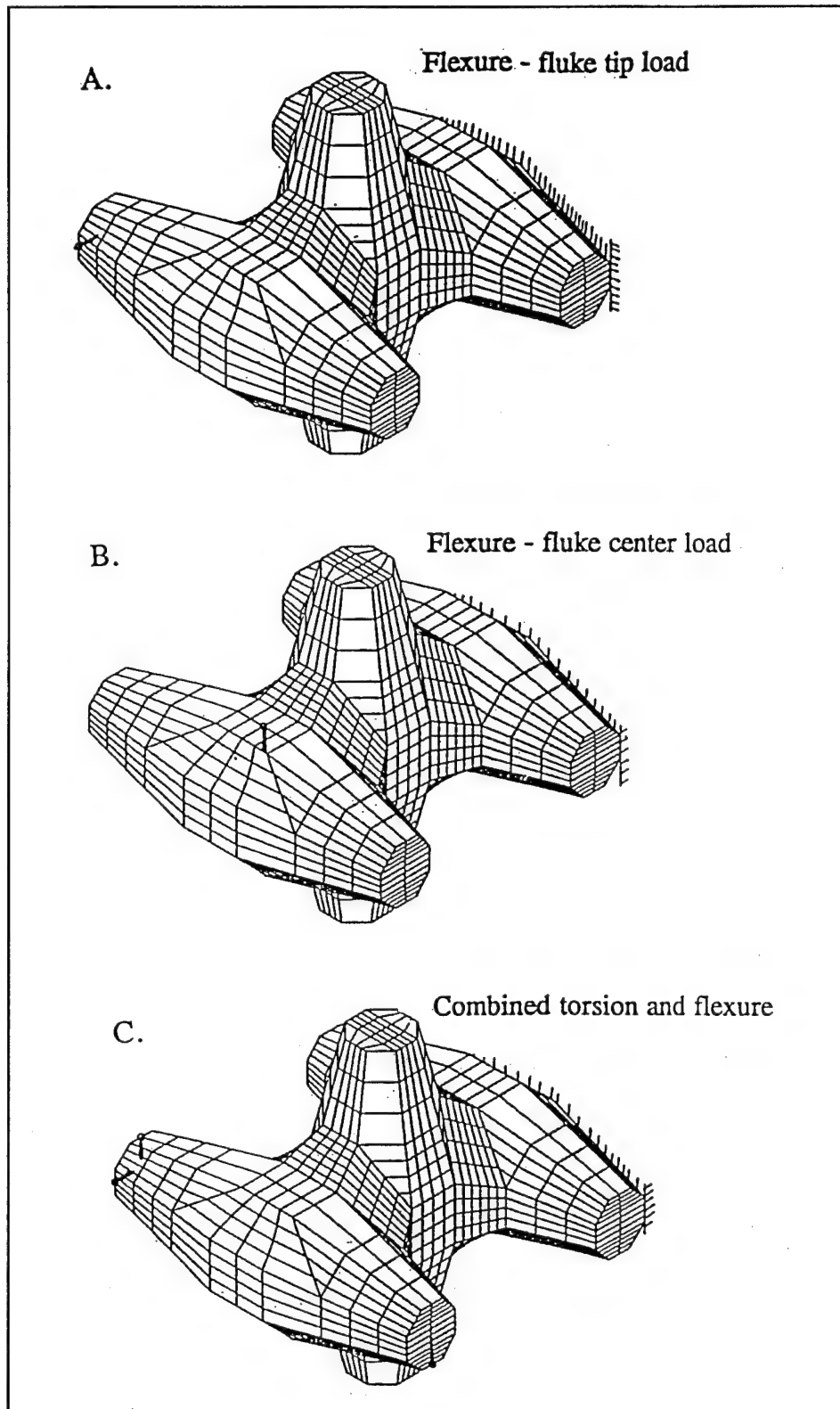
Figure A3. Loading and boundary conditions for various loading conditions
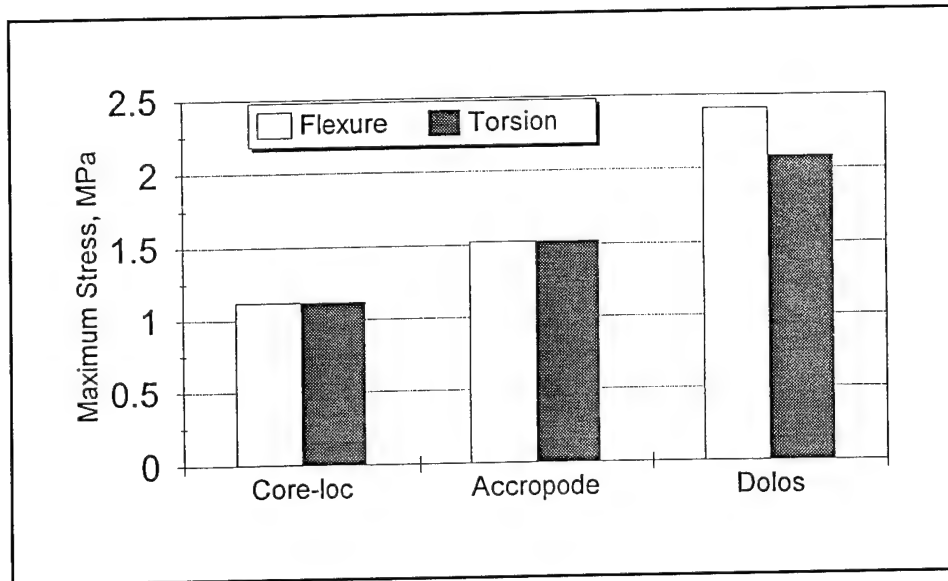
Figure A4.  Finite element structural response comparison

The concrete used should possess the following qualities:

a.  28-day compressive strength = 45 MPa.

b.  28-day splitting tensile strength = 4.5 MPa.

c   Slump = 5 to 10 cm.

d.  Air entrainment = < 5% ± 1%.

The specification baseline values for a trial mix design are as follows:

a.  Cement.

(1)  Type II or III with the optional 8% limit of $C_3A$ invoked.

(2)  374-392 kg/m$^3$.

(3)  Water/cement ratio 0.33-0.38.

b.  Aggregate.

(1)  Non-alkali-silica reactive.

(2)  Max. size = 3.8 cm.

(3)  Gradation conforms to ASTM C33.

(4)  Fineness modulus for fine aggregate 0.24-0.30.

    (5)  30% of coarse aggregate to be crushed.

  *c.*  Water - potable, free from high concentration of sodium or potassium.

  *d.*  Admixtures.

    (1)  Appropriate air entrainment.

    (2)  Superplastizers, increases workability and reduce water content.

The concrete mixture design tests should utilize the same materials as will be used in the prototype and meet the minimum requirements for *both* of the suggested tensile strength tests. During the casting of the concrete armor units, six cylinders should be cast and tested for every concrete batch. No armor unit should be accepted if the concrete batch fails to produce the minimum tensile strength required.


# Reinforcement

To date, both conventional deformed-bar steel reinforcing and steel fiber reinforced concrete (SFRC) have been used in prototype dolosse. The main problem with conventional reinforcing, besides additional cost, is that the steel bars do not contribute to the tensile strength until the concrete cracks. Depending on the depth of cover and the magnitude of the tensile strain, these cracks may provide a conduit for water to initiate corrosion of the steel bars. So while conventional steel reinforcing may keep components of an armor unit intact during a major design event, cracking can lead to corrosion and eventual failure of the unit. Yet, although most U.S. conventionally reinforced concrete units show signs of reinforcement corrosion and resultant spalling, no armor units have been observed to fail due to reinforcement corrosion. Very few reinforced units have been observed to be cracked through crucial cross sections that were not broken. They typically have stresses well below the strength or, when rocking, have stresses well above the concrete strength. This confirms stress measurements made in the LSDFS and discussed above, where stable dolos stresses were quite small relative to impact stresses.

At one time SFRC held promise as a strength enhancement for concrete armor units. In testing of Crescent City prototype dolos concrete, Gutschow reports a 7.2-percent increase in concrete tensile strength of SFRC over unreinforced concrete under laboratory conditions. SFRC also has been shown to have a slightly improved impact strength. However, using the steel fibers during construction of the Crescent City breakwater proved to be difficult. Steel fibers had a tendency to "ball up" during mixing, resulting in a non-homogeneous concrete matrix. Without uniform consistent fiber dispersion throughout the concrete, strength enhancement is negligible. Although fiber

dispersion improved during casting, the workability problems coupled with the added expense of the steel make SFRC only marginally effective.

At this time no recommendation is made as to the use of steel reinforcing for the Noyo Project because the design stresses are considered low enough to provide sufficient reserve capacity in the Core-Loc, Accropode, and dolos units.

## Conclusions

The following is a summary of the conclusions from this report of the acceptable concrete armor unit design for the Noyo Harbor breakwater:

*a.* The design dolos factored tensile stresses are below the factored strength using a 28-day compressive strength of 45 MPa, provided they do not rock in place or move about on the breakwater. This stability was verified in a two-dimensional flume physical model study.

*b.* Based on a high-resolution finite element analysis, the design Core-Loc and Accropode will have maximum tensile stress levels over 35 percent less than the 3.5-MPa design stress level in the dolos, and maximum compressive stress levels well below the strength of normal strength concrete, provided they also do not rock on the breakwater. Stability was verified in two-dimensional and three-dimensional physical model studies. Therefore, a conservative design tensile strength of 3.5 MPa should be adequate, provided the units do not undergo large displacements such as rollovers.

*c.* A moderate strength concrete has been specified to provide armor units that will not crack or break under normal nonimpact design conditions. Steel or plastic fibers may be added to the mix in lieu of additional cement.

## References

Gutschow, R. A. (1985). "The use of steel fiber reinforced concrete for casting large dolos," *Western Coast Regional Design Conference*, Oakland, CA. ASCE, New York.

Howell, G. L., Rhee, J. P., and Rosati, J. (1990). "Stresses in dolos armor units due to waves." *ASCE/WPCO seminar on stresses in concrete armor units*. New York, NY.

Kendall, T. R., and Melby, J. A. (1990). "Continued monitoring of 42-ton dolos movements and static stresses at Crescent City." *ASCE/WPCO seminar on stresses in concrete armor units*. New York, NY.

Melby, J. A. (1992). "Application of a dolos structural design procedure." *Proc. Coast. Engrg Practice Conf.*, ASCE, 830-846.

Melby, J. A. (1993). "Dolos design procedure based on Crescent City proto-type data," Technical Report CERC-93-10, U.S. Army Engineer Waterways Experiment Station, Vicksburg, MS.

Melby, J. A., and Turk, G. F. (1992). "Dolos design using reliability methods." *Proc. 23rd Int. Conf. Coast. Engrg.*, ASCE, 1385-1399.

Melby, J. A., and Turk, G. F. (1993). "Large scale dolos flume study: post-experiment progress report." Progress report for the Breakwater Concrete Armor Units for Repair work unit under the REMR program, U.S. Army Engineer Waterways Experiment Station, Vicksburg, MS.

Melby, J. A., and Turk, G. F. (1995). "CORE-LOC concrete armor units," in preparation, U.S. Army Engineer Waterways Experiment Station, Vicksburg, MS.

# Appendix B
# Two-Dimensional Stability Photographs
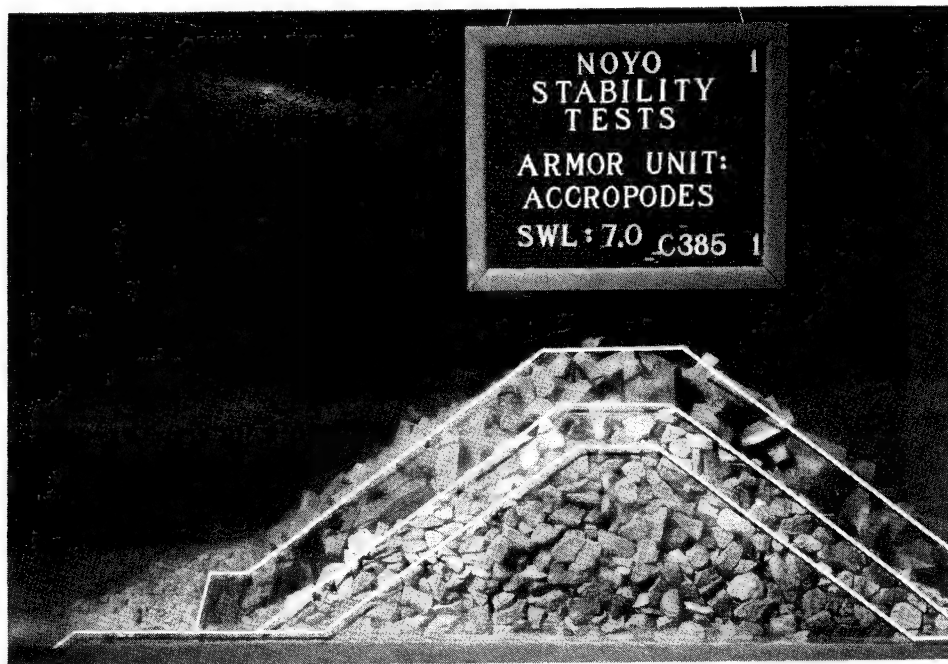
Photo B1. Plan 1, Side view, before testing
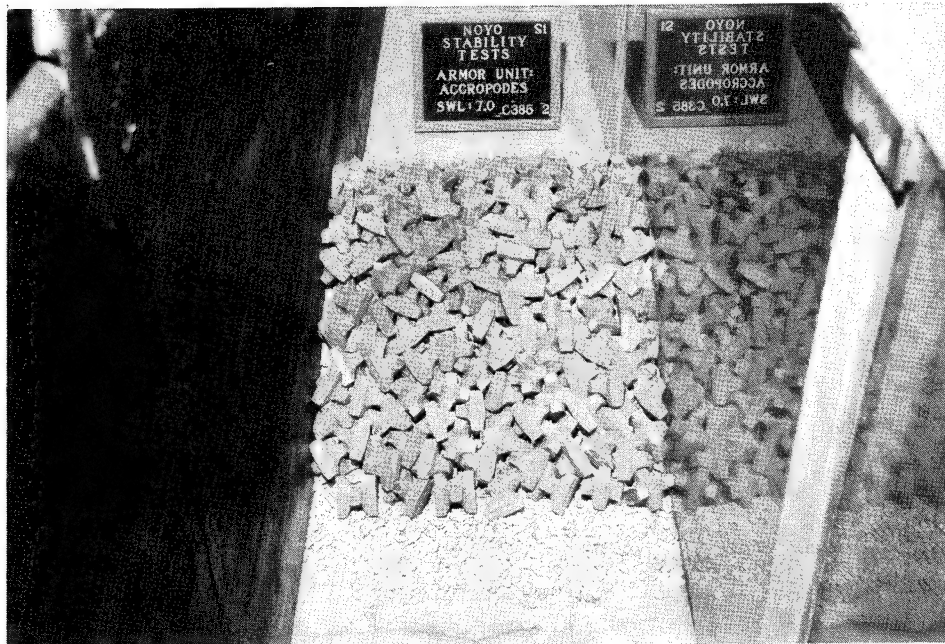


Photo B2. Plan 1, Seaside view, before testing
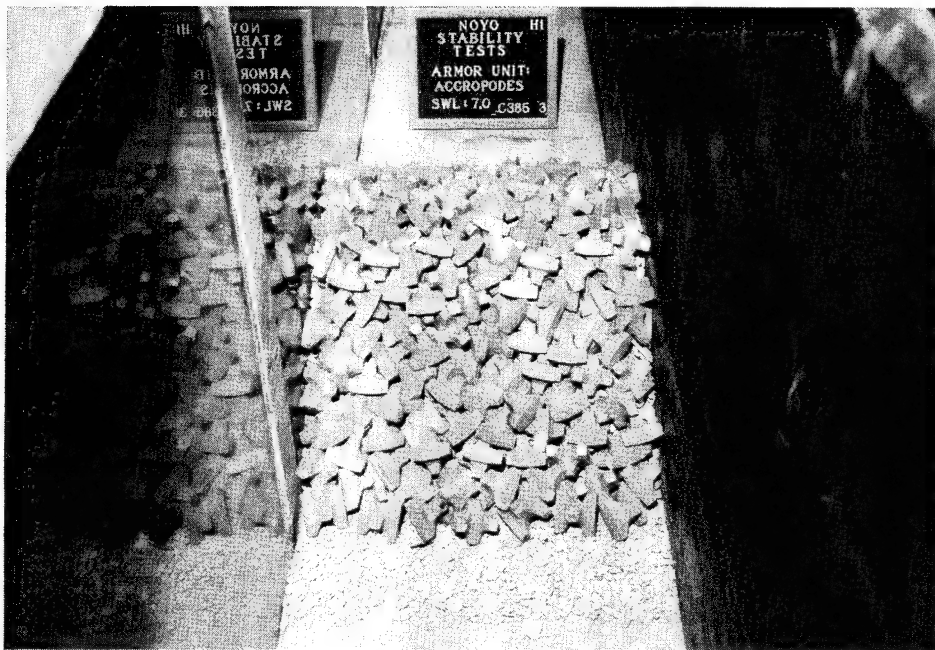
Photo B3. Plan 1, Leeside view, before testing
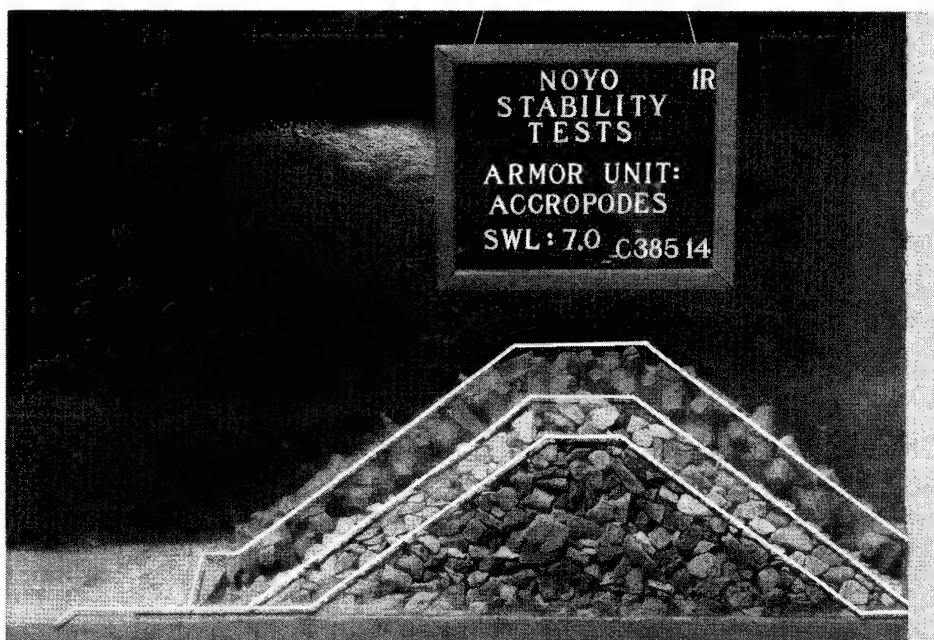


Photo B4. Plan 1, Side view, after testing
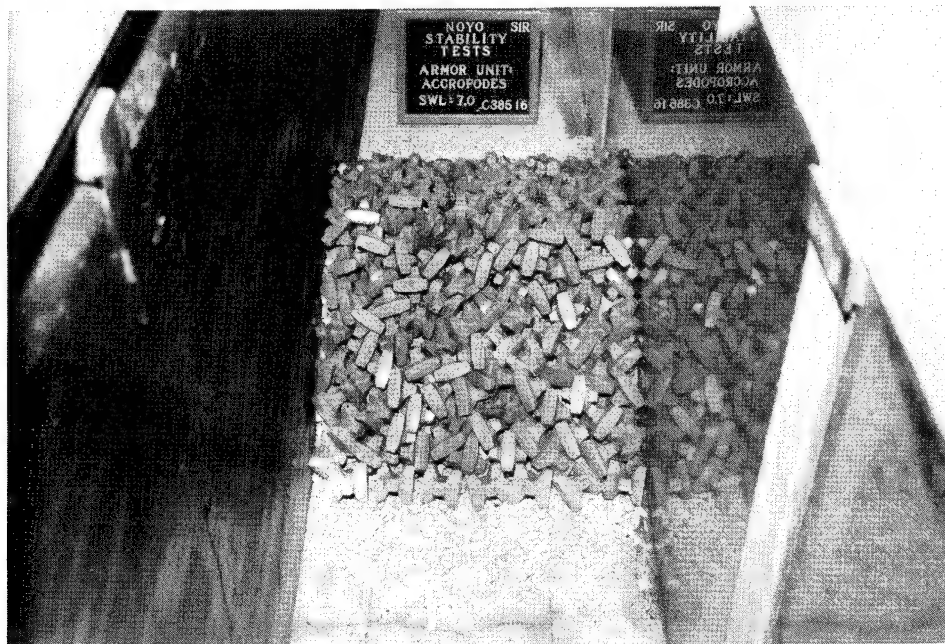
Photo B5. Plan 1, Seaside view, after testing
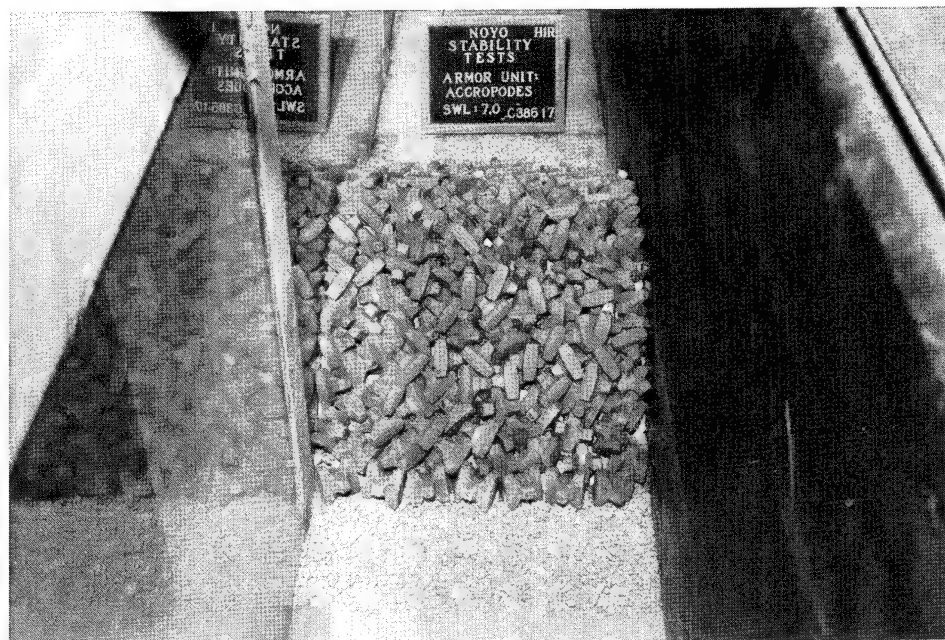


Photo B6. Plan 1, Leeside view, after testing
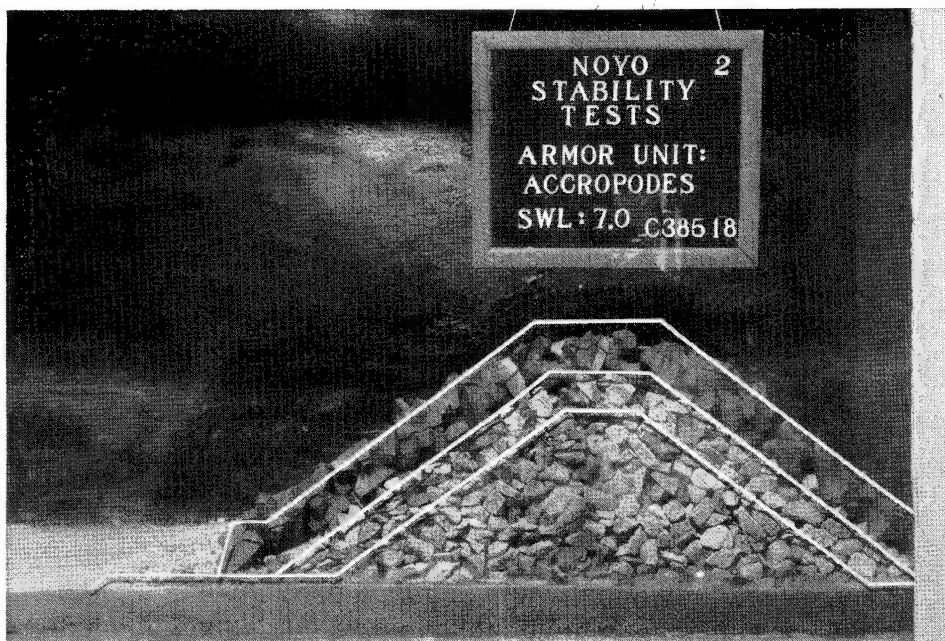
Photo B7. Plan 2, Side view, before testing
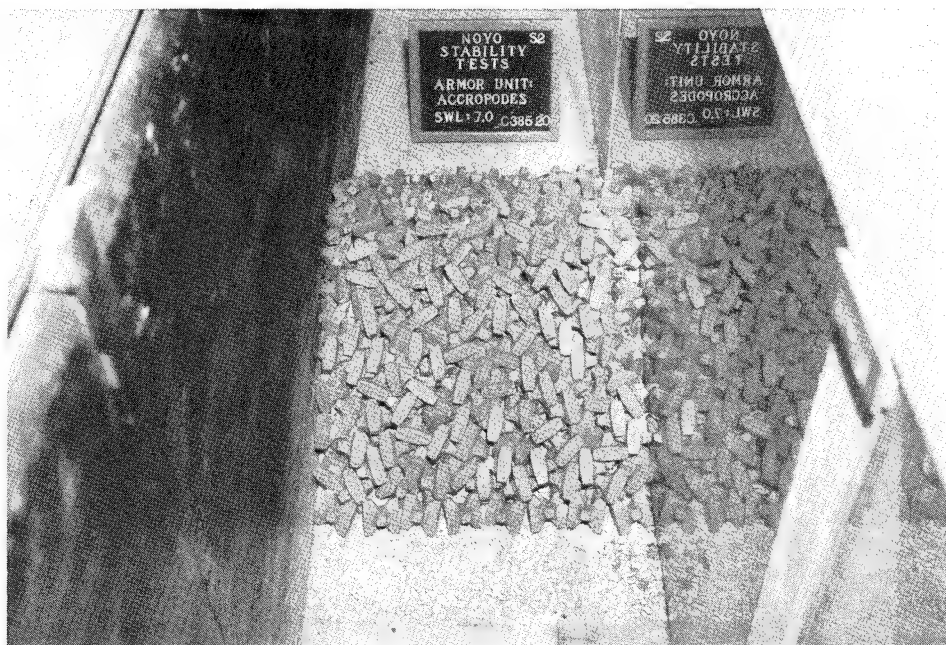


Photo B8. Plan 2, Seaside view, before testing

Appendix B  Two-Dimensional Stability Photographs
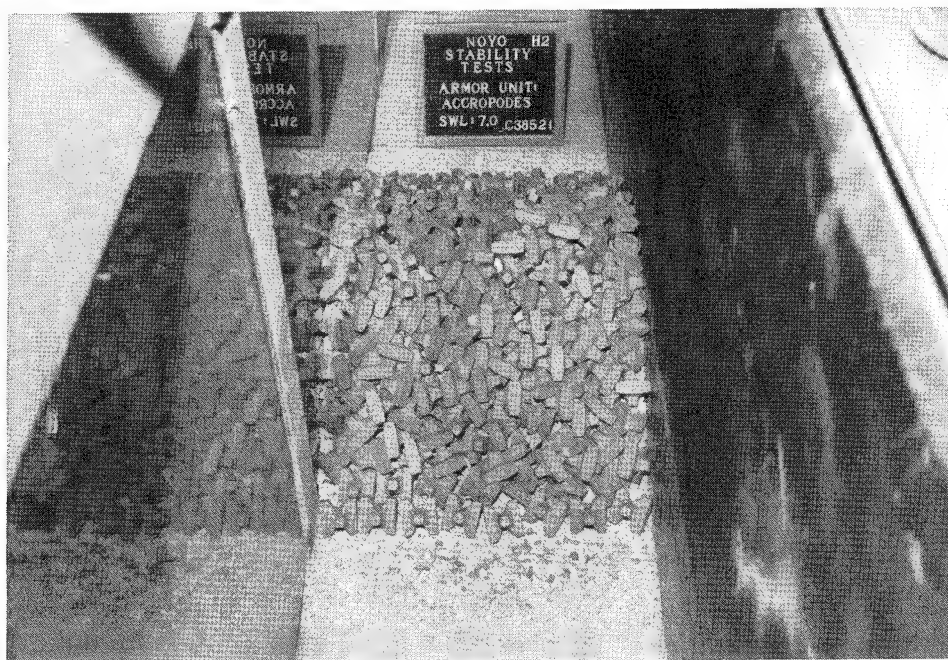
Photo B9. Plan 2, Leeside view, before testing



Photo B10. Plan 2, Side view, after testing

Photo B11. Plan 2, Seaside view, after testing
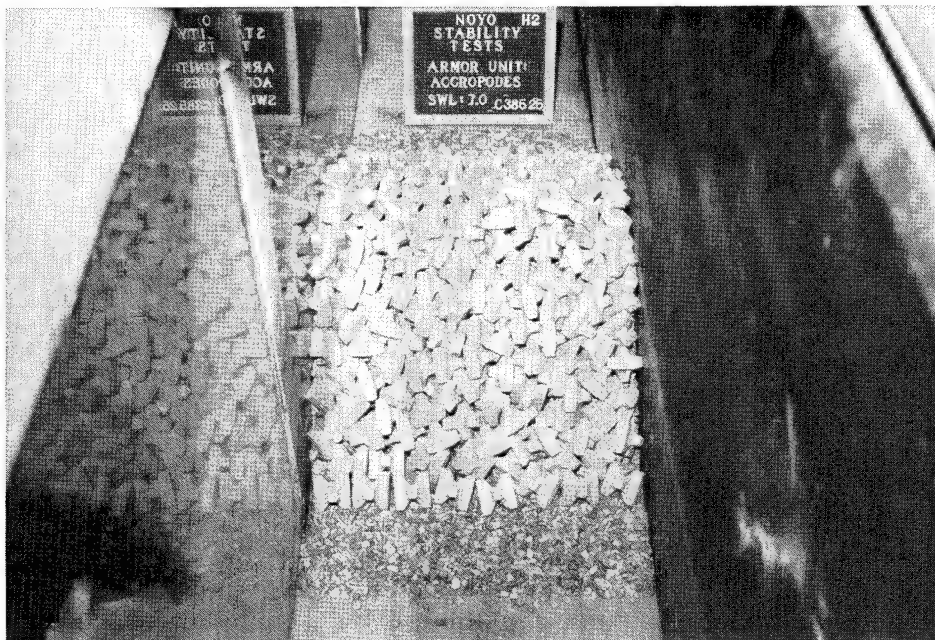


Photo B12. Plan 2, Leeside view, after testing
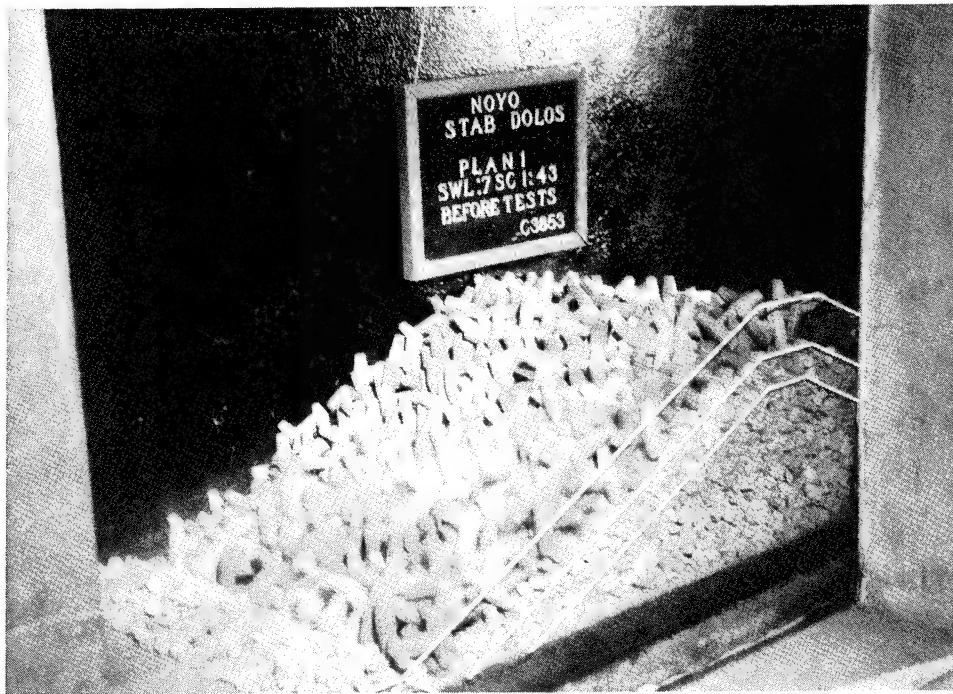
Photo B13. Plan 3, Side view, before testing
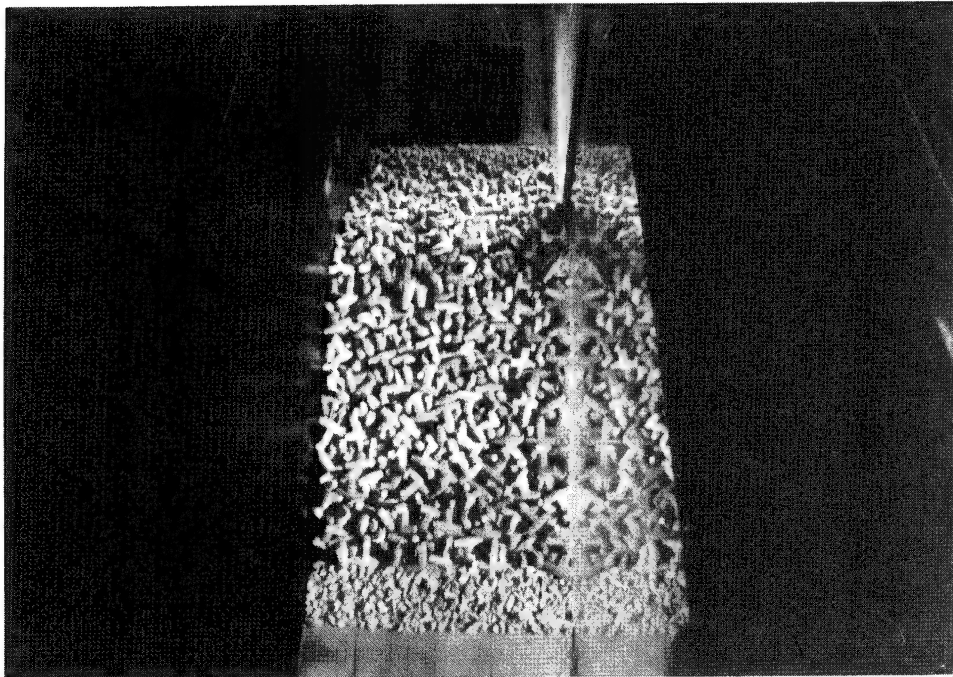


Photo B14. Plan 3, Seaside view, before testing
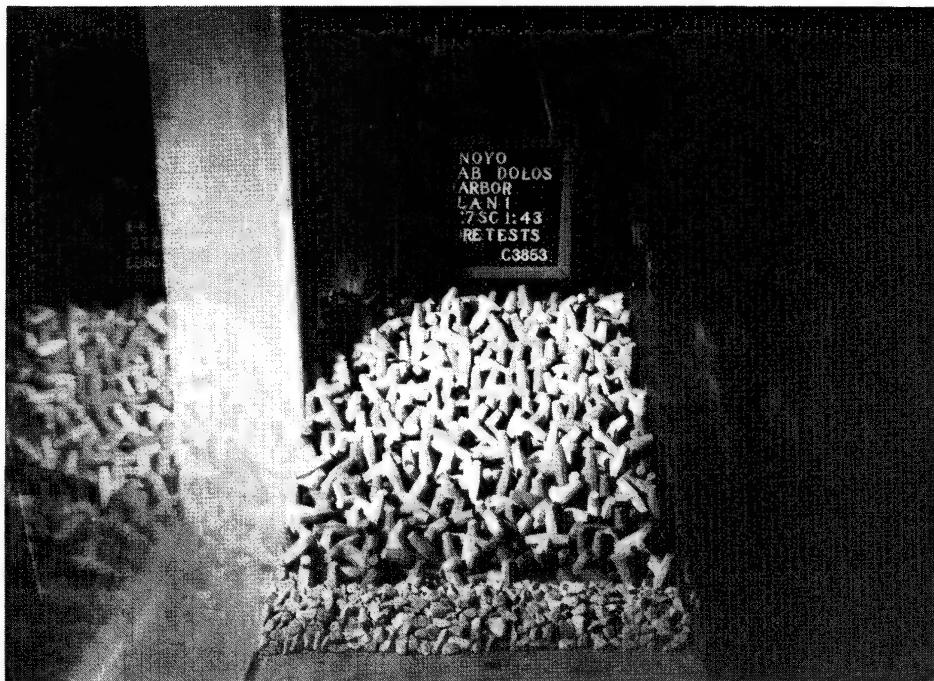
Photo B15. Plan 3, Leeside view, before testing



Photo B16. Plan 3, Seaside view, after testing
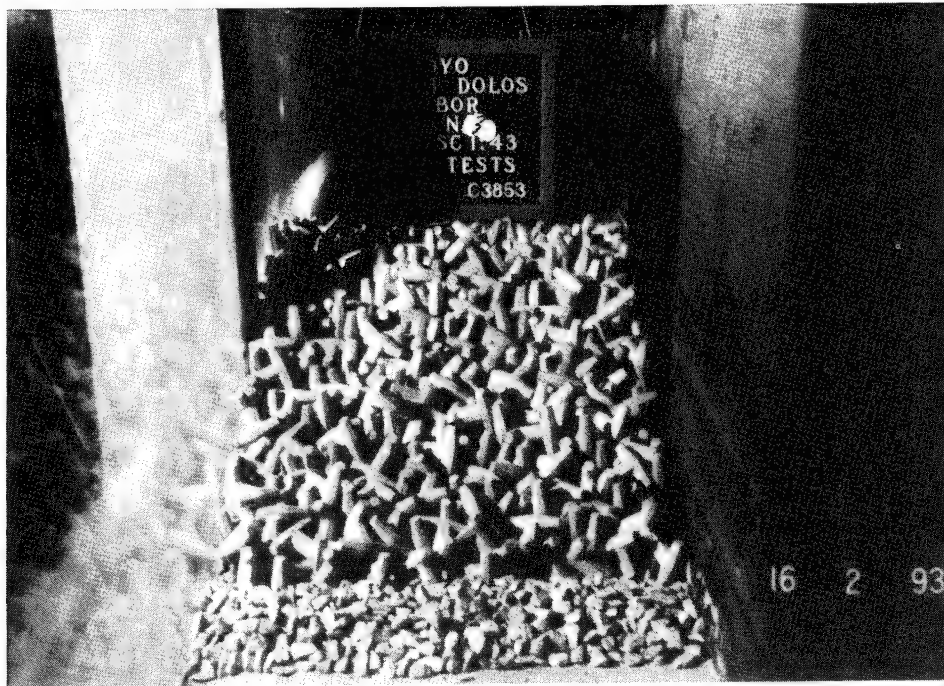
Photo B17. Plan 3, Leeside view, after testing
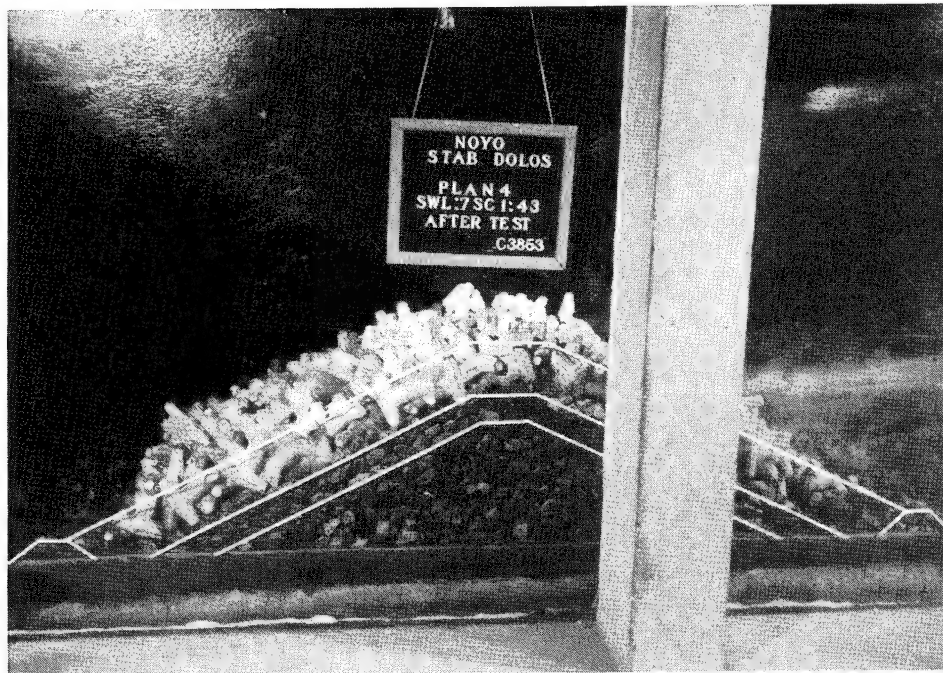


Photo B18. Plan 4, Side view, after testing
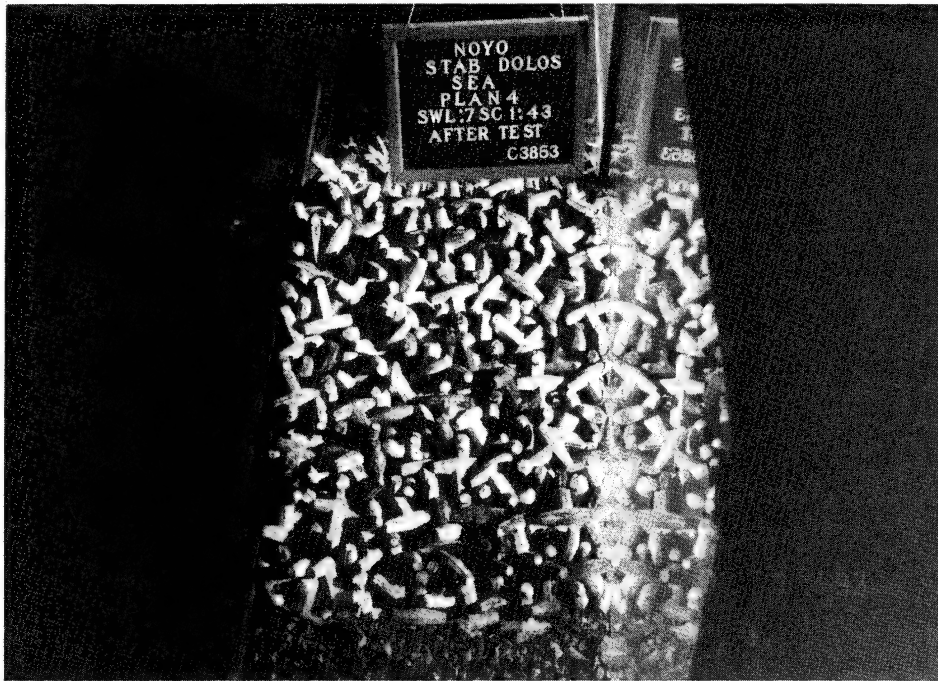
Photo B19. Plan 4, Seaside view, after testing
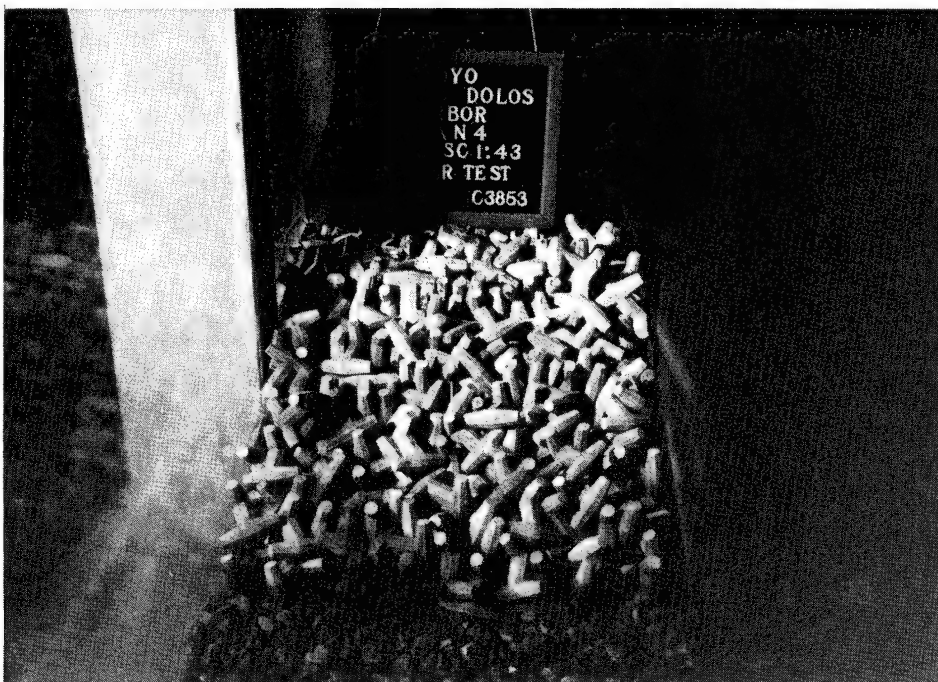


Photo B20. Plan 4, Leeside view, after testing

Photo B21.  Plan 5, Side view, before testing
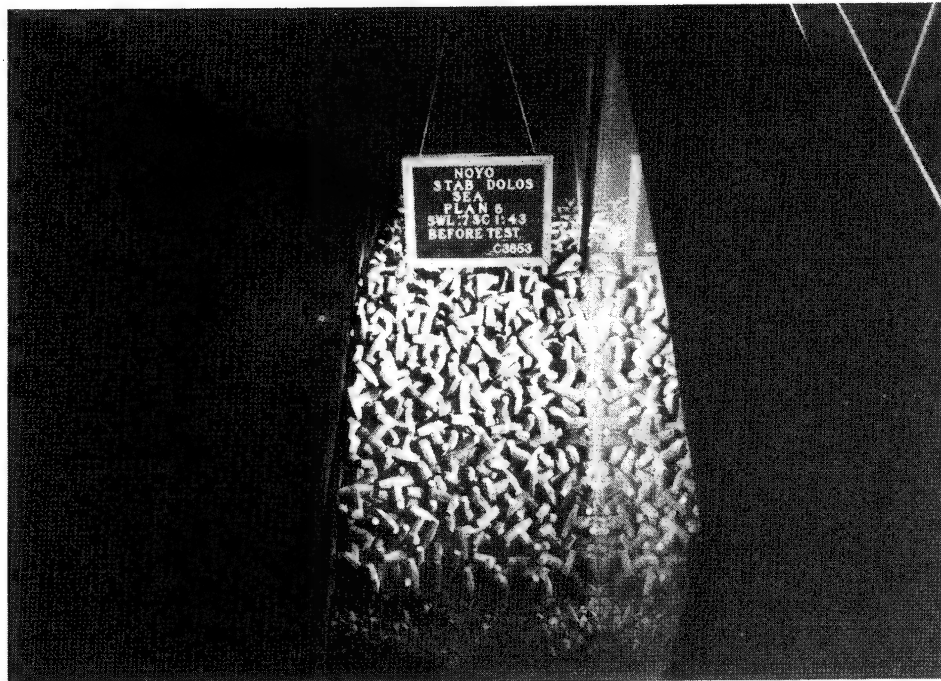


Photo B22.  Plan 5, Seaside view, before testing

Photo B23. Plan 5, Leeside view, before testing

# Appendix C
# Three-Dimensional Stability Photographs
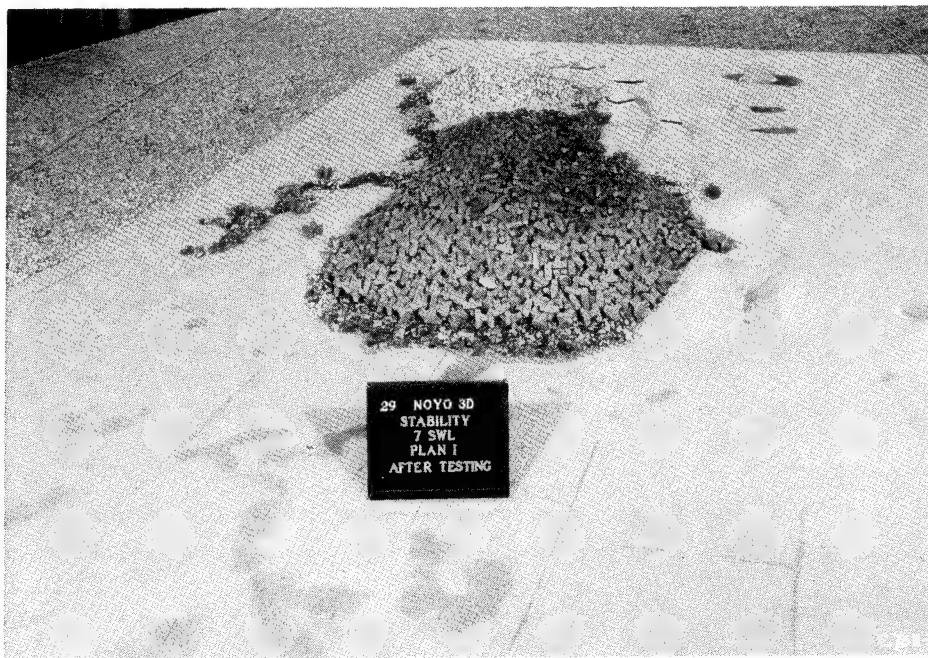
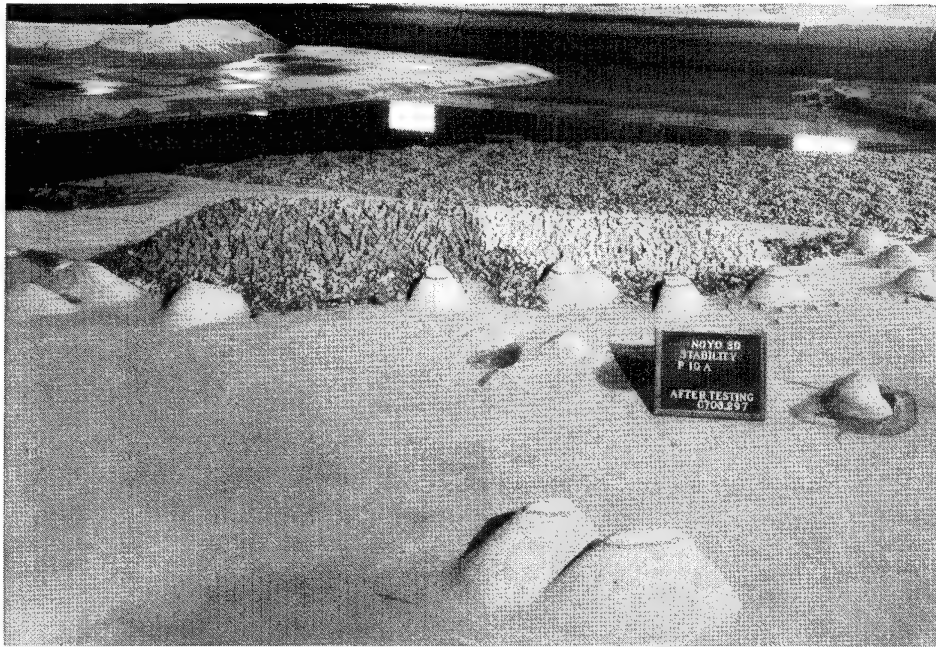Photo C1. Plan 1, north roundhead after Storm I waves



Photo C2. Leeside view of Plan 1 after Storm I waves
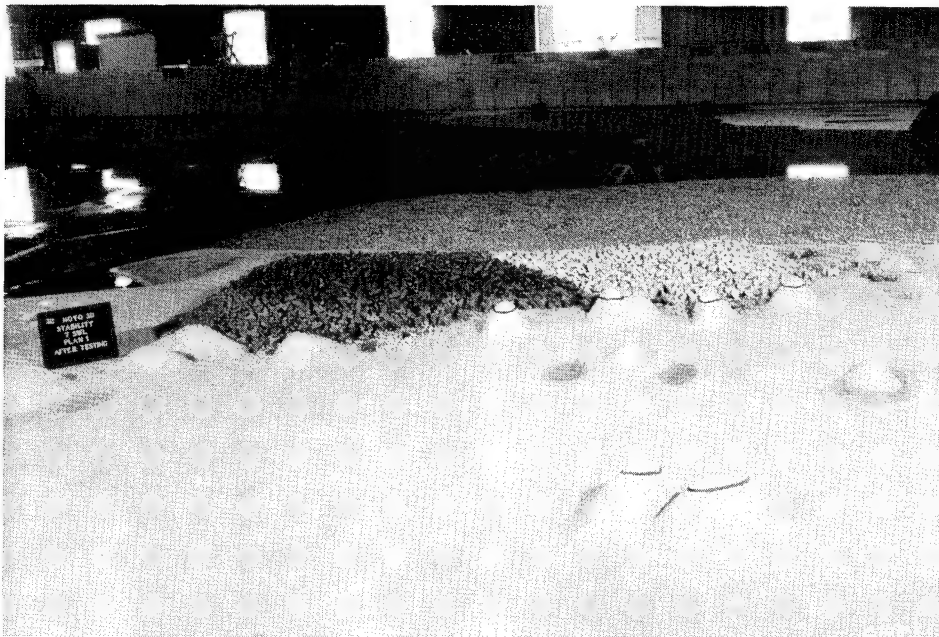
Photo C3.  Sea-side view of Plan 1 after Storm I waves
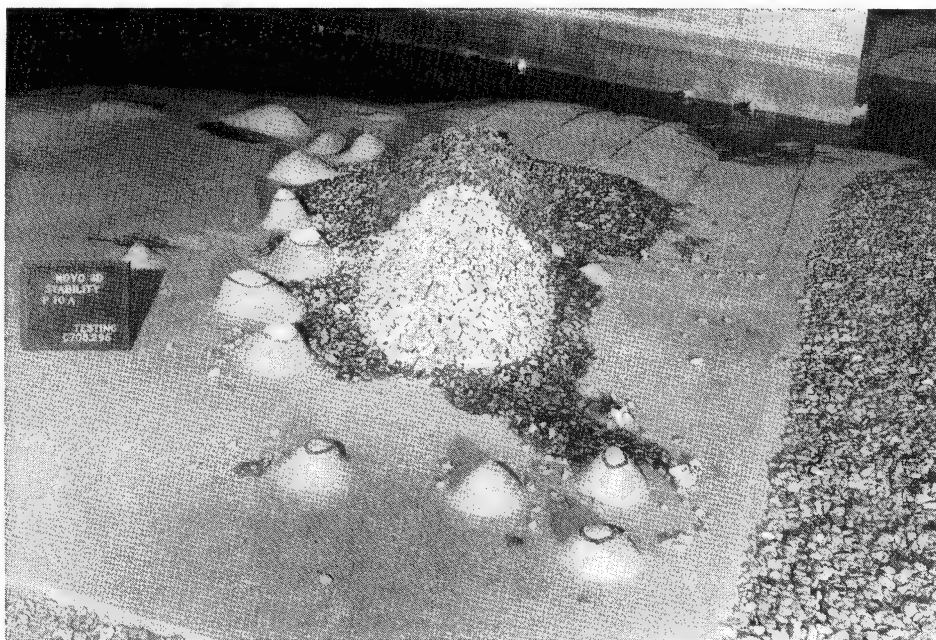


Photo C4.  Plan 1, south roundhead after Storm I waves
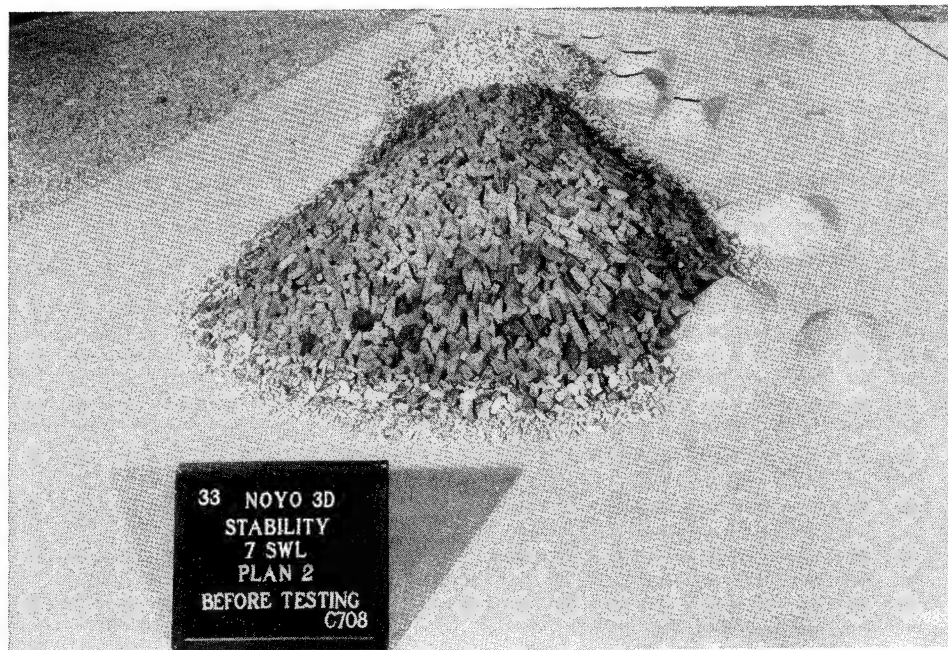
Photo C5. Plan 2, north roundhead before testing
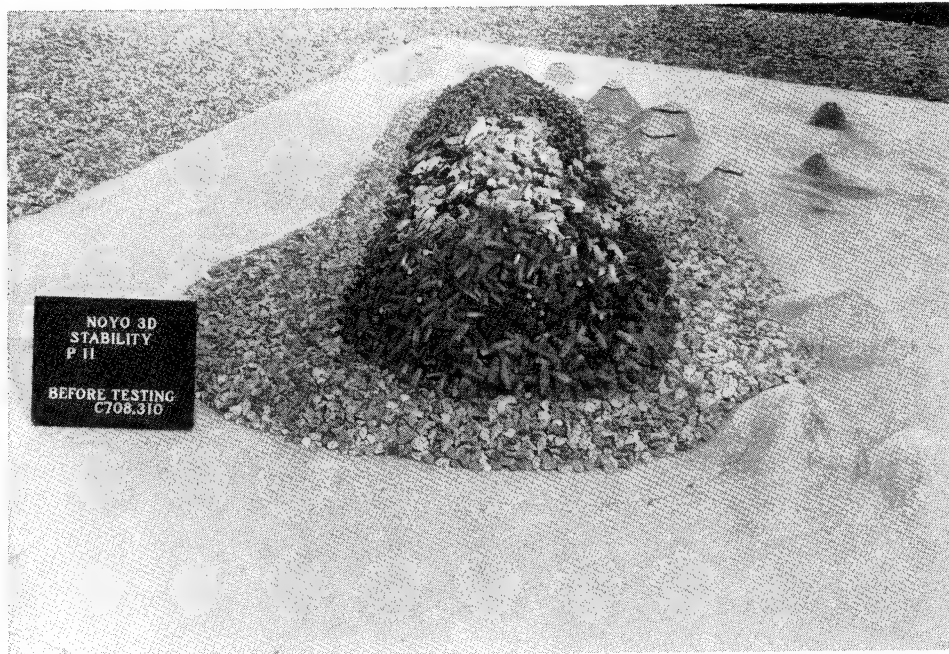


Photo C6. Leeside view of Plan 2 before testing

Appendix C  Three-Dimensional Stability Photographs
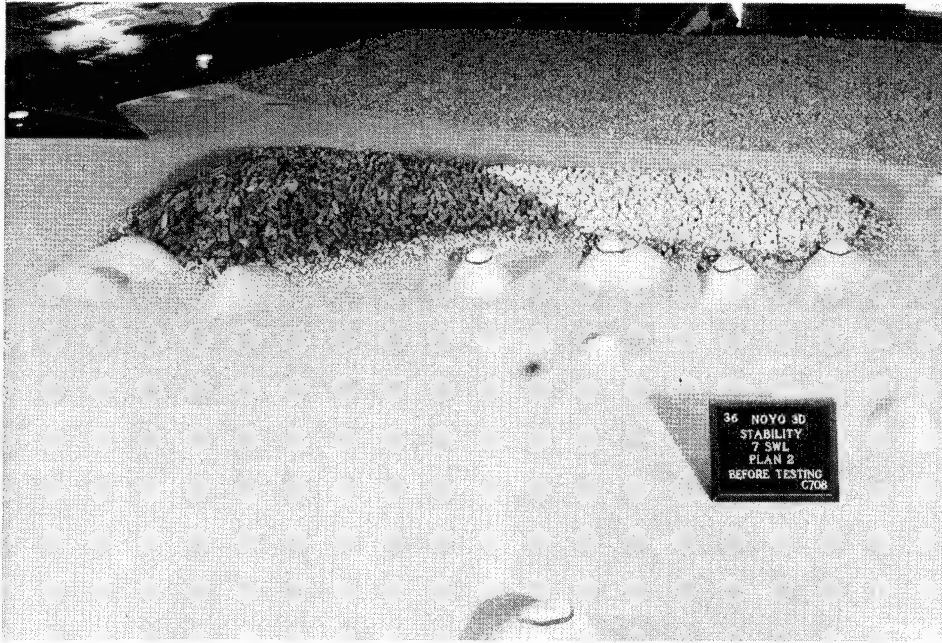
Photo C7.  Sea-side view of Plan 2 before testing
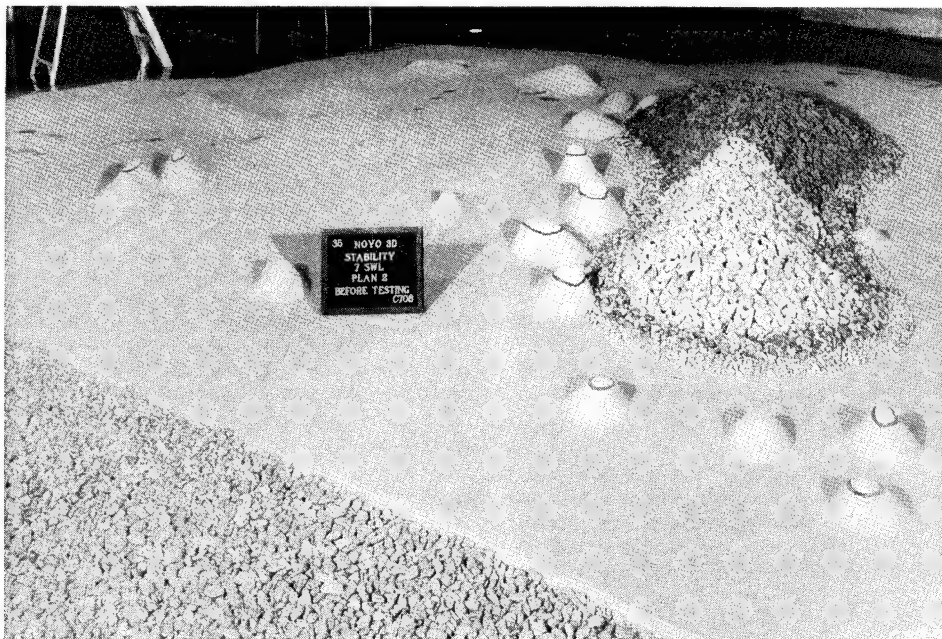


Photo C8.  Plan 2, south roundhead before testing

Photo C9.  Plan 2, north roundhead after Storm I waves
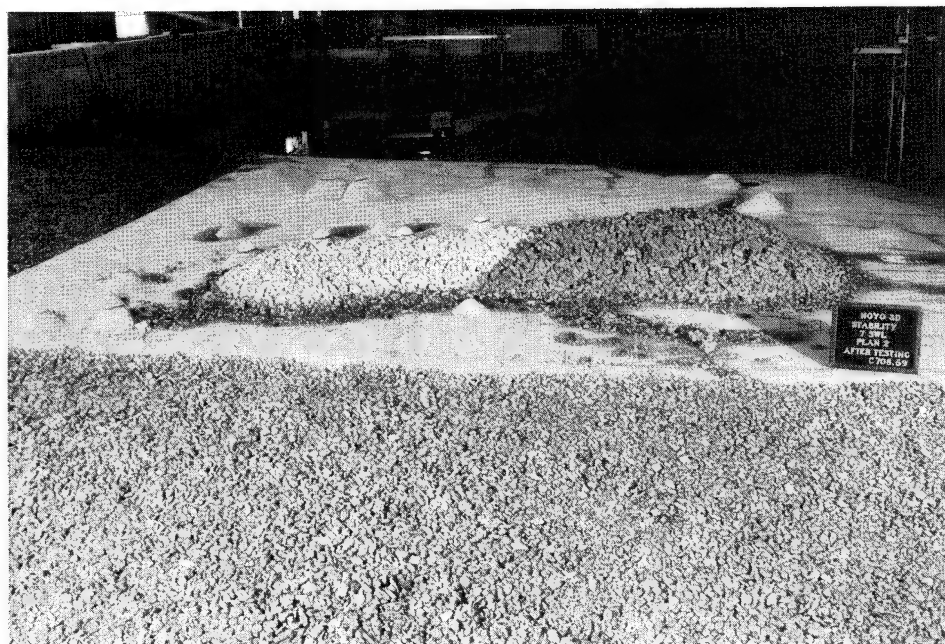


Photo C10.  Leeside view of Plan 2 after Storm I waves
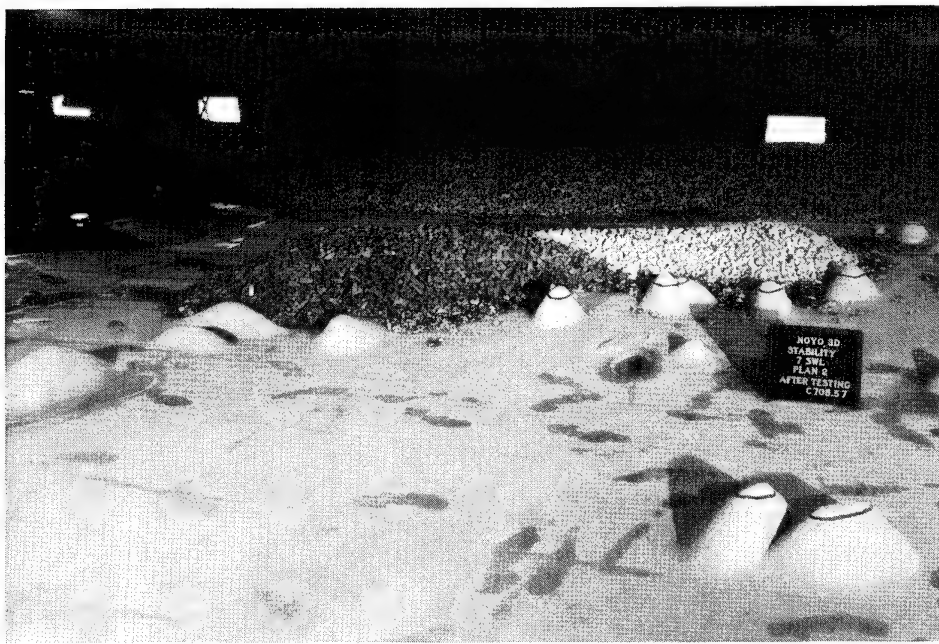
Photo C11.  Sea-side view of Plan 2 after Storm I waves



Photo C12.  Plan 2, south roundhead after Storm I waves
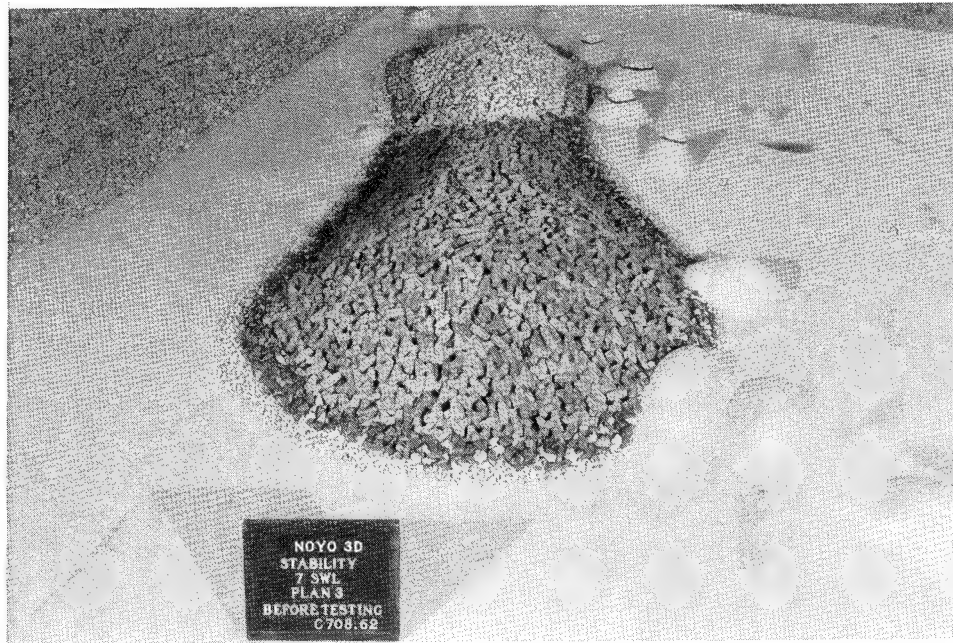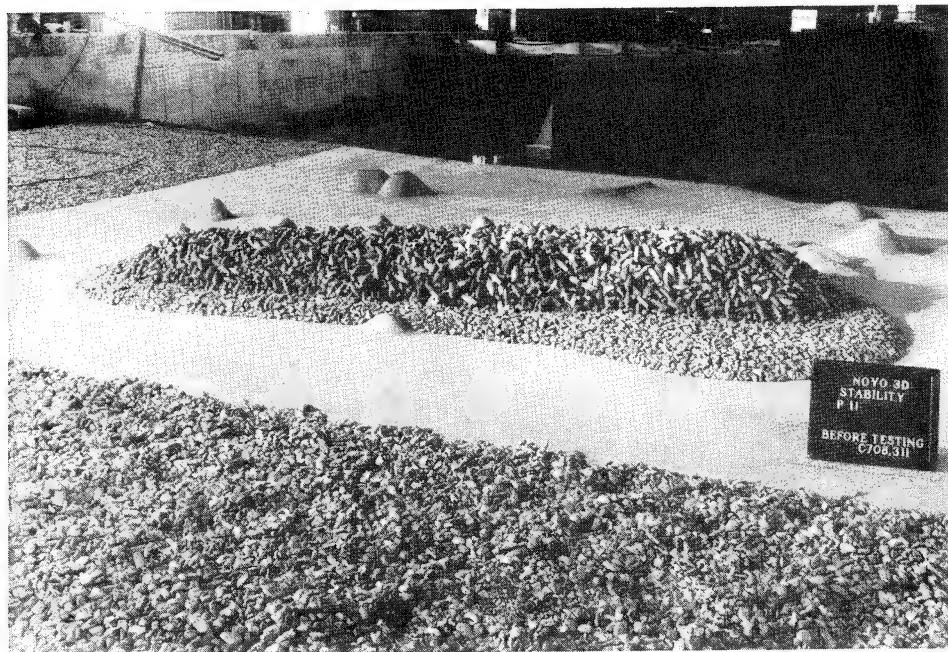
Photo C13. Plan 3, north roundhead before testing
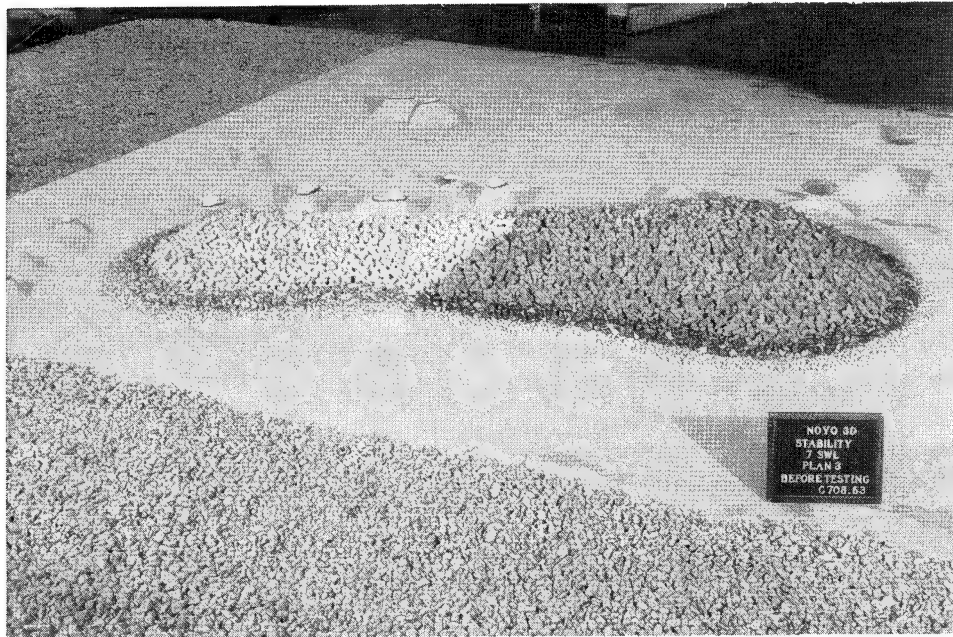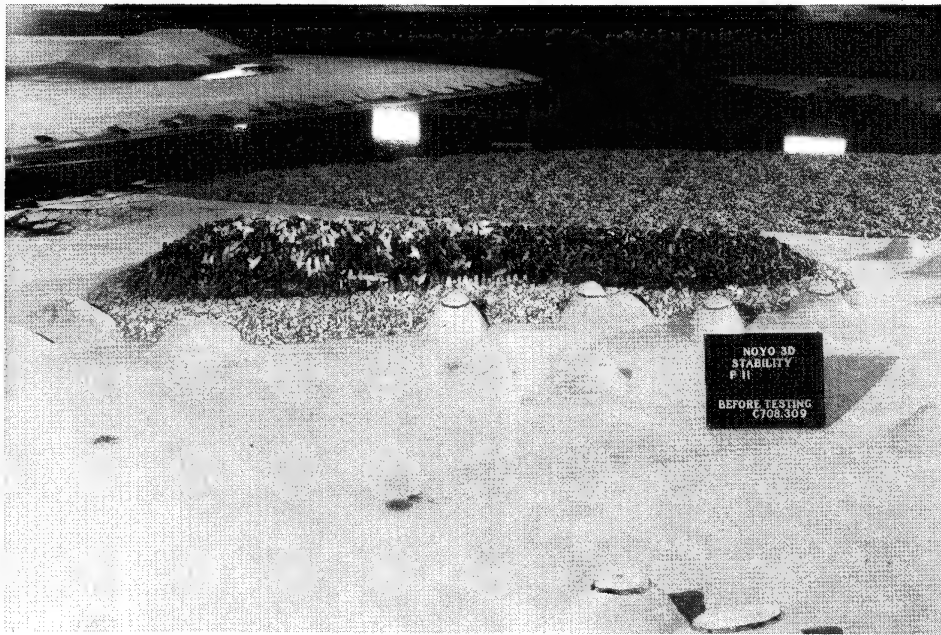


Photo C14. Leeside view of Plan 3 before testing
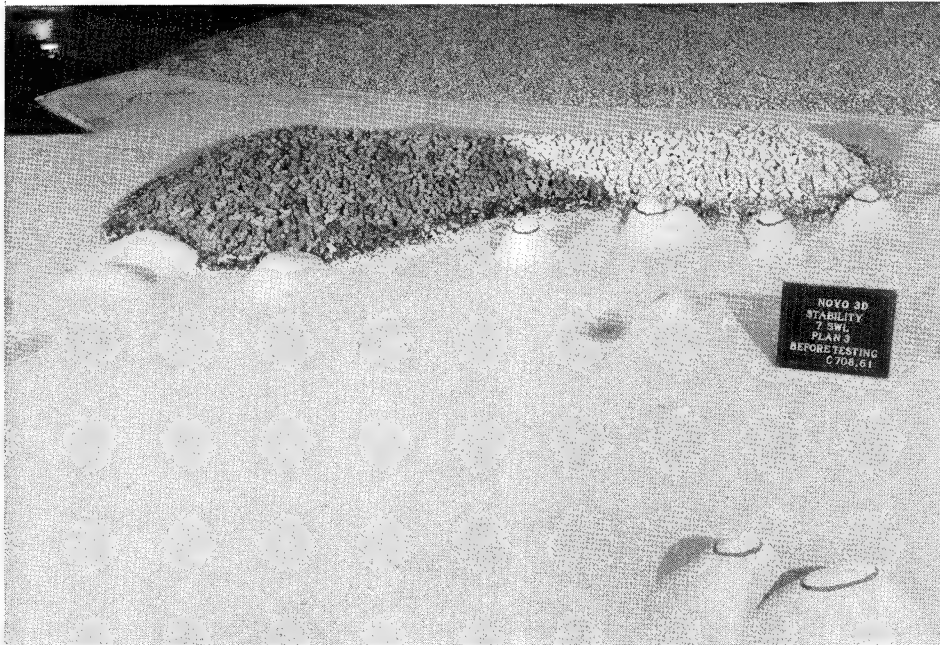
Photo C15.  Sea-side view of Plan 3 before testing
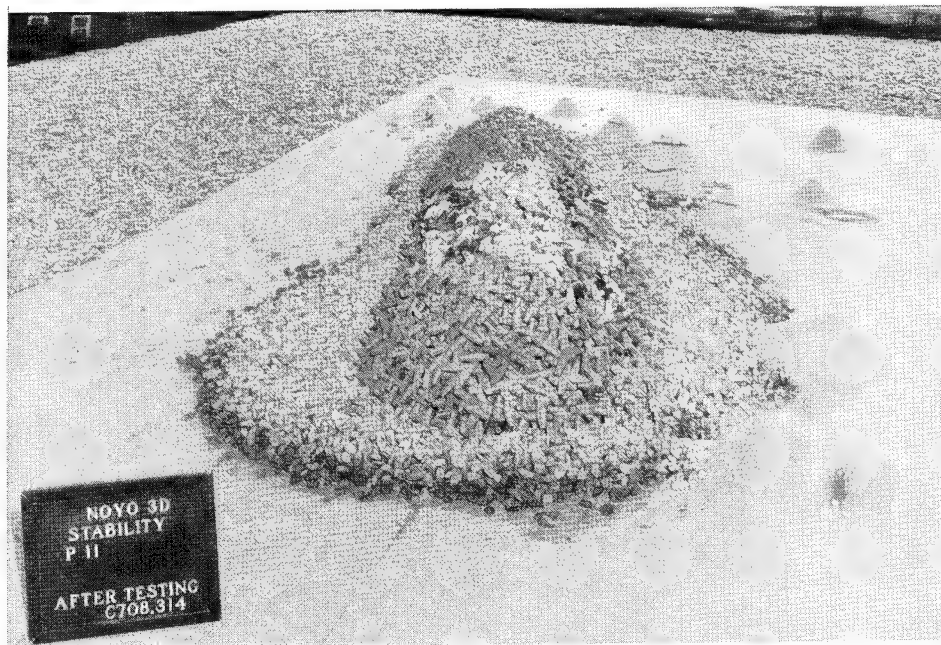


Photo C16.  Plan 3, south roundhead before testing

Photo C17. Plan 3, north roundhead after Storm I waves
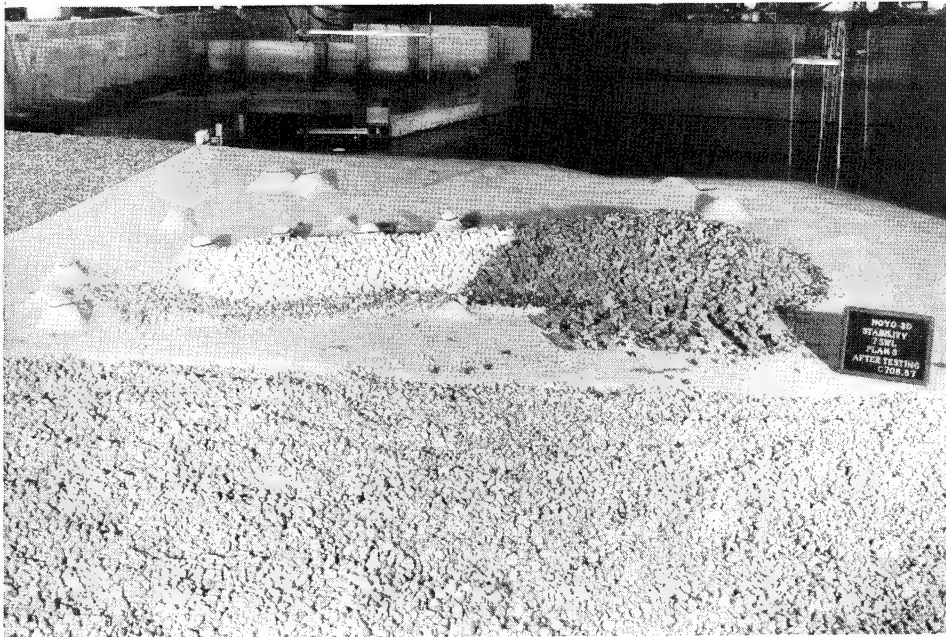


Photo C18. Leeside view of Plan 3 after Storm I waves
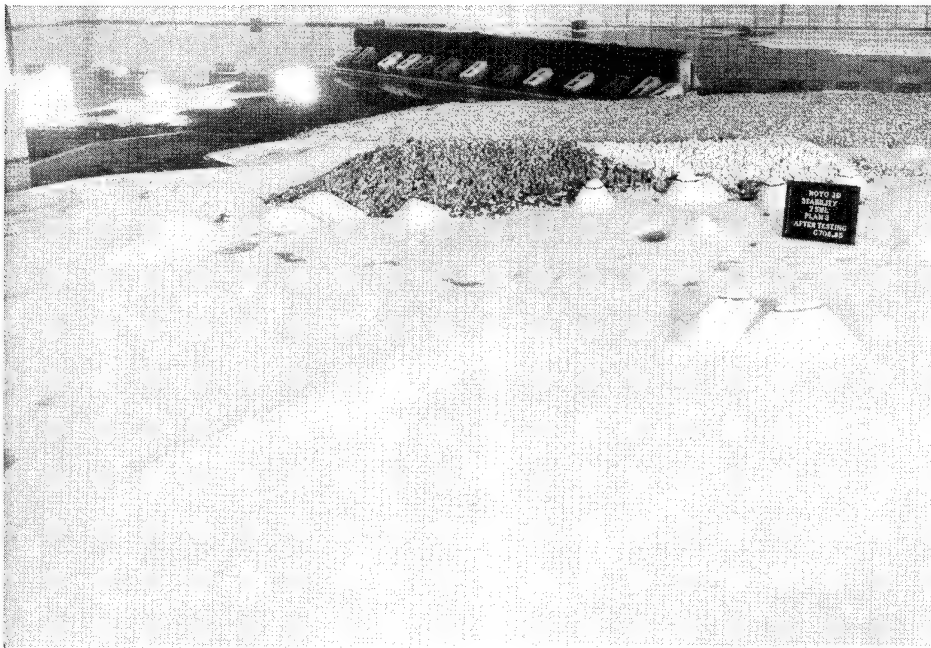
Photo C19. Sea-side view of Plan 3 after Storm I waves



Photo C20. Plan 3, south roundhead after Storm I waves
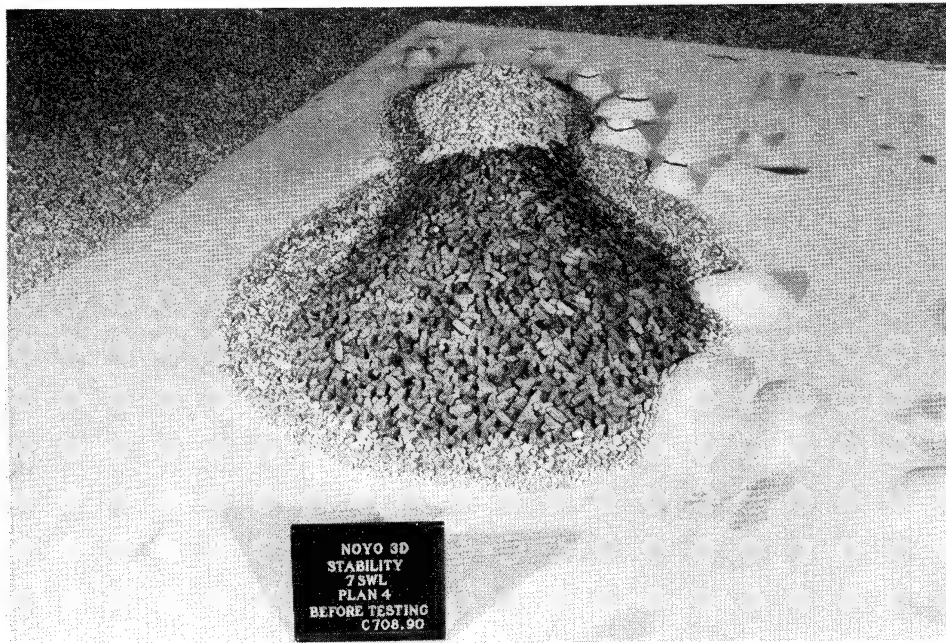
Photo C21. Plan 4, north roundhead before testing
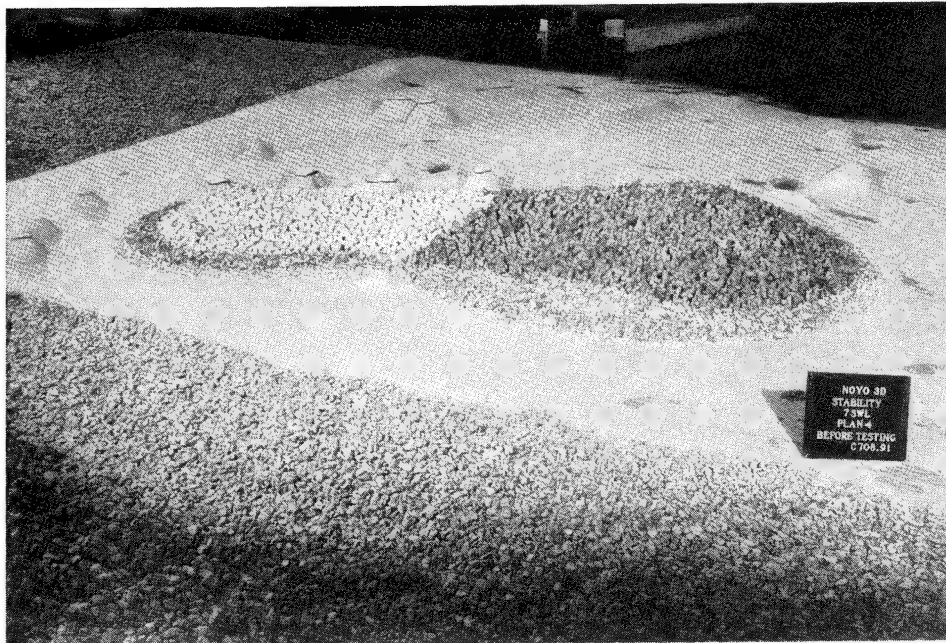


Photo C22. Leeside view of Plan 4 before testing

Appendix C  Three-Dimensional Stability Photographs

Photo C23. Sea-side view of Plan 4 before testing



Photo C24. Plan 4, south roundhead before testing
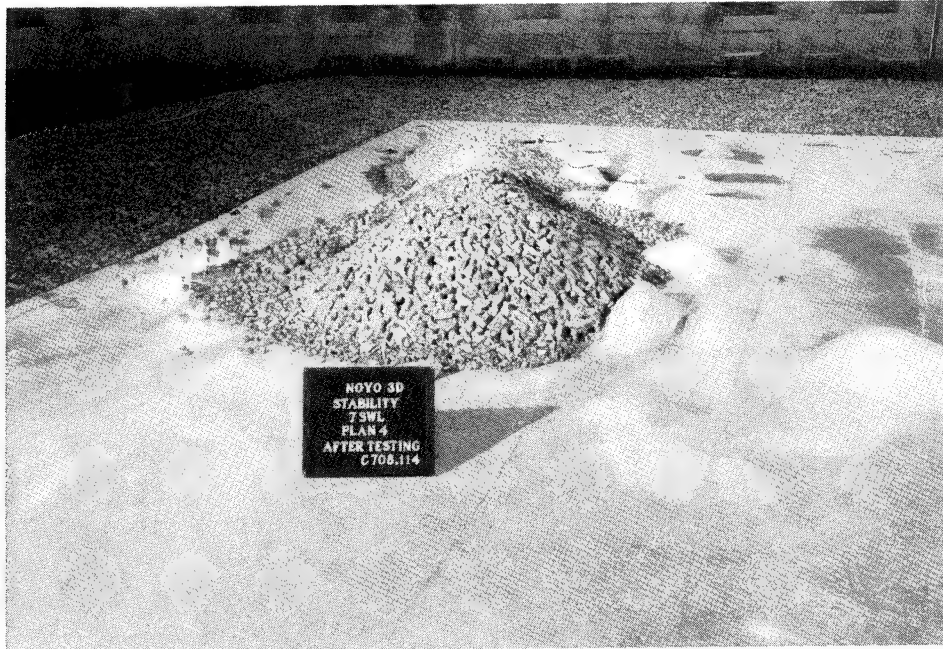
Photo C25. Plan 4, north roundhead after Storm I waves



Photo C26. Leeside view of Plan 4 after Storm I waves
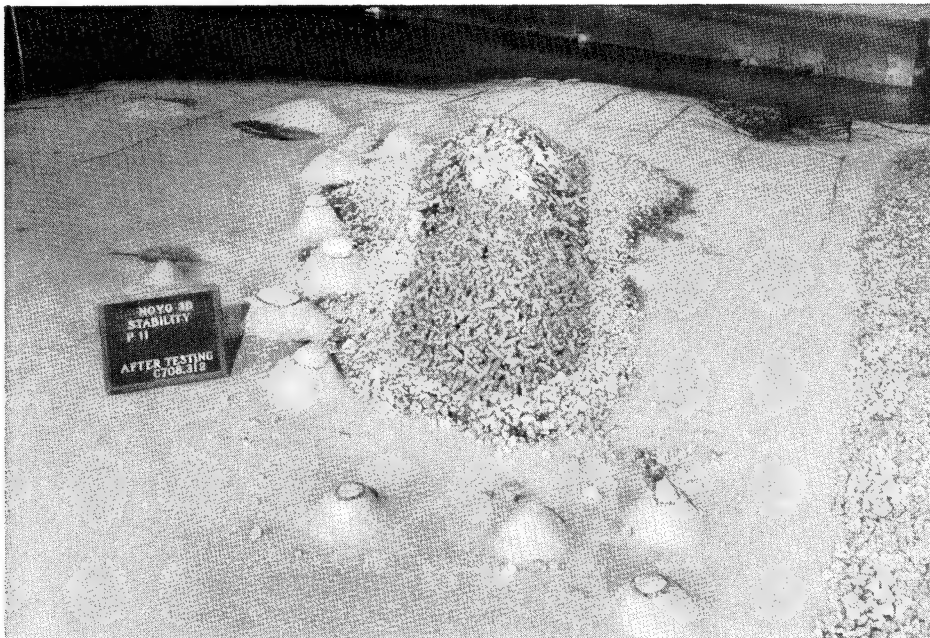
Photo C27.  Sea-side view of Plan 4 after Storm I waves
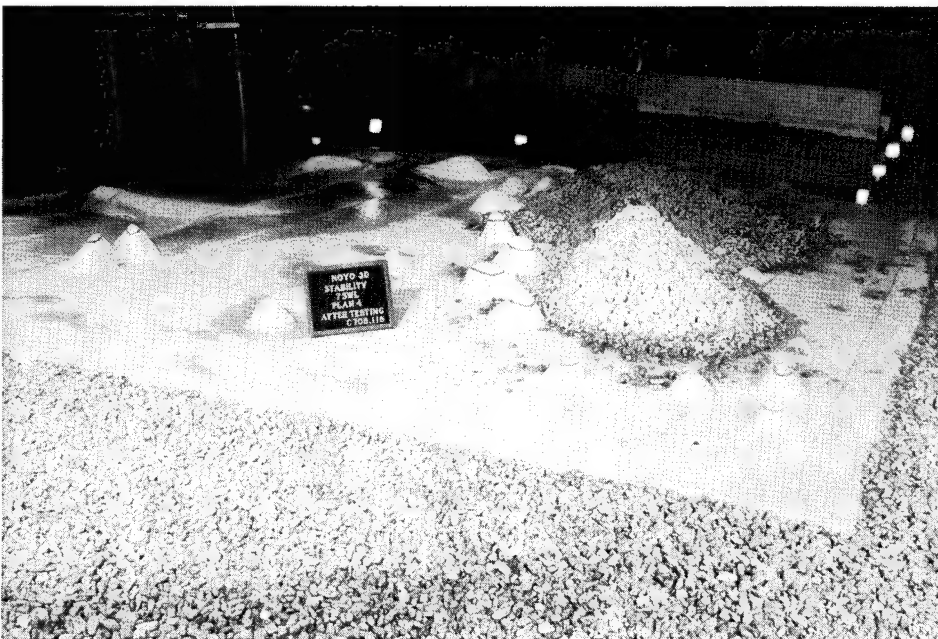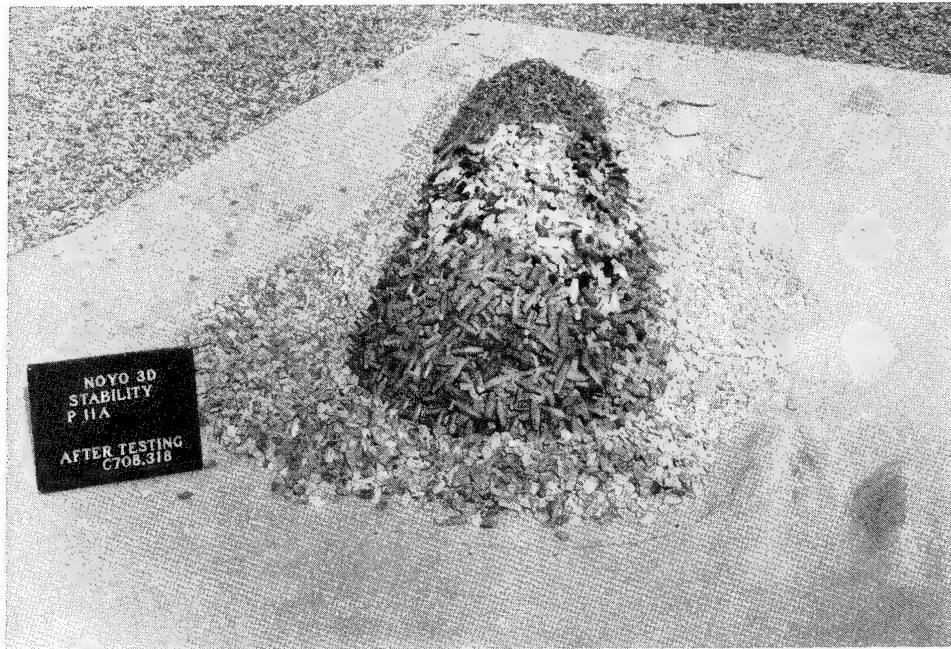


Photo C28.  Plan 4, south roundhead after Storm I waves
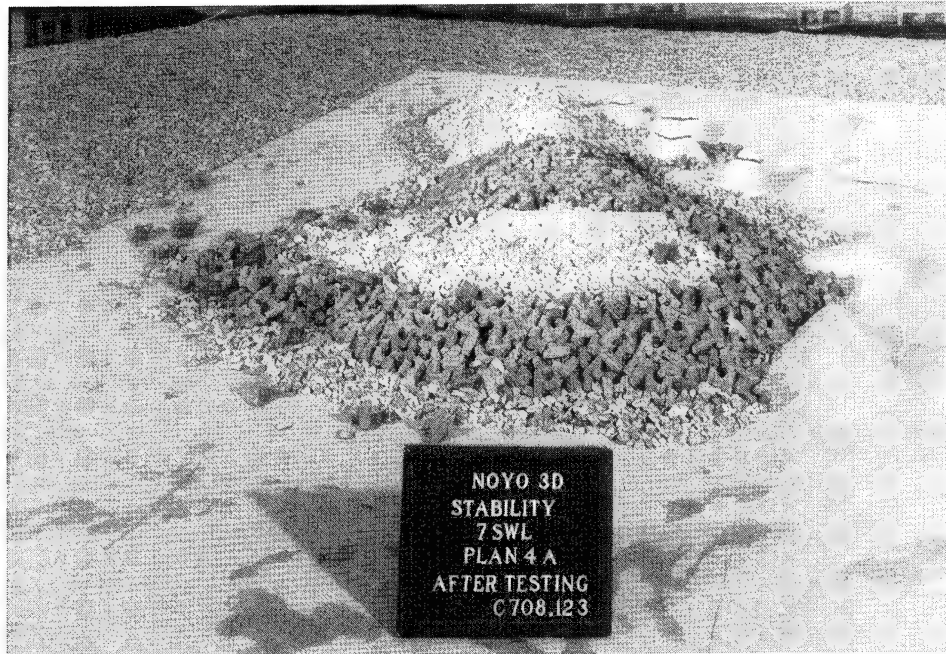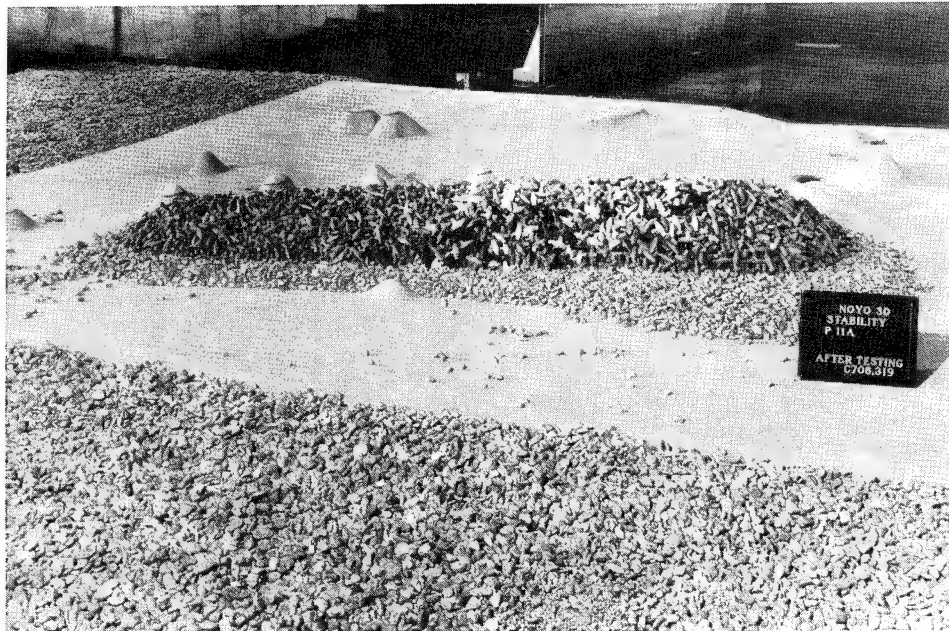
Photo C29.  Plan 4, north roundhead after Storm IA waves
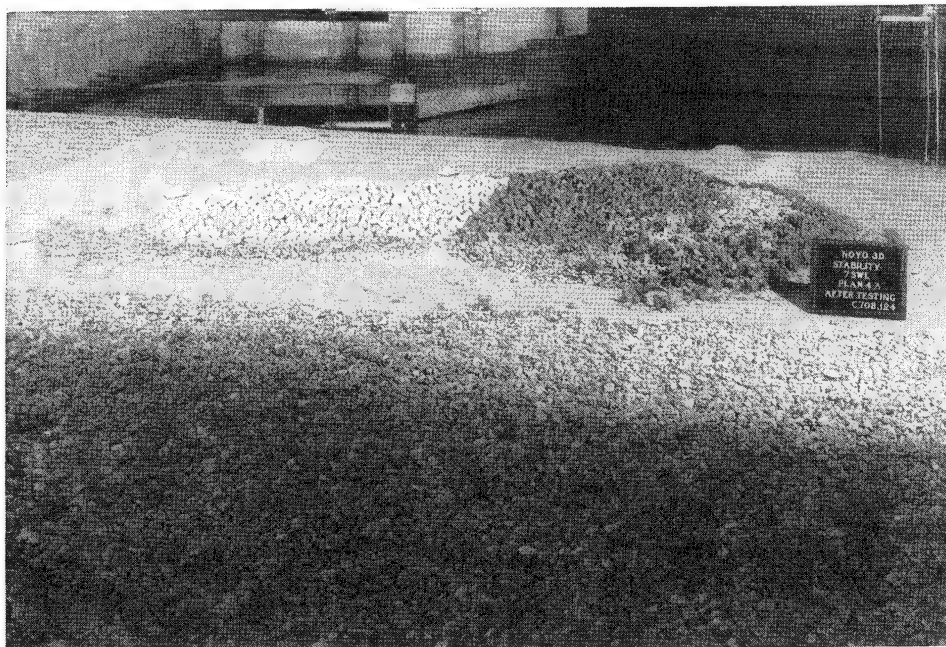


Photo C30.  Leeside view of Plan 4 after Storm IA waves
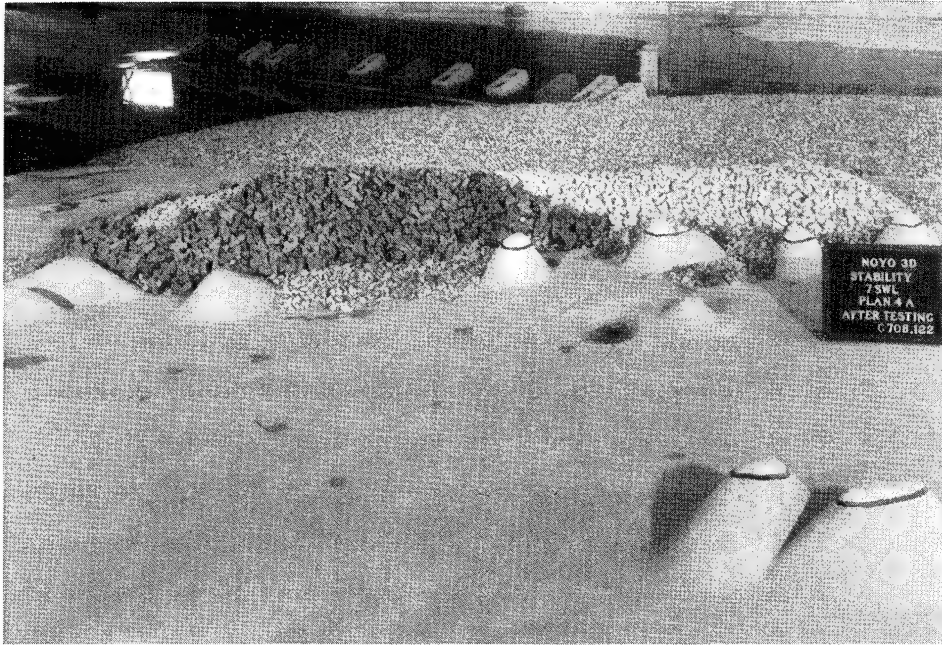
Photo C31. Sea-side view of Plan 4 after Storm IA waves



Photo C32. Plan 4, south roundhead after Storm IA waves
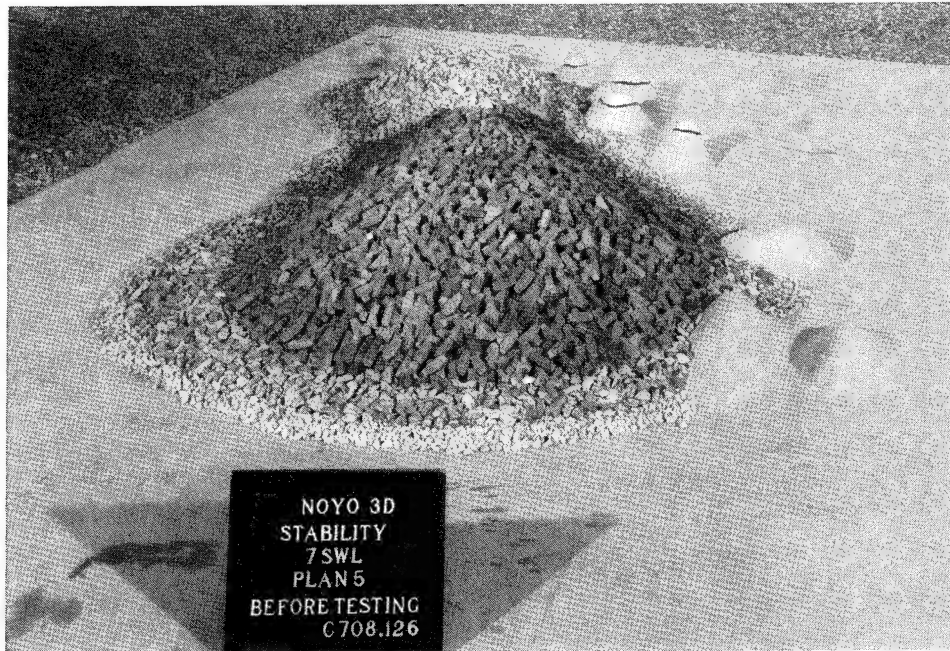
Photo C33.  Plan 5, north roundhead before testing
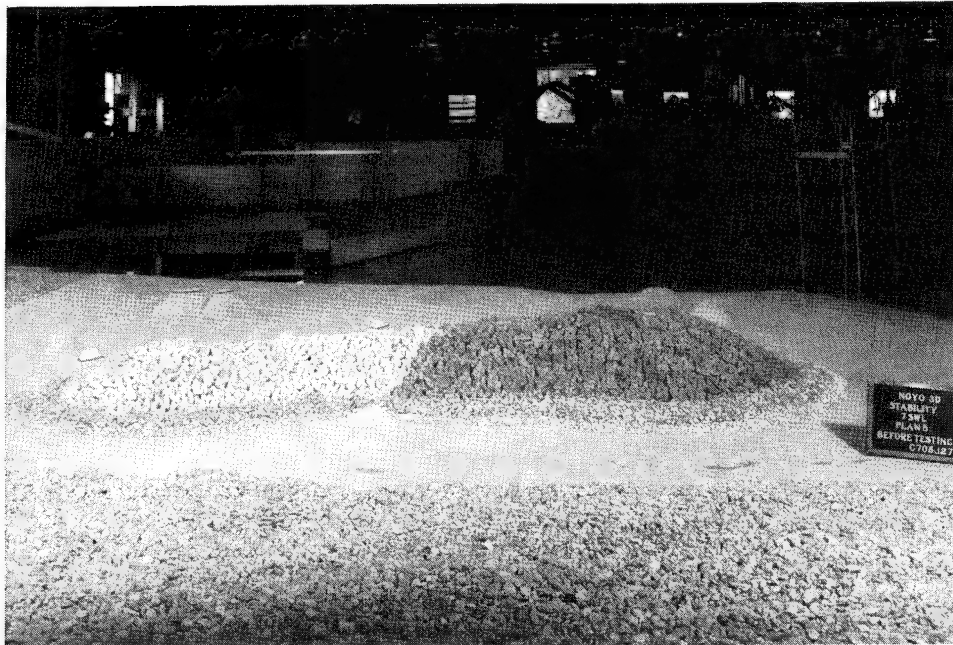


Photo C34.  Leeside view of Plan 5 before testing
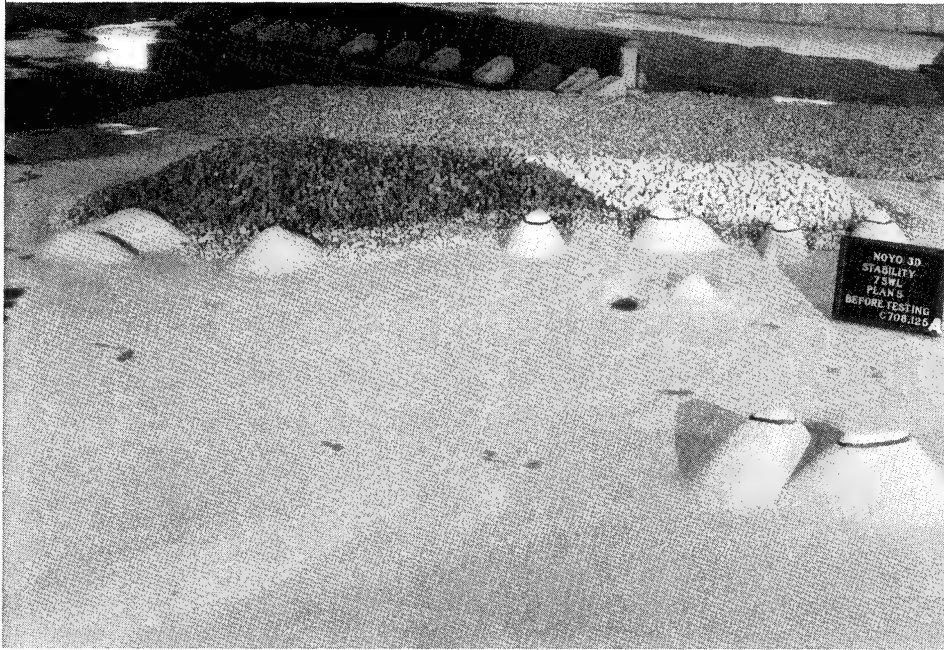
Photo C35. Sea-side view of Plan 5 before testing
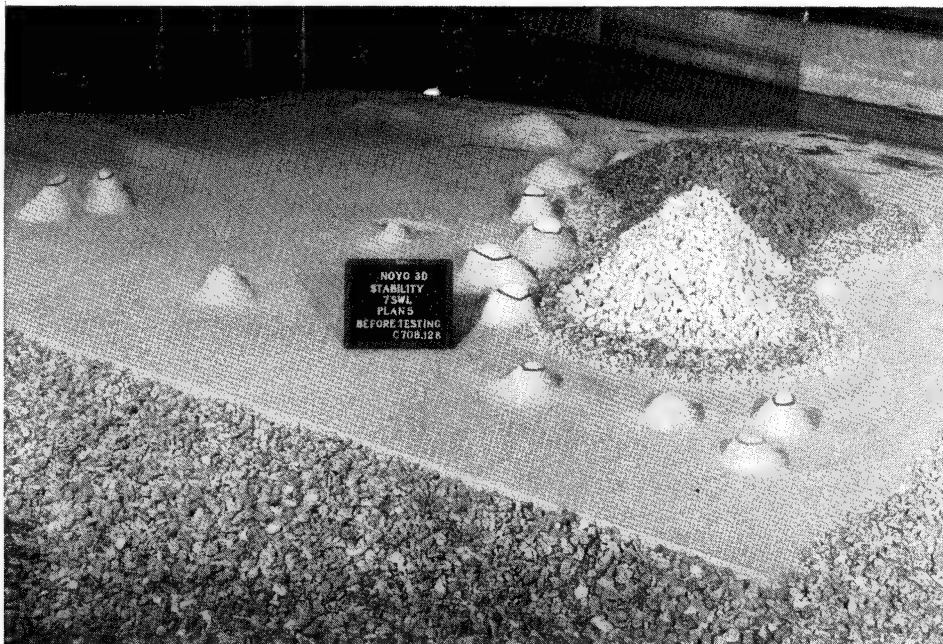


Photo C36. Plan 5, south roundhead before testing
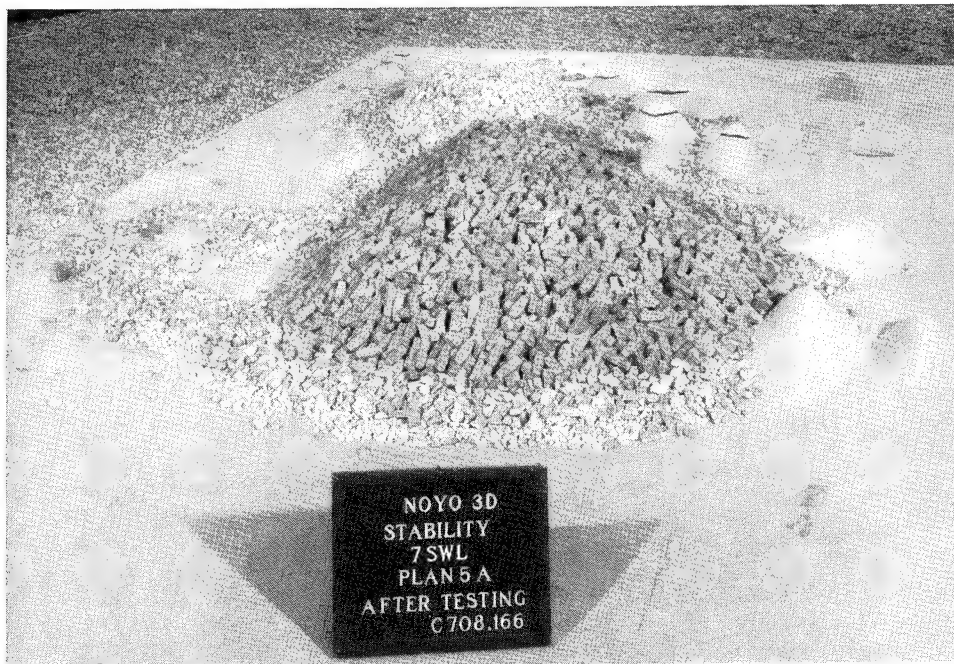
Photo C37. Plan 5, north roundhead after Storm IA waves
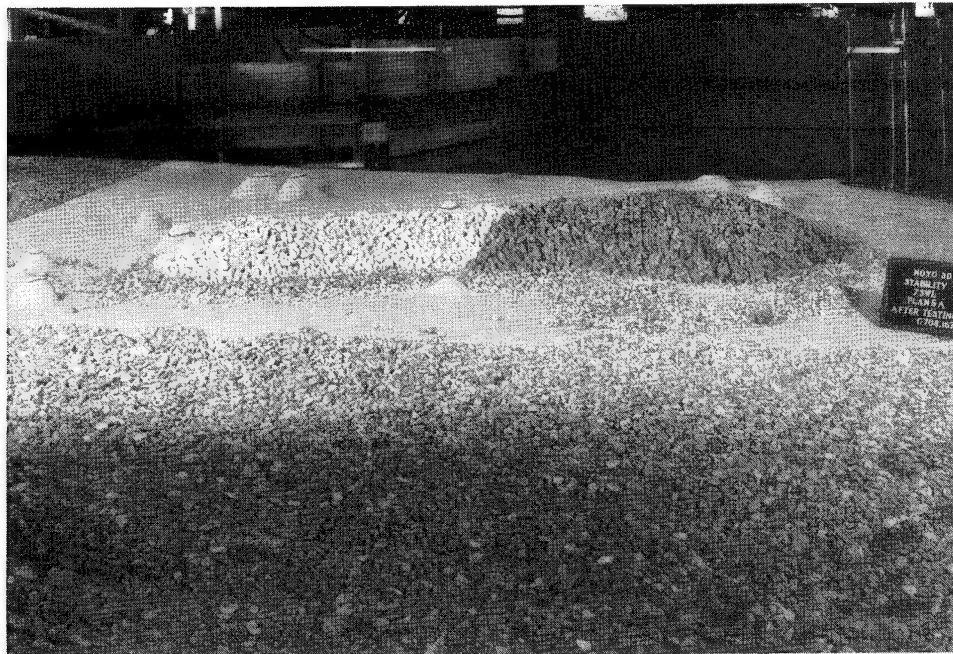


Photo C38. Leeside view of Plan 5 after Storm IA waves
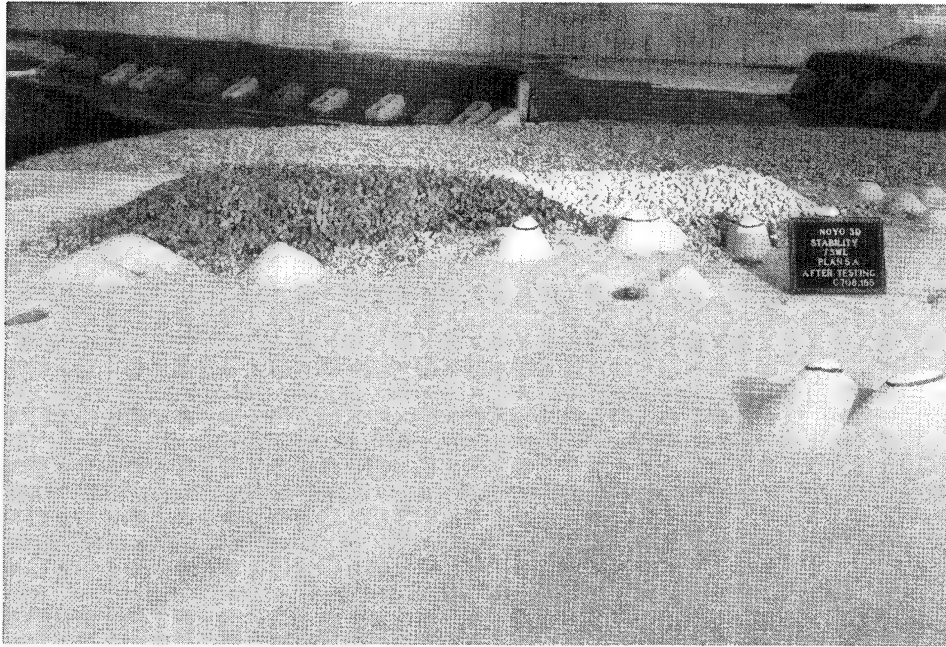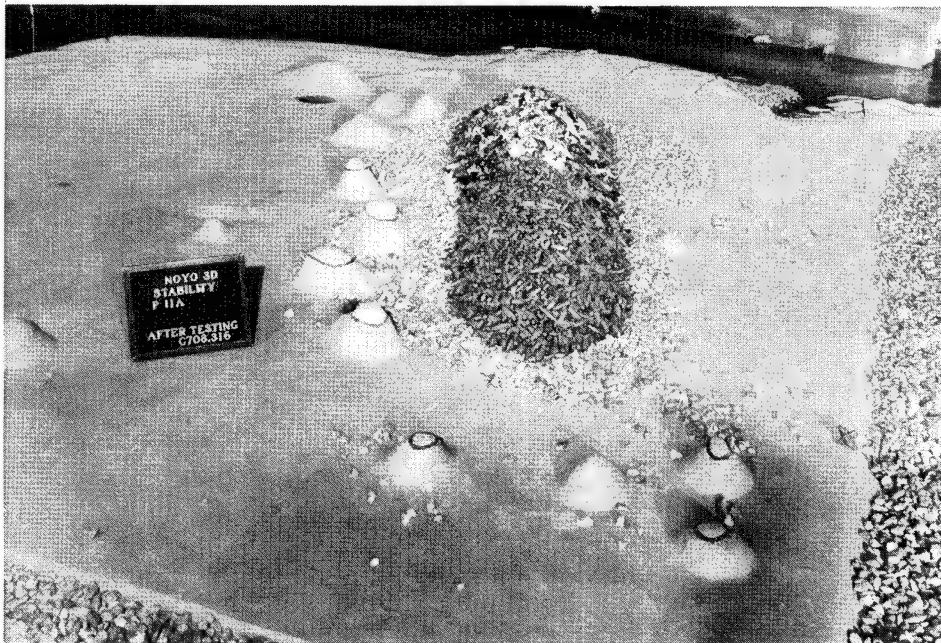
Photo C39. Sea-side view of Plan 5 after Storm IA waves


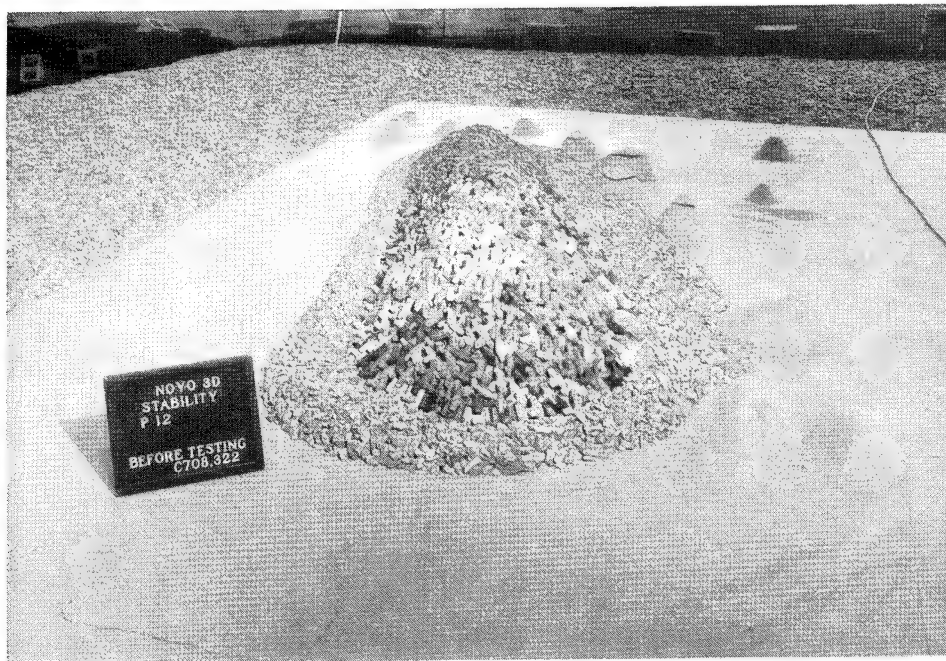
Photo C40. Plan 5, south roundhead after Storm IA waves
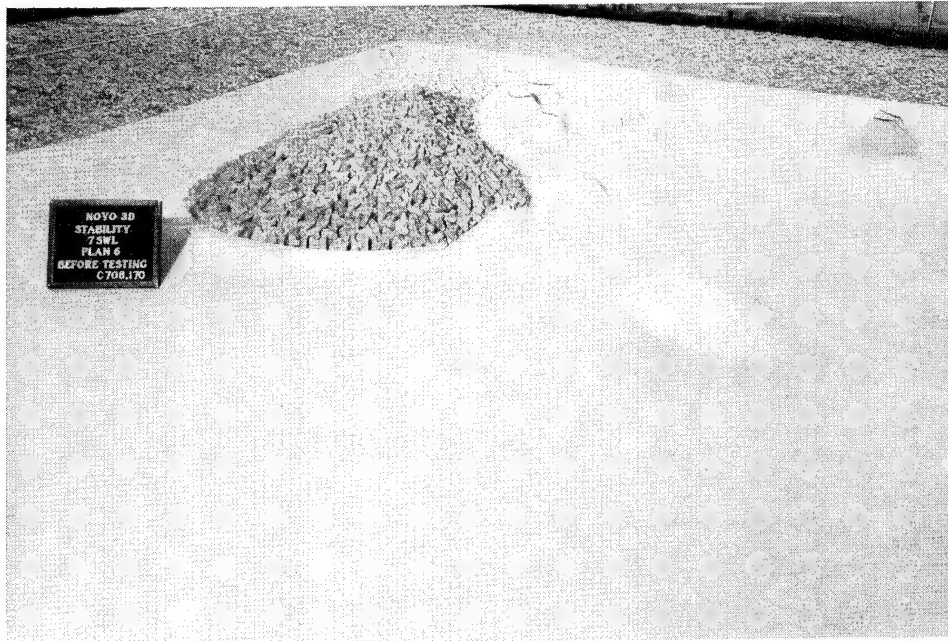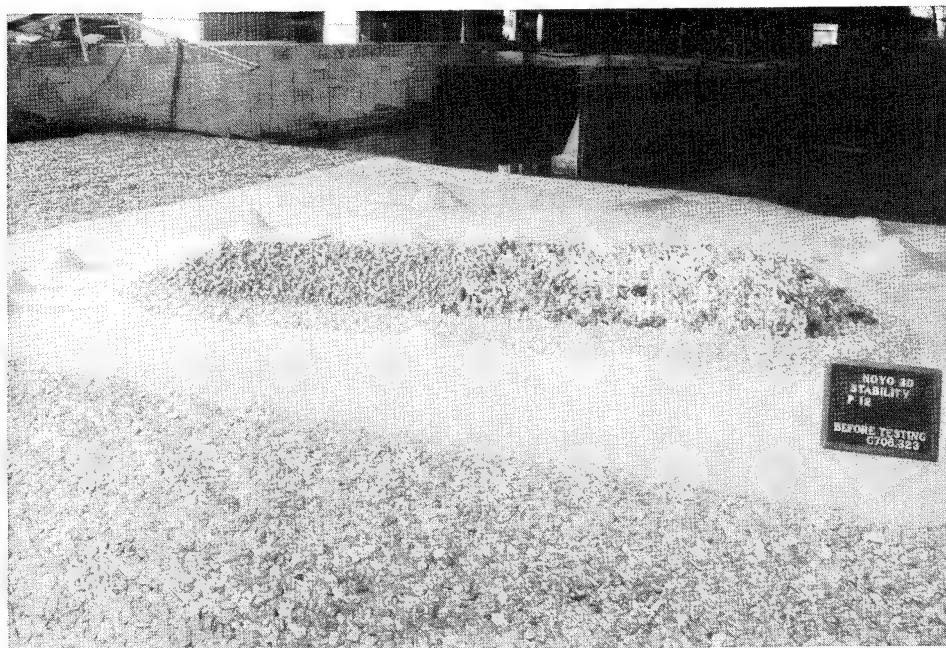
Photo C41. Plan 6, north roundhead before testing
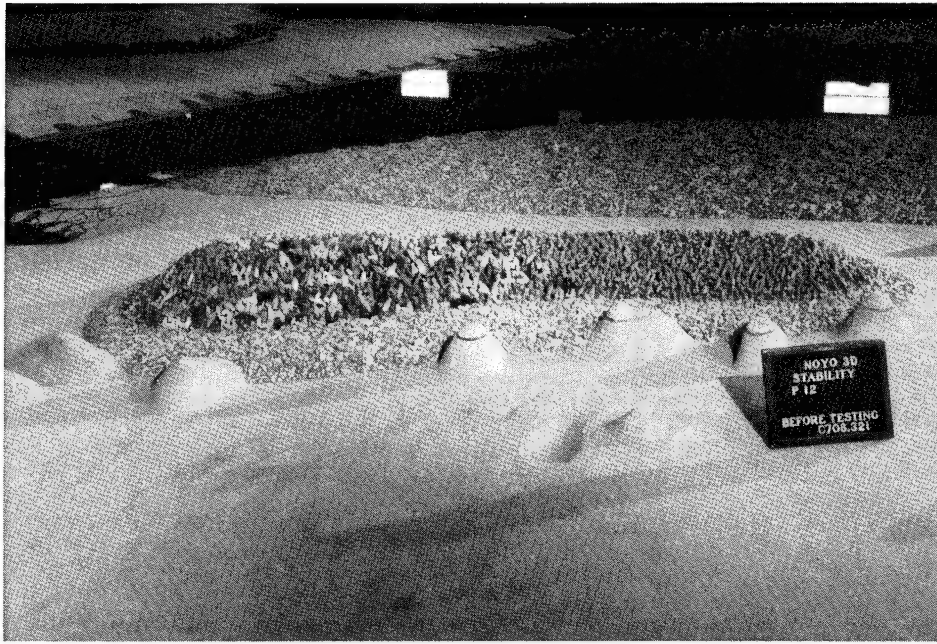


Photo C42. Leeside view of Plan 6 before testing
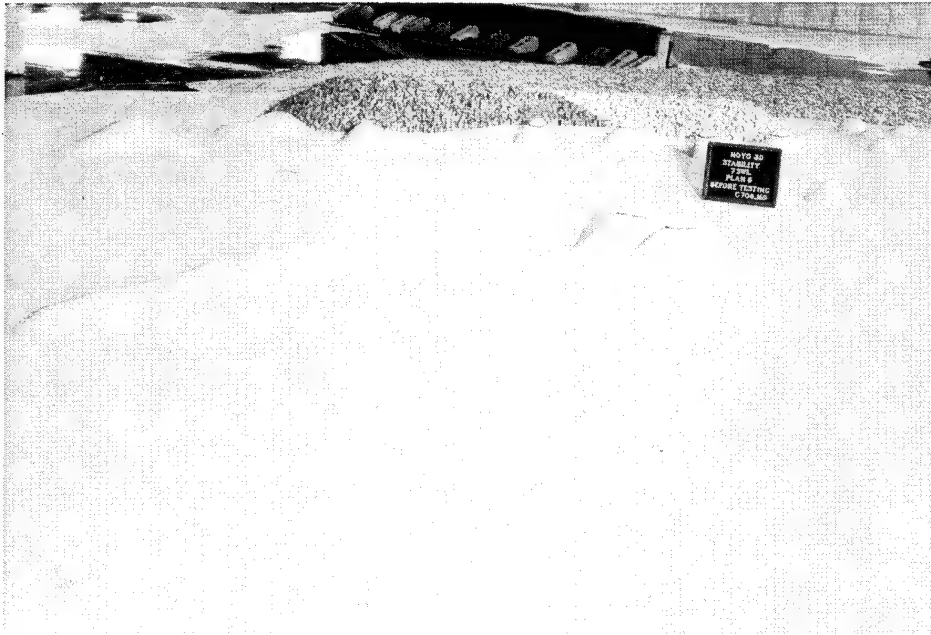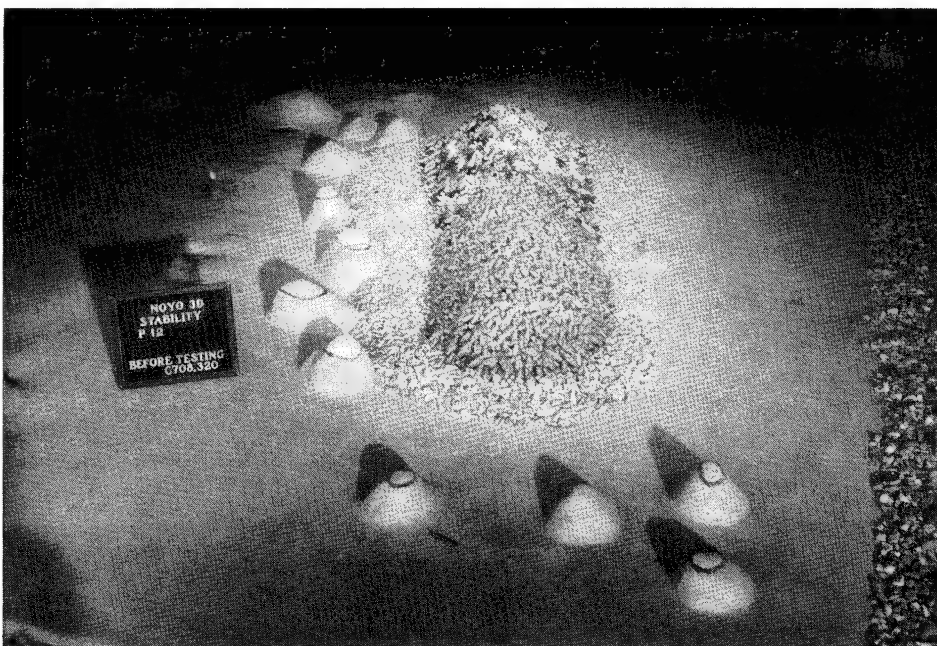
Photo C43.  Sea-side view of Plan 6 before testing
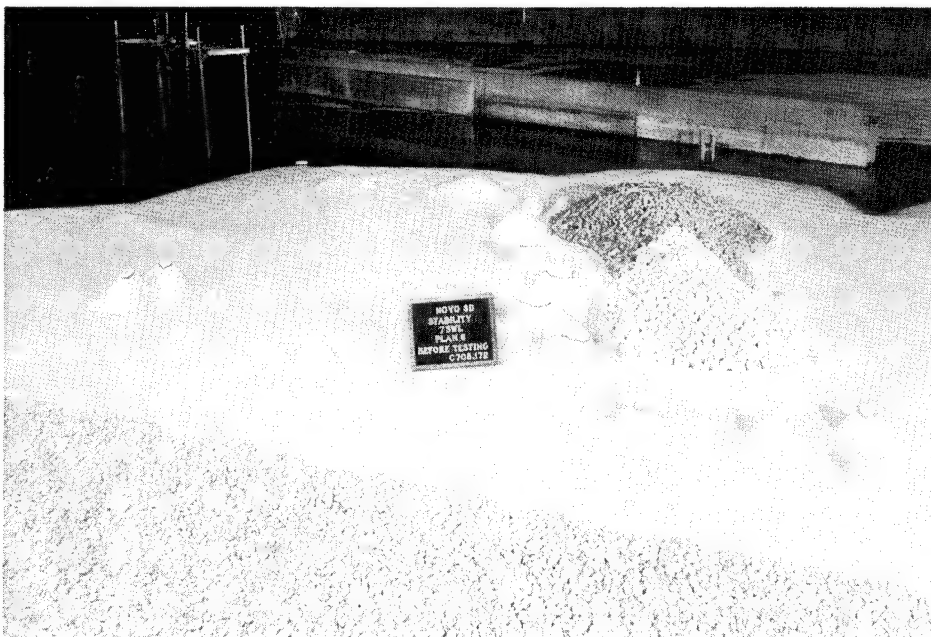


Photo C44.  Plan 6, south roundhead before testing
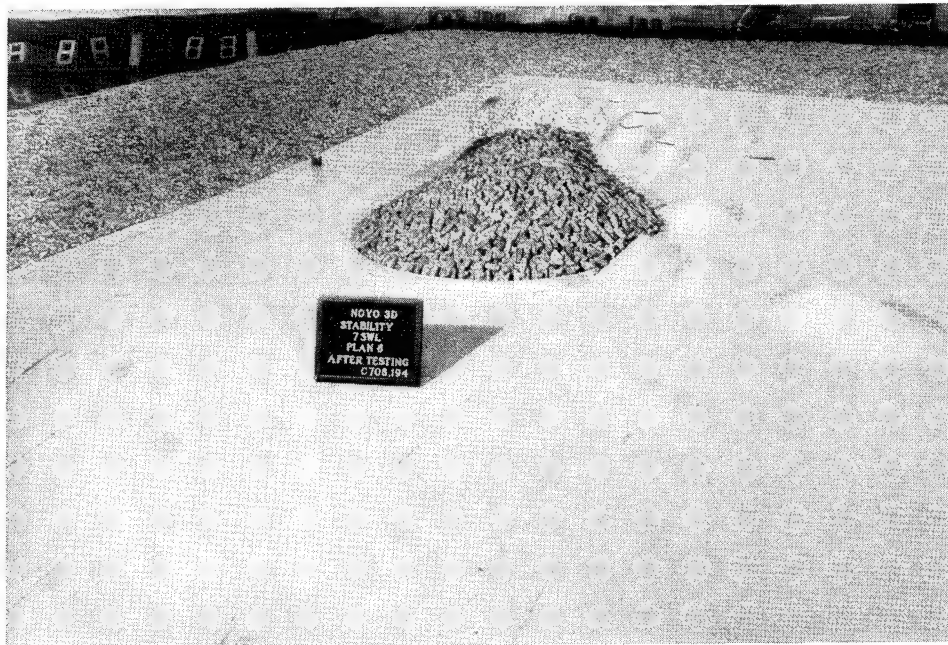
Photo C45.  Plan 6, north roundhead after Storm I waves
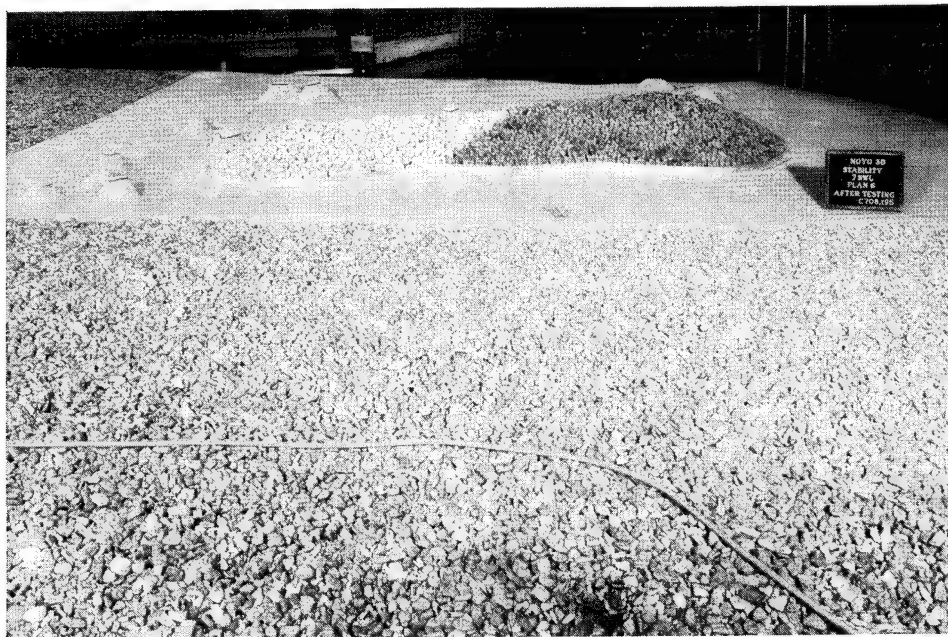


Photo C46.  Leeside view of Plan 6 after Storm I waves
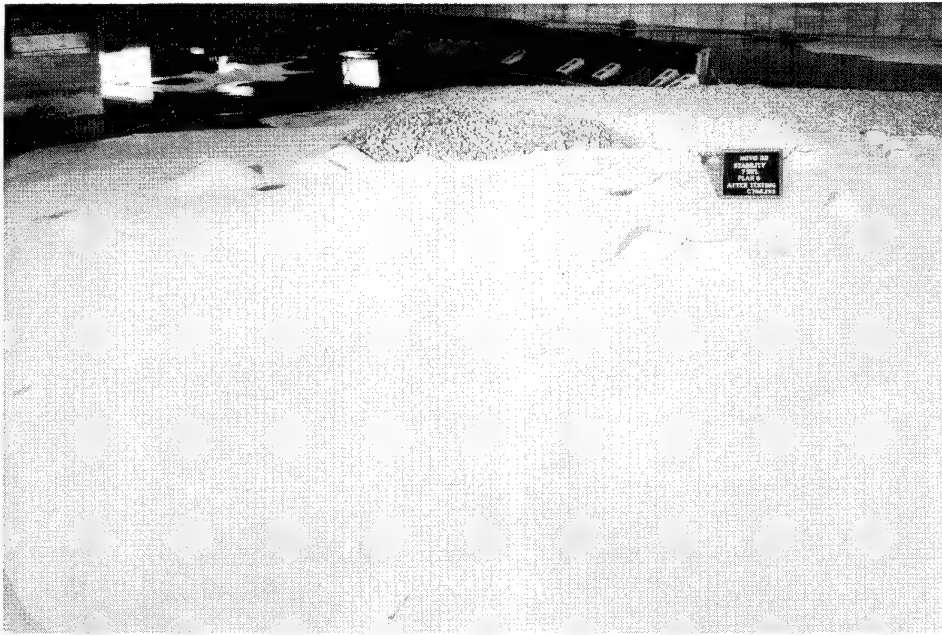
Photo C47.  Sea-side view of Plan 6 after Storm I waves
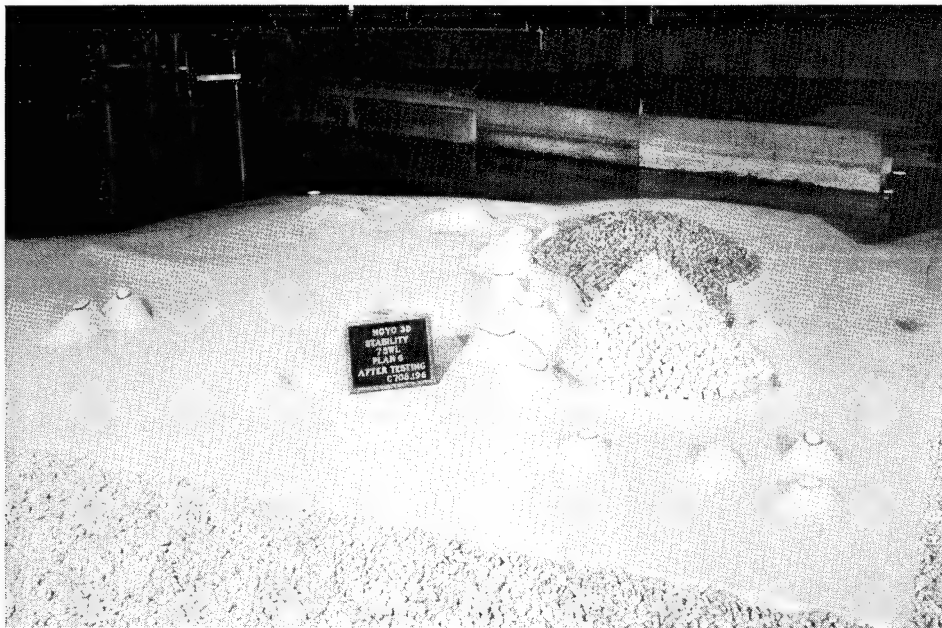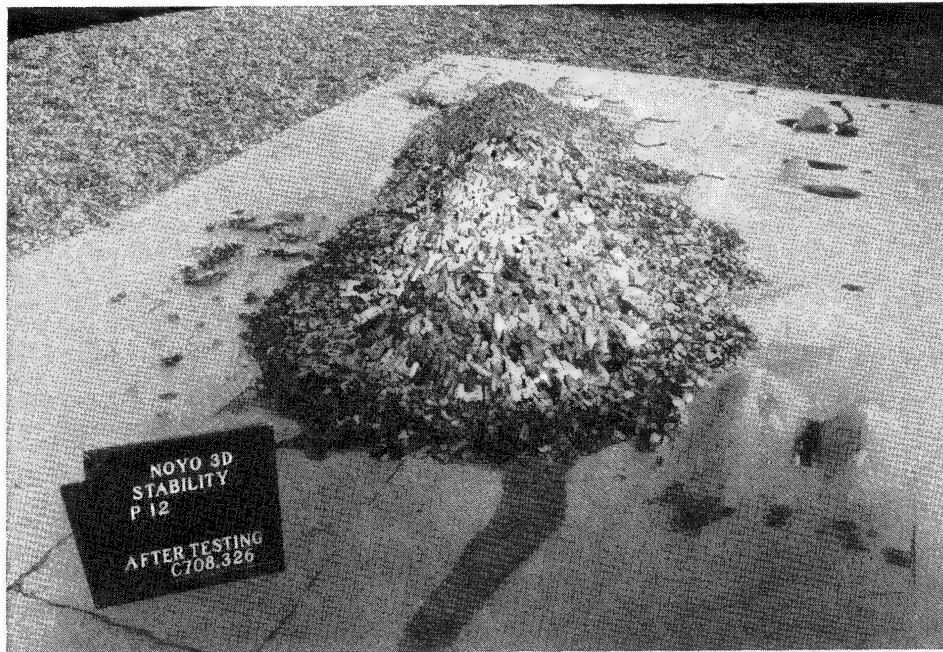


Photo C48.  Plan 6, south roundhead after Storm I waves
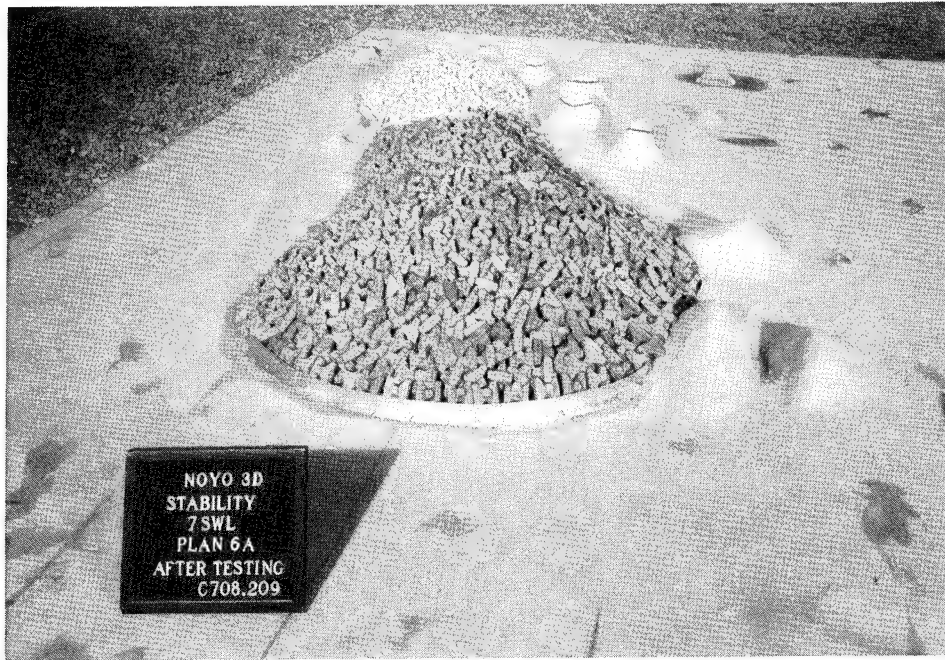
Photo C49. Plan 6, north roundhead after Storm IA waves
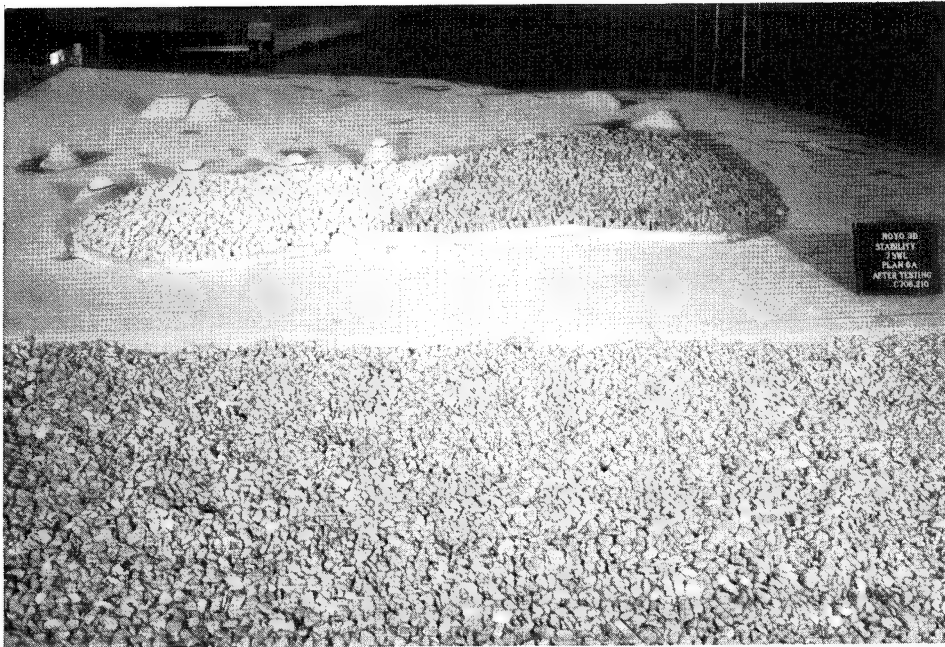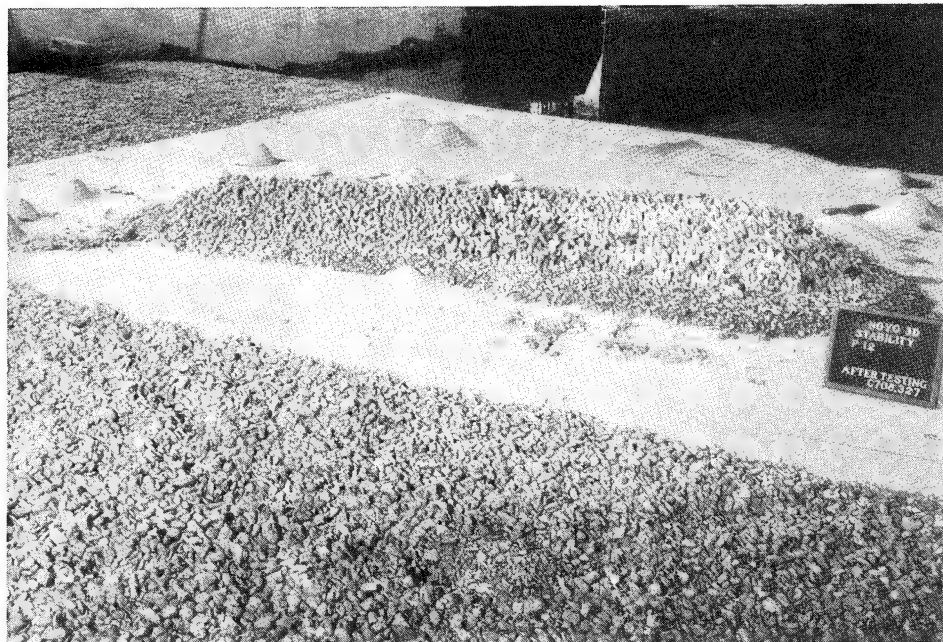


Photo C50. Leeside view of Plan 6 after Storm IA waves
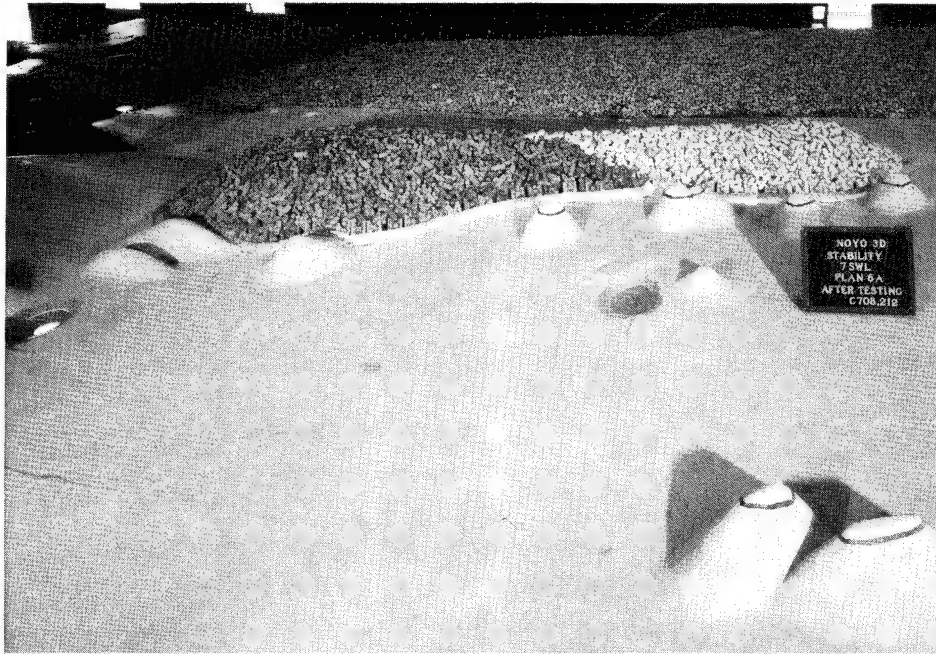
Photo C51. Sea-side view of Plan 6 after Storm IA waves
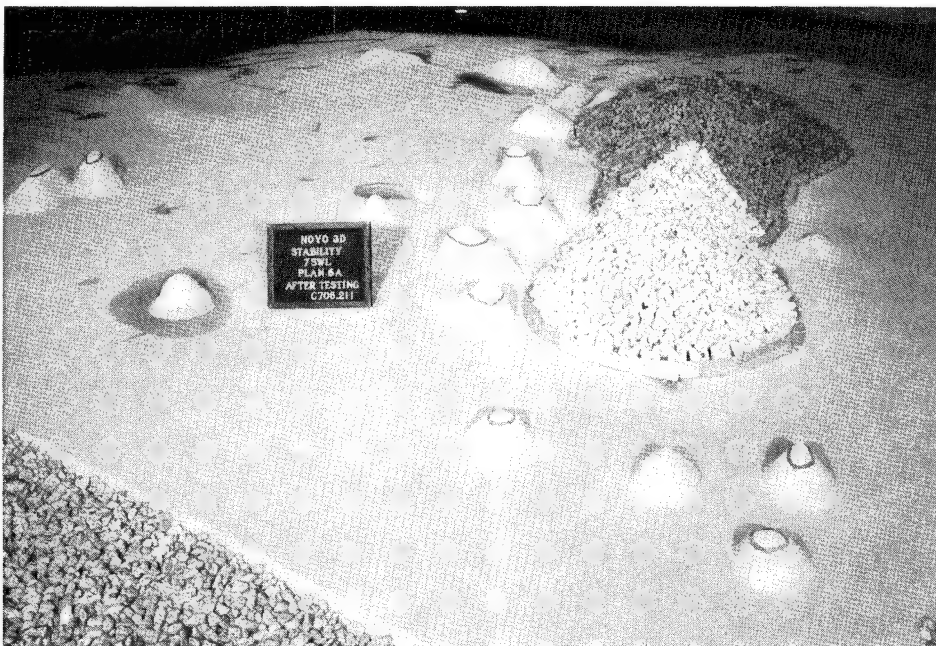


Photo C52. Plan 6, south roundhead after Storm IA waves
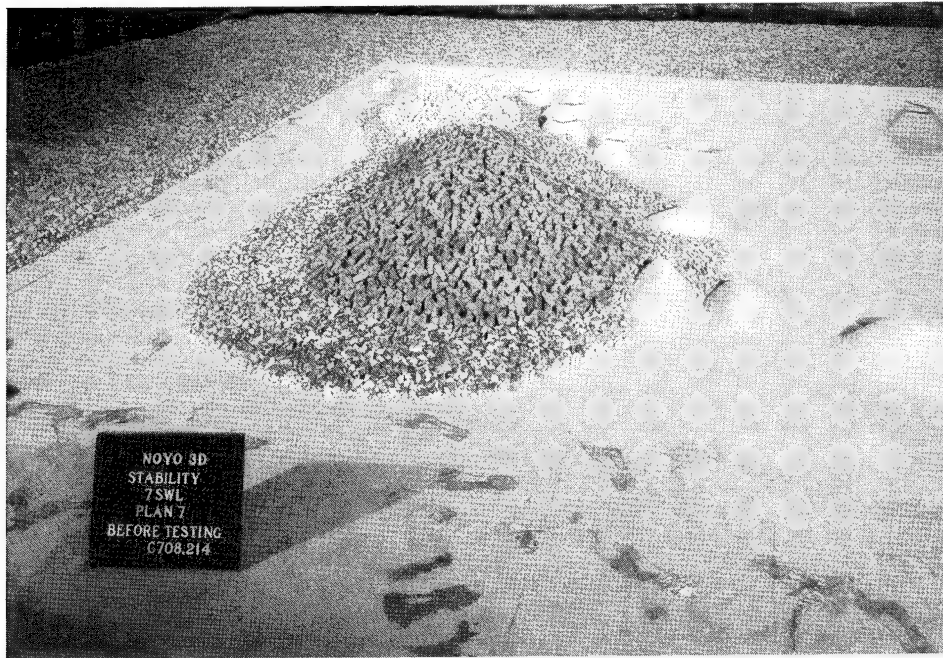
Photo C53. Plan 7, north roundhead before testing
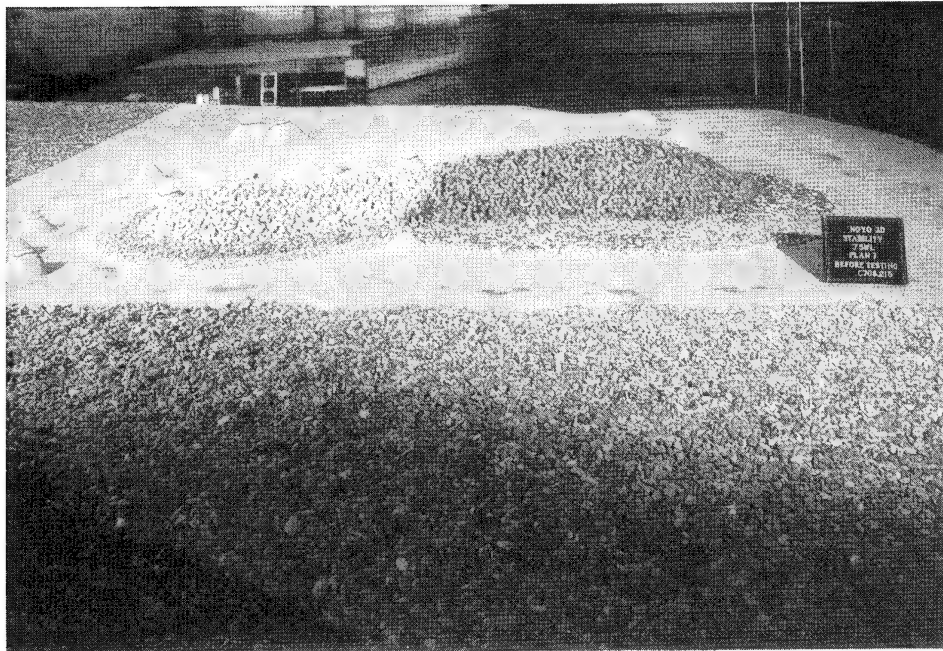


Photo C54. Leeside view of Plan 7 before testing
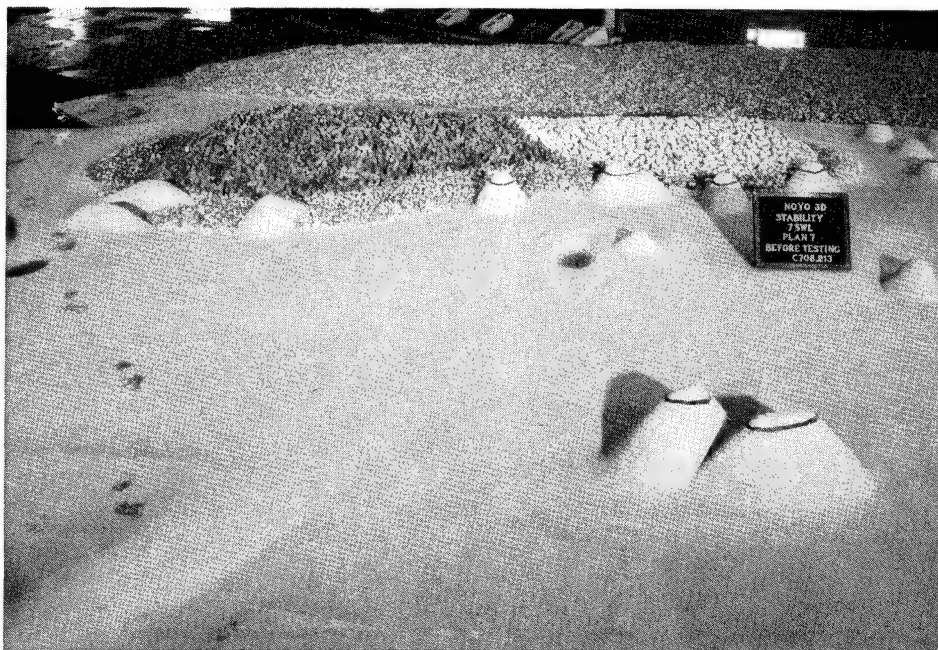
Photo C55. Sea-side view of Plan 7 before testing
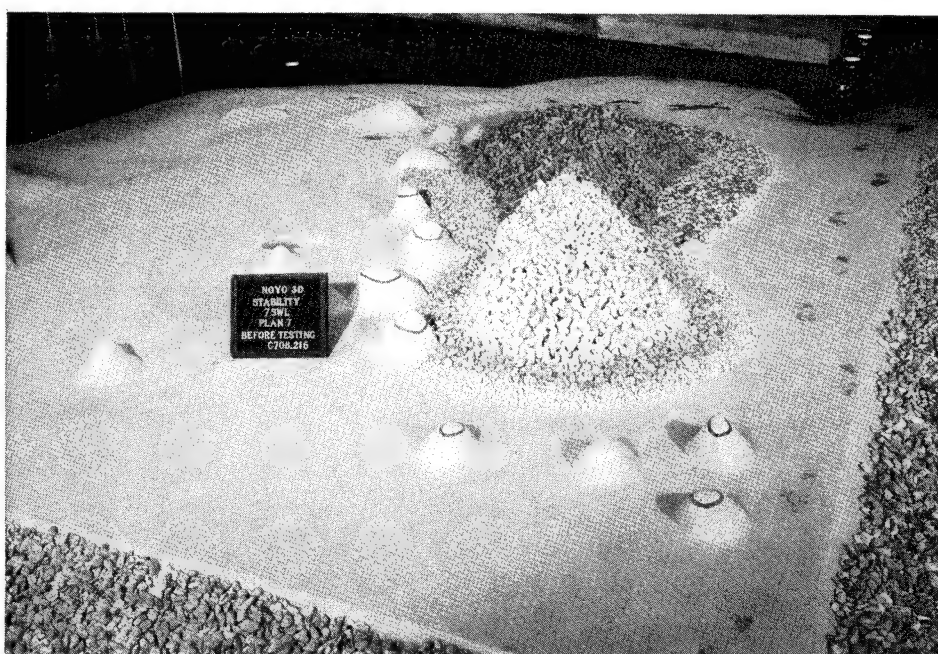


Photo C56. Plan 7, south roundhead before testing

Appendix C  Three-Dimensional Stability Photographs
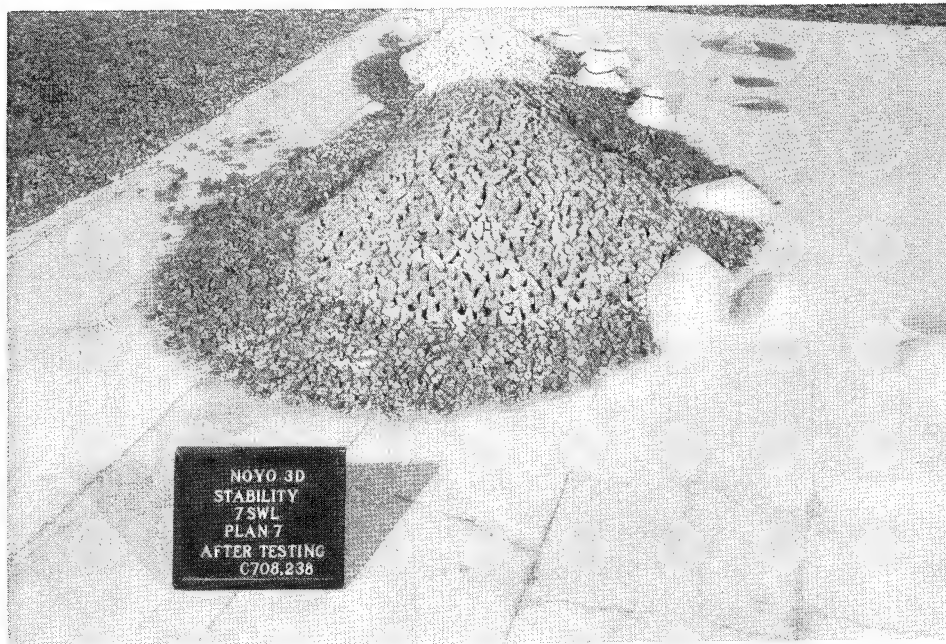
Photo C57.  Plan 7, north roundhead after Storm I waves



Photo C58.  Leeside view of Plan 7 after Storm I waves
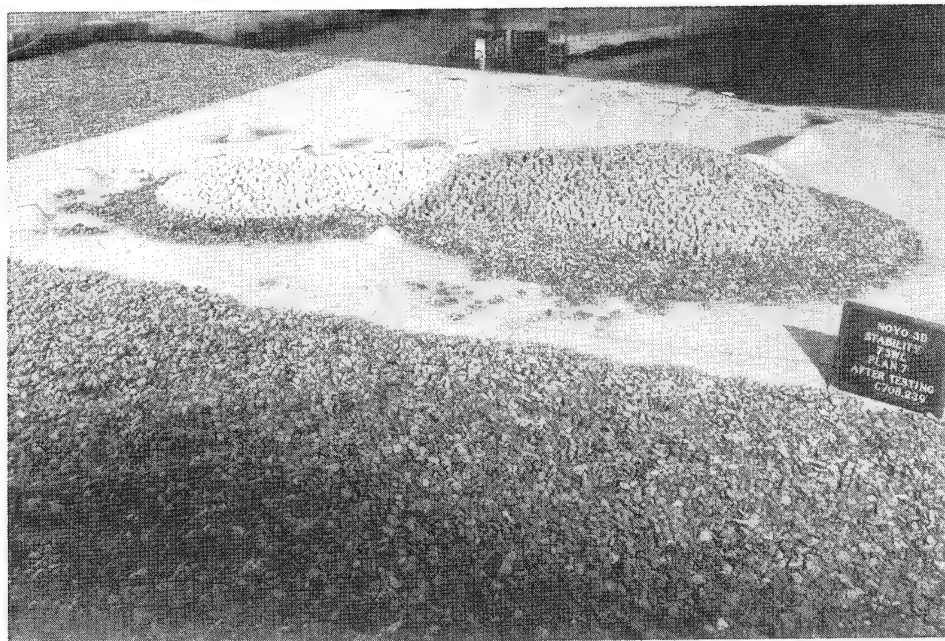
Appendix C  Three-Dimensional Stability Photographs
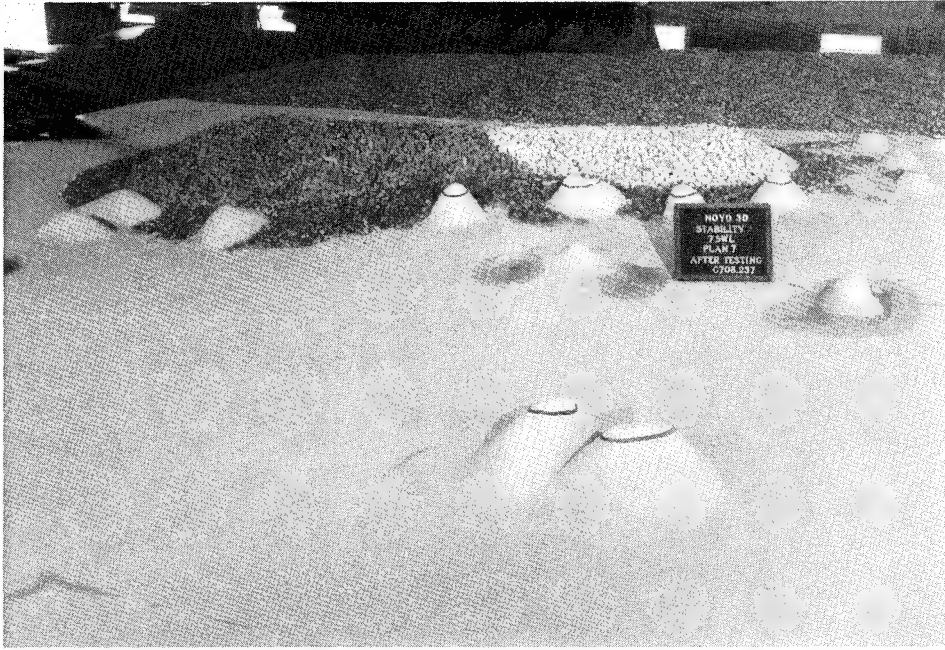
Photo C59.  Sea-side view of Plan 7 after Storm I waves



Photo C60.  Plan 7, south roundhead after Storm I waves
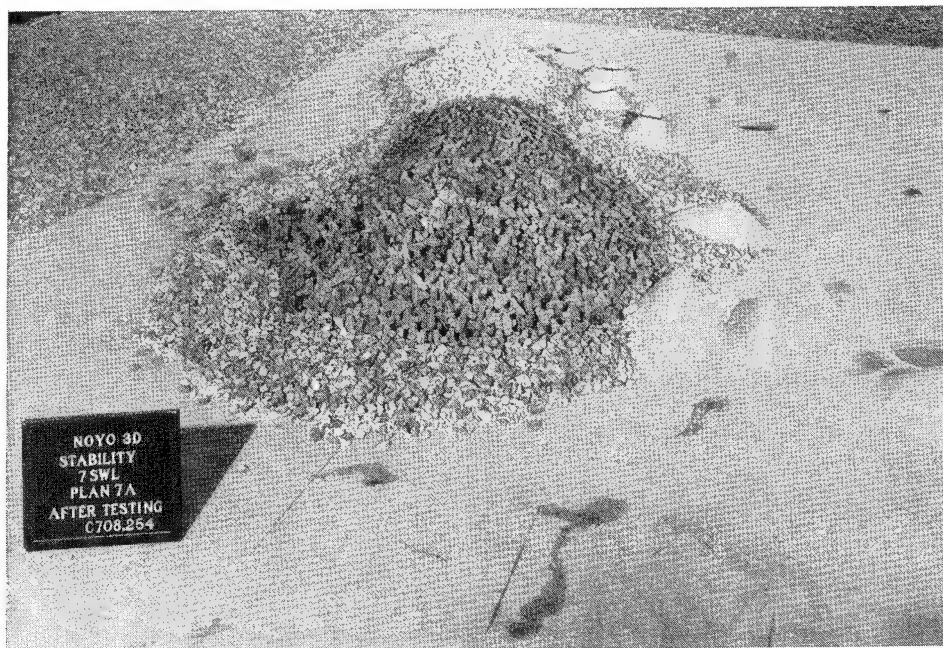
Photo C61. Plan 7, north roundhead after Storm IA waves
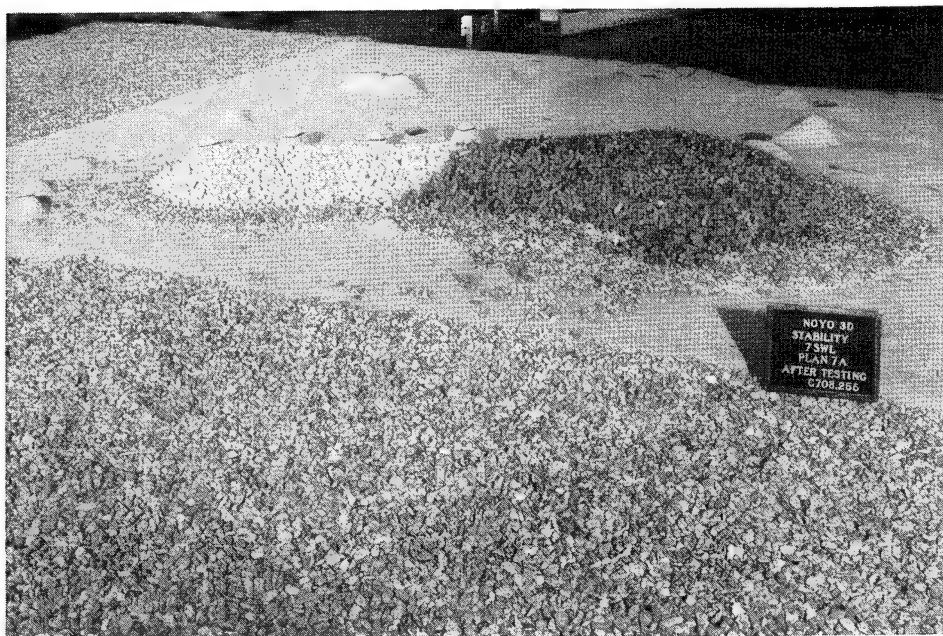


Photo C62. Leeside view of Plan 7 after Storm IA waves

Photo C63. Sea-side view of Plan 7 after Storm IA waves
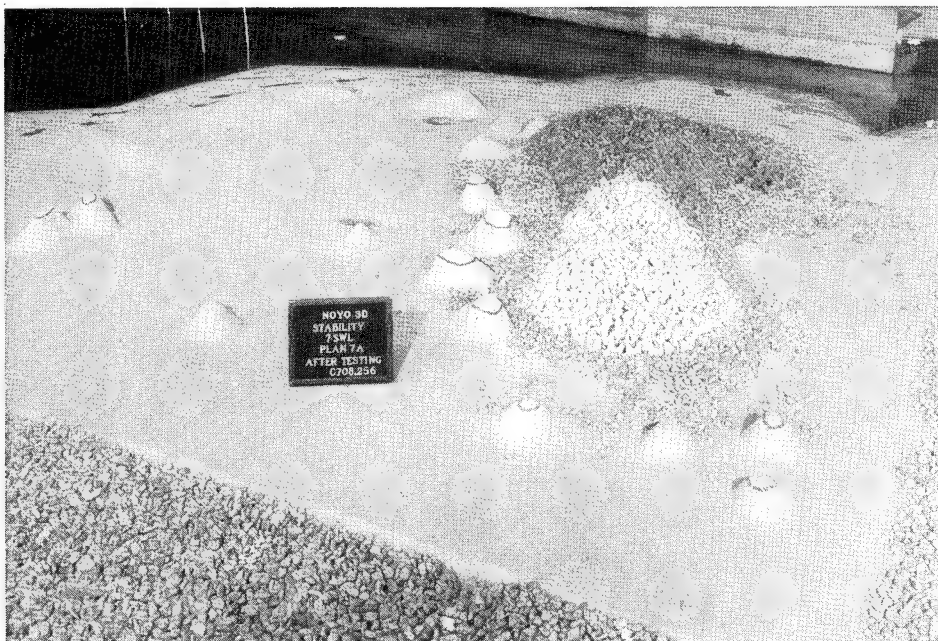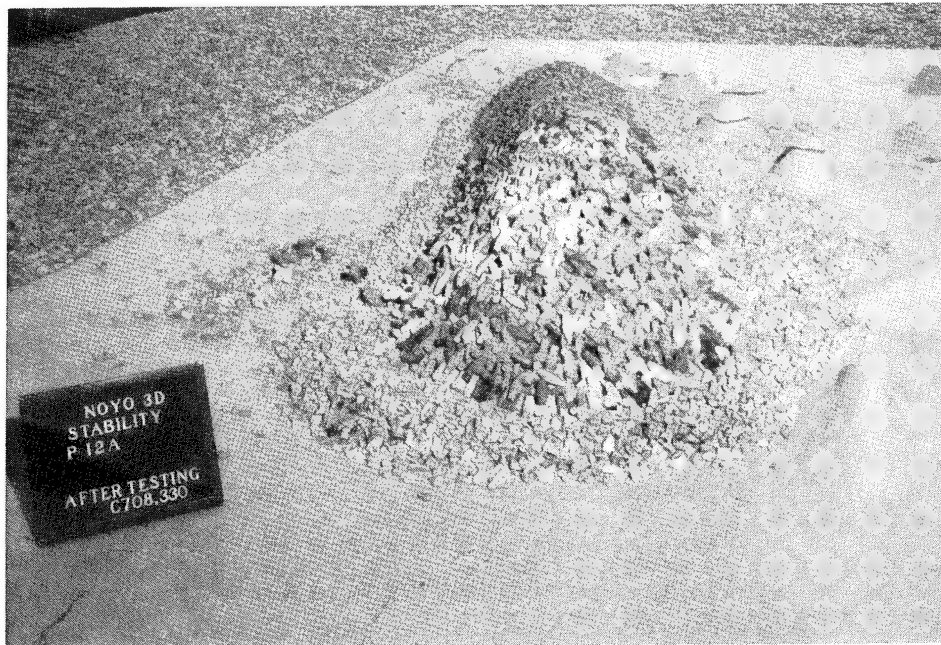


Photo C64. Plan 7, south roundhead after Storm IA waves
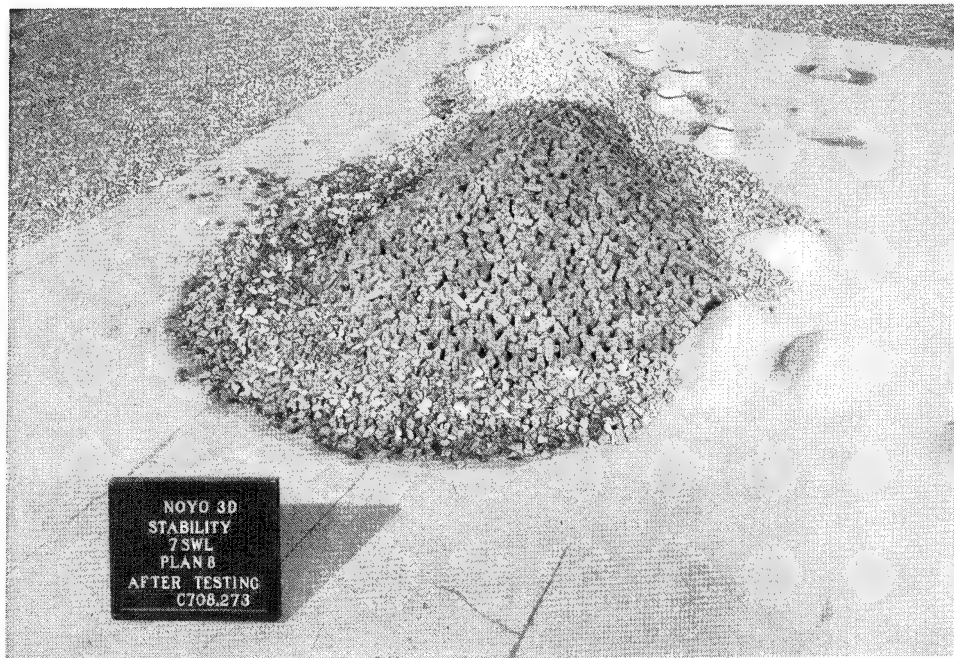
Photo C65. Plan 8, north roundhead after Storm IA waves



Photo C66. Leeside view of Plan 8 after Storm IA waves
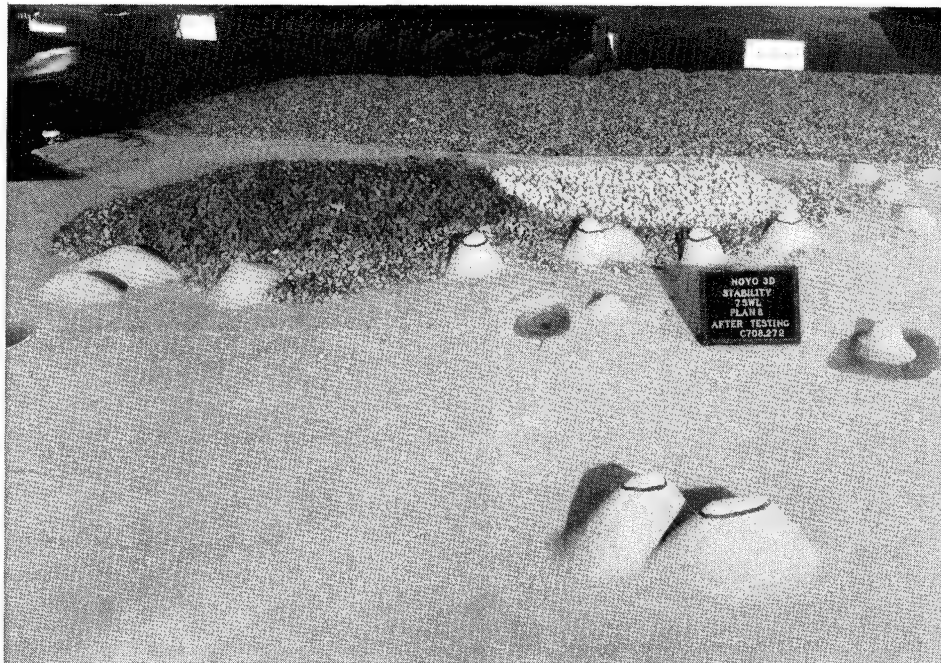
Photo C67.  Sea-side view of Plan 8 after Storm IA waves
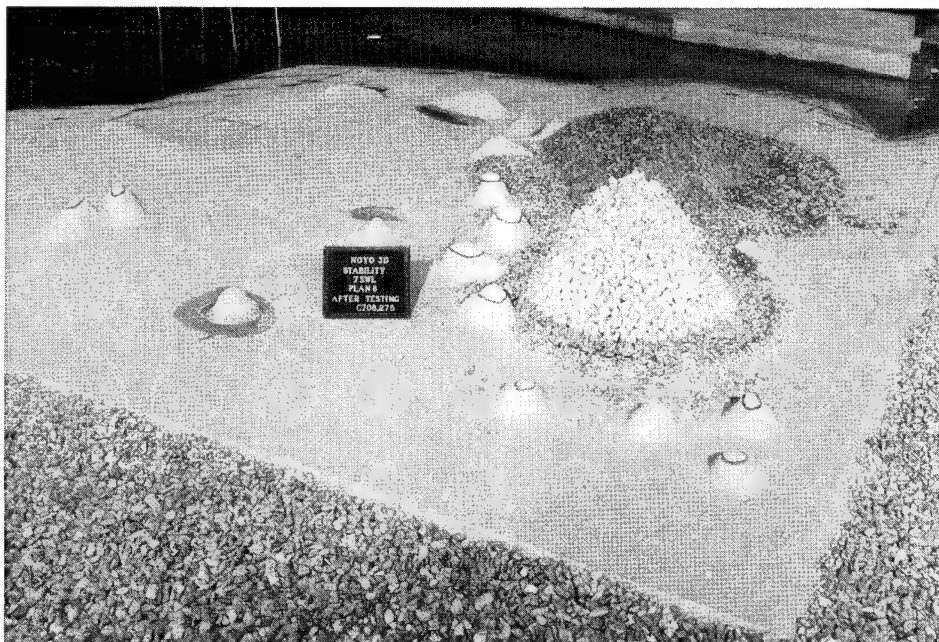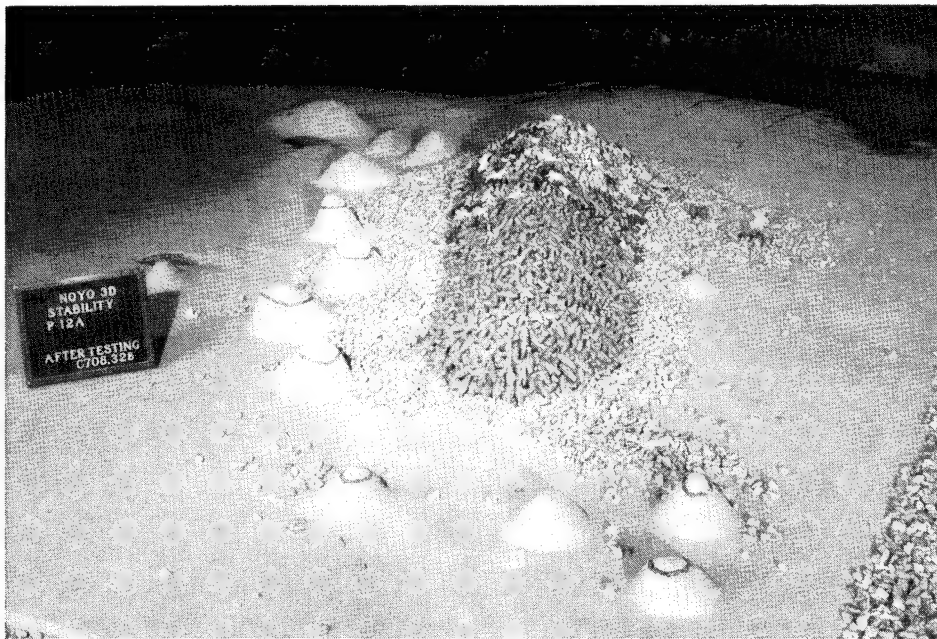
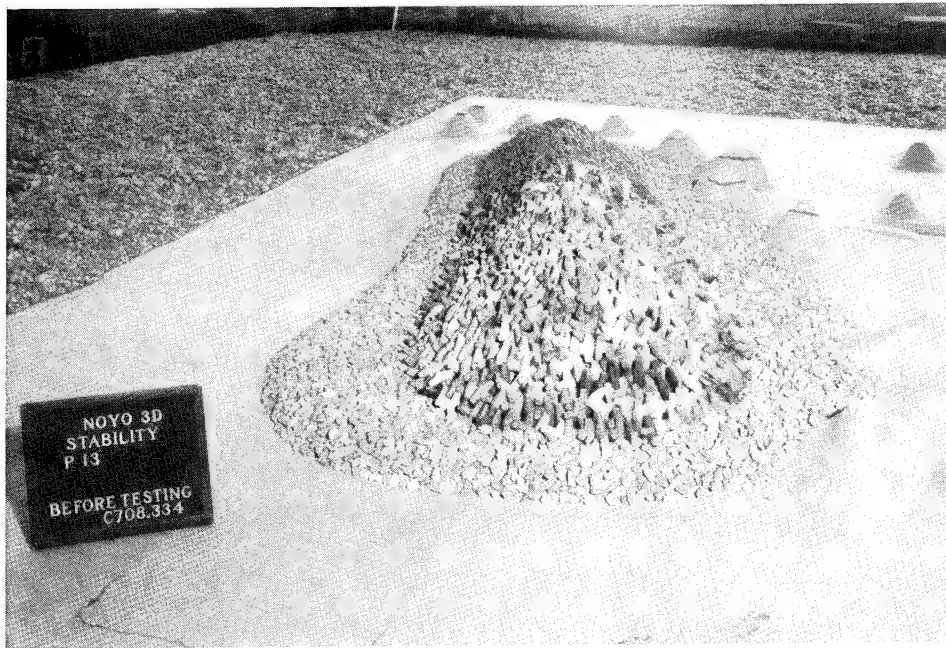

Photo C68.  Plan 8, south roundhead after Storm IA waves
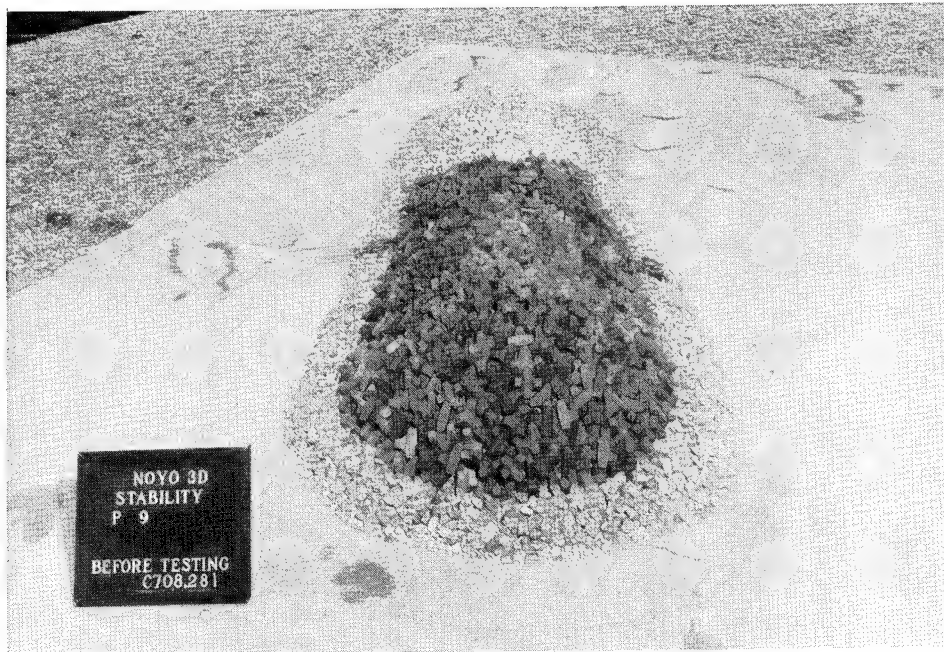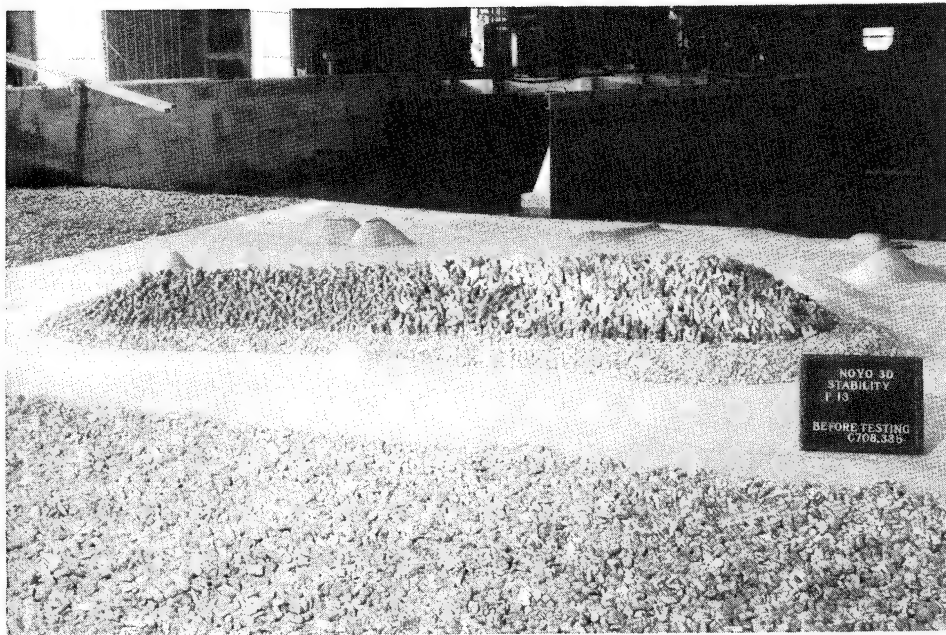
Photo C69. Plan 9, north roundhead before testing
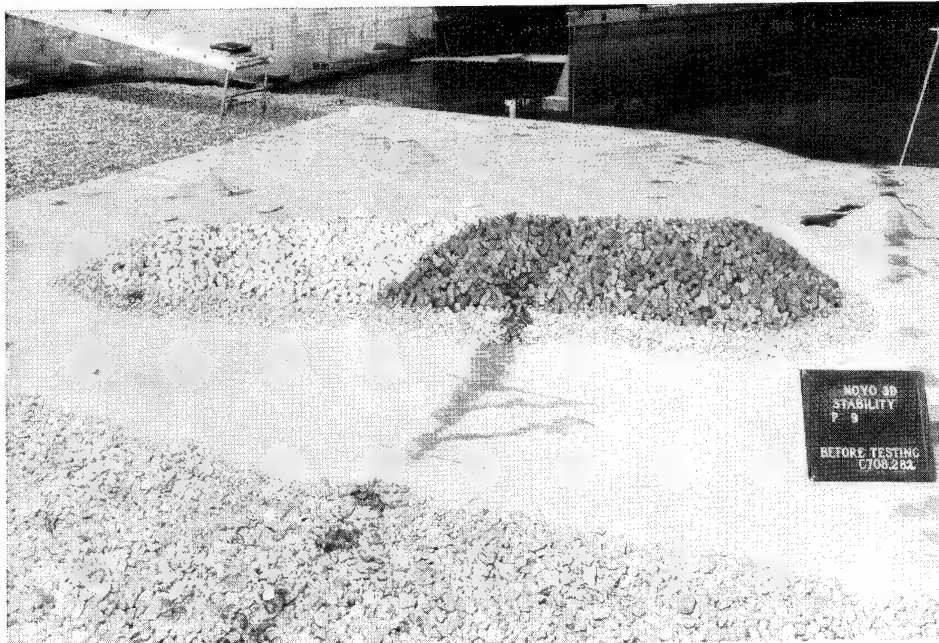


Photo C70. Leeside view of Plan 9 before testing
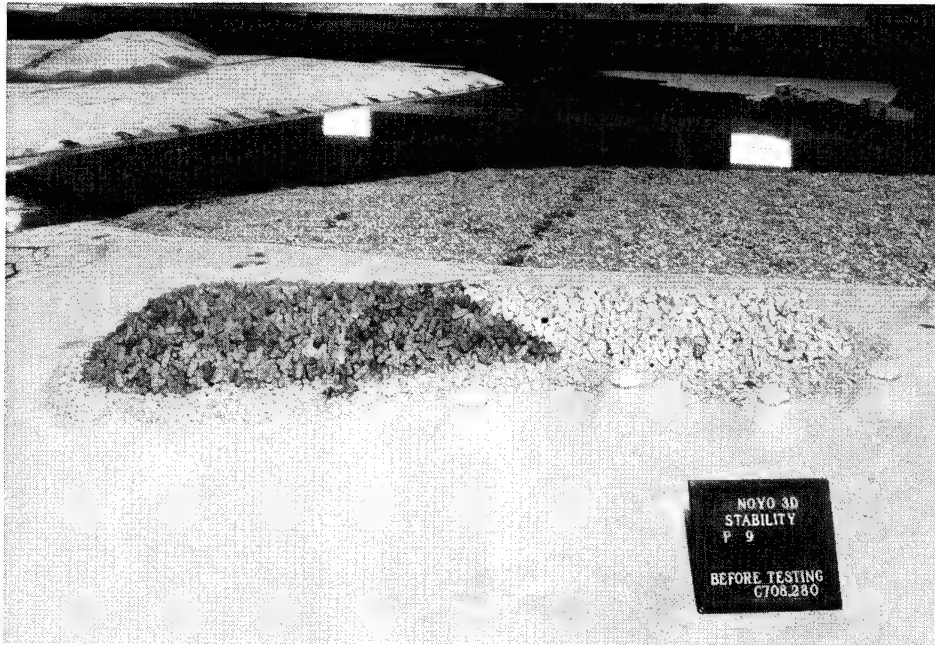
Photo C71.  Sea-side view of Plan 9 before testing
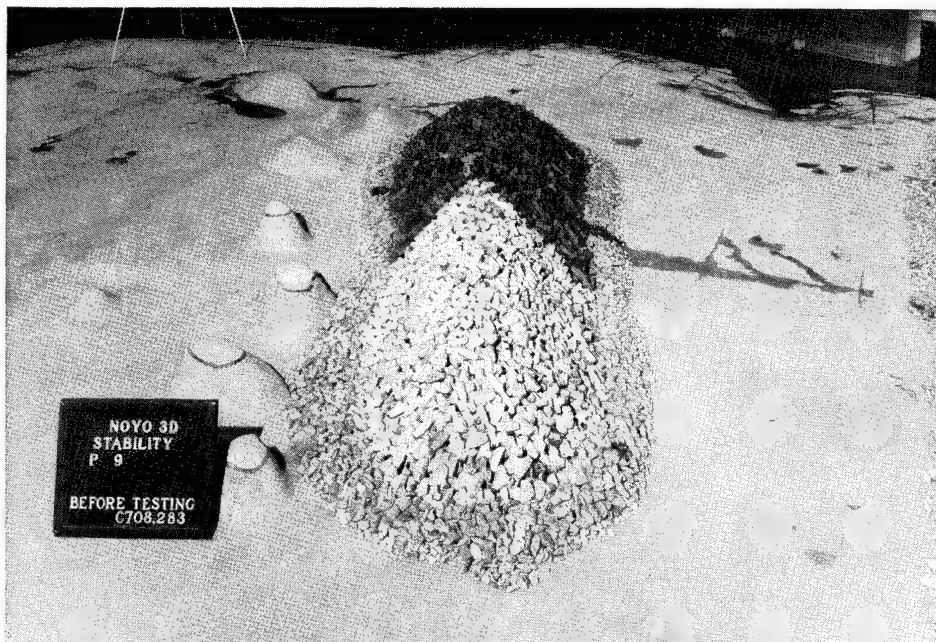


Photo C72.  Plan 9, south roundhead before testing

Photo C73. Plan 9, north roundhead after Storm I waves
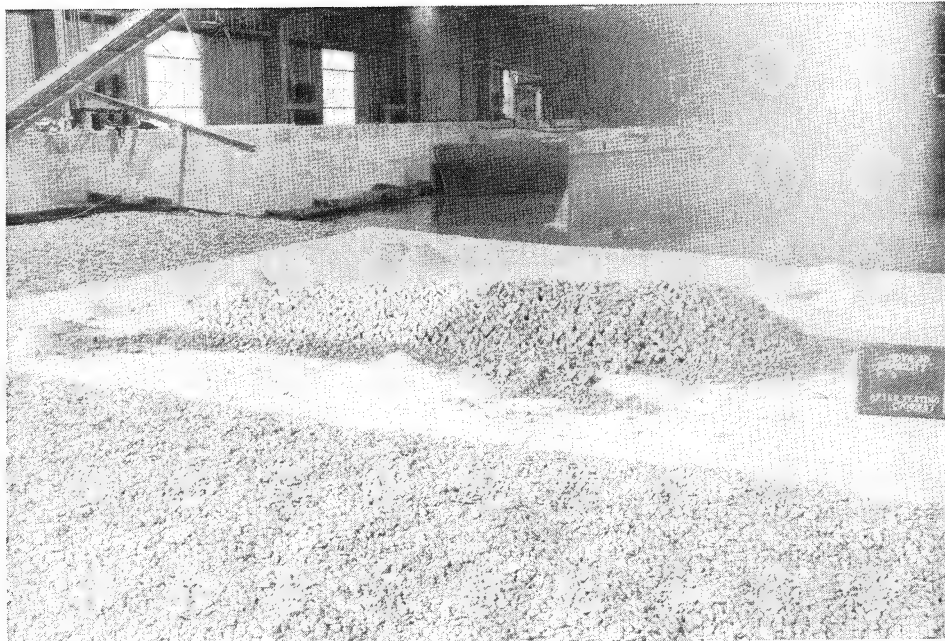


Photo C74. Leeside view of Plan 9 after Storm I waves
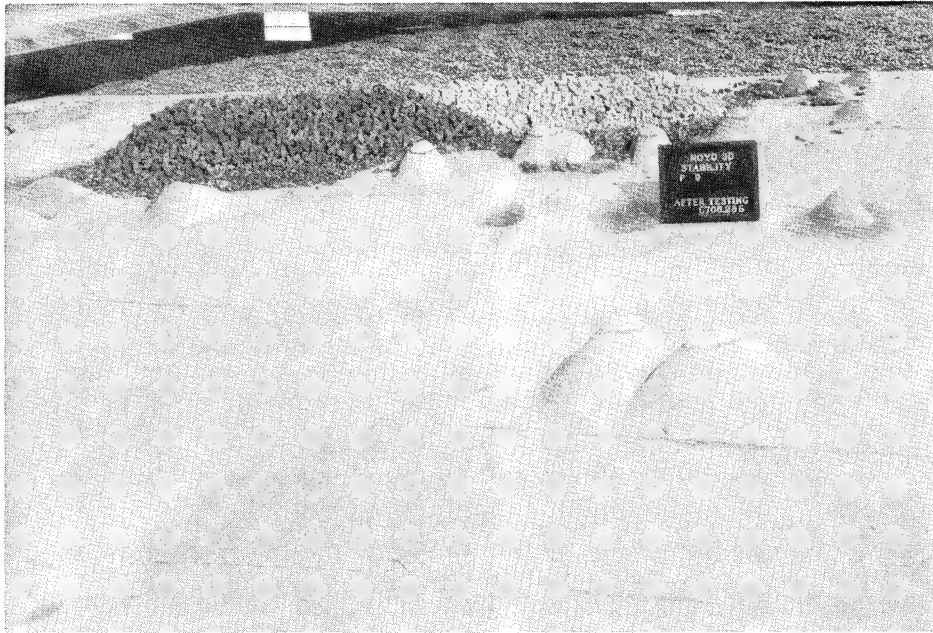
Photo C75. Sea-side view of Plan 9 after Storm I waves
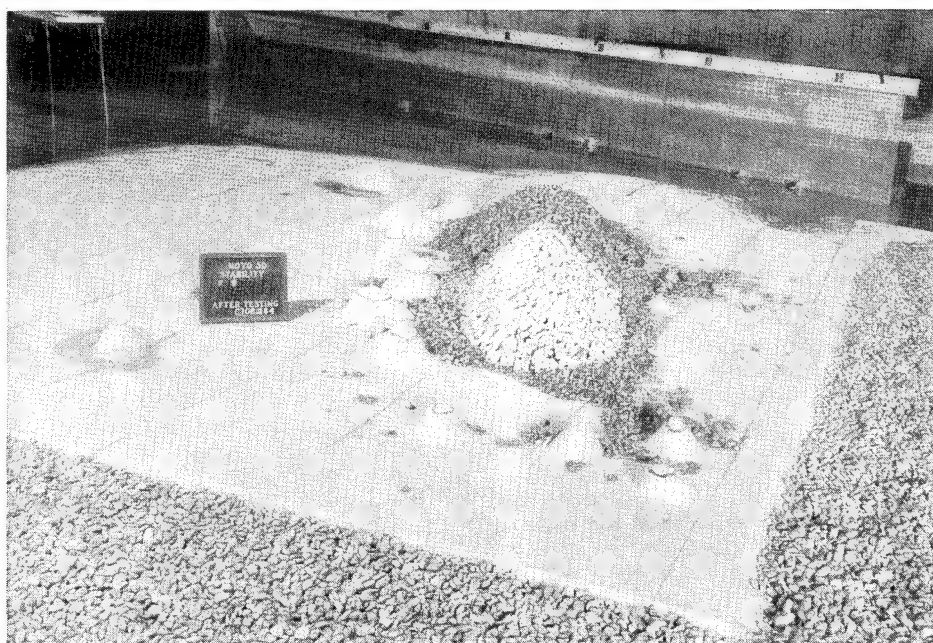


Photo C76. Plan 9, south roundhead after Storm I waves
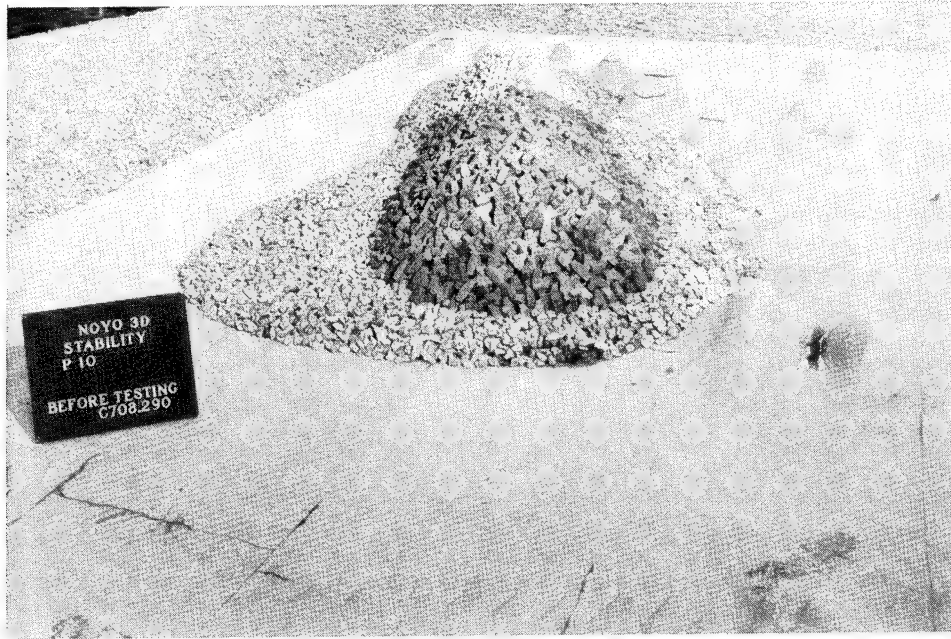
Photo C77. Plan 10, north roundhead before testing

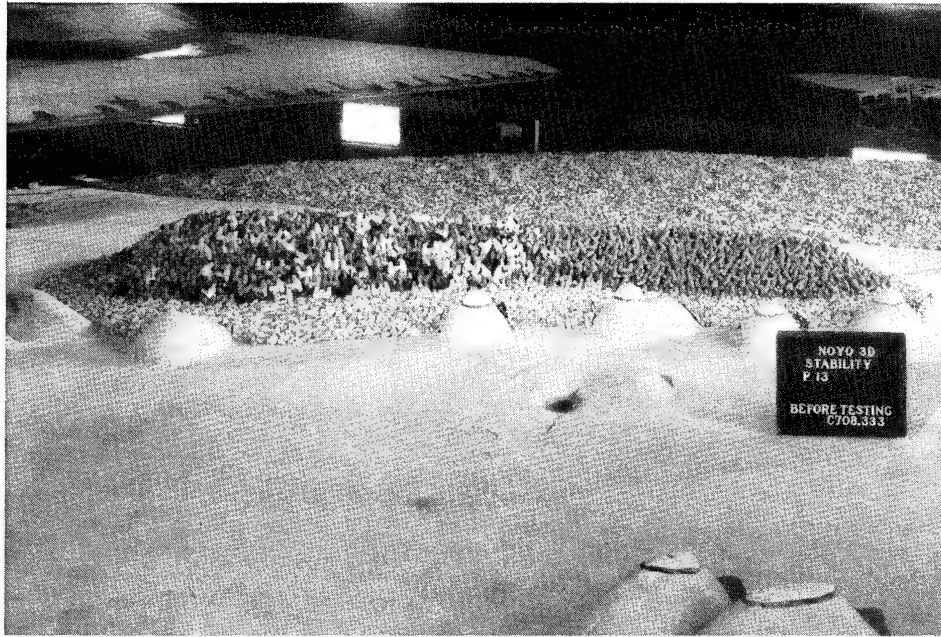

Photo C78. Leeside view of Plan 10 before testing
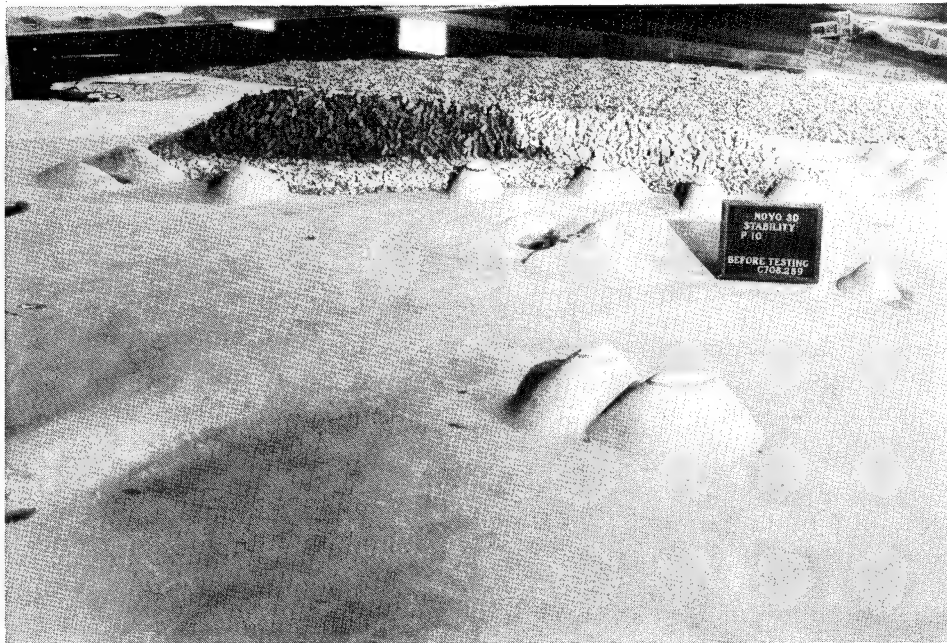
Photo C79.   Sea-side view of Plan 10 before testing
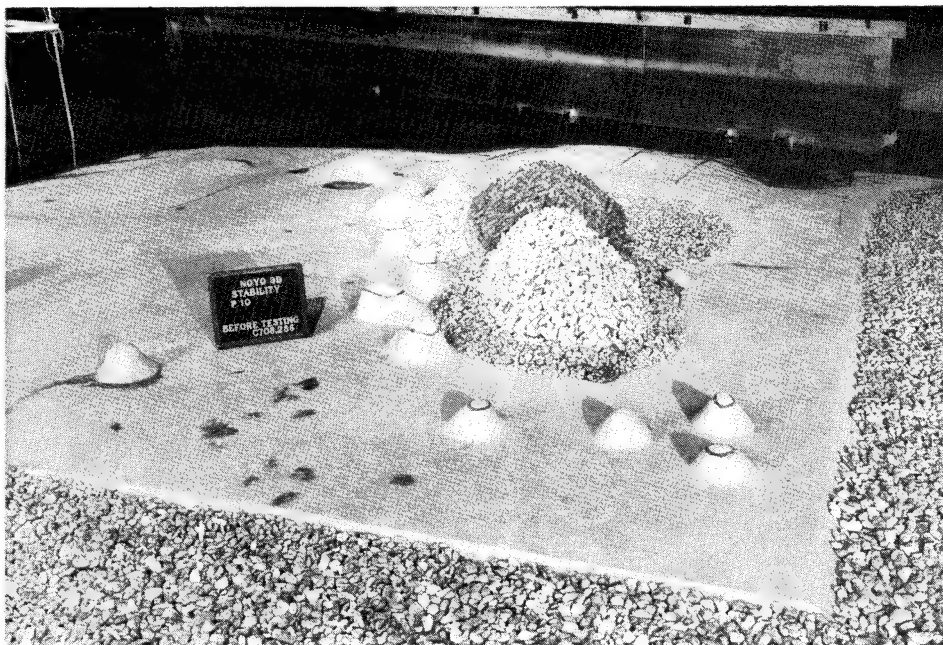


Photo C80.   Plan 10, south roundhead before testing
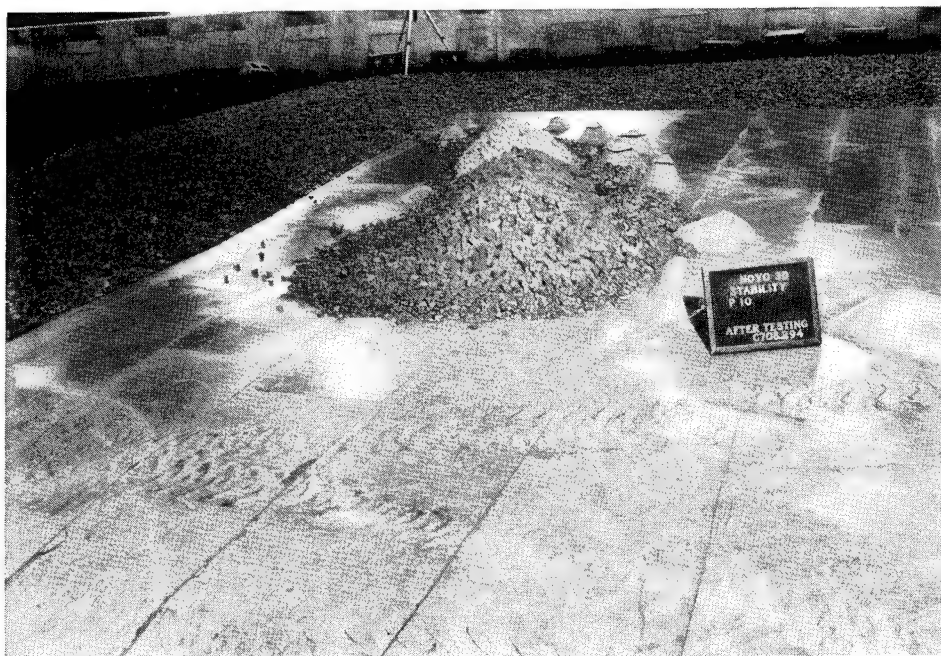
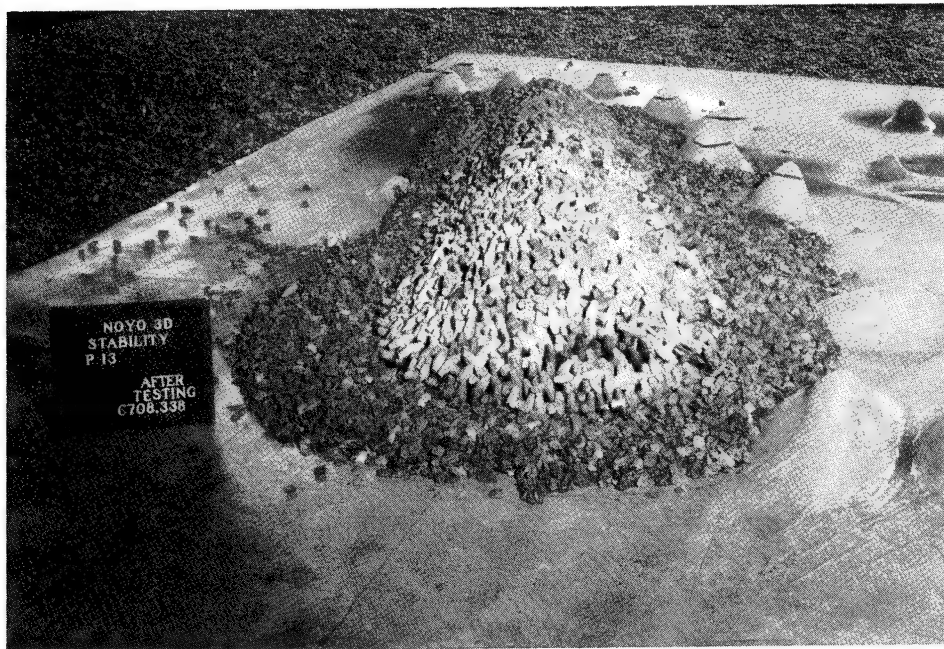Photo C81.  Plan 10, north roundhead after Storm IA waves
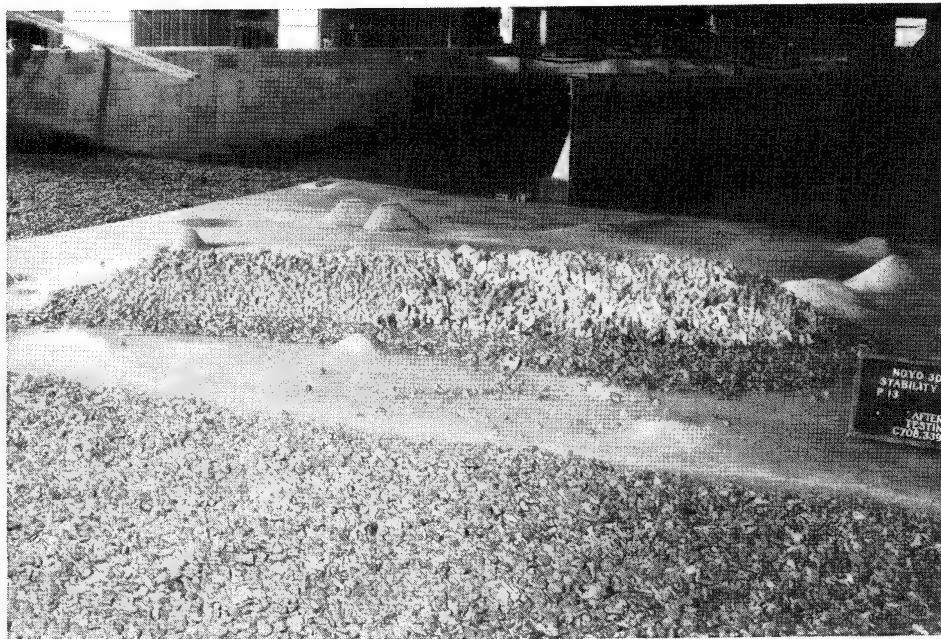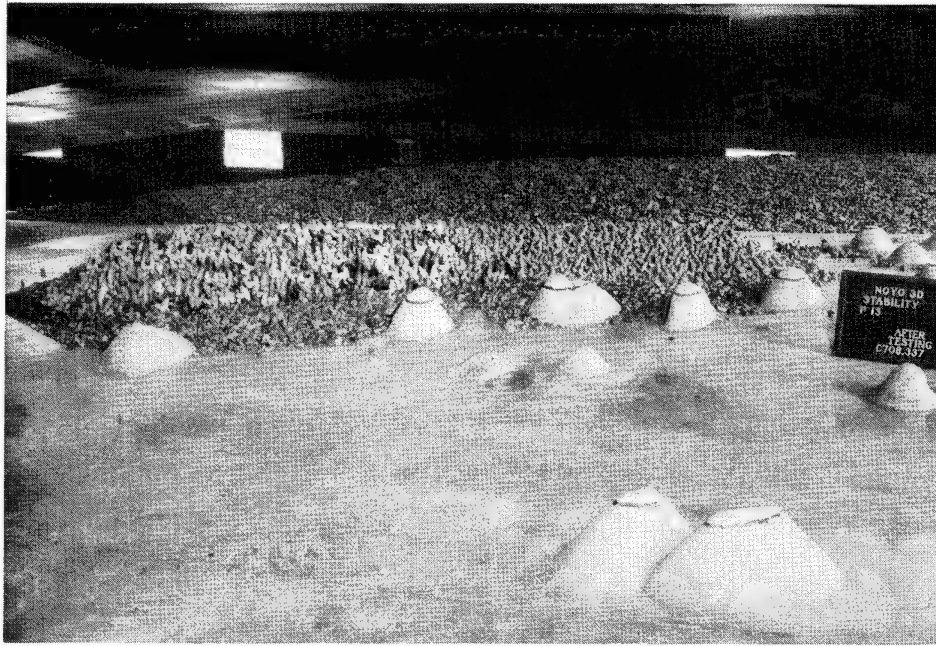


Photo C82.  Leeside view of Plan 10 after Storm IA waves
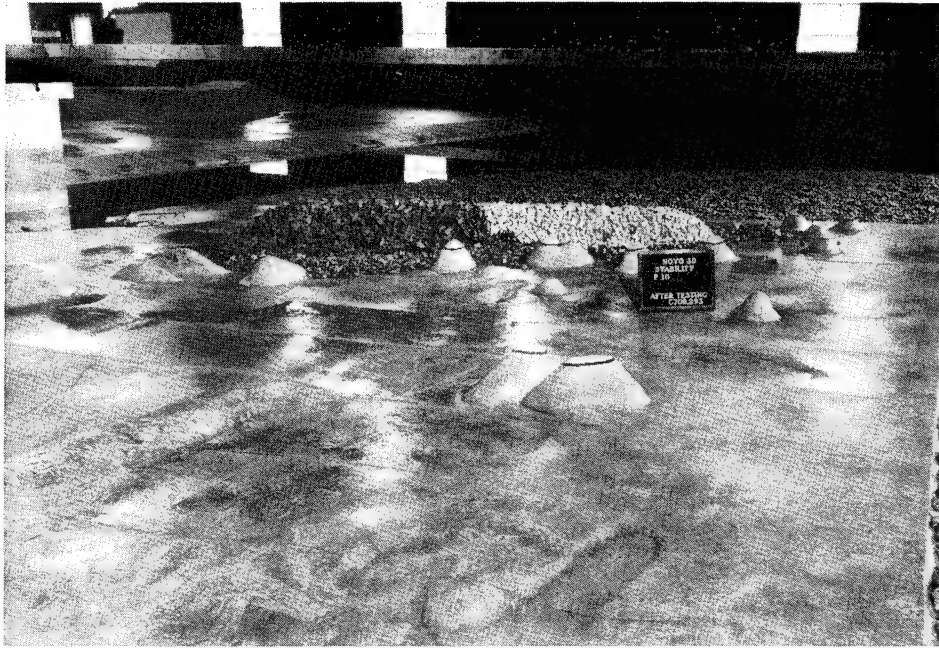
Photo C83.  Sea-side view of Plan 10 after Storm IA waves
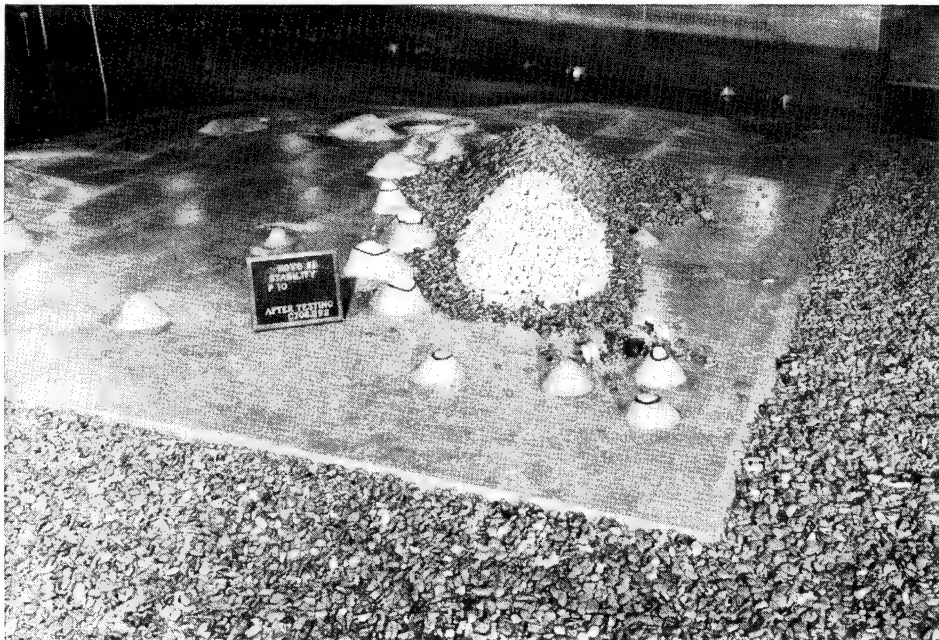


Photo C84.  Plan 10, south roundhead after Storm IA waves
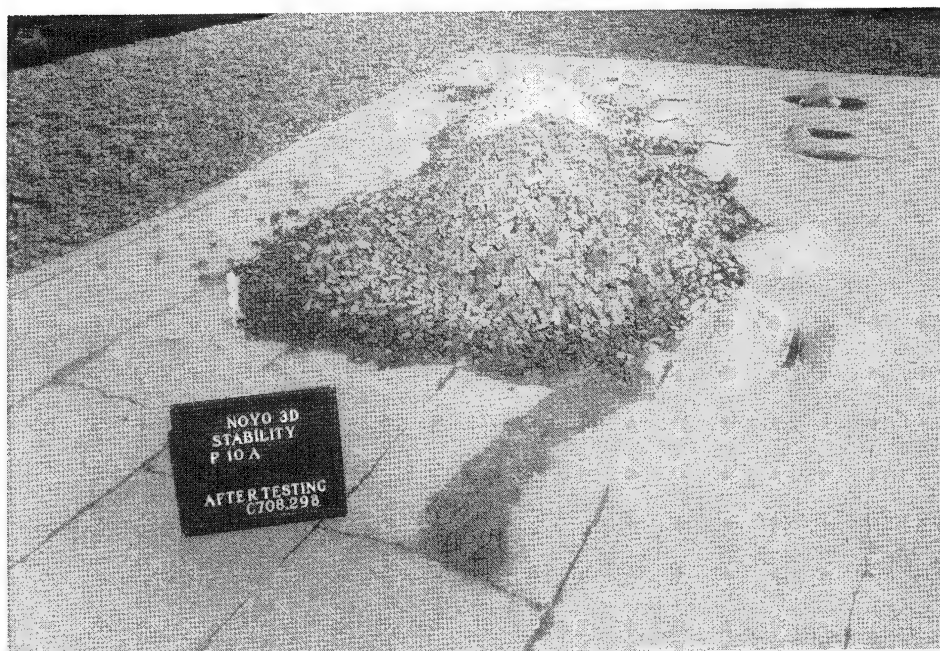
Photo C85.  Plan 10, north roundhead after two series of Storm IA waves
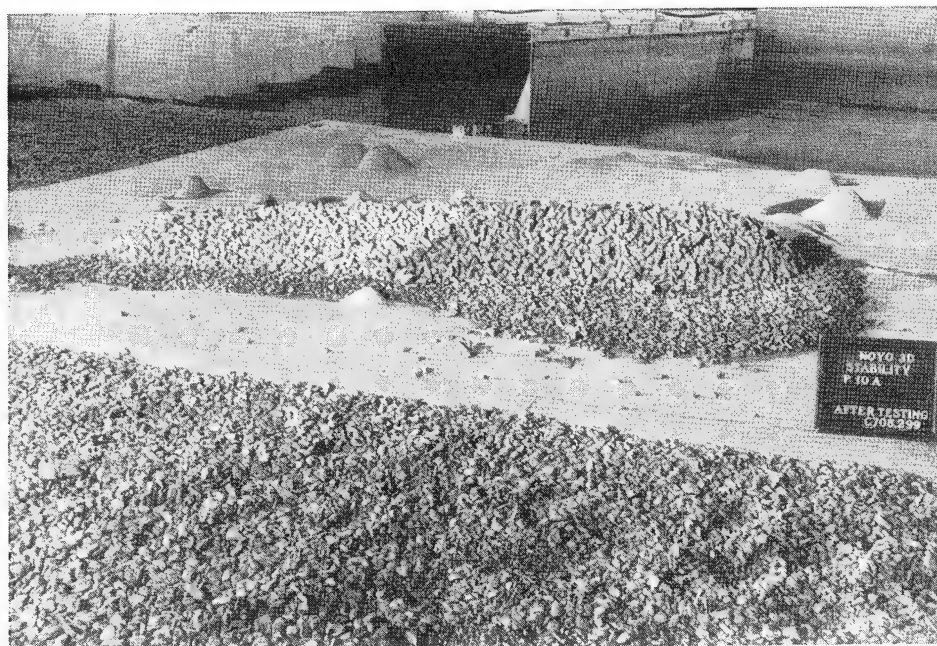


Photo C86.  Leeside view of Plan 10 after two series of Storm IA waves

Photo C87.  Sea-side view of Plan 10 after two series of Storm IA waves



Photo C88.  Plan 10, south roundhead after two series of Storm IA waves

Photo C89. Plan 11, north roundhead before testing



Photo C90. Leeside view of Plan 11 before testing

Photo C91.  Sea-side view of Plan 11 before testing



Photo C92.  Plan 11, south roundhead before testing

Photo C93. Plan 11, north roundhead after Storm IA waves
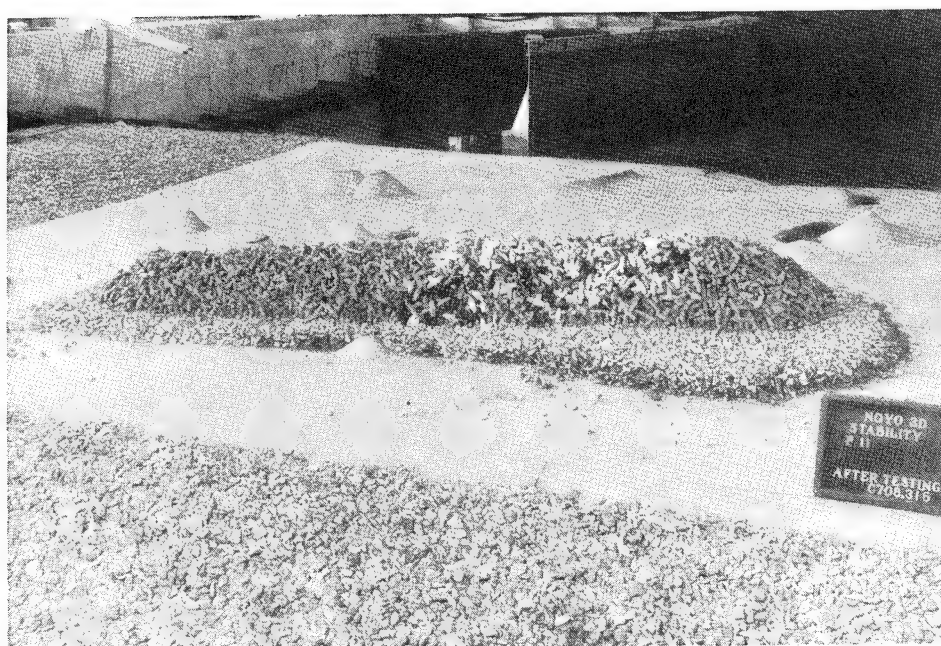


Photo C94. Leeside view of Plan 11 after Storm IA waves
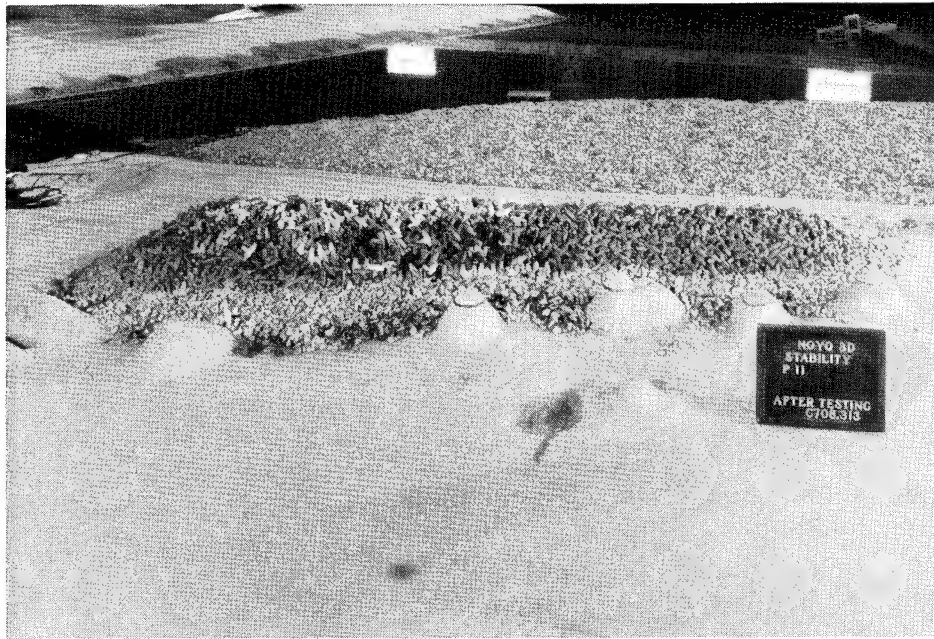
Photo C95.  Sea-side view of Plan 11 after Storm IA waves
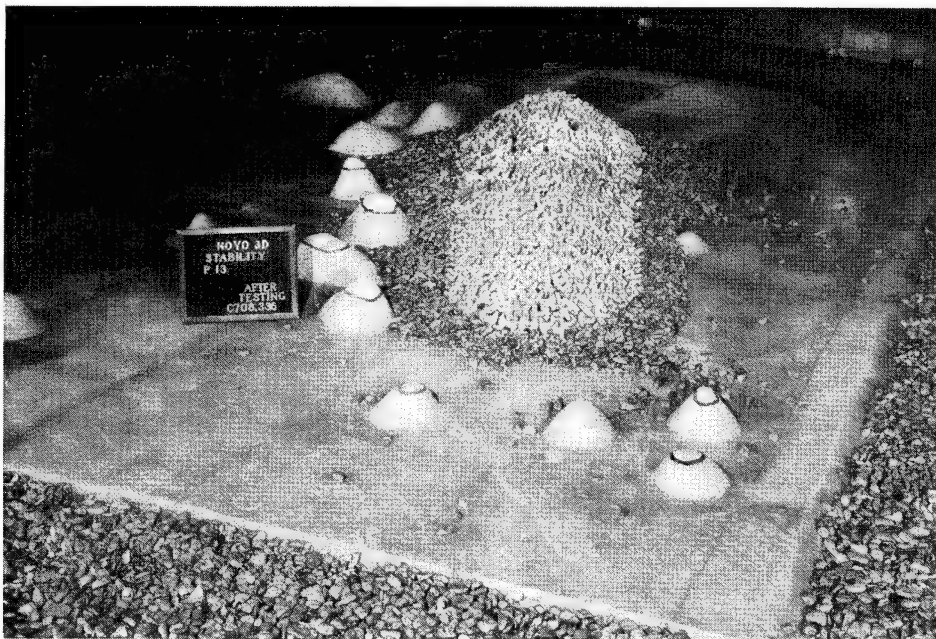
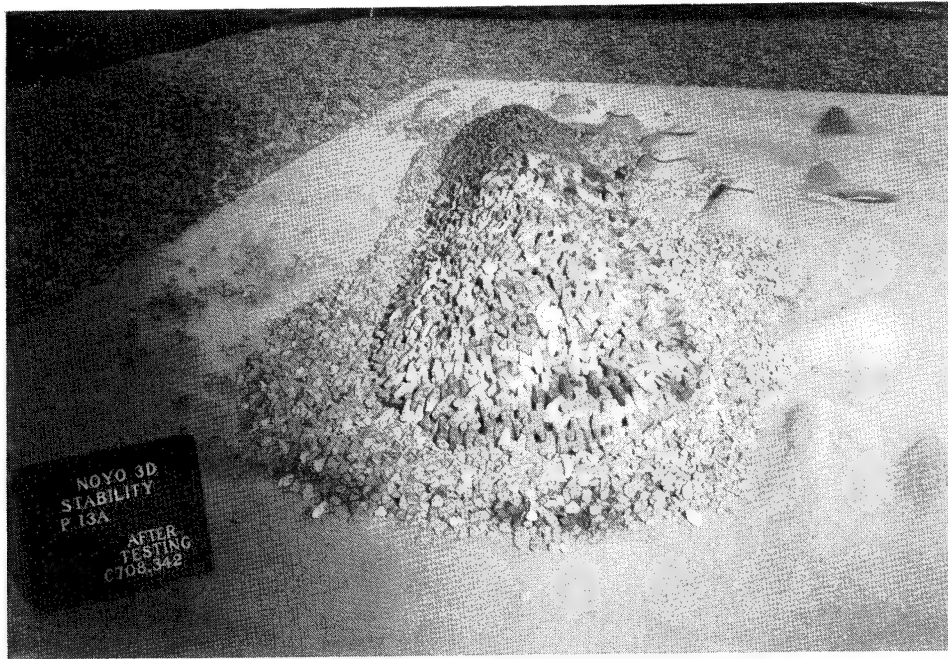

Photo C96.  Plan 11, south roundhead after Storm IA waves

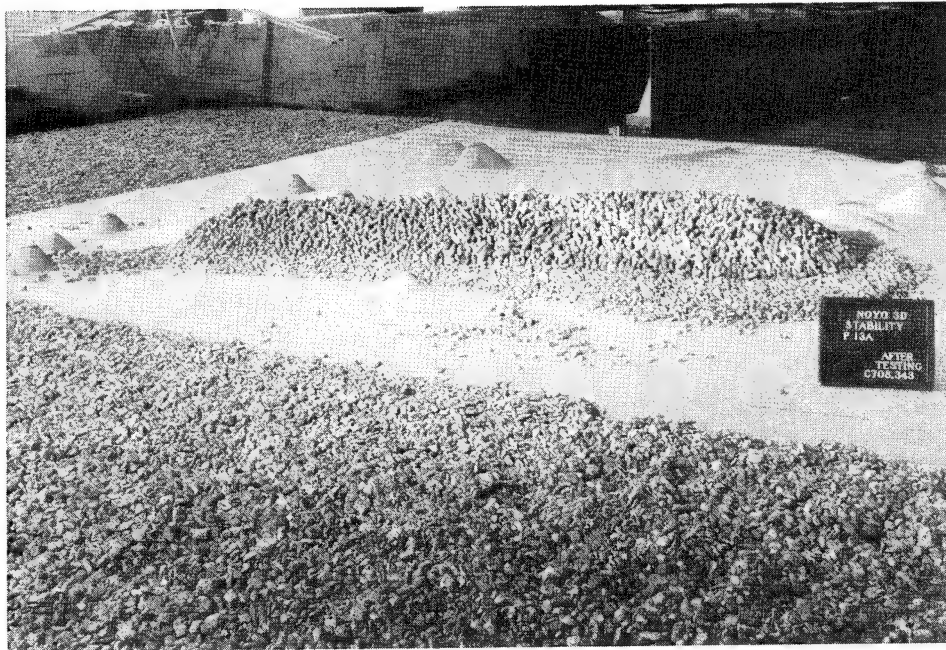Photo C97. Plan 11, north roundhead after two series of Storm IA waves



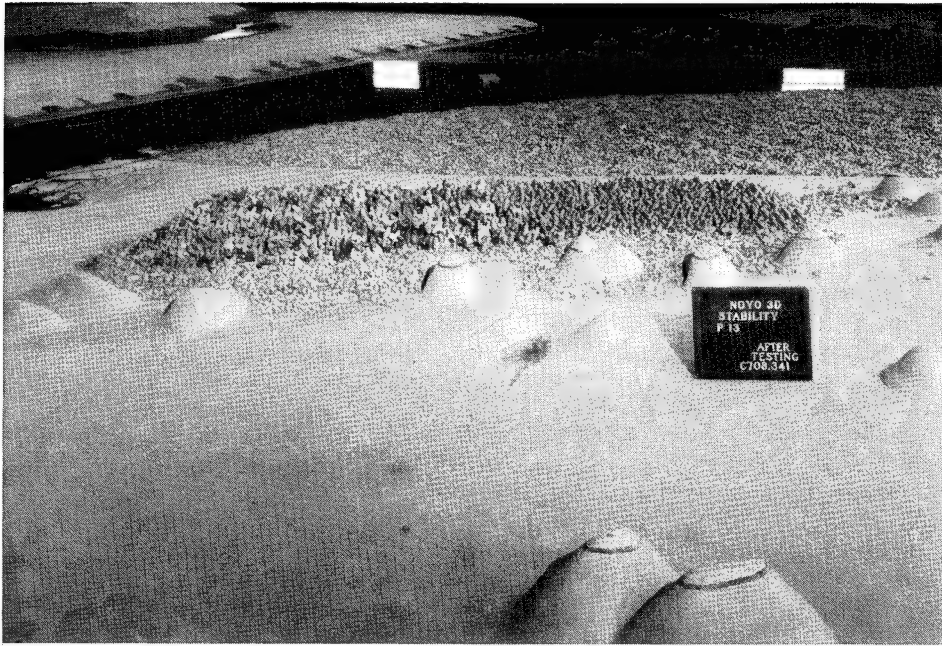Photo C98. Leeside view of Plan 11 after two series of Storm IA waves
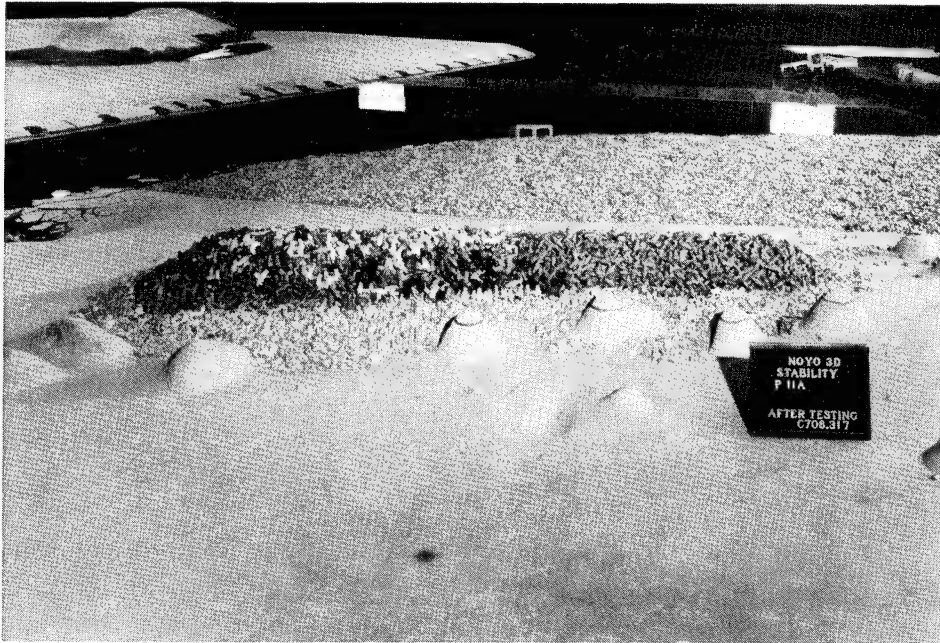
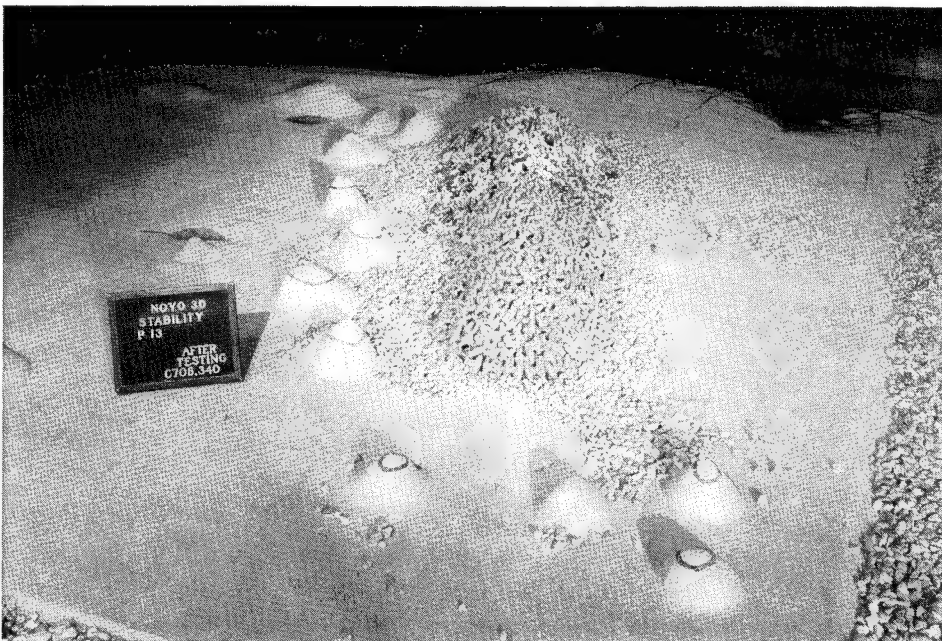Photo C99.  Sea-side view of Plan 11 after two series of Storm IA waves



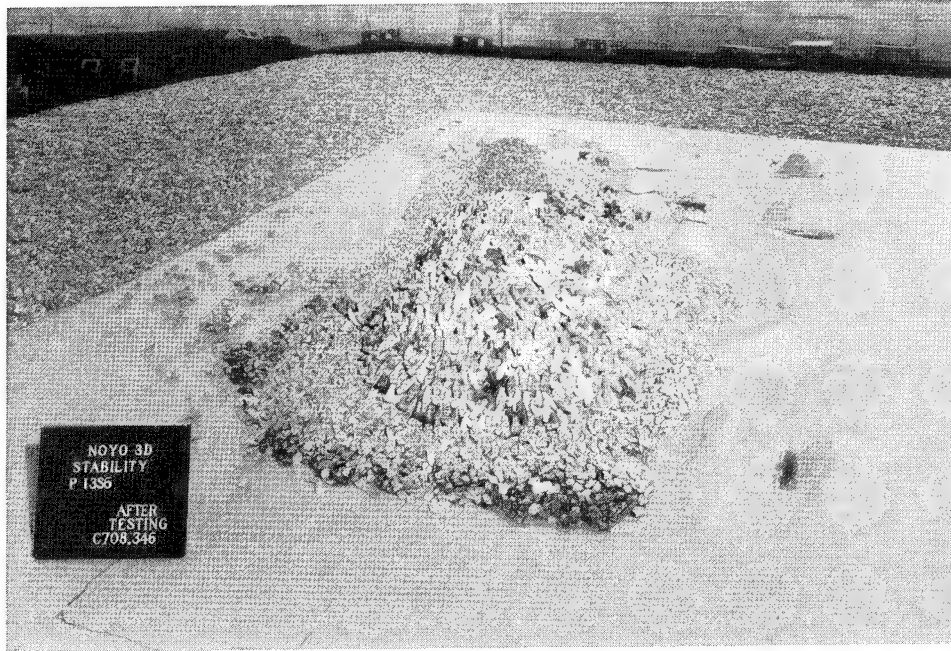Photo C100.  Plan 11, south roundhead after two series of Storm IA waves

Photo C101. Plan 12, north roundhead before testing



Photo C102. Leeside view of Plan 12 before testing

Photo C103. Sea-side view of Plan 12 before testing



Photo C104. Plan 12, south roundhead before testing

Photo C105. Plan 12, north roundhead after Storm IA waves



Photo C106. Leeside view of Plan 12 after Storm IA waves

Photo C107. Sea-side view of Plan 12 after Storm IA waves



Photo C108. Plan 12, south roundhead after Storm IA waves

Photo C109. Plan 12, north roundhead after two series of Storm IA waves



Photo C110. Leeside view of Plan 12 after two series of Storm IA waves
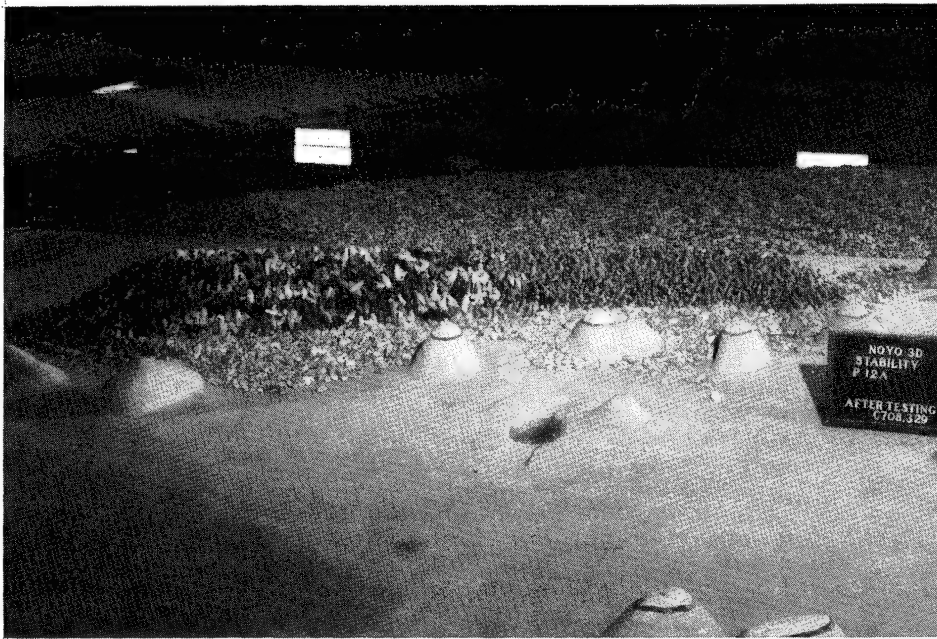
Photo C111. Sea-side view of Plan 12 after two series of Storm IA waves



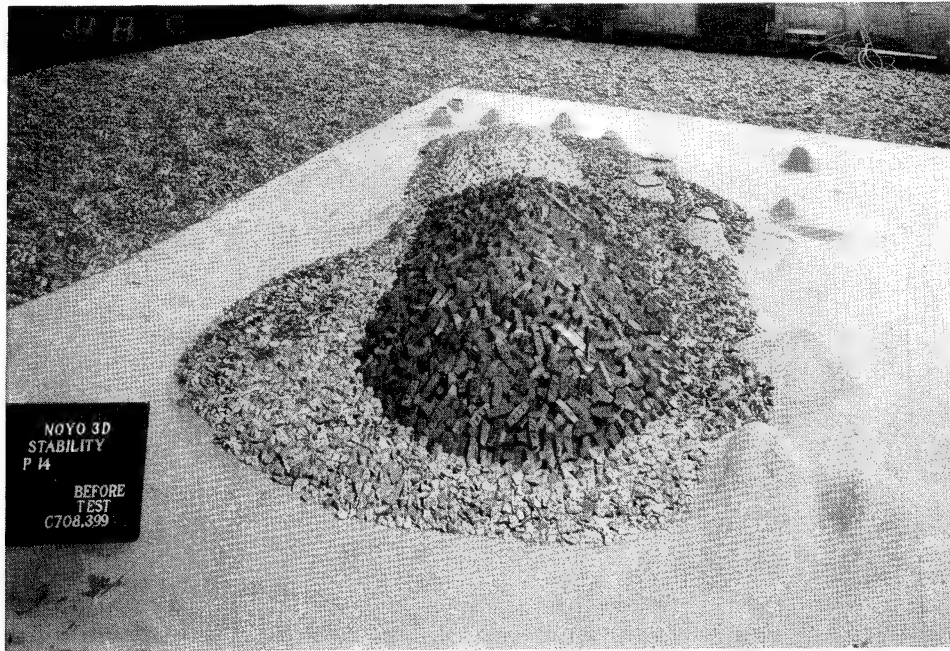Photo C112. Plan 12, south roundhead after two series of Storm IA waves

Photo C113.  Plan 13, north roundhead before testing



Photo C114.  Leeside view of Plan 13 before testing

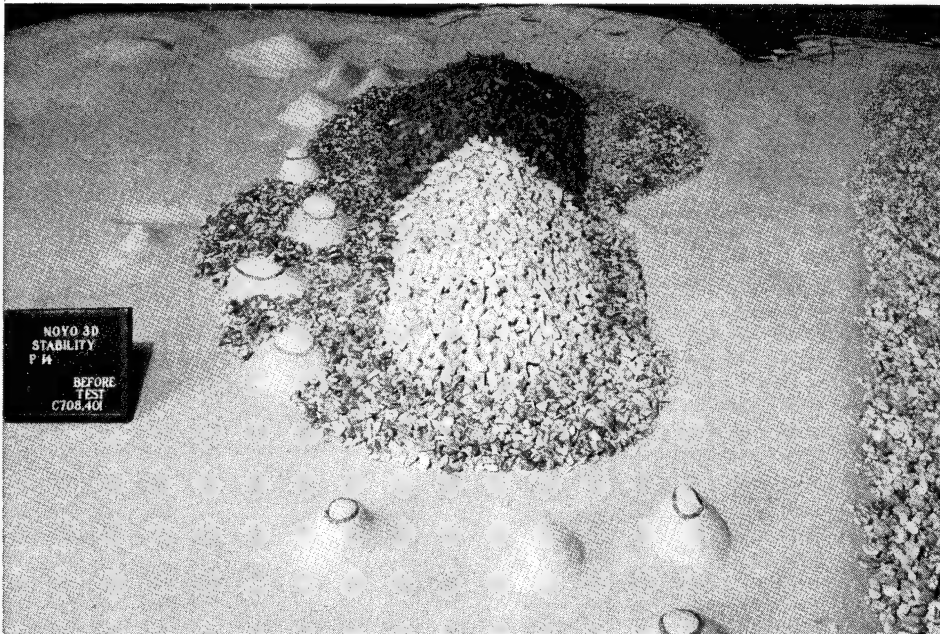Photo C115. Sea-side view of Plan 13 before testing



Photo C116. Plan 13, south roundhead before testing
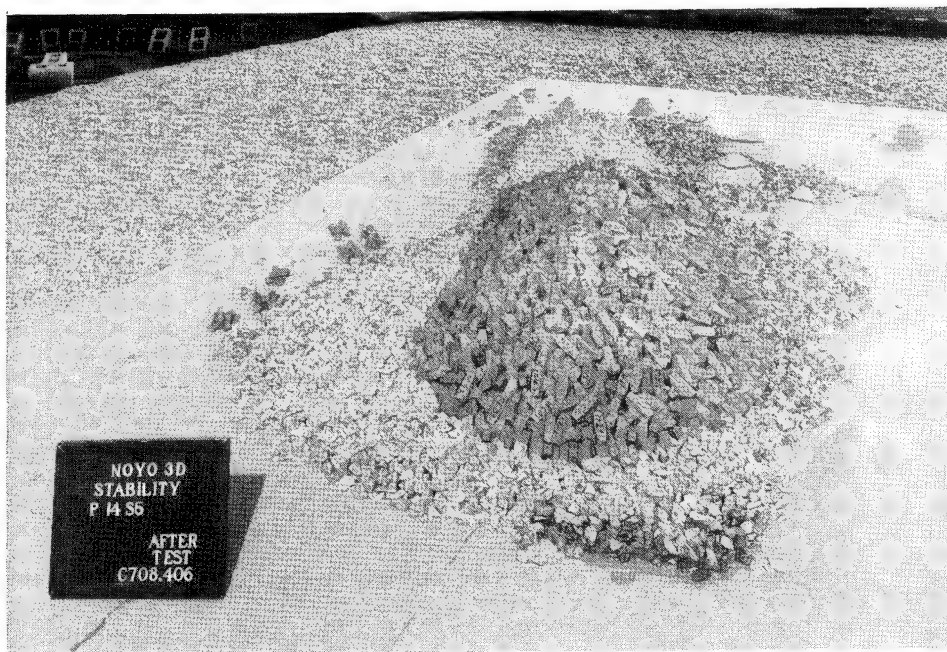
Photo C117.  Plan 13, north roundhead after Storm IA waves



Photo C118.  Leeside view of Plan 13 after Storm IA waves

Photo C119. Sea-side view of Plan 13 after Storm IA waves



Photo C120. Plan 13, south roundhead after Storm IA waves

Photo C121. Plan 13, north roundhead after two series of Storm IA waves



Photo C122. Leeside view of Plan 13 after two series of Storm IA waves

Photo C123.  Sea-side view of Plan 13 after two series of Storm IA waves



Photo C124.  Plan 13, south roundhead after two series of Storm IA waves

Photo C125.  Plan 13, north roundhead after two series of Storm IA waves and
three series of Storm IB waves
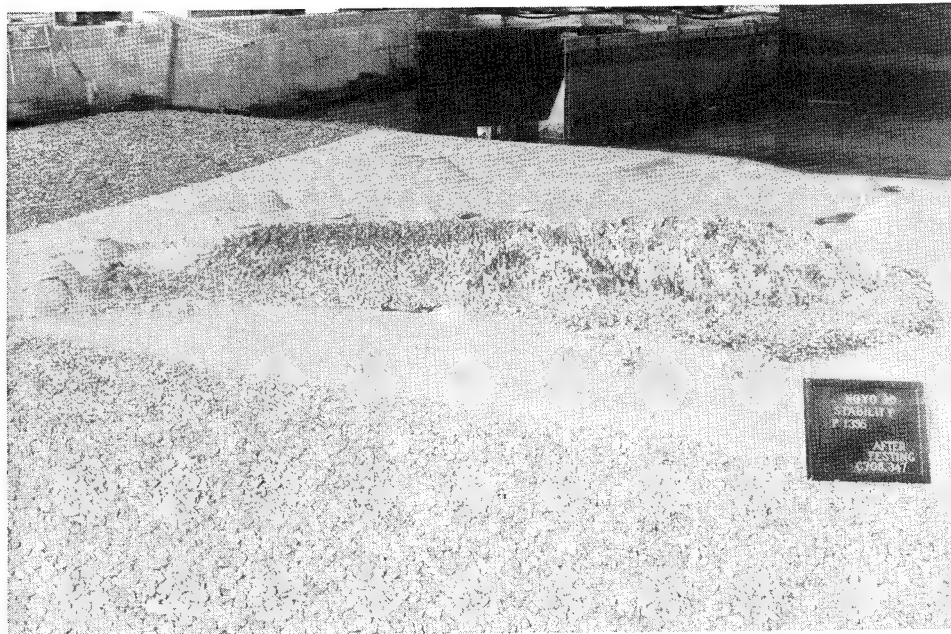


Photo C126.  Leeside view of Plan 13 after two series of Storm IA waves and
three series of Storm IB waves
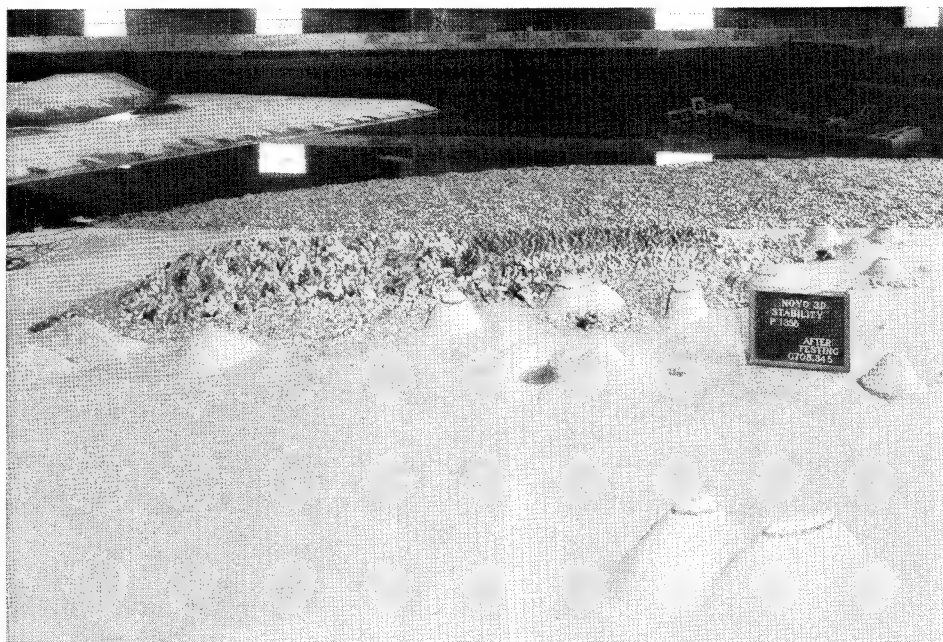
Photo C127.  Sea-side view of Plan 13 after two series of Storm IA waves and three series of Storm IB waves
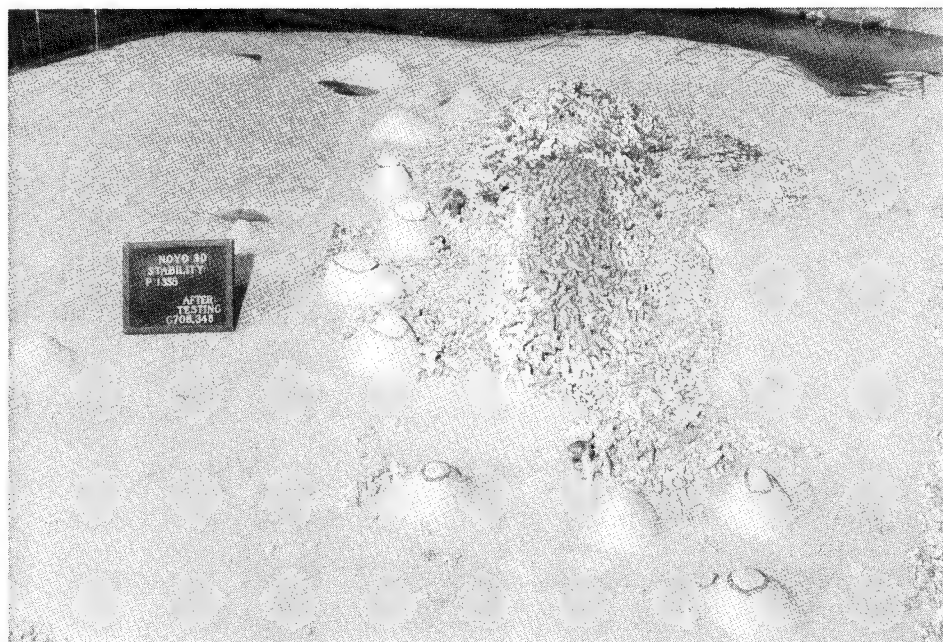


Photo C128.  Plan 13, south roundhead after two series of Strom IA waves and three series of Storm IB waves

Photo C129. Plan 14, north roundhead before testing



Photo C130. Leeside view of Plan 14 before testing

Photo C131. Sea-side view of Plan 14 before testing



Photo C132. Plan 14, south roundhead before testing

Photo C133. Plan 14, north roundhead after five series of Storm IB waves
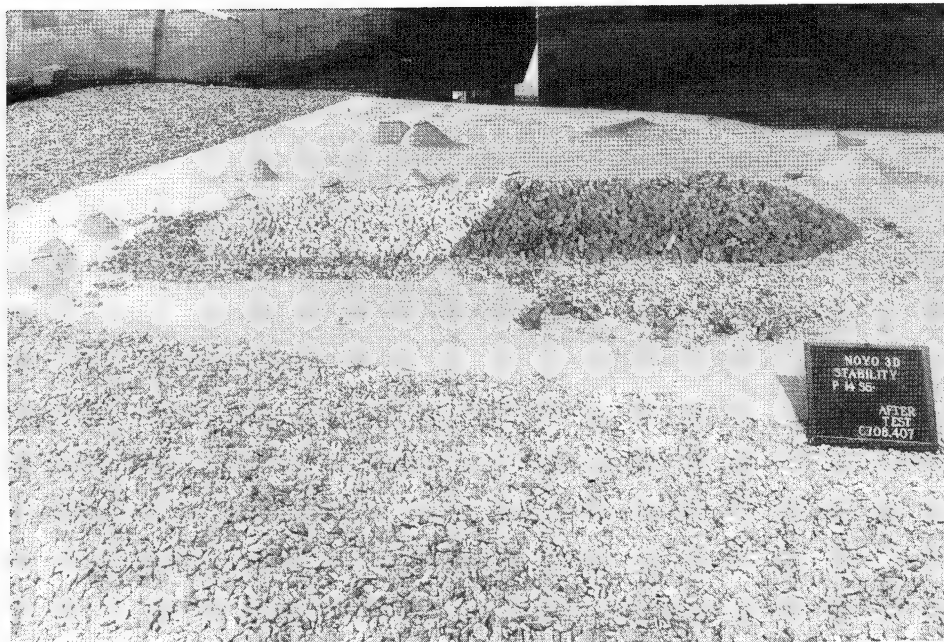


Photo C134. Leeside view of Plan 14 after five series of Storm IB waves
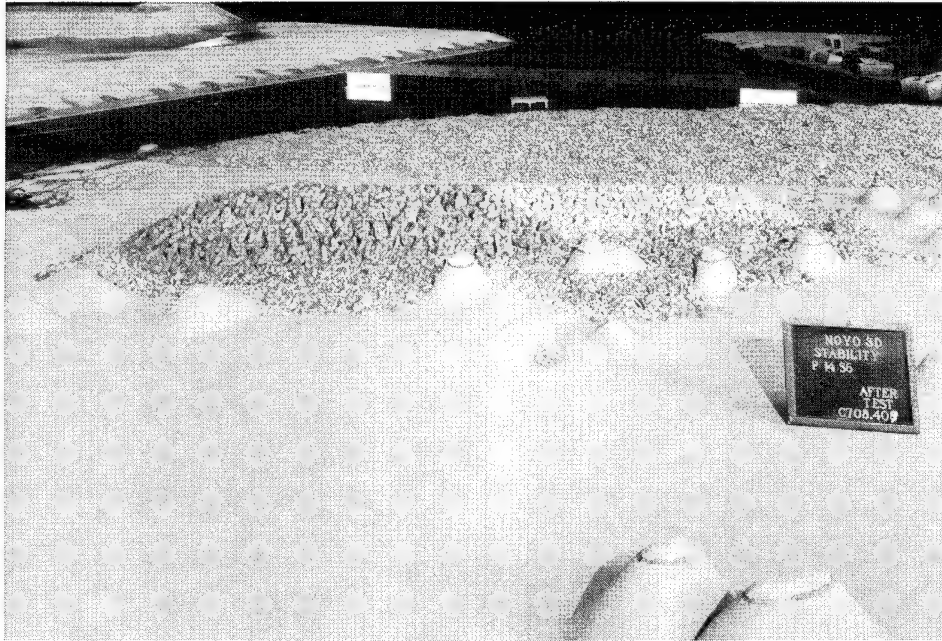
Photo C135. Sea-side view of Plan 14 after five series of Storm IB waves
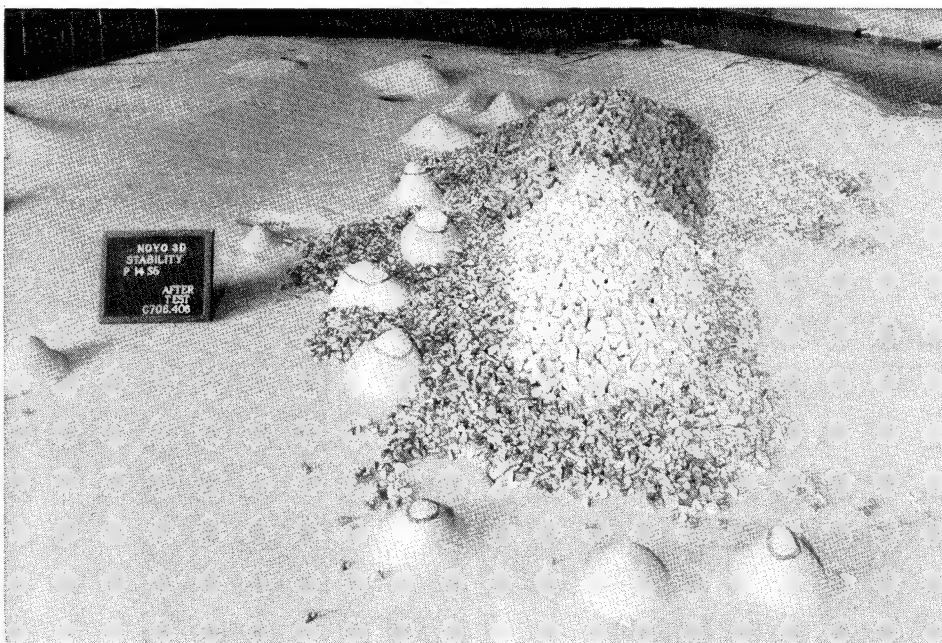


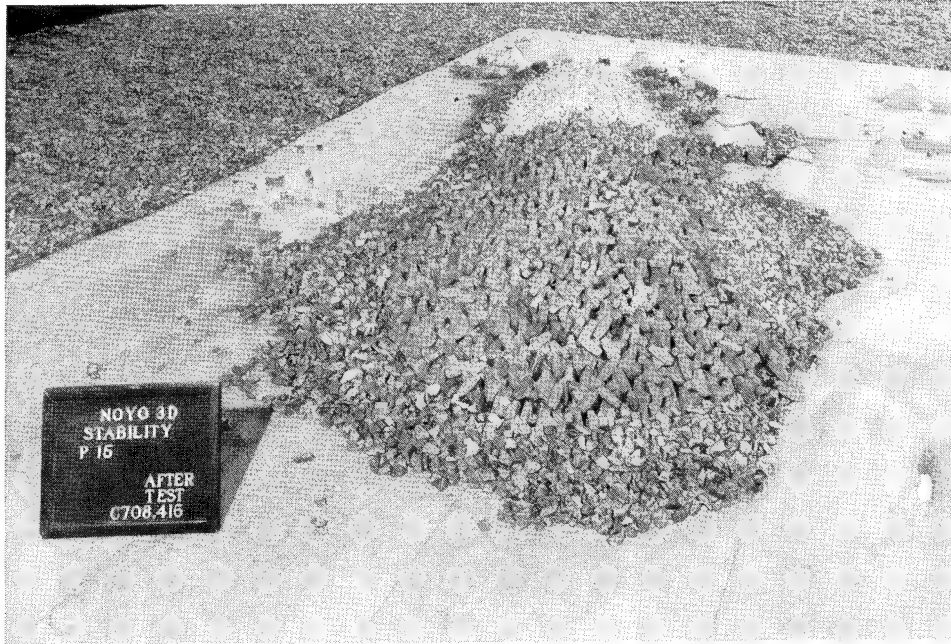Photo C136. Plan 14, south roundhead after five series of Storm IB waves

Photo C137. Plan 15, north roundhead after five series of Storm IB waves



Photo C138. Leeside view of Plan 15 after five series of Storm IB waves

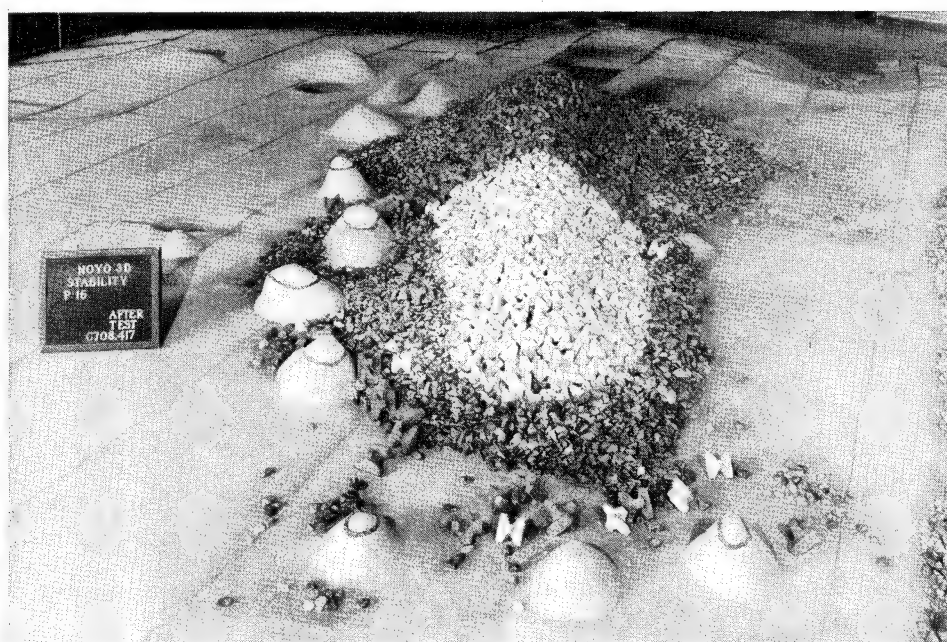Photo C139. Sea-side view of Plan 15 after five series of Storm IB waves



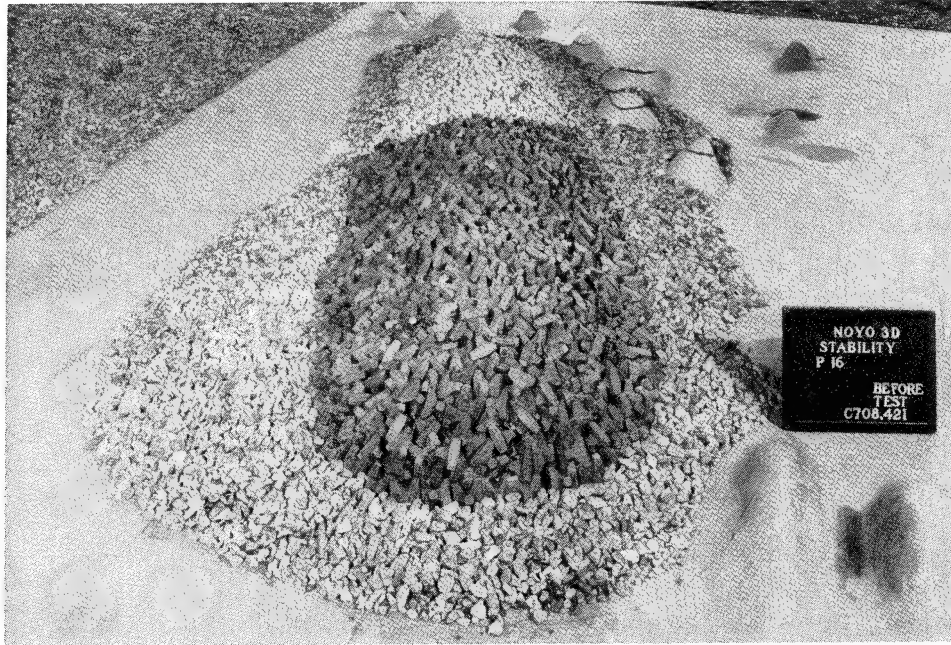Photo C140. Plan 15, south roundhead after five series of Storm IB waves

Photo C141. Plan 16, north roundhead before testing



Photo C142. Leeside view of Plan 16 before testing
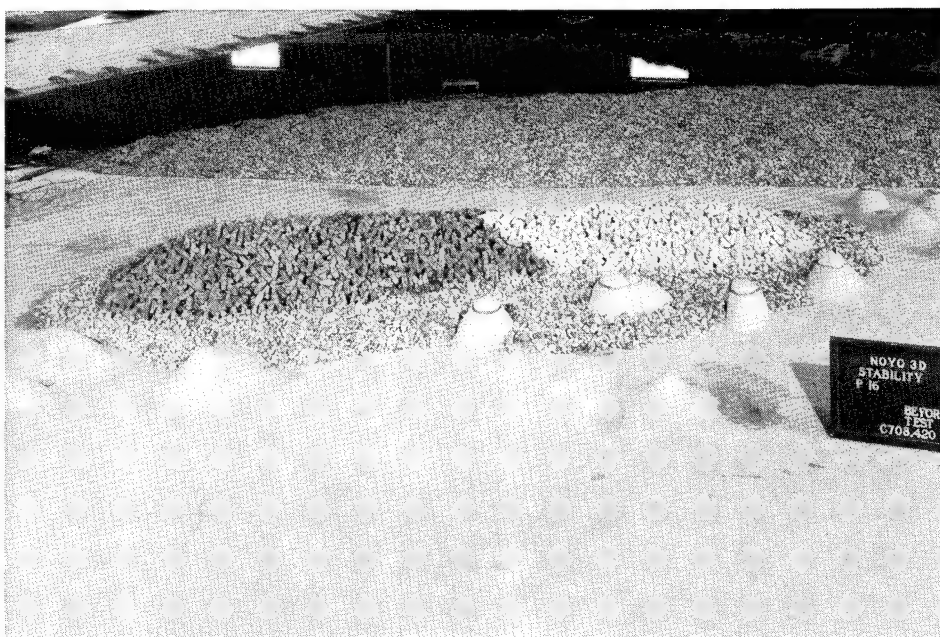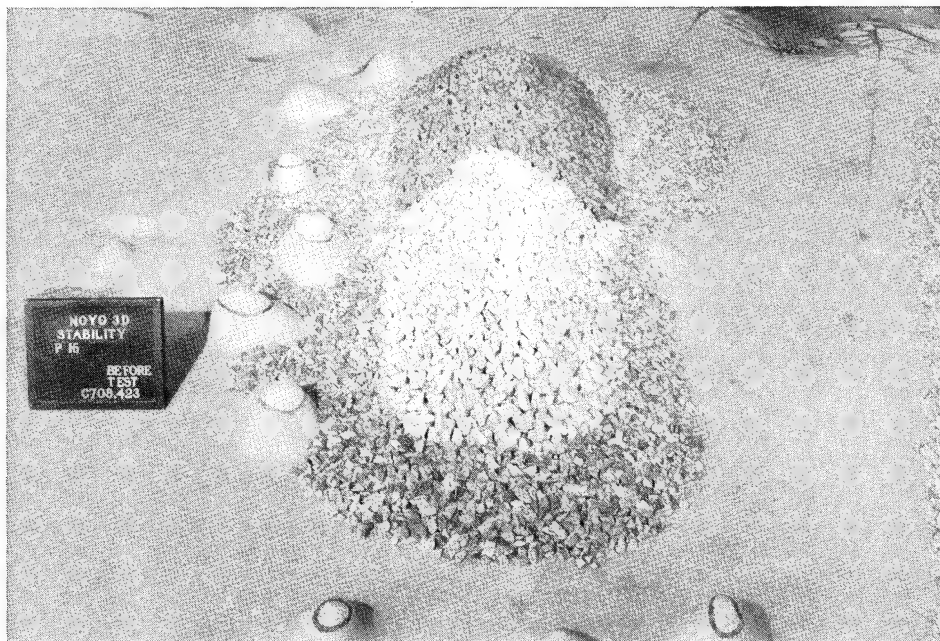
Photo C143. Sea-side view of Plan 16 before testing



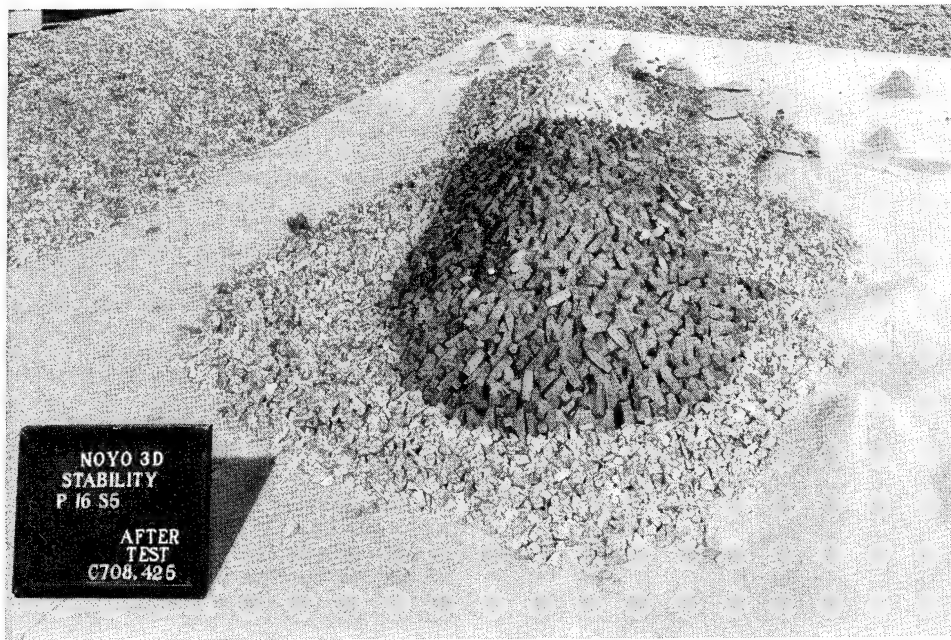Photo C144. Plan 16, south roundhead before testing

Photo C145. Plan 16, north roundhead after five series of modified Storm IB waves



Photo C146. Leeside view of Plan 16 after five series of modified Storm IB waves

Photo C147.  Sea-side view of Plan 16 after five series of modified Storm IB
waves



Photo C148.  Plan 16, south roundhead after five series of modified Storm IB
waves

Photo C149. Plan 17, north roundhead before testing



Photo C150. Leeside view of Plan 17 before testing
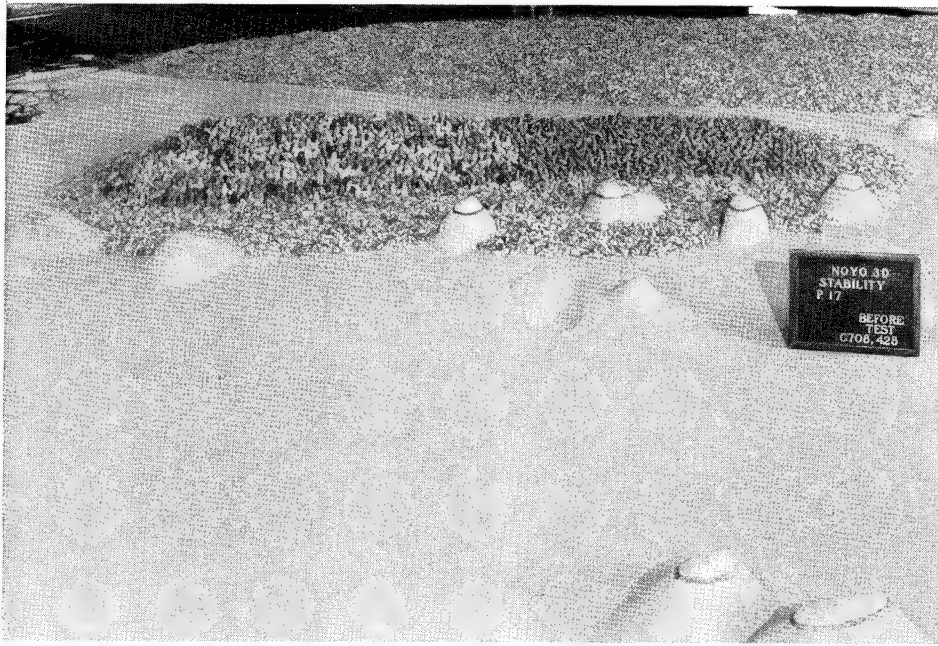
Photo C151. Sea-side view of Plan 17 before testing
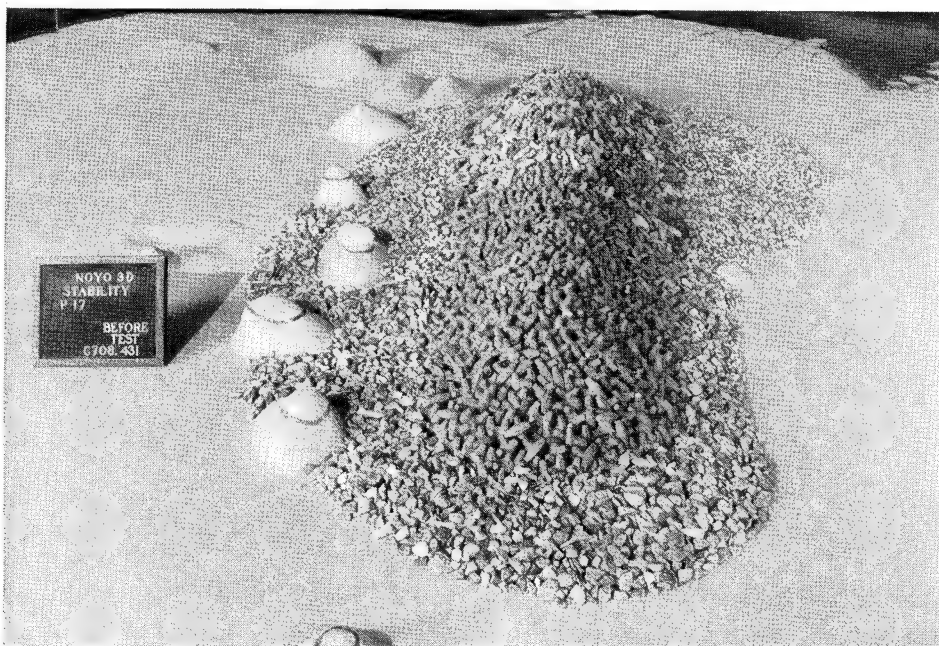


Photo C152. Plan 17, south roundhead before testing

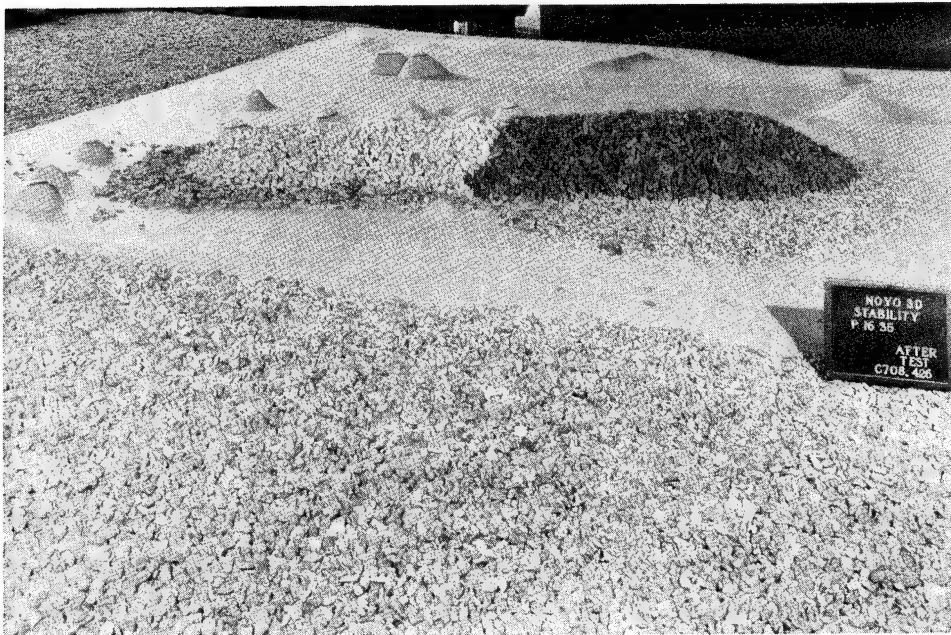Photo C153.  Plan 17, north roundhead after five series of modified Storm IB
waves



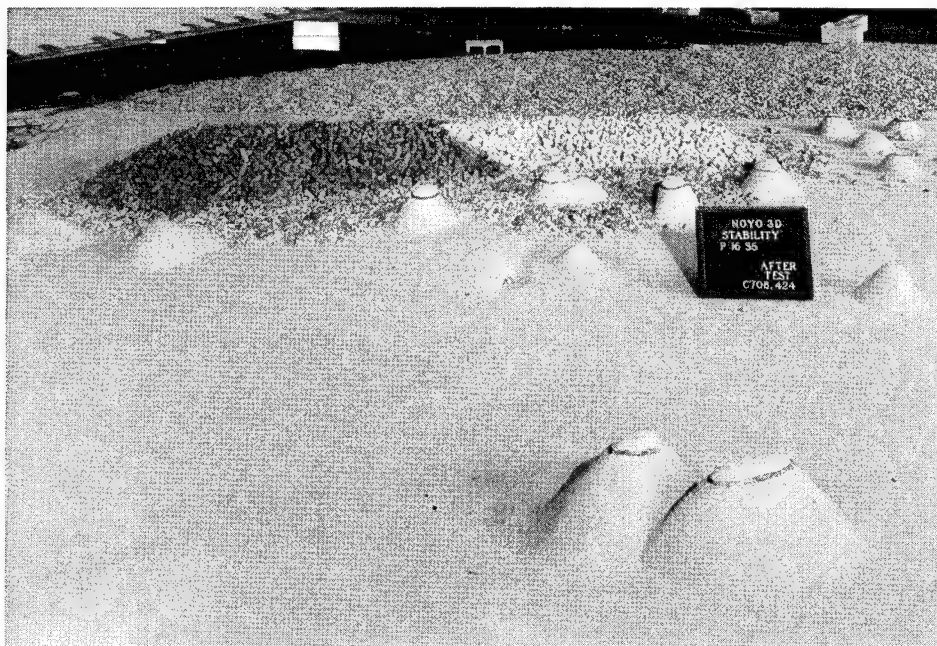Photo C154.  Leeside view of Plan 17 after five series of modified Storm IB
waves

Photo C155.  Sea-side view of Plan 17 after five series of modified Storm IB waves
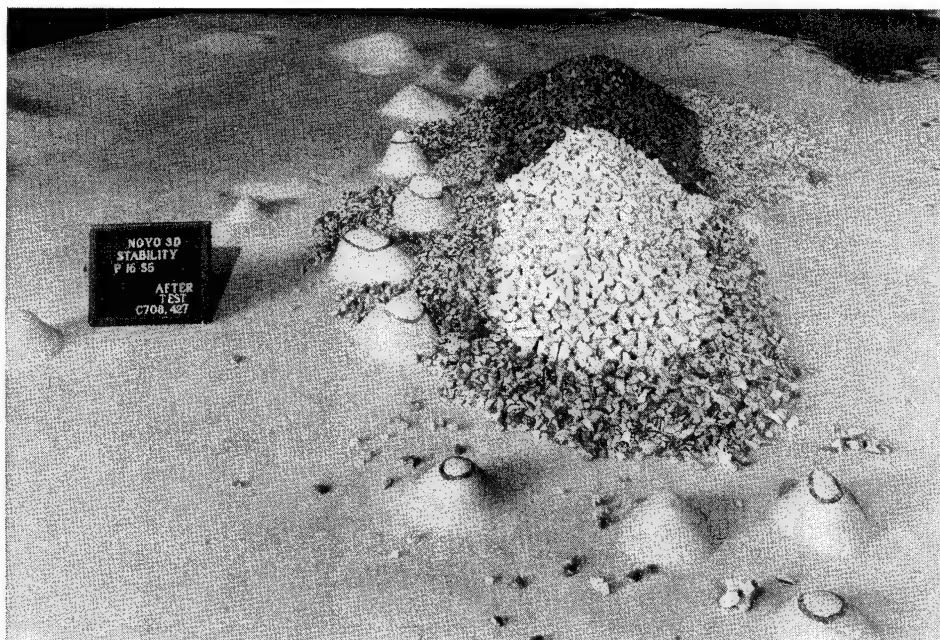


Photo C156.  Plan 17, south roundhead after five series of modified Storm IB waves
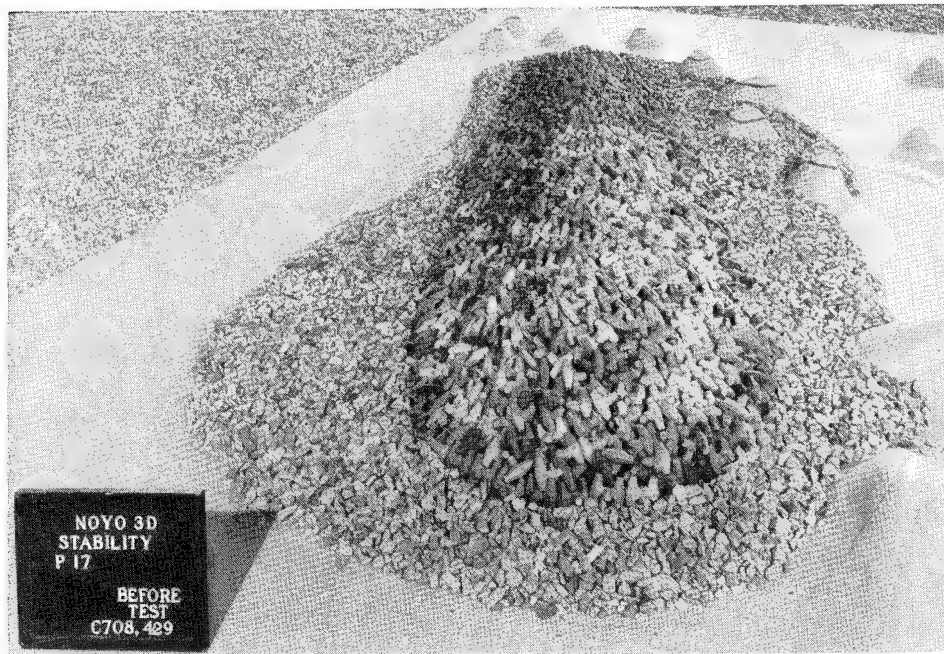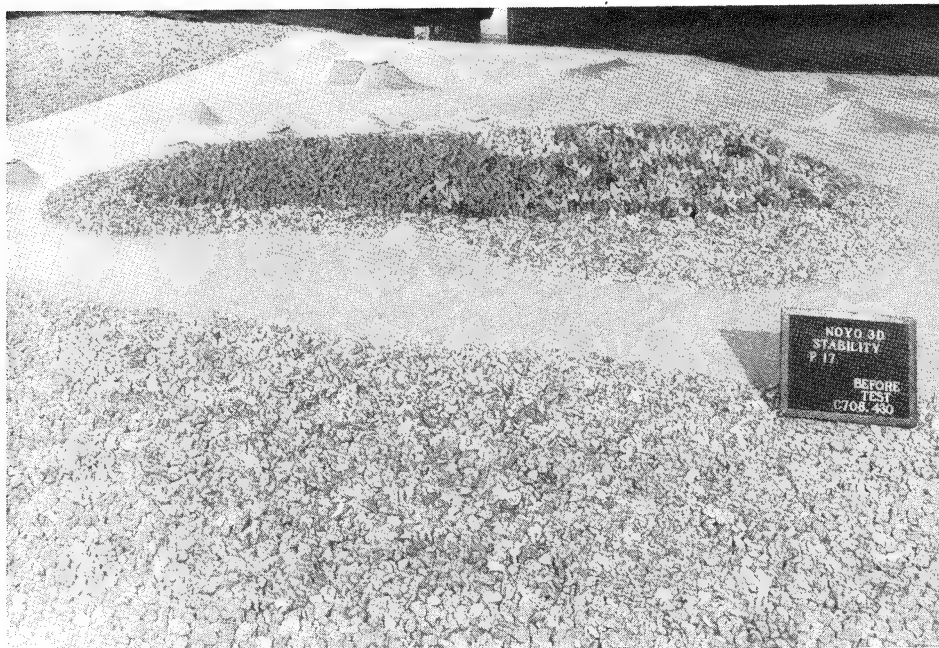
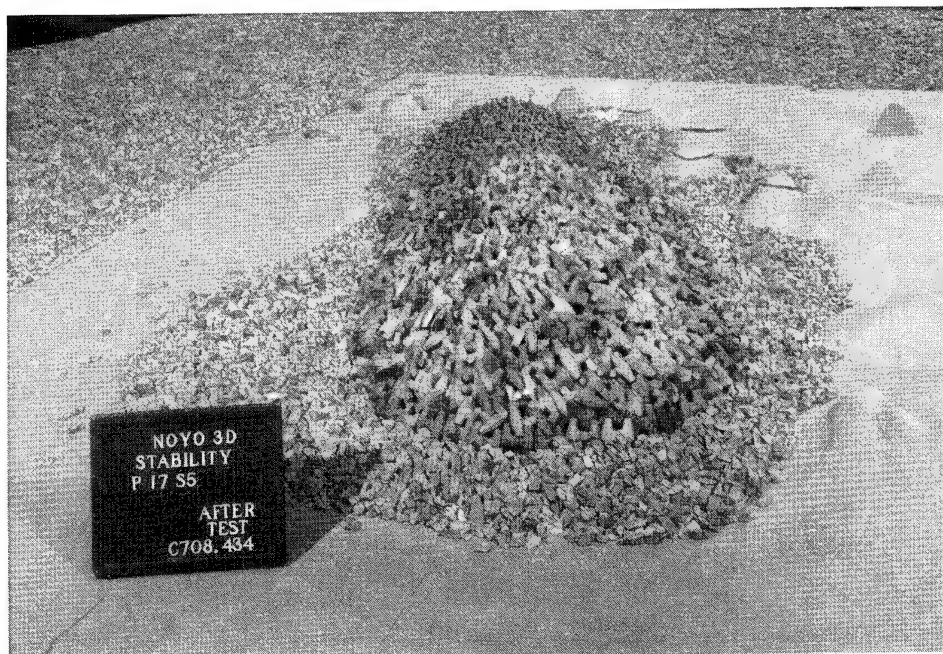Photo C157. Plan 17, north roundhead after five series of modified Storm IB
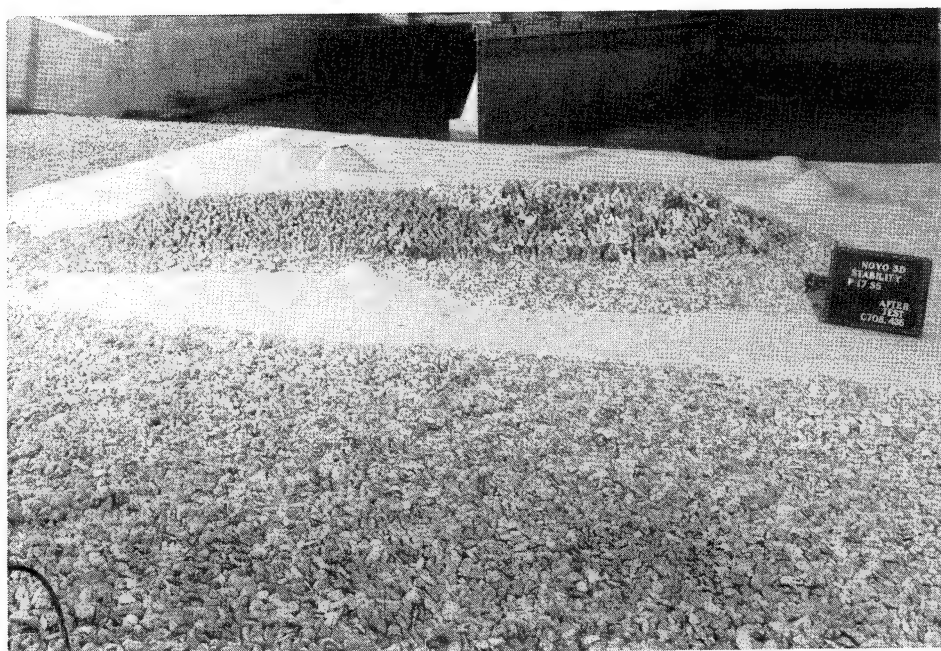waves at +0 m mllw



Photo C158. Leeside view of Plan 17 after five series of modified Storm IB
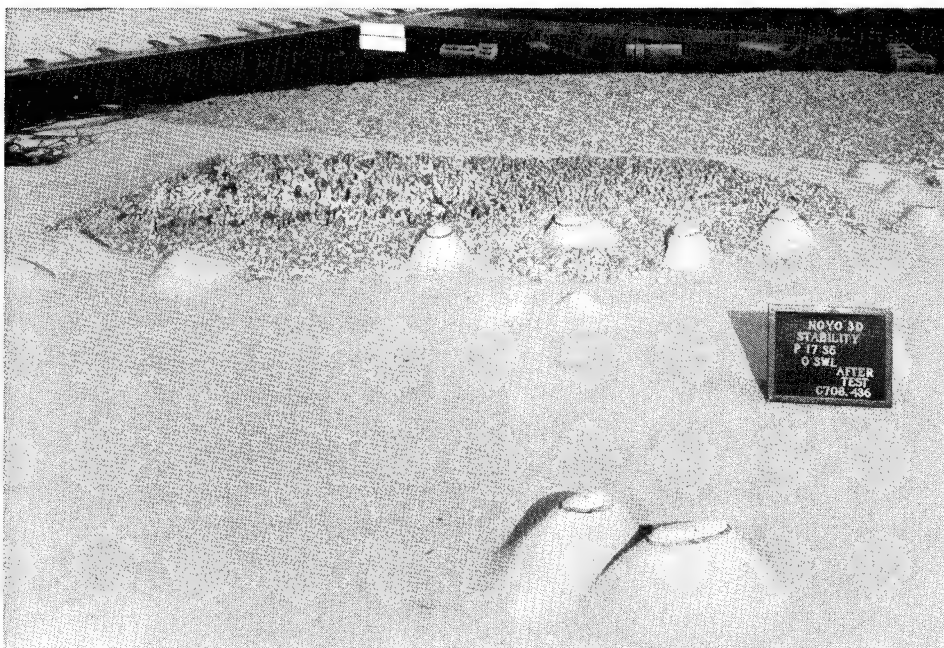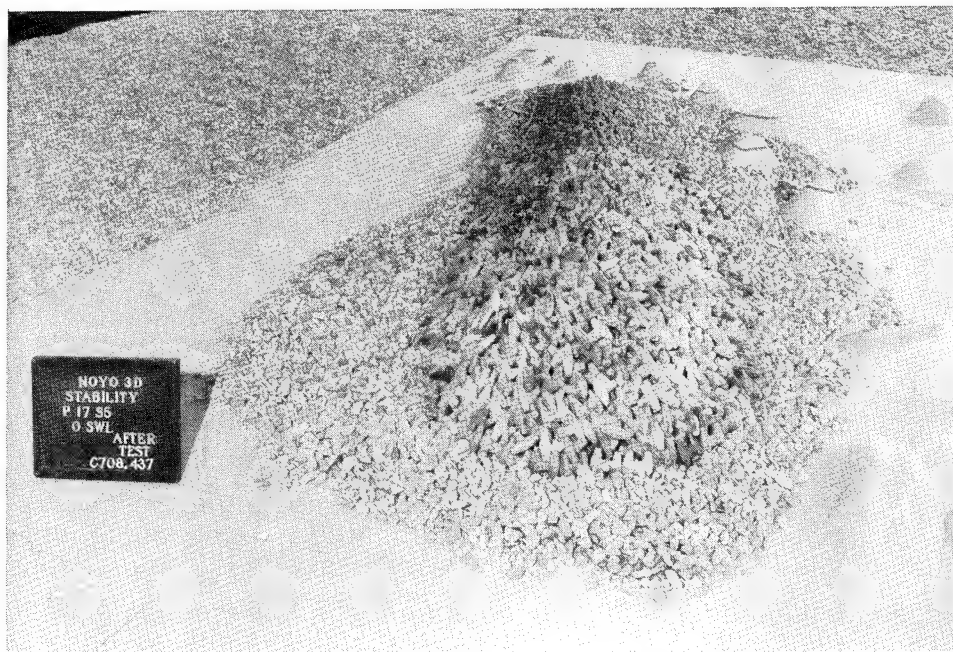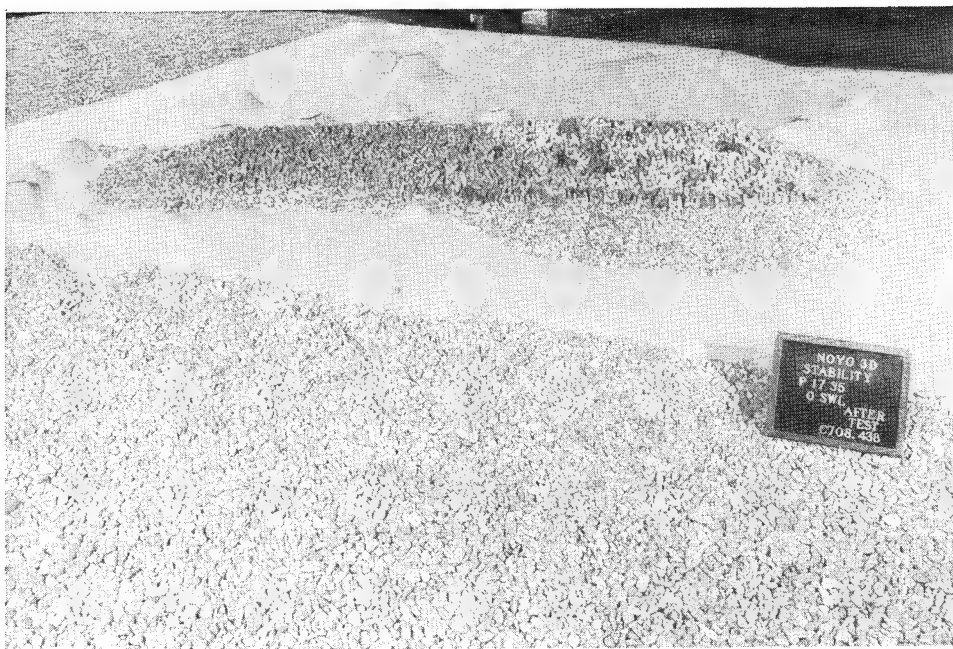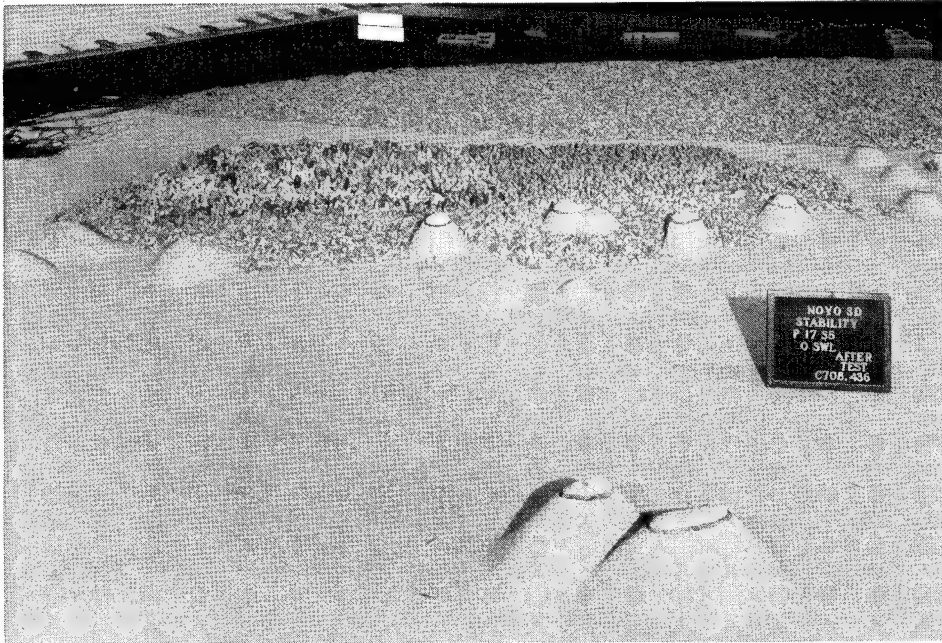waves at +0 m mllw

Photo C159.  Sea-side view of Plan 17 after five series of modified Storm IB
waves at +0 m mllw
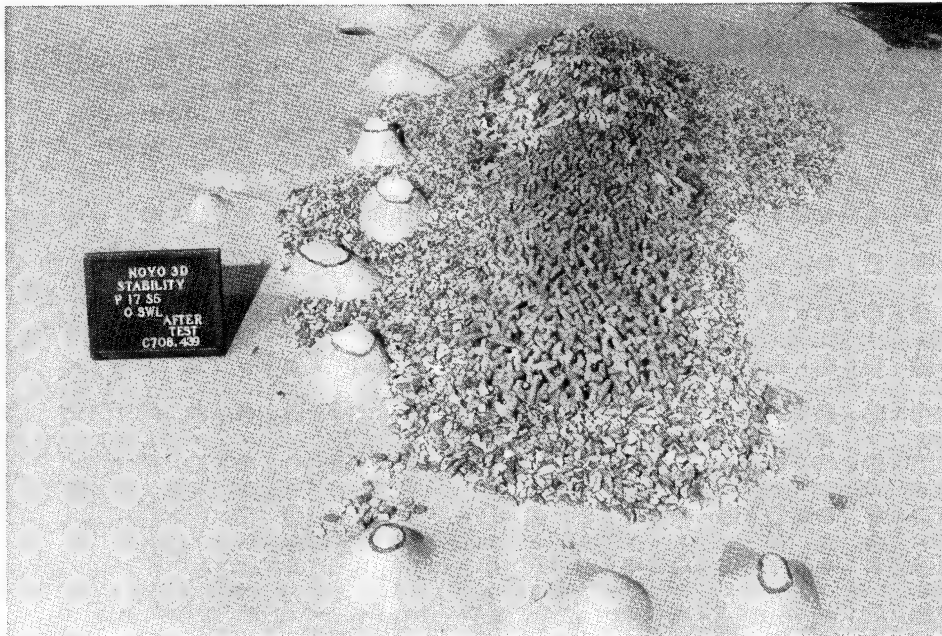


Photo C160.  Plan 17, south roundhead after five series of modified Storm IB
waves at +0 m mllw

# Appendix D
# Notation

| | |
|---|---|
| $a$ | Area scale |
| $E$ | Elastic modulus |
| $f_t$ | Splitting tensile strength |
| $FS$ | Factor of safety |
| $H$ | Wave height |
| $H_d$ | Highest wave height at the structure that causes no damage |
| $H_i$ | Incident wave height |
| $H_{mo}$ | Zero-moment wave height |
| $(H_{mo})_{24}$ | Offshore zero-moment wave height, three-dimensional tests |
| $(H_{mo})_d$ | Zero-moment wave height at north roundhead, three-dimensional tests |
| $(H_{mo})_o$ | Offshore zero-moment wave height, two-dimensional tests |
| $H_{max}$ | Maximum wave height |
| $(H_{max})_d$ | Maximum wave height at north roundhead, three-dimensional tests |
| $H_s$ | Significant wave height |
| $(H_s)_d$ | Significant wave height at north roundhead, three-dimensional tests |
| $H_t$ | Transmitted wave height |
| $k_M$ | Stress contribution factor |
| $K_d$ | Stability coefficient |
| $K_t$ | Transmission coefficient |
| $l$ | Length scale |
| $m$ | Model quantity |
| $M_{cr}$ | Critical moment |
| $M_n$ | Nominal moment |
| $p$ | Prototype quantity |
| $P$ | Exceedance probability |
| $Q$ | Applied loading |
| $r$ | Subscript denoting model to prototype |
| $r_w$ | Dolos waist ratio |
| $R$ | Structural resistance |
| $S$ | Specific gravity |
| $S_a$ | Specific gravity of an individual armor unit relative to the water in which it is placed, $S_a = \gamma_a/\gamma_w$ |
| $S_m$ | Section modulus |

| | |
|---|---|
| $t$ | Time scale |
| $T$ | Average wave period |
| $T_p$ | Peak wave period |
| $v$ | Volume scale |
| $W$ | Armor weight |
| $W_1$ | Weight of an individual unit in armor layer |
| $W_2$ | Weight of stone in first underlayer |
| $W_2'$ | Weight of stone in second underlayer |
| $W_3$ | Weight of stone in core |
| $W_4$ | Weight of stone in toe berm |
| $W_a$ | Weight of an individual armor unit |
| $Y_1$ | Vertical distance below crest elevation of transmission barrier |
| $Y_2$ | Vertical distance above crest elevation of transmission barrier |
| $\theta$ | Angle of the structure slope measured from horizontal in degrees ($\theta$) |
| $\phi$ | Resistance factor ($\phi$) |
| $\sigma_1$ | Principal tensile stress ($\sigma$) |
| $\gamma$ | Load factor ($\gamma$) |
| $\gamma_a$ | Specific weight of an individual armor unit ($\gamma$) |
| $\gamma_w$ | Specific weight of water ($\gamma$) |
| $\nu$ | Poisson's ratio ($\nu$) |

# REPORT DOCUMENTATION PAGE

Public reporting burden for this collection of information is estimated to average 1 hour per response, including the time for reviewing instructions, searching existing data sources, gathering and maintaining the data needed, and completing and reviewing the collection of information. Send comments regarding this burden estimate or any other aspect of this collection of information, including suggestions for reducing this burden, to Washington Headquarters Services, Directorate for Information Operations and Reports, 1215 Jefferson Davis Highway, Suite 1204, Arlington, VA22202-4302, and to the Office of Management and Budget, Paperwork Reduction Project (0704-0188), Washington, DC20503.

| 1. AGENCY USE ONLY (Leave blank) | 2. REPORT DATE <br> October 1995 | 3. REPORT TYPE AND DATES COVERED <br> Final report |
|---|---|---|

| 4. TITLE AND SUBTITLE <br> Noyo Harbor, California, Breakwater Stability and Transmission Tests | 5. FUNDING NUMBERS |
|---|---|
| 6. AUTHOR(S) <br> Ernest R. Smith, Leland L. Hennington | |

| 7. PERFORMING ORGANIZATION NAME(S) AND ADDRESS(ES) <br> U.S. Army Engineer Waterways Experiment Station <br> 3909 Halls Ferry Road, Vicksburg, MS   39180-6199 | 8. PERFORMING ORGANIZATION REPORT NUMBER <br> Technical Report CERC-95-17 |
|---|---|

| 9. SPONSORING/MONITORING AGENCY NAME(S) AND ADDRESS(ES) <br> U.S. Army Engineer District, San Francisco <br> 211 Main Street <br> San Francisco, CA   94105-1905 | 10. SPONSORING/MONITORING AGENCY REPORT NUMBER |
|---|---|

**11. SUPPLEMENTARY NOTES**

Available from National Technical Information Service, 5285 Port Royal Road, Springfield, VA   22161.

| 12a. DISTRIBUTION/AVAILABILITY STATEMENT <br><br> Approved for public release; distribution is unlimited. | 12b. DISTRIBUTION CODE |
|---|---|

**13. ABSTRACT (Maximum 200 words)**

Stability tests were conducted in two and three dimensions to identify a stable breakwater cross section for a proposed breakwater at Noyo Harbor, California. Additionally, two-dimensional transmission tests were performed to determine a small-scale cross section that reproduced transmission of the proposed breakwater cross section.

Five two-dimensional stability plans were tested in a wave tank at a 1:43.3 scale. Plans 1 and 2 consisted of Accropode armor units, and Plans 3 through 5 were performed with dolos armor units. Plans 1 and 3, constructed of 9.0-m$^3$ Accropodes and 7.9-m$^3$ dolosse, were stable but conservative in design. Plan 2, consisting of 7.6-m$^3$ Accropodes, was stable. Plans 4 (3.8-m$^3$ dolosse) and 5 (5.9-m$^3$ dolosse) were moderately stable.

Three-dimensional stability tests were conducted for 17 plans with two breakwater configurations. Approximately 425 by 425 m of prototype bathymetery was reproduced in a basin at a 1:50 scale. The original breakwater configuration consisted of 14- and 8.3-m$^3$ Accropode armor units. It was necessary to place a metal strip at the base of the structure, which simulated a toe trench in prototype, to obtain toe stability with the original breakwater configuration. Results of tests with the modified breakwater indicated a stone buttress was sufficient to stabilize the toe. Armor units tested with the modified plan included 14- and 8.3-m$^3$ Accropodes, 11.9- and 7.0-m$^3$ Core-Locs, and 19- and 8.3-m$^3$ Accropodes.

(Continued)

| 14. SUBJECT TERMS <br> Accropode     Dolos     Toe stability <br> Breakwaters     Harbors, California     Wave transmission <br> Breakwater stability     Hydraulic models <br> Core-Loc     Noyo Harbor, California | 15. NUMBER OF PAGES <br> 184 |
|---|---|
| | 16. PRICE CODE |

| 17. SECURITY CLASSIFICATION OF REPORT <br> UNCLASSIFIED | 18. SECURITY CLASSIFICATION OF THIS PAGE <br> UNCLASSIFIED | 19. SECURITY CLASSIFICATION OF ABSTRACT | 20. LIMITATION OF ABSTRACT |
|---|---|---|---|

## 13. ABSTRACT (Concluded).

The 19-m$^3$ Accropode was required to stabilize the north roundhead for five successive storms of depth-limited waves for the design periods. A heavier model Core-Loc unit was not available for testing, but based on observations, a Core-Loc weight of at least 16.9 m$^3$ would be necessary for stability. The lighter armor units were stable if wave conditions that exceeded wave hindcast information were omitted for three of the five successive storms.

Two-dimensional transmission tests were conducted at 1:75 scale for nine cross sections. Results of the tests were compared to transmitted wave heights of two-dimensional stability Plan 1. Two plans consisting of a vertical barrier placed in the cross section were necessary to reproduce transmission of the larger scale for all design periods. The cross sections were used during harbor model tests conducted by Bottin (1994).